



ICFAST 2022

12th India-Japan Science and Technology Conclave
INTERNATIONAL CONFERENCE ON FRONTIER AREAS OF
SCIENCE AND TECHNOLOGY
(ICFAST-2022)

ABSTRACT BOOKLET





Message

Message from Prof. B.J. Rao, Vice Chancellor, University of Hyderabad to the participants of International Conference on Frontier Areas of Science and Technology (ICFAST-2022).

On behalf of the organizers, I extend a warm welcome to all the scientists, researchers, faculty and students from Japan, India and elsewhere to the verdant and naturally endowed campus of University of Hyderabad (UoH). We are extremely proud and happy that IJAA, on behalf of JSPS, has chosen University of Hyderabad to host the 12th edition of the International Symposium ICFAST 2022. I am also happy to note that all the science schools of the University – School of Physics, School of Chemistry and School of Life Sciences have come forward to organize this premier event.

University of Hyderabad, established in 1974 as a Central University, is one of the premier institutions in the country for under-graduate, post-graduate and doctoral level teaching and research. The motto of the University is to disseminate and advance knowledge by providing instructional and research facilities in such branches of learning as it may deem fit and by the example of its corporate life, and in particular to make special provisions for integrated courses in humanities and science in the educational programmes of the University and to take appropriate measures for promoting inter-disciplinary studies and research in the University. Our relentless endeavour to realize these objectives accorded us several international and national recognition. We consistently rank among the top 50 universities in the world which are under 50 years old. In 2019 Government of India accorded UoH the Institution of Eminence (IOE) status in recognition of our standing, ability and potential to move into the league of the world's best institution. Our students are considered assets in all the organizations they associate themselves and our faculty are beacons of knowledge and research achievements who collaborate with eminent researchers across the world.

In the emerging world India and Japan are natural allies in the scientific and technological worlds apart from other spheres of life. Several of our students go on to pursue their research career in Japan and faculty have collaborative work with their counterparts as well. However, the numbers are currently not at the level where it should be considering the synergy between the two countries. I am sure hosting ICFAST 2022 in UoH and other such and related efforts in the future will give a fillip to increasing the numbers to benefit both countries and scientific communities. From this perspective this is an enormous opportunity to showcase our eminent status among scientific peers.

I am sure that the faculty coordinators of the event have made arrangements to ensure a scientifically and collaboratively wonderful event. Wishing them a successful event, I join my faculty colleagues in extending a warm welcome to all the participants of the ICFAST 2022 conference, which I am sure will be mutually and scientifically beneficial to the community at large.

Basuthkar Jagadeeshwar Rao
vice chancellor
University of Hyderabad



Message

Message from JSPS President SUGINO Tsuyoshi on Occasion of IJAA's 12th International Symposium

Writing on behalf of the Japan Society for the Promotion of Science, we are very happy that the Indian JSPS Alumni Association is holding its 12th India-Japan Science & Technology Symposium there in Hyderabad on the theme “International Conference on Frontier Areas of Science and Technology (ICFAST-2022).”

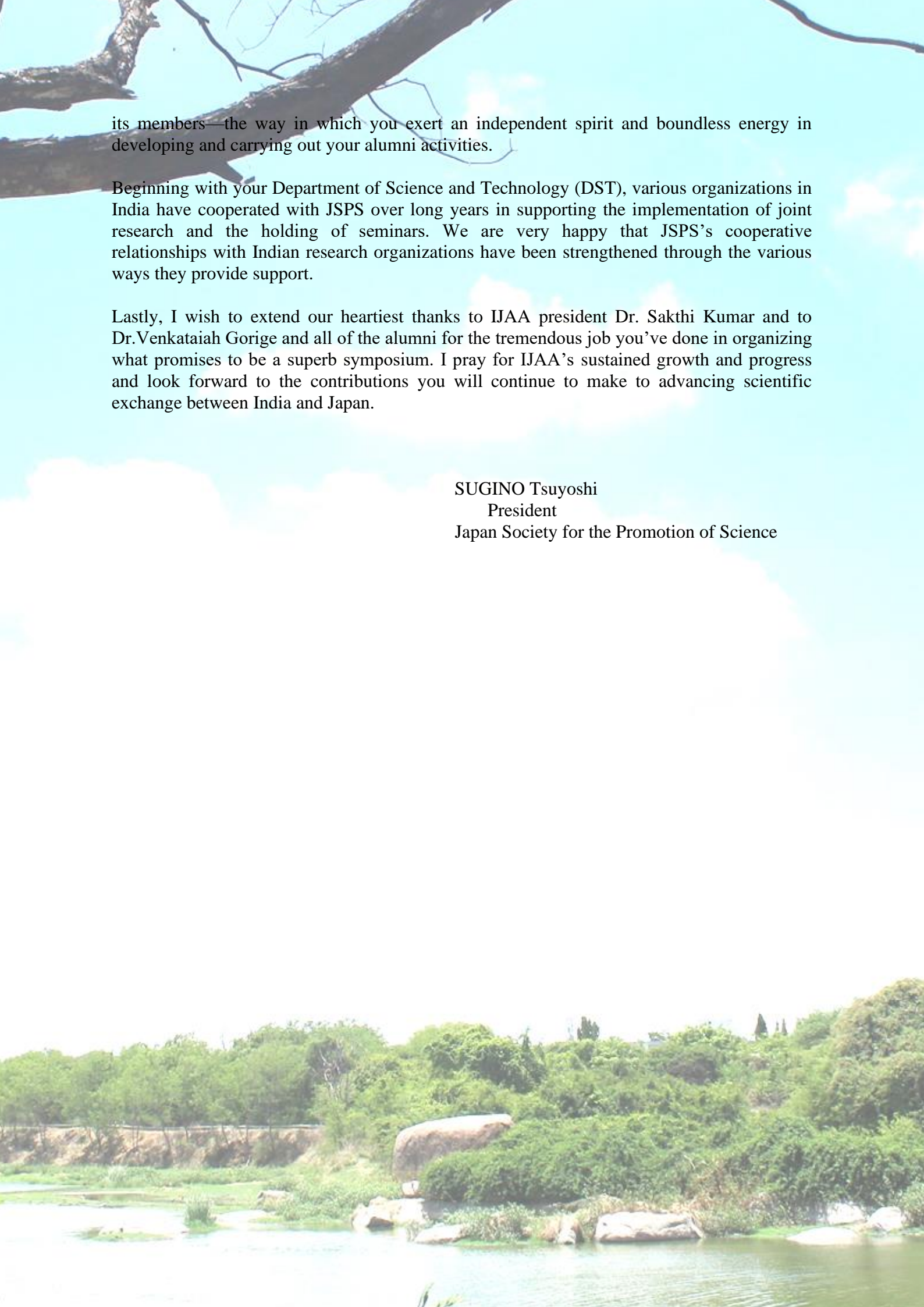
Every year, this symposium enjoys a wide spectrum of participation including students, researchers, university faculty and administrators, and corporate people who gather for it from both in and outside India. It always attracts strong interest and wide attention as an event that strengthens scientific exchange between India and Japan.

To effectively advance science, the free and diverse ideas of researchers must be respected and their activities must be given sustained support. This symposium provides an important platform for the participants to share information on a wide range of science and technology being advanced through cutting-edge research in India and Japan. While addressing the importance of basic research and basic science, the symposium offers a valuable opportunity to consider the state of scientific cooperation enjoyed between our two countries.

Though I merely state the obvious, India is one of Japan's most important partners in both the scientific and many other areas of bilateral exchange. A great many joint research projects have and are being carried out between our countries, producing results that advance science and benefit society. As one vehicle of exchange, the Inter-university Exchange Project, spearheaded by Japan's Ministry of Education, Culture, Sports, Science and Technology (MEXT), has steadily advanced the exchange of many excellent students between India and Japan. The achievements that they have and will make provide foundations for propelling exchange between our nations long into the future. I look forward to the continued thriving of our scientific partnership.

The persistent effect of the new coronavirus pandemic has hampered active international exchange among researchers. Before the pandemic occurred, more than 4,500 researchers from other countries were invited and came to Japan each year through JSPS's international exchange programs. Concurrently, about the same number of Japanese researchers were dispatched abroad. Among the researchers coming to Japan, more than 1,700 of them were invited from India. Building networks while in Japan, many of these researchers return home to engage in joint projects with Japanese colleagues.

Established in 2006, IJAA is the organizer of this symposium. It is JSPS's sixth official alumni association of researchers who have stayed in Japan while participating in JSPS programs. In addition, IJAA is both the first JSPS alumni association to be established in Asia and in a country without a JSPS overseas office. We at JSPS are very proud of IJAA and



its members—the way in which you exert an independent spirit and boundless energy in developing and carrying out your alumni activities.

Beginning with your Department of Science and Technology (DST), various organizations in India have cooperated with JSPS over long years in supporting the implementation of joint research and the holding of seminars. We are very happy that JSPS's cooperative relationships with Indian research organizations have been strengthened through the various ways they provide support.

Lastly, I wish to extend our heartiest thanks to IJAA president Dr. Sakthi Kumar and to Dr. Venkataiah Gorige and all of the alumni for the tremendous job you've done in organizing what promises to be a superb symposium. I pray for IJAA's sustained growth and progress and look forward to the contributions you will continue to make to advancing scientific exchange between India and Japan.

SUGINO Tsuyoshi
President
Japan Society for the Promotion of Science

भारत के राजदूत
AMBASSADOR OF INDIA



भारत का राजदूतावास
Embassy of India
2-2-11 Kudan Minami, Chiyoda-ku
Tokyo 102 0074



MESSAGE

I congratulate the Indian JSPS Alumni Association (IJAA) for organizing the 12th India-Japan Science and Technology Seminar on 9-10 September 2022 in association with the University of Hyderabad. The theme of the Seminar – International Conference on Frontier Areas of Science and Technology (ICFAST) – has great relevance to India-Japan collaboration in the field of Science and Technology. Today scientific and technological endeavour is breaching new frontiers, bringing in its wake both opportunities and challenges.

I sincerely hope that the Seminar will provide innovative information to the scientific community in India and Japan and help develop collaboration and partnership between institutes of the two countries.

I am confident that the 12th India-Japan Science and Technology Seminar will be a great success.


(Sanjay Kumar Verma)

Tokyo
05 September 2022



Message

I am really happy to invite you all for Indian JSPS Alumni Association's (IJAA), 12 th India – Japan Science and Technology seminar, that IJAA is organizing in collaboration with university of Hyderabad at Hyderabad during September 9-10, 2022 and our annual get together. This seminar we are conducting under the celebration of 70 th Anniversary of India-Japan Diplomatic Relations as well as 75th Anniversary of Independence of India. IJAA is really committed to spread and augment S&T collaboration between India and Japan and for achieving the same, we had conducted 11 India-Japan S&T seminar in various places in India and 1 S&T seminar in Tokyo. Ever increasing number of participants in our seminar, clearly says that we have achieved our goal.

This time our South Chapter of IJAA is organizing the seminar in Hyderabad. IJAA is very much thankful to Dr. Venkataiah Gorige and his team for organizing our 12th seminar in Hyderabad.

Once again I welcome all delegates to our seminar and hope that it would provide a great experience.

Prof. D. Sakthi Kumar,
Chairman,
Indian JSPS Alumni Association

Professor, Bio Nano Electronics Research Center,
Toyo University, Kawagoe, Saitama, Japan



12th India-Japan Science and Technology Conclave
International Conference on Frontier Areas of Science and Technology (ICFAST-2022)
School of Physics [SoP]
University of Hyderabad [UoH]
 C.R. Rao Road, Gachibowli, Hyderabad-500046, India
 September 09-10, 2022

Conference Venue: Auditorium and Seminar Room, School of Life Sciences [SLS], University of Hyderabad

Stream – 1 (Chemistry, Life Sciences, Medical Sciences & Interdisciplinary)

Schedule of the Program for Day-1 (09 September 2022)

08:30 - 09:00		Registration [for guests]	
Session-I	Inauguration	Inauguration by	
Venue: SLS Auditorium	09:00 - 09:40	Hon. Ambassadors of Japan and India, President (JSPS), Vice-Chancellor (University of Hyderabad), President of the IJAA, General Secretary of the IJAA, Dean (School of Physics, UoH), and Convener (ICFAST-2022)	
Chairperson: Prof. B J Rao VC, UoH	Keynote Lecture 09:40 - 10:40	Prof. G. Ravindra Kumar TIFR (M), India	<i>Science with Extreme Laser Light (SELL)</i>
10:40-11:00		High Tea	
Session-II (A) (Chemistry) Venue: SLS Auditorium Chairperson: Prof. Aanunay Samanta UoH, India	11:00 - 11:30	Prof. Rajadurai Chandrasekar UoH, India	<i>Mechanophotonics & Crystal-photonics foundry: A Roadmap to All-Organic, Single-Crystal, Photonic Integrated Circuits</i>
	11:30 - 12:00	Prof. Vijayamohanan Pillai IISER (T), India	<i>Simultaneous doping and un-zipping of carbon nanotubes at room-temperature in different electrolytes</i>
	12:00 - 12:30	Prof. D. B. Ramachary UoH, India	<i>Discovery of sustainable organocatalytic reactions: expansion of substrate/catalysts scope</i>
	12:30 - 13:00	Prof. Chilla Malla Reddy IISER (K), India	<i>Adaptive soft molecular crystals: from bending to self-healing</i>
13:00-14:00		Lunch & University booths	
14:00-16:00		Poster Session and University booths	

15:00 – 16:00		IJAA Executive and General Committee meeting (Only for IJAA members)	
Session-III (A) (Life Sciences) Venue: SLS Auditorium Chairpersons: Prof. Appa Rao P & Prof. S Rajagopal UoH, India	16:00 - 16:30	Prof. Deepak Sharma IMTECH, India	<i>The cell-penetrating peptide penetratin prevents neurodegeneration in mice models of Parkinson's disease</i>
	16:30 - 17:00	Prof. Jagadis Gupta Kapuganti NIPGR, India	<i>Nitric oxide signaling in plants and its role in plant tolerance to low oxygen stress</i>
17:00-17:15		Tea	
Session-IV (Cultural Program) Venue: DST Auditorium, UoH Chairpersons: Prof. J Anuradha UoH, India	17:15 - 18:30	Team from Sarojini Naidu School of Arts and Communication, UoH, India	<i>Cultural Program</i>
19:00-21:00 Venue: Ellaa Hotel, Gachibowli, Hyderabad		Gala Dinner	

Schedule of Program for Day-2 (10 September 2022)

09:00 - 09:10		Registration [for guests]	
Session-I: Venue: SLS Auditorium & Seminar Hall Chairpersons: Prof. D Basavaiah UoH, India	Keynote Lecture 09:10 - 09:55 <i>(online)</i>	Nobel Laureate Prof. Ryōji Noyori Nagoya Univ., Japan	<i>Where am I from? Where are you going?</i>
	Session-II: (A) Venue: SLS Auditorium Chairpersons: Prof. Anand K Kondapi, UoH, India	10:00 - 10:30	Prof. Rajender K. Motiani RCB, India

10:30-10:45		Tea	
Session-III (A) (Chemistry and Biology) Venue: SLS Auditorium Chairperson: Prof. T P Radhakrishnan UoH, India	10:45 - 11:15	Prof. Kana M. Sureshan IISER (TVM), India	<i>Gels and their Applications</i>
	11:15 - 11:45	Prof. Melepurath Deepa IIT-H, India	<i>Solution Processed High Performance Devices: Solar Cells and Photoelectrochromic Devices and Photo-supercapacitors</i>
	11:45 - 12:15	Prof. S. Venkata Mohan CSIR-IICT (H), India	<i>Low-carbon and green hydrogen production through a biorefinery approach</i>
	12:15 - 12:45	Prof. Kundan Sengupta IISER (P), India	<i>Lamins – mechanoprotector of the nucleus</i>
12:45-14:00		Lunch, Poster & University booths	
Session-IV (A) (Life Sciences and) Venue: SLS Auditorium Chairpersons: Prof. N Siva Kumar & Prof. Krishnaveni Mishra UoH, India	14:00 - 14:30	Prof. Ullas Kolthur Seetharam TIFR (M), India	<i>Investigating order in chaos: Unraveling emergent mechanisms that cumulatively dictate aging and emergence of diseases</i>
	14:30 - 15:00	Prof. M. Subba Reddy CDFD, India	<i>Mapping interaction network of human phosphatases</i>
	15:00 - 15:30	Prof. Subba Rao IISc, India	<i>Golgi localized small G-protein regulates cell adhesion</i>
	15:30 - 16:00	Prof. Renu John IIT-H, India	<i>Quantitative Phase Microscopy for Clinical Diagnosis</i>
16:00-16:15		Tea	
Session-V (A) (Interdisciplinary Topics) Venue: SLS Auditorium Chairpersons: Prof. Prakash Babu & Prof. K Srinivasulu, UoH India	16:15 - 16:45	Prof. Yuichiro Takahashi RIIS, Japan	<i>Structure and dynamics of photosystem I supercomplex in the green alga Chlamydomonas reinhardtii</i>
	16:45 - 17:15	Prof. Aki Yonehara Toyo Univ., Japan & IIT-D, India	<i>A mechanism and impact of translocational learning: A trial of international educational exchange program between India and Japan</i>
	17:15 - 17:45	Prof. Eri Ikeda IIT-D, India	<i>Global economy and economics</i>
Venue: SLS Auditorium	17:45-18:00	<i>JST Presentation: Sakura Science Program</i>	
	18:00-18:15	<i>NEDO Presentation: Introducing NEDO activities and opportunities for India-Japan joint programs</i>	
18:15-19:00 Venue: SLS Auditorium		Poster Award and Concluding Session	

12th India-Japan Science and Technology Conclave
International Conference on Frontier Areas of Science and Technology (ICFAST-2022)
School of Physics [SoP]
University of Hyderabad [UoH]
 C.R. Rao Road, Gachibowli, Hyderabad-500046, India
 September 09-10, 2022

Conference Venue: Auditorium and Seminar Hall, School of Life Sciences [SLS], University of Hyderabad

Stream – 2 (Physics, Engineering & Mathematics)

Schedule of the Program for Day-1 (09 September 2022)

08:30 - 09:00		Registration [for guests]	
Session-I <u>Venue:</u> SLS Auditorium	<u>Inauguration</u> 09:00 - 09:40	Inauguration by Hon. Ambassadors of Japan and India, President (JSPS), Vice-Chancellor (University of Hyderabad), President of the IJAA, General Secretary of the IJAA, Dean (School of Physics, UoH), and Convener (ICFAST-2022)	
<u>Chairperson:</u> Prof. B J Rao VC, UoH, India	<u>Keynote Lecture</u> 09:40 - 10:40	Prof. G. Ravindra Kumar, TIFR (M), India	<i>Science with Extreme Laser Light (SELL)</i>
10:40-11:00		High Tea	
Session-II (B) (Atomic, Molecular, and Optical Physics) <u>Venue:</u> SLS Seminar Hall <u>Chairpersons:</u> Prof. M Ghanashyam Krishna & Prof. Nirmal K V, UoH, India	11:00 - 11:30	Prof. Takashige Omatsu Chiba Univ., Japan	<i>Structured light fields revolutionize materials science</i>
	11:30 - 12:00	Prof. Achanta Venugopal NPL, India	<i>Active metamaterials</i>
	12:00 - 12:30	Prof. Yoko Miyamoto UEC, Japan	<i>Optical mode manipulation for quantum technologies</i>
	12:30 - 13:00	Prof. Yoshiro Azuma IIT-D, India	<i>A big jump from Japan joining IIT Delhi in the wake of Covid 19: Atomic and molecular physics, higher education, and life in general</i>
13:00-14:00		Lunch	
14:00-16:00		Poster Session	

15:00-16:00		IJAA Executive and General Committee meeting (Only for IJAA members)	
Session-III (B) (Theoretical Condensed Matter Physics) Venue: SLS Seminar Hall Chairpersons: Prof. V Subramanyam & Prof. Vaitheeswaran UoH, India	16:00 - 16:30	Prof. Subroto Mukerjee IISc, India	<i>Many body localization: a Fock space perspective</i>
	16:30 - 17:00	Prof. Chandan Dasgupta IISc, India	<i>Living glass: active matter at high densities</i>
17:00-17:15		Tea	
Session-IV (Cultural Program) Venue: DST Auditorium, UoH Chairpersons: Prof. J Anuradha UoH, India	17:15 - 18:30	Team from Sarojini Naidu School of Arts and Communication, UoH, India	<i>Cultural Program</i>
19:00-21:00		Gala Dinner	
Venue: Ellaa Hotel, Gachibowli, Hyderabad			

Schedule of Program for Day-2 (10 September 2022)

09:00 - 09:10		Registration [for guests]	
Session-I: Venue: SLS Auditorium & Seminar Hall Chairpersons: Prof. D Basavaiah UoH, India	Keynote Lecture 09:10 - 09:55 (<i>online</i>)	Nobel Laureate Prof. Ryōji Noyori Nagoya Univ., Japan	<i>Where am I from? Where are you going?</i>
	Session-II: (B) (Statistical Mechanics) Venue: SLS Seminar Room Chairpersons: Prof. B V R Tata UoH, India	10:00 - 10:30	Prof. Smarajit Karmakar TIFR (H), India

10:30-10:45		Tea	
Session-III (B) (Experimental Condensed Matter Physics) Venue: SLS Seminar Hall Chairpersons: Prof. S Srinath & Prof. Dibakar Das UoH, India	10:45 - 11:15	Prof. Tomoyasu Taniyama Nagoya Univ., Japan	<i>Artificial multiferroic heterostructures for spin-wave applications</i>
	11:15 - 11:45	Prof. P. S. Anil Kumar IISc, India	<i>Spin chirality induced large topological Hall effect in magnetic Weyl semi-metallic $\text{Eu}_2\text{Ir}_2\text{O}_7$ (111) thin films</i>
	11:45 - 12:15	Prof. Yoichi Kamihara Keio Univ., Japan	<i>Review on a mixed anion layered compound (MALC) polycrystalline $\text{LaCu}_{1-\delta}\text{S}_{0.5}\text{Se}_{0.5}\text{O}$ ($\delta \sim 0.01$) as a degenerate semiconductor</i>
	12:15 - 12:45	Prof. Kalobaran Maiti TIFR (M), India	<i>Electron spectroscopy for the physics of quantum materials</i>
12:45-14:00		Lunch	
Session-IV (B) (Applied Physics, Engineering, and Technology) Venue: SLS Seminar Hall Chairpersons: Prof. D Narayana Rao & Prof. S Ananthamurthy UoH, India	14:00 - 14:30	Prof. Anil Shaji IISER (TVM), India	<i>Using machine learning in the design and implementation of quantum algorithms</i>
	14:30 - 15:00	Prof. Surajit Dhara UoH, India	<i>Exploitation of topological defects in liquid crystals</i>
	15:00 - 15:30	Prof. P. Sudharshan Phani ARCI, India	<i>High speed nanoindentation mapping - a new paradigm in small scale mechanical testing</i>
	15:30 - 16:00	Prof. M. Senthil Kumar ISRO, India	<i>OPTICS: Space borne remote sensing and beyond</i>
16:00-16:15		Tea	
Session-V (B) (Particle Physics, Astrophysics, and Space Science) Venue: SLS Seminar Hall Chairpersons: Prof. P K Suresh & Prof. R Mohanta UoH, India	16:15 - 16:45	Prof. Amitava Raychaudhuri CU, India	<i>The future of neutrino physics</i>
	16:45 - 17:15	Prof. Brajesh C. Choudhary DU, India	<i>India's contributions to the CMS Experiment and its Physics</i>
	17:15 - 17:45	Prof. Annapurni Subramaniam IIA, India	<i>AstroSat, the first Indian space observatory</i>
Venue: SLS Auditorium	17:45-18:00	<i>JST Presentation: Sakura Science Program</i>	
	18:00-18:15	<i>NEDO Presentation: Introducing NEDO activities and opportunities for India-Japan joint programs</i>	
18:15-19:00 Venue: SLS Auditorium		Poster Award and Concluding Session	

Table of Contents

Keynote Lectures		
	Science with Extreme Laser Light (SELL)	1
	Where am I from? Where are you going?	2
Invited Lectures		
IL-01	Mechanophotonics & Crystal-photonics Foundry: All-Organic, Single-Crystal, Photonic Integrated Circuits	3
IL-02	Simultaneous Doping and Un-zipping of Carbon Nanotubes at Room-temperature in Different Electrolytes	4
IL-03	Discovery of Sustainable Organocatalytic Reactions: Expansion of Substrate/Catalysts Scope	5
IL-04	Adaptive Soft Molecular Crystals: From Bending to Self-Healing	6
IL-05	The cell-penetrating peptide penetratin prevents neurodegeneration in mice models of Parkinson's disease.	7
IL-06	Nitric oxide signaling in plants and its role in plant tolerance to low oxygen stress	8
IL-07	Calcium dynamics: a critical regulator of human skin pigmentation	9
IL-08	Gels and their Applications	10
IL-09	Solution Processed High Performance Devices: Solar Cells and Photoelectrochromic Devices and Photo-supercapacitors	11
IL-10	Low-Carbon and Green Hydrogen Production Through a Biorefinery Approach	12
IL-11	"Lamins - mechanoprotector of the nucleus"	13
IL-12	Investigating order in chaos: Unraveling emergent mechanisms that cumulatively dictate aging and emergence of diseases	14
IL-13	Mapping Interaction Network of Human Phosphatases	15
IL-14	Golgi localized small G-protein regulates cell adhesion	16
IL-15	Quantitative Phase Microscopy for Clinical Diagnosis	17
IL-16	Structure and dynamics of photosystem I supercomplex in the green alga <i>Chlamydomonas reinhardtii</i>	18
IL-17	A mechanism and impact of translocal learning: A trial of international educational exchange program between India and Japan	19
IL-18	Global economy and economics	20
IL-19	Structured light fields revolutionize materials science	21
IL-20	Active Metamaterials	22
IL-21	Optical mode manipulation for quantum technologies	23
IL-22	A big jump from Japan joining IIT Delhi in the wake of Covid 19: Atomic and molecular physics, higher education, and life in general	24
IL-23	Many Body Localization: A Fock space perspective	25
IL-24	Living Glass: Active Matter at High Density	26

IL-25	Strong Dynamical Heterogeneity in Active Glass-forming Liquids and its implications in the Physics of Glasses	27
IL-26	Artificial Multiferroic Heterostructures for Spin-Wave Applications	28
IL-27	Spin chirality induced large topological Hall effect in magnetic Weyl semi-metallic Eu ₂ Ir ₂ O ₇ (111) thin films	29
IL-28	Review on a Mixed Anion Layered Compound (MALC) Polycrystalline LaCu ₁ -S _{0.5} Se _{0.5} O (0.01) as a Degenerate Semiconductor	30
IL-29	Electron spectroscopy for the physics of quantum materials	31
IL-30	Using machine learning in the design and implementation of quantum algorithms	32
IL-31	Exploitation of topological defects in liquid crystals	33
IL-32	High speed nanoindentation mapping - A new paradigm in small	34
IL-33	OPTICS: Space borne remote sensing and beyond	35
IL-34	The Future of Neutrino Physics	36
IL-35	India's contributions to the CMS Experiment and its Physics	37
IL-36	AstroSat, the first Indian Space Observatory	38
Poster presentation		
Physics		
PC-01	The Optimized Sparse Davidson Algorithm: A modern numerical approach for finding extreme eigenpairs for large Hermitian matrices	1
PC-02	Analysis of Congestive heart failure signals using normalized entropy	2
PC-03	Network properties of healthy and epileptic brain signals	3
PC-04	Thermodynamic properties of a particle scattering by rotating trapped quantum gases	4
PC-05	Synthesis and Characterization of Sb ₂ Se ₃ Thin Films and Numerical Simulation of p-Sb ₂ Se ₃ /n-ZnSe Heterojunction Solar Cell	5
PC-06	Electrodeposited NiO nanoflakes for electrochromic energy storage applications	6
PC-07	Photocatalytic Self-Cleaning and Stain Removing Properties of Carbon Nitride /PEDOT Composite for Smart Textile Application	7
PC-08	A theorem on the generic form of the quantum cluster integral	8
PC-09	Non-equilibrium work distribution of a 3-d harmonic oscillator with time varying angular frequency in a rotating frame	9
PC-10	Thermal Decomposition of Iron(III)citrate in Presence of Glucose Leading to Iron Oxide Nanoparticles	10
PC-11	Role of A-site Cationic Ordering on Structural and Magnetic Properties of Mixed-Valent Manganites	11
PC-12	Enhanced light absorption in ultrathin CIGS solar cells using plasmonic nanoparticles	12
PC-13	Structural and magnetic properties of NiCuMgZn/SiO ₂ nanocomposites	13
PC-14	Studies on aluminium and indium co-doped ZnO thin films for gas sensing application	14

PC-15	Gamma Radiation Shielding parameters of Li ₂ O Doped Lead Vanado Tellurite Glasses.	15
PC-16	Temperature-dependent dielectric relaxation and ac-conductivity of Ca ₃ PO ₄ :Tm ³⁺ /Yb ³⁺ impedance spectroscopy	17
PC-17	Effect of Site Disorder on Structural and Magnetic Relaxation in Co ₂ Fe _{0.5} Ti _{0.5} Si Quaternary Heusler Alloy Thin Film	18
PC-18	Nitrosamine Clusters in Water Solvent: Spectroscopy and Many-body Interactions	19
PC-19	Determination of natural radioactivity in some building materials	20
PC-20	Transport Spectroscopy in a Low Phosphorous Doped Silicon Nano-Transistor	21
PC-21	Correlation between structural, static and dynamic magnetic properties in Co ₂ FeAl _{0.5} Si _{0.5} Heusler alloy thin films.	23
PC-22	Effect of oxygen partial pressure on the microwave tunability of the pulsed laser deposited Ba _{0.5} Sr _{0.5} TiO ₃ thin films	24
PC-23	Green Synthesis of Hematite Nanoparticles using Tabernaemontana Divaricata Flower Extract: Structure, Optical, Morphology and Dielectric Studies	25
PC-24	Effect of Strontium Substitution on the Structural and Magnetic Properties of Barium Hexaferrite	26
PC-25	Variation of Gilbert Damping Constant via Interface Induced Magnetic Anisotropy in LSMO/PMN-PT Heterostructures	27
PC-26	Particle-Tracking Microrheology in Yeast	28
PC-27	Effects of Gamma Irradiation on Tantalum oxide based Resistive Random access memory devices	29
PC-28	Structural properties, lattice dynamics, and metallization of van der Waals solid iodanil (C ₆ I ₄ O ₂) studied using density functional theory	30
PC-29	Interactions between active rotors studied using dual optical tweezer.	31
PC-30	Effect of gallium substitution on formation of X-ferrite phase in a mixed ferrite system and its magnetic and dielectric properties	32
PC-31	Active Material Host For Sodium-Ion Battery From Mechanically Stable Freestanding Carbon Nanotube (CNT)	33
PC-32	Radiation tolerance of modified Ferroelectric thin films for Micro-Electro-Mechanical system applications in Nuclear Industries	34
PC-33	Spray deposited iron tungstate thin film memristive device for non-volatile memory application	35
PC-34	An AFM probe of RBCs topographical structures during deformability under various physics and chemical influences.	36
PC-35	Bias and Frequency dependence of Metal/TaO _x /GaAs Capacitor	37
PC-36	Studies on the effect of Bovine serum albumin on human red blood cell membrane stiffness using an atomic force microscope	38
PC-37	Spin-filtering effect in a correlated single-molecular spintronics-transistor: Anderson-Holstein-Caldeira-Leggett-Rashba model	39
PC-38	Non-equilibrium Transport In a Bi-molecular Transistor: Effect of External Magnetic Field And Temperature	40

PC-39	Dielectric and electrocaloric properties of BCTZ composite with cobalt zinc ferrite nanoparticles	41
PC-40	Dielectric Properties and AC Conductivity of Li ₂ O Doped Zinc Borophosphate Glasses	42
PC-41	Synthesis, Characterization and STM study of Single QD Fe:CdS Rectifying Diode	43
PC-42	Study of Thermo Optics Coefficients and Thermo Polarizable Coefficients in LiNbO ₃ Open Type Optical Waveguide using Point Dipole Approximation	44
PC-43	Structural Stabilization and Optical, Electrical analysis of Al _{1-x} Ga _x O ₃ at different Ga- compositions prepared by Mechanical alloying method	45
PC-44	Temperature Dependence of Electrical conductivity of ZnO-V ₂ O ₅ -B ₂ O ₃ -MnO Glass nano composites	46
PC-45	Microwave Characterization of PVDF-TrFE-Nafion blended films	48
PC-46	Detection of milk adulteration based on principal component analysis of absorption and transmission spectra	49
PC-47	Highly Enhanced SQ Efficiency in ZnS/CdSe Core/Shell nanowire: An Ab-Initio Study	50
PC-48	Mixed-valence iron phosphate: Superhydrophilic multi-plated microflakes towards symmetric supercapacitor	51
PC-49	Electrical Transport Mechanism Studies in Borotellurite Glasses	52
PC-50	Synthesis of Self Assembled Poly (methyl Methacrylate) layers for Resistive Random Access Memory Application on Flexible Substrate	54
PC-51	The electronic and adsorption properties of tyramine neurotransmitter based on fullerene nanocage- A DFT approach	55
PC-52	Mesoporous and Phase Pure Anatase TiO ₂ Nanospheres for Enhanced Photocatalysis	56
PC-53	DFT Investigation of Adsorption of NH ₃ by Sensing Arrays of PtAs ₂ Monolayer	57
PC-54	Nontrivial Electrophoresis of Silica Nano and Microrods in a Nematic Liquid Crystal	58
PC-55	Enhanced Electrochemical and Photocatalysis Using CZTS-MWCNT Nanocomposites	59
PC-56	Indigenous Development of Laser Diffraction Setup for Characterizing the Structure of Photonic Crystals	60
PC-57	One-Step Synthesis of Bismuth Ferrite by Microwave Assisted Solvothermal Method	61
PC-58	Finite element method simulation studies on Photonic Crystal templates with and without defects with emphasis on Q-modes	62
PC-59	Rheology of lyotropic chromonic liquid crystals	63
PC-60	Power spectral analysis on colloidal suspensions of thermo-responsive poly(N-isopropyl acrylamide) PNIPAM microgels	64
PC-61	Investigation of Room Temperature Structural and Electrical properties of Ti doped CuO Nano particles	65
PC-62	Electronic structure and magnetic properties of Ruthenium based full Heusler alloy Ru ₂ CrX (X = Si, Ge)	66

PC-63	2TBA functionalized silver clusters as active SERS substrates for D-glucose detection and metering	67
PC-64	Reddish-orange emissions from Sm ³⁺ doped Sm ₂ Si ₂ O ₇ -based glass ceramics for solid-state lighting applications	68
PC-65	Lattice Dynamics of 5-ATZN predicted from first principle studies	69
PC-66	Topological study of nonsymmorphic Dirac semimetal phase in layered Matlockites ACdSb (A = Rb, Cs)	70
PC-67	Role of annealing ambience on the electrical properties of Ge MOS Capacitors with HfO ₂ /Ge ₃ N ₄ as gate dielectric	71
PC-68	Flexible PVDF-HFP based SERS active substrates with biosynthesized Au nanoparticles	72
PC-69	Enhanced photocatalytic hydrogen evolution from reduced graphene oxide-defect rich TiO _{2-x} nanocomposites	73
PC-70	Defect – Polymorphism – Controlled Electrophoretic Propulsion of Anisometric Microparticles in a Nematic Liquid Crystal	74
PC-71	Investigating The Effect Of Morphology Of Titanium Dioxide Nanostructures On The Electronic Properties Of A Diode Device	75
PC-72	Vertical distribution of natural radionuclides and health assessment in sediment samples of the northeast coast of Tamil Nadu	76
PC-73	Mineral and thermal analysis of ancient potteries of Tami Nadu	77
PC-74	Analysis of Heavy metal Contamination of sediments of Kovalam, Tamilnadu using X-ray Fluorescence Spectroscopic Technique	78
PC-75	Investigation of molecular interaction studies of ethylene glycol /sulfolane binary mixtures at different temperatures using volumetric, dielectric relaxation, and DFT methods	79
PC-76	Effect of Reaction Atmosphere on the Solid State Reaction of 1-Ferrocenyl Ethanol	80
PC-77	An Electronically Tunable Metal-Insulator-Metal (MIM) varactors with & without floating metal	81
PC-78	Aliovalent (Sr, Zr) co-doping on BiFeO ₃ for improved multiferroic characteristics	83
PH-01	Characterization of Atmospheric Aerosols at an urban site: Hyderabad	84
PH-02	Magnetic reconnection in the wakes of cosmic strings	85
PH-03	Maximal Acceleration in DFR space-time	86
PH-04	A Study of Photoionized Gas in Two HII Regions of the N44 Complex in the LMC Using MUSE Observations.	87
PH-05	Magnetic field evolution in the wakes of cosmic string.	88
PH-06	The CMS Level-1 Calorimeter Trigger for the HL-LHC	89
PH-07	Deviations from isotropic turbulence of heavy-ion collision plasma	90
PH-08	A search for dark matter in Higgs to $\tau\tau$ + ET miss final state by using p-p collision data of CMS detector at $\sqrt{s}=13\text{TeV}$	91
PH-09	Abstracts for 12th India-Japan Science and Technology seminar	92

PH-10	Neutrino Phenomenology in A4 Modular Symmetry with Type-III Seesaw and Leptogenesis	93
PH-11	Superdense star in kappa-deformed space-time	94
PH-12	3+1 sterile neutrino study of Super-ORCA	95
PH-13	Rational Extension of Quantum Theories	96
PH-14	Extracting the best physics sensitivity from T2HKK: a study on optimal detector volume at Japan and Korea	97
PH-15	Exploring astronomical PAHs in the epoch of JWST	98
PH-16	Complex dynamical properties of coupled Van der Pol-Duffing oscillators with balanced loss and gain	99
PH-17	Non-linear Schrödinger equation with time-dependent balanced loss gain and space-time modulated non-linear interaction	100
PH-18	sulfate reducing bacteria based bio	101
PH-19	Search for Dark Matter (DM) using monophoton final state data at LHC using CMS detector	102
PO-01	Resonating Photonic Nanostructures and its Applications	103
PO-02	Three photon transition in a four-level atomic system	105
PO-03	Optical switching in probe field propagation through microwave driven inverted-Y type atomic system	106
PO-04	Probe response characteristics of a twelve-level atomic system under cascade configuration	107
PO-05	Ultrafast Nonlinear Optical Switching and Sensing Response of Bimetallic Nanoparticles Produced Using Bessel Beam	108
PO-06	Understanding the Laser-Aerosol Interaction: Simulation of the Laser Beam Propagation through Optical System and Aerosol clouds	109
PO-07	Real Time Terahertz Imaging of Organic and Inorganic materials.	110
PO-08	Study of PEDOT polymer based charge transfer mechanisms for the demonstration of photons- electron interaction in the green line fluorescence spectra of plant leaves	111
PO-09	Growth and Photoluminescence Properties of α -MoO ₃ Nanoneedles	112
PO-10	Bound State of Solitons	113
PO-11	Modelling Spin-to-Orbital Angular Momentum Conversion of in Tightly-focused Circularly-polarized Light	114
PO-12	Bifurcation of complex singular points due to circular birefringence in a uniaxial crystal plate	115
PO-13	Picosecond Laser Ablated GaAs Surface Structures for Antireflective and SERS Applications	116
PO-14	A study of the spin-Hall effect of light at different incident angle	117
PO-15	Electron-atom scattering in Ultracold Plasma	118
PO-16	Unravelling the intraband ultrafast carrier dynamics in few layer MoS ₂ by probing with mid IR pulses	119

PO-17	Excited state relaxation dynamics study of IR-780 dye using home-built broadband multicolour transient absorption spectrometer	120
PO-18	Plasmonics on optical nanofibers: a versatile platform for strong light-matter interaction	121
PO-19	Compact Optical Scheme for mid-IR Spectrum Generation	122
PO-20	Z-Scan technique for measurement of nonlinear refractive index in Ag-nano particles	123
PO-21	Does Surface Roughness Affect Contact Angle?	124
PO-22	Ultrafast Pump-Probe Signal Detection using a Box-car and Lock-in Amplifier	125
PO-23	Insitu Fiber Diameter Measurement Using Whispering Gallery Modes	126
PO-24	Ladder like Laser Induced Periodic structures for SERS applications	127
PO-25	Fiber-Coupled Single Photon Source Using Optical Nanofiber Tip	128
PO-26	Near perfect ultra-broad band absorbing surfaces fabricated by ultrafast lasers	129
PO-27	Ultrashort pulse compression and pulse measurement	131
PO-28	Fabrication of Titanium nanoparticles by Picosecond Laser Irradiation of Titanium nitride Suspension in DMF solvent	132
ES-01	Applicability of Fitts' Law to the Interaction of Young Adults with Touchscreen	133
ES-02	Multi-class cancers classification using neural networks from non-invasive factors	134
ES-03	Role of Artificial Intelligence in Cyber Security: Pros and Cons	135
Chemistry		
CI-01	Additive engineering in MAPbBr ₃ single crystals for tunable high order harmonics	136
CI-02	Facile synthesis of Ni-Cr bimetallic oxide grafted with ethylenediamine for sequestration of Malachite Green from aqueous solution	137
CI-03	Dissolution of soft magnetic FeSiAl alloy cores from spent printed circuit boards and synthesis of α -Fe ₂ O ₃ nanoparticles for methylene blue dye degradation	138
CI-04	Synthesis, Structural Design and Effect of Substituents on Acylhydrazones: Evaluation of Cytotoxicity, Cytocompatibility and Hemolytic Activity: Structure-Activity Relationship Using DFT and in silico Molecular Docking Studies	139
CI-05	Synthesis and electrical properties of Nanocrystalline CuTiO ₃ for fuel cell applications	140
CO-01	A Unified Radical Sulfonylation-Cyclization of 1,6-Enynes with Sodium Sulfinates: A General Access for the Synthesis of Sulfonylated Benzofurans and its analogues	141
CO-02	Design, Synthesis, Optimization and In-vivo Validation of New Imidazopyridine Scaffold as Dual hTLR7 and hTLR9 Antagonists	142
CO-03	Target Based Design Synthesis and Development of Small Molecules for Treatment of Non-Alcoholic Fatty Liver Disease (NAFLD)	144
CO-04	A "chemical switch" to convert a TLR7 agonist into an antagonist and structural optimization leading to dual TLR7/9 antagonist relevant to psoriasis model	146
CO-05	Development of a chemical biology tool enabling reversible optical control of protein labeling: A promising new direction in photopharmacology	147
CO-06	Design, synthesis, and antimicrobial evaluation of novel 10-undecenoic acid based lipidic triazoles against plant pathogens	149

CO-07	Design, synthesis, and antimicrobial evaluation of novel 10-undecenoic acid based lipidic triazoles against plant pathogens	150
CO-08	Synthesis of Novel Indolizine Derivatives with Biological Activity	151
CO-09	Efficient Synthesis of Functionalized pyrrolo[1,2-a]quinolines and their biological profile	152
CO-10	Biodegradable-Biocompatible Renewable Amino Acid Derived Polyhydroxyurethanes	153
CO-11	Additive-Free Efficient and Regioselective Construction of Functionalised Isoxazolines from Chloro-Oxime and Boc-Anhydride	155
CO-12	Hydrogen Bond Assisted Reactivity of Ylideneketoneitriles with 1° Amines: A Chemo Selective Synthesis of 2-Pyridone and 2-Aminopyridine Derivatives.	156
CO-13	Reagent-Based Diversity-Oriented Synthesis Approach to Fused 1,4-Dihydropyrimidines, Dihydroisoxazolines, 2,3-Dihydrofurans, Substituted 4H-pyran and Cyclohexane-1,3-diones from 2-(2,2,2-trifluoro-1-aryl-ethylidene)cyclohexane-1,3-diones as Scaffold	157
CO-14	Dual Metallation in a Two-Dimensional Covalent Organic Framework for Photocatalytic C–N Cross-Coupling Reactions	158
CO-15	Enantioselective C–H bond functionalization of aromatic ketones with 1,6-enynes via photoredox/cobalt dual catalysis	159
CO-16	A Biogenic Cu ₂ O/Cu Nanocatalyst for Sonogashira and Chan-Lam Cross Coupling	160
CO-17	[DDQM][HSO ₄] Ionic liquid as a Bifunctional Catalyst for the Synthesis of 2-Phenylquinazolin-4(3H)-ones under Microwave Irradiation	161
CO-18	Mn(OAc) ₃ -Promoted Cycloannulative-Sulfonyl Migration of (E)-β-Iodovinyl Sulfones with 2-(arylethynyl)phenols for the Synthesis of Chromene Derivatives.	162
CO-19	Pd-Catalyzed Interrupted Benzofuran-Vinylation of 2-(Arylethynyl)-phenols/anilines with (E)-β-Iodovinyl Sulfones to Access 2,3-Disubstituted	163
CP-01	Insights into the Cren7 mediated structural stabilization of DNA in Crenarchaea	164
CP-02	A Minimum Energy Path Exploration of Chemical Reaction Mechanisms Through the FFoRCE Method	165
CP-03	A New Recurrent Neural Network (RNN)-Based Method for Designing Onsite Druglikeness Molecules	166
CP-04	A Rapid Deep-Learning Algorithm to Predict Systematic Growth Patterns of Atomic Clusters	167
CP-05	Feature Vector Driven Global Optimization of Molecular Cluster	168
CP-06	Base-triggerable lauryl sarcosinate-dodecyl sulfate catanionic liposomes. Structure, biophysical characterization, and drug entrapment/release studies	169
CP-07	Purification, Biophysical Characterization, Lipid Binding Properties and Chaperone-like Activity of The Major Donkey Seminal Plasma Protein, DSP-1	170
CP-08	Modeling Covid-19 transmission dynamics using diffusion based hybrid model	171
CP-09	Phase Behaviour and Supramolecular Organization of O-acyl-β-alaninols and Characterization of Equimolar Catanionic Complex	172
CP-10	De novo design of peptides as hydrolase model	173

CP-11	Effect Of Macromolecular Crowding On Lectin-Carbohydrate Interaction	174
CP-12	Study of Transport Properties of a Driven Brownian Ratchet in a Rough Periodic Potential	175
CP-13	Micromechanically-Powered Rolling Locomotion of Twisted-Crystal Optical-Waveguide-Cavity as a Mobile Light Polarization Rotor	176
CP-14	Micromanufacturing of Geometrically- and Dimensionally-Precise Molecular Single-Crystal Photonic Micro-Resonators via Focused Ion Beam Milling	177
CP-15	A Generalized Langevin Equation Approach for Barrier Crossing Dynamics in Conformational Transitions of Proteins	178
CP-16	The importance of d-metal Ion in determining the Fate of NIR emission from LnIII ions: Ligand Influence Versus Electronic Configuration	179
CP-17	Ferrous ion - Carboxylate coordination-based crosslinking in XNBR	180
CP-18	Regulating the 'Locally excited states' to facilitate spin-flip processes in efficient 'acceptor free' TADF emitters	181
CP-19	Organic Spiral waveguides for Photonic Circuit Applications	182
CP-20	ANTI-INFLAMMATORY, ANTI-CANDIDAL ACTIVITY AND INSILICO PREDICTION OF PHARMACOKINETIC PROPERTIES OF NARDOSTACHYS JATAMANSI	183
Life Science / Bioscience		
LA-01	Knockdown of Sperm associated antigen 11 A (Spag11a) enhances the susceptibility of epididymis and prostate to chemically induced carcinogenesis	184
LA-02	Bioaccumulation of heavy metals in different fishes of Gangetic river system in Varanasi and its health risk assessment	185
LA-03	Chromatin Association Dynamics Of Wip1	186
LA-04	Mechanistic Insights on Mitochondrial Transport Defects in P301L Neurons	187
LA-05	Role of hydrophobic hydration on the cold-induced denaturation of protein	188
LBC-01	Restoration of Mitochondrial Fusion Reduces Ovarian Cancer Progression by modulating AMPK/mTOR/ERK axis	189
LBC-02	Refolding and Biophysical characterization of leptospiral complementRegulator-acquiring protein A (LcpA)	190
LBC-03	Regulation of protein homeostasis via SUMOylation in Candida glabrata	191
LBC-04	Hydroxynitrile Lyase Employed Asymmetrization of Environmentally Challenging Aliphatic Aldehydes Into Value Added Chiral β -Nitroalcohols	192
LBC-05	Podocyte Derived TNF- α Mediates Monocyte Differentiation and Contributes to Glomerular Injury	193
LBC-06	Beta N-acetyl-hexosaminidase from Snake Gourd: Purification and Biochemical Characterization	194
LBC-07	Proteomic study of purified alpha-mannosidase from bitter gourd seeds: understanding possible potential application in plant glycosylation	195
LBC-08	Characterization of Lysosomal Enzymes From Hydra: An Attempt to Understand the Role of Lysosomal Enzymes During Hydra Regeneration	196

LBC-09	Characterization of cyanobacterial isocitrate dehydrogenase enzyme under the influence of citrate	197
LBC-10	Zn Tolerance Exhibited By Carbon And Nitrogen Fixation Machinery Of A Cyanobacterium Isolated From Coal Mine Wastewater: A Potential Zn Bioremediator	198
LBC-11	Toxicity of the herbicide 2,4-D on cyanobacterial CO ₂ and N ₂ fixations is mediated via molecular interaction with some vital proteins	199
LBC-12	Enzymatic And Non-Enzymatic Antioxidant Response To Cd ²⁺ Stress In A Cyanobacterium	200
LB-01	Comparative Analysis of Relative Efficacy of Synthetic and Natural Drugs in Endometriosis Through Computational Approach	201
LB-02	Metastable Intermediates During Fibril Formation of Mutant Forms α -Synuclein and Their Relation with Fibril Stability and Disease Progression	202
LB-03	An in-silico investigation on the role of Oleuropein aglycone on the aggregation propensity of α -Synuclein	203
LB-04	Effect of pY39 Post-translational modification on the interactions between α -Synuclein and Lipid Membrane	204
LB-05	Immunoinformatics Analysis of Antigenic Epitopes and Designing of a Multi-epitope Peptide Vaccine from Putative Nitro-reductases of Multi-epitope Peptide Vaccine from Putative Nitro-reductases of	205
LB-06	CHOLAR: Characterization of lncRNA from raw reads	206
LB-07	Screening Of Disease Candidates in Hepatocellular Carcinoma by Gene Ontology inferred through a Protein-Protein Interaction Graph	207
LB-08	Effect of mutations on the RBD of spike protein on its interaction with the ACE2 receptor of human host	208
LB-09	Microsatellite Based Molecular Diversity Among Selected Segregants Derived from Mahateora X Biol-212 and Berhampore Local X Mahateora In Grasspea	210
LB-10	Assessing Biochemical Descriptors Affecting Fibre Quality of Tossa Jute	211
LB-11	Differential Effect Of Dihydric Alcohols On Thermo- And Cryo-Stability Of Apomyoglobin	212
LB-12	Characterization of leishmanial arginyl synthetase for the development of novel therapeutics	213
LB-13	Advanced Glycated End-Products Activate Notch1 Signaling In Podocytes: Implications In Diabetic Nephropathy	214
LB-14	Utilization Of Tannery Solid Waste For Enzyme Induced Carbonate Precipitation Process	215
LB-15	Preferential Anti-Apoptotic and Imaging Potentials of Dual Acting Oleyl Chitosan Coated Quercetin Nanocomposite: In Vitro Perspectives	216
LB-16	Fleshings Extract As An Alternate Nitrogen Source For Production Of Industrial Enzymes	217
LB-17	Preparation and Characterization of Bioactive Composite Material for Tissue Regeneration Application	218
LB-18	Genetically Encoded Fluorescent Protein as a Sensor for Cancer Theranostics	219

LB-19	Enzyme mediated Biofuel production using nanomaterials	220
LB-20	Role of dengue virus capsid protein on mitochondrial homeostasis	221
LB-21	Designing Inhibitors Against Cathepsin Targeting HIV-1 Viral Infection	222
LB-22	Importance of Mitochondrial Electron Transport Chain in Sustaining Brassinosteroid Enhanced Photosynthesis in Arabidopsis thaliana Mesophyll Protoplasts	223
LB-23	Structural and functional attributes of Microrchidia family of chromatin remodelers	224
LB-24	iMCLAPE: A multi-class classifier for epistatic interaction	225
LB-25	GREEN ENGINEERED SILVER NANOPARTICLES OF SPONDIAS PINNATA LEAVES & ITS APPICATIONS – AN ECO-FRIENDLY APPROACH	227
MS-01	A Tendon Substitute For Orthopaedic Reconstructive Surgery - Acellular Tissue Matrix With Phyto-extract of Cuminum cyminium	228
MS-02	Treatment of Ischemic Brain Injury with optimized mesenchymal stem cells and their secretome through the intermittent hypoxic physiological environments	230
MS-03	Mobile Health (mHealth) Technology for Non-Communicable Disease Services: Enhancing the Performance of Community Health Workers.	231
MS-04	Streptozotocin-induced Animal Model as a model to study Diabetic Complications	232
MS-05	A gelatin based 3D matrix with adipose derived stem cells and exclusive ascorbic acid signalling emerged as a novel neural tissue engineering construct	234
MS-06	Synthesis Of Cysteine Graphene Oxide And Assessing Its Antimicrobial Activity.	235
MS-07	Revisiting the Effects of Ocimum sanctum Shade-Dried Leaves Powder on Body Length and Wing Length of Drosophila melanogaster	236
MS-08	New approach for Dry Eye Diagnosis: using Tear Film Lipid Layer Thickness and Meibomian Gland Loss	237
MS-09	Dimensions of access to mobile based tobacco cessation services among Municipal waste workers in Hyderabad, Telangana.	238
MS-10	Internalization of exosomes in Retinoblastoma tumor progression	240
MS-11	Ocular Surface Analyser as an emerging diagnostic modality for Dry Eye Disease and Meibomian Gland Dysfunction	242
MS-12	Application of Technology for Diagnostics Devices and Tools for Life Sciences	243
MS-13	Nanoparticles enhance infection susceptibility: a multi-parametric cellular analysis using ECIS	244
MS-14	Title- In-vitro model to study Clostridium sporogenes interaction with the gut epithelial cells.	245
MS-15	Screening the Perception of Quality of Life among Parents of Retinoblastoma(Rb) Survivors of 2-5 years of age group in Tertiary Care Eye Hospital in Hyderabad: A Crosssectional Study	246
MS-16	Mobile Based Health Interventions for Health Promotion among adults with Non-alcoholic Fatty Liver Disease.	248
MS-17	Analysis of Wing Expansion Behaviour in Rice Grasshopper Hieroglyphus banian	250
MS-18	Prevention and Control of Workplace Violence Among Health Care Professionals: Use of Technology	251

LP-01	Melatonin modulates the nitrogen metabolism and autophagy differentially under drought stress in upland cotton (<i>Gossypium hirsutum</i> L.)	252
LP-02	Functional elucidation of a Phosphorus starvation inducible Respiratory burst oxidase SIRbohH gene in the reprogramming of root system architecture.	253
LP-03	Genetic polymorphism revealed by RAPD and ISSR markers in different accessions of <i>Pterocarpus santalinus</i> L.	254
LP-04	Silencing of a ripening-associated UDP-glycosyltransferase SIUGT1 gene leads to inhibited ripening in tomato fruits	255
LP-05	Cryo-milled nano-DAP for enhanced growth of plants	256
LP-06	Insights into the chitin-active repertoire of <i>Paenibacillus</i> sp. LS1 and its implication in chitooligosaccharides production	257
LP-07	<u>Understanding[RK1] the genetic regulatory mechanism controlling PUE and PAE upon mycorrhizal colonization in tomato</u>	258
LP-08	Heterologous expression of Melon Necrotic Spot Virus recombinant Coat Protein for invitro assembly studies	259
LP-09	Insights into the chitinolytic machinery of <i>Streptomyces</i> sp. UH6	260
LP-10	Molecular cloning and characterization of a new chitinase from <i>Flavobacterium johnsoniae</i>	261
LP-11	Understanding PGPR Mediated Salt Stress Tolerance In Tomato Plants	262
LP-12	<i>Azolla</i> plants attenuate Aluminium toxicity in Rice plants, and escalate their development under acidic soil conditions	263
LP-13	Tolerance of cotton to Aluminum is regulated by GhMATE1 and overexpression of GhMATE1 intensifies acid soil tolerance of <i>Arabidopsis</i>	264

KL-01**Science with Extreme Laser Light (SELL)**G. Ravindra Kumar

Tata Institute of Fundamental Research, Colaba, Mumbai 400 005

e-address: grk@tifr.res.inWebpage: www.tifr.res.in/uphill

Stars and their violent explosions in the sky and volcanoes erupting from deep within cells (ASCs), the earth are ready testimonies to the fact that the universe is predominantly hot and dense. In recent times, such extreme states containing high energy density have been studied in the laboratory focusing ‘extreme light’ namely, high peak power, ultrashort pulsed laser light, to micron spatial scales. As laser technology marches on inexorably to higher powers, we can expect to simulate such matter better in lab experiments and learn more about the complex interactions and dynamics. At the same time, we can exploit the rich emissions of high energy photons and material particles from such matter to fashion novel, tabletop sources of radiation for a variety of applications in science, technology and medicine [1 and the references therein].

This talk will attempt to describe in a broad perspective, some of the science and applications of dense, hot matter, with reference to the research at TIFR – creation of gigantic magnetic pulses (100s of megagauss), ultrafast plasma dynamics, passage of relativistic electrons through dense, hot matter and its consequences in terms of MeV ion production, ultrafast hard x-ray emission etc.²⁻⁸.

Gerard Mourou and Donna Strickland won half the Nobel prize in physics in 2018 for the invention of chirped pulse amplification that made ultrahigh power laser, femtosecond laser pulses. The most powerful, ultrashort pulse laser emitting 10 petawatt, 25 femtosecond pulses was inaugurated in Nov 2020 at the ‘Extreme Light Infrastructure- Nuclear Physics’ in Romania]

References:

1. S.V. Bulanov et al., Plasma Physics Reports, 2015, 41, 1
2. G. Chatterjee et al., Phys. Rev. Lett. 2012, 108, 235005
3. M. Shaikh et al., Phys. Rev. Lett. 2018,120, 065001
4. S. Mondal et al., Proc. Natl. Acad. Sci. (USA) 2012, 109, 8011
5. S. Mondal et al., Phys. Rev. Lett. 2010, 105, 105002
6. A. Adak et al., Phys. Rev.Lett. 2015, 114, 115001
7. K. Jana et al., Phys. Rev. Res. 2021, 3, 033034
8. G. Chatterjee et al., Nat. Commun. 2017, 8,15970; A. Das et al., Phys. Rev. Res. 2020, 3, 033405

KL-02**Where am I from? Where are you going?**Ryoji Noyori^{a,b}^a Nagoya University, Department of Chemistry and Research Center for Material Science, Chikusa, Nagoya 464-8602, Japan^b Japan Science and Technology Agency (JST), Center for Research and Development Strategy (CRDS), Chiyoda, Tokyo 102-0076, Japan,e-address: noyori@chem3.chem.nagoya-u.ac.jp, noyori@jst.go.jp

Scientific research is a never-ending “journey of knowledge”. There is more meaning in experiencing various encounters and making a good journey itself than reaching the destination. I have myself travelled to some extent on this journey. In 1960s, I began my particular brand of chemistry research in what was at the time an impoverished hinterland of the world. Still, I was able to proceed, thanks to the guidance of many people, and eventually attain a degree of worldwide recognition. I was patient, diligent, and hardworking. Most importantly, I fully enjoyed academic freedom without any kind of outside pressure or restriction. This is a very key for promoting academic research.

In today’s civilized society, we have been blessed with a range of innovations which are founded upon scientific principles and superb technologies. The benefits are crystal clear. A bright light also casts a dark shadow, however. Society is now riddled with contradictions, and science and technology are no exception. On the one hand, we highly value science-based technologies, but on the other, we are wary of their consequences. Uncontrolled and excessive human activities are triggering drastic climate fluctuations and environmental changes, depleting resources and energy, widening economic disparity, and leading our human society to a crisis situation.

These are all problems that we have created, but no one is willing to take responsibility for resolving these problems. New generations are asked to make full use of scientific knowledge and technology of the highest standard to find solutions. The 20th century was an era of international competition, symbolized by war and economic rivalry. In the 21st century, however, we will have to cooperate globally for the survival of our species with the limits of this planet.

IL-01**Mechanophotonics & Crystal-photonics Foundry: All-Organic, Single-Crystal, Photonic Integrated Circuits**

Rajadurai Chandrasekar

Advanced Organic Photonic Materials and Technology Laboratory School of Chemistry, University of Hyderabad, Hyderabad – 500046, INDIA

e-address: r.chandrasekar@uohyd.ac.inWebpage: / <https://www.rajaduraichandrasekar.com/>

Recently, nano/micro organic solids have emerged as promising materials for producing miniaturized organic photonic components, such as optical waveguides (active/passive), lasers, resonators (including chiral ones), filters, and modulators suitable for constructing organic photonic integrated circuits (OPICs).^{1,2} Miniature crystal (rigid/flexible) optical waveguides³⁻⁸ are useful for controlling and manipulating light propagation down to microscale. In optical resonators, their mirror-like geometry allows them to trap photons tightly by repeated total internal reflection at the air-matter interface and produce multimodal optical emissions. Low-optical-loss (high Q) resonators are good optical gain media, therefore potential elements for microlasers. Selective reabsorbance of broad-band optical emission in microcrystal waveguides lessens the bandwidth of the propagating light signal producing a long-pass filter effect. We have shown that atomic force microscopy (AFM) is an effective technique to mechanically micromanipulate miniature organic photonic components towards OPICs - an approach that we named Mechanophotonics. I will introduce examples of miniature organic photonic components in my talk. I will also discuss the construction of OPICs with active, passive, and energy-transfer attributes using mechanophotonics. The fabricated OPICs switch, split, direct, and filter optical signals useful for signal enhancement, sensing, information processing and switchable photonic device applications.^{9,10} If time permits, I will discuss about Crystal-photonics foundry a new discipline developed in our group to shape organic crystals into various photonic geometries via FIB milling.¹¹

Keywords:

Mechanophotonics, Organic Photonic Integrated Circuits, Crystal-photonics foundry

References:

1. R. Chandrasekar, Chem. Commun. 2022, 58, 3415-3428.
2. R. Chandrasekar, Small, 2021, 17, 2100277.
3. R. Chandrasekar et al. Adv. Opt. Mater. 2020, 8, 2000959.
4. R. Chandrasekar, Phys. Chem. Chem. Phys. 2014, 16, 7173
5. R. Chandrasekar et al. Adv. Opt. Mater. 2018, 6, 1800343.
6. D. Venkatakrishna et al. Adv. Mater. 2017, 29, 1605260.
7. P. Hui et al. Adv. Mater. 2013, 25, 2963.
8. N. Chandrasekar, et al. Angew. Chem. Int. Ed. 2012, 51, 3556.
9. M. Annadhasan et al. Angew. Chem. Int. Ed. 2020, 59, 13852-1385; (ii) Angew. Chem. Int. Ed. 2020, 59, 13821-13830S.
10. J. Ravi et al, Adv. Funct. Mater. 2021, 31, 2105415 and Adv. Funct. Mater. 2021, 31, 2100642.
11. V.V. Pradeep and R. Chandrasekar, Indian Patent Application, TEMP/E-1/18625/2022-CHE; arXiv:2203.14218v1 [physics.optics; Adv. Opt. Mater, 2022, <https://doi.org/10.1002/>

IL-02**Simultaneous Doping and Un-zipping of Carbon Nanotubes at Room-temperature in Different Electrolytes**Vijayamohanan K Pillai

IISER Tirupati

e-address: vijay@iisertirupati.ac.in

Carbon nanotubes can be transformed into graphene nano-ribbons (GNRs) or Graphene quantum Dots (GQDs) by an electrochemical approaches at room temperature in different environment. For example, when an superacid like trifluoromethane sulfonic acid is used an electrolyte fluorinated graphene nanoribbons are formed while nonaqueous electrolytes like acetonitrile or dichloromethane gives doped graphene quantum Dots. This lecture deals with strategies involving longitudinal unzipping of carbon nanotubes (oxidation) in various aqueous and nonaqueous electrolytes, super acids, ionic liquids, to produce oxygen functionalities and their subsequent reduction to form GNRs and GQDs. The application of electric field at room temperature results in the unzipping of carbon nanotubes with concomitant functionalization and Doping. Potential applications of fluorinated GNRs(F-GNRs) include electrocatalysis, biosensing, Li- Batteries, and solar energy conversion.

IL-03

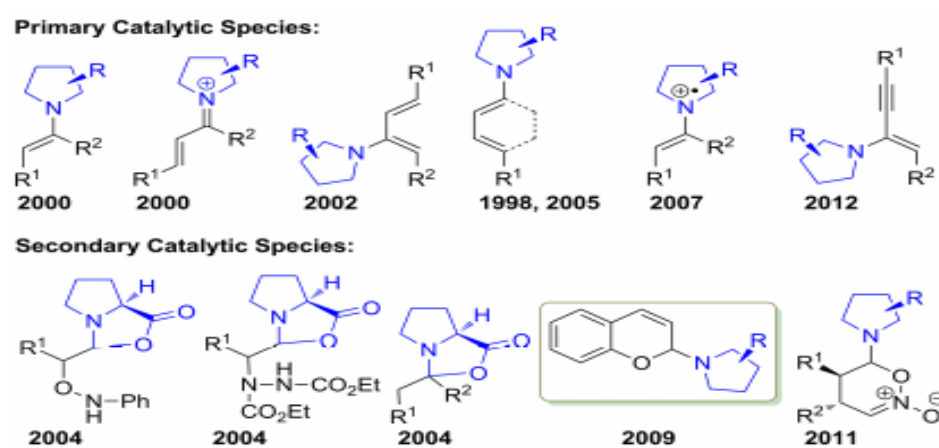
Discovery of Sustainable Organocatalytic Reactions: Expansion of Substrate/Catalysts Scope

Dhevalapally B. Ramachary

FTAS, FRSC, FASc, FNASc Catalysis Laboratory, School of Chemistry, University of Hyderabad Prof. CR Rao Road, Gachibowli, Hyderabad-500 046

e-address: ramsc@uohyd.ac.in, ramchary.db@gmail.comWebpage: <http://chemistry.uohyd.ac.in/dbr/index.htm>

The discovery of in situ generated novel reactive primary catalytic species like enamines, iminium ions, dienamines, trienamines and aminoenynes from the reaction of variety of carbonyls with catalytic amount of chiral primary- or secondary amines or amino acids will be discussed. Their direct applications in a variety of selective green bond formations to furnish the chiral functionalized molecules, drugs, drug-like molecules, natural products, and pharmaceuticals will be discussed¹⁻⁹.



References:

1. C. F. Barbas III, *Angew. Chem. Int. Ed.* 2008, 47, 42-47.
2. D. W. C. MacMillan, *Nature* 2008, 455, 304-308.
3. S. Mukherjee, J. W. Yang, S. Hoffmann, B. List, *Chem. Rev.* 2007, 107, 5471-5569.
4. A. G. Doyle, E. N. Jacobsen, *Chem. Rev.* 2007, 107, 5713-5743.
5. B. S. Donslund, T. K. Johansen, P. H. Poulsen, K. S. Halskov, K. A. Jørgensen, *Angew. Chem. Int. Ed.* 2015, 54, 13860-13874.
6. D. Enders, O. Niemeier, A. Henseler, *Chem. Rev.* 2007, 107, 5606-5655.
7. Y. Hayashi, *Chem. Sci.* 2016, 7, 866-880.
8. D. B. Ramachary, M. A. Pasha, G. Thirupathi, *Angew. Chem. Int. Ed.* 2017, 56, 12930-12934.
9. M. Raj, V. K. Singh, *Chem. Commun.* 2009, 6687-6703.

IL-04**Adaptive Soft Molecular Crystals: From Bending to Self-Healing**

C Malla Reddy

Department of Chemical Sciences, Indian Institute of Science Education and Research (IISER) Kolkata, Mohanpur 741 246, India
e-address: cmreddy@iiserkol.ac.in, cmallareddy@gmail.com

High crystallinity, although desired in materials for a wide range of high-performance engineering applications, generally it comes with undesirable attributes such as high brittleness and fragility¹. This makes crystalline materials incompatible with many future technologies, such as flexible devices and soft-robotics. Recent progress in crystal engineering has brought into light many possible opportunities to address these issues, enabling the design of adaptive crystalline materials that respond to external stimuli with exceptional qualities.¹⁻⁷ For instance, crystals that bend (elastically or plastically), twist, curl, wind, jump, exfoliate, laminate, and explode, under external stresses, such as mechanical stress, pressure, light, heat, solvent, etc., have been shown. On the other hand, until very recent times, self-healing was observed only in soft and amorphous materials, mostly involving approaches that use chemical reactions, diffusion, solvent, vapour, electricity, etc., with typical healing time scales in minutes to weeks⁸. A new self-healing mechanism that we recently introduced⁹ in materials science, enables ultra-fast, near 100% autonomous diffusion-less repair in crystalline materials that uses electrostatic surface potentials generated on the freshly created fracture surfaces, inherent to certain types of non-centrosymmetric single crystals. My talk will cover structure-property correlation for crystal engineering of adaptive soft crystals.

References:

1. Saha, S., Mishra, M. K., Reddy, C. M. & Desiraju, G. R. (2018) *Acc. Chem. Res.* 51, 2957.
2. Reddy, C. M., Gundakaram, R. C., Basavoju, S., Kirchner, M. T., Padmanabhan, K. A. & Desiraju, G. R. (2005), *Chem. Commun.* 3945.
3. Ghosh, S. & Reddy, C. M. (2012) *Angew. Chem. Int. Ed.*, 51, 10319.
4. Krishna. G. R., Devarapalli, R., Lal, G. & Reddy, C. M. (2016) *J. Am. Chem. Soc.*, 138, 13561.
5. Naumov, P., Chizhik, S., Panda, M. K., Nath, N. K. & Boldyreva, E. (2015) *Chem. Rev.*, 115, 12440.
6. Mondal, A., Bhattacharya, B., Das, S., Bhunia, S., Chowdhury, R., Dey, S. & Reddy, C. M. (2020) *Angew. Chem. Int. Ed.* 59 ,10971.
7. Takamizawa, S. & Miyamoto, Y. (2014) *Angew. Chem. Int. Ed.* 53, 6970.
8. Yanagisawa, Y., Nan, Y., Okuro, K. & Aida, T. (2018) *Science*, 359, 72.
9. Bhunia, S., Chandel, S., Karan, S. K., Dey, S., Tiwary, A., Das, S., Kumar, N., Chowdhury, R., Mondal, S., Ghosh, S., Mondal, A., Khatua, B. B., Ghosh, N & Reddy, C. M. (2021), *Science*, 373, Issue 6552, pp. 321-327.

IL-05**The cell-penetrating peptide penetratin prevents neurodegeneration in mice models of Parkinson's disease.**

Deepak Kumar Sharma
Principal Scientist, CSIR-IMTECH

Parkinson's disease (PD) is the second most common neurodegenerative disorder. The accumulation of Lewy bodies, composed primarily of α -synuclein (α -syn) aggregates, in the substantia nigra region of brain is a characteristic feature of Parkinson's disease (PD). We screened numerous peptides and discovered that penetratin is a potent inhibitor of α -syn aggregation. Similar to penetratin, its cyclic derivative also prevented α -syn aggregation, enhanced worm motility, and restored dopamine signaling in the *C.elegans* model. Penetratin treatment improved locomotor coordination and halted disease progression in mice models of PD. Overall, this study identifies a potential therapeutic agent for the treatment of PD.

IL-06**Nitric oxide signaling in plants and its role in plant tolerance to low oxygen stress**

Kapuganti Jagadis Gupta

National Institute of Plant Genome Research, Aruna Asaf Ali Marg, 110067, New Delhi, India

e-address: jgk@nipgrac.in

The free radical nitric oxide (NO) emerged as an important signal molecule in plants. Various reductive, oxidative pathways operative for NO biosynthesis. The reductive pathway utilizes nitrite as substrate, which is exclusively produced by cytosolic nitrate reductase (NR) and mitochondria. Using plant mitochondria, we show that nitrite reduction to NO is strongly increased with the decrease in oxygen, which is a general consequence under flooding stress. The reaction is linked to ATP synthesis under hypoxia. NO diffuses from the mitochondria to the cytosol where it is scavenged to nitrate by the non-symbiotic haemoglobins. I will present experimental data supporting these reactions and showing that under low oxygen, the plant mitochondrion serves as a nitrite: NO reductase and becomes a major component in the anoxic nitrogen cycling where it directly contributes to a decrease of cell reduction level and to a limited ATP synthesis. We also found that NO inhibits aconitase protein levels and its activity that leads to increases in citrate levels which then act as a potent inducer of AOX pathway. The NO production, inhibition of aconitase, and induction of AOX protein and activity leads to a shift of plant metabolism towards amino acid biosynthesis. Mitochondrial NO also play role in signalling via protein S nitrosylation. Mitochondrial produced NO also play role stabilisation of supercomplexes. Under normoxic conditions NO regulates respiration, internal oxygen, carbohydrate utilization, and ROS levels in roots. We show that a decrease in NO, leads to a drop in internal oxygen, an increase in glucose consumption, further elevation of ROS in chickpea. Thus, NO is required for maintaining steady-state oxygen concentrations and to keep ROS low. In deepwater rice NO plays a role in enhancing energy metabolism and submergence tolerance.

IL-07**Calcium dynamics: a critical regulator of human skin pigmentation**

Dr. Rajender K Motiani

Assistant Professor and DBT/Wellcome Trust Intermediate Fellow Regional Centre for Biotechnology, Faridabad

Skin pigmentation plays a vital role in protection against harmful ultraviolet (UV) rays. Indeed, tanning is a protective response of the melanocytes for guarding skin from UV induced cancers. Perturbations in pigmentation pathways result in pigmentary disorders like solar lentigo, melasma, and vitiligo. Further, inefficient pigmentation can lead to skin cancers that are one of the leading causes of cancer-associated deaths. To identify novel regulators of human pigmentation, we performed microarrays on hyperpigmented and hypopigmented primary human melanocytes and observed significant changes in Ca^{2+} homeostasis genes in differentially pigmented cells. The expression profile of several key Ca^{2+} handling proteins vary between hyperpigmented and hypopigmented human melanocytes (Motiani et al., EMBO J, 2018). We then performed in-depth functional assays and in vivo zebrafish studies, which established an ER Ca^{2+} sensor STIM1 (Stromal Interaction Molecule 1) as a novel regulator of pigmentation (Motiani et al., EMBO J, 2018). An interesting observation of this study was that STIM1 expression augments in melanocytes while they pigment. In our more recent work, we have delineated the molecular mechanism that drives STIM1 expression in pigmenting melanocytes (Motiani and colleagues, JBC, 2022, under minor revision). We demonstrated that physiological melanogenic stimuli αMSH increases STIM1 mRNA and protein levels. Further, αMSH stimulates STIM1 promoter driven luciferase activity thereby suggesting transcriptional upregulation of STIM1. We show that downstream of αMSH , MITF transcription factor drives STIM1 expression and activity. Next, we conducted extensive bioinformatics analysis and identified MITF binding sites on the STIM1 promoter. We validated significance of the MITF binding sites in controlling STIM1 expression by performing CHIP and luciferase assays with truncated STIM1 promoters. Importantly, analysis of publicly available datasets substantiated a positive correlation between STIM1 and MITF expression in sun-exposed tanned human skin thereby highlighting physiological relevance of this regulation. Taken together, we have identified that cellular Ca^{2+} dynamics plays a critical role in regulating human skin pigmentation.

IL-08**Gels and their Applications**Kana M. SureshanSchool of Chemistry, Indian Institute of Science Education and Research Thiruvananthapuram, Maruthamala,
Thiruvananthapuram-695551, India.e-address: kms@iisertvm.ac.in

Gels are attractive materials that find application in many areas. Based on the size of the gelators, they are classified as polymeric gelators and Low molecular Weight gelators (LMWG). Based on the nature of solvent, the gels are divided into organogels and hydrogel. LMWGs are especially attractive as the gels formed by them are reversible. The reversibility, order and the weak linkage of LMWGs are often advantageous for several applications. Exploiting these features, we have developed a few organogels and demonstrated their application in soft optics, oil spill recovery, CO₂ absorption, deionization of water etc. In some cases the gels were used as such, in some cases we have transcribed the fragile gel structure to more robust polymers and in some case we have used a blend with covalent polymers¹⁻¹⁶. In this talk, I will be giving glimpse of our work on these areas.

References:

1. C. Raju, L. A. Mathew, K. M. Sureshan, *Adv. Sust. Sys.* 2022, 6, 2100521
2. R. Rai, K. M. Sureshan, *Angew. Chem. Int. Ed.*, 2022, 61, e202111623
3. R. Mohanrao, H. Kuntrapakam, K. M. Sureshan, *ACS Appl. Polym. Mater.* 2020, 2, 4985-4992.
4. A. M. Vibhute, K. M. Sureshan, *ChemSusChem* 2020, 13, 5343-5360.
5. A. Prathap, A. Ravi, J. R. Pathan, K. M. Sureshan, *CrystEngComm* 2019, 21, 5310-5316.
6. A. Prathap, C. Raju, K. M. Sureshan, *ACS Appl. Mater. Interfaces* 2018, 10, 15183.
7. A. Prathap, K. M. Sureshan, *Angew. Chem. Int. Ed.* 2017, 56, 9405-9409.
8. B. P. Krishnan, K. M. Sureshan, *J. Am. Chem. Soc.*, 2017, 139, 1584-1589.
9. B. P. Krishnan, S. Raghu, S. Mukherjee and K. M. Sureshan, *Chem. Commun.*, 2016, 52, 14089-14092.
10. A. M. Vibhute, V. Muvvala, K. M. Sureshan, *Angew. Chem. Int. Ed.* 2016, 55, 7782-7785.
11. A. Prathap, M. M. Shaijumon, K. M. Sureshan, *Chem. Commun.*, 2016, 52, 1342-1345.
12. B. P. Krishnan, S. Mukherjee, P. M. Aneesh, M. A. G. Namboothiry, K. M. Sureshan, *Angew. Chem. Int. Ed.* 2016, 55, 2345-2349.
13. A. Vidyasagar, K. M. Sureshan, *Angew. Chem. Int. Ed.* 2015, 54, 12078-12082.
14. B. P. Krishnan, S. Ramakrishnan, K. M. Sureshan, *Chem. Commun.* 2013, 49, 1494-1496.
15. A. Prathap, K. M. Sureshan, *Chem. Commun.* 2012, 48, 5250-5252.
16. A. Vidyasagar, K. Handore, K. M. Sureshan, *Angew. Chem. Int. Ed.* 2011, 50, 8021-8024.

IL-09**Solution Processed High Performance Devices: Solar Cells and Photoelectrochromic Devices and Photo-supercapacitors**

Melepurath Deepa , Ankita Kolay, Debanjan Maity, Aparajita Das
Department of Chemistry, IIT Hyderabad

The power conversion efficiency of solution processed liquid junction solar cells has over the recent years reached about 16%. In view of the advanced level of research on identifying suitable approaches which are effective in enhancing solar cell performances, concerted efforts are being devoted to engineering electrodes for either panchromatic absorption and conversion of solar radiation or for a self-powered- smart window (photoelectrochromic device, PECVD) or supercapacitor (photosupercapacitor, PSC), while being easy-to-fabricate at a low cost. By replacing the traditional counter electrode (CE) with a photosensitive cathode and by use of electron or hole conducting and/or light harvesting nanostructures, plasmonic metal nanoparticles etc at the anode and/or cathode, high power conversion efficiencies (PCEs) can be achieved. Furthermore, by using electrochromic materials or by using energy storage materials in the photovoltaic devices, dual function devices which can convert/save energy or convert/store energy can be developed. Such devices have In this talk, I will focus on how by the use of the above-mentioned strategies, high performance solar cells, PECVDs and PSCs can be developed by using easy-to-implement processing methods.

IL-10**Low-Carbon and Green Hydrogen Production Through a Biorefinery Approach**

Dr. S Venkata Mohan, Ankita Kolay, Debanjan Maity, Aparajita Das

Bioengineering and Environmental Sciences Lab, Department of Energy and Environmental Engineering, CSIR-Indian Institute of Chemical Technology (CSIR-IICT), Hyderabad-500 007, India

e-address: svmohan@iict.res.in, vmohan_s@yahoo.com

Renewable/Green hydrogen (H₂) production is now being considered a sustainable alternative. The dark-fermentation/acidogenic process is one of the key processes that can produce a significant amount of H₂ production by using wastewater, agri-biomass and biodegradable waste as feedstock. Integration of dark-fermentation with other processes (mostly biological) showed promise in maximizing resource recovery by putting back the unutilized carbon into the ecological loop with a biorefinery approach. Acidogenesis as a versatile process that has the potential to play an important role in biorefineries for the transformation of waste into primary fermented products viz., fatty acids and hydrogen, which can be further converted to platform chemicals and fuels. Integration with anaerobic digestion for CH₄ production or hybrid process towards biohythane (H₂ compressed natural gas, H-CNG) production is feasible to influx into the existing infrastructure. This communication will discuss the research being carried out at CSIR-IICT on H₂ production employing a closed-loop design with a multi-product portfolio.

IL-11**“Lamins - mechanoprotector of the nucleus”**

Kundan Sengupta,

Chromosome Biology Lab (CBL), IISER PUNE

It is well established that the nucleus is protected by an intricate organization of proteins involving the LINC (linker to nucleoskeleton and cytoskeleton) complex along with the type V intermediate filament proteins - lamins. Nuclear lamins are primarily of 3 types - Lamin A/C, B1 and B2, which provide structural and mechanical integrity to the nucleus. Here, we have examined the remarkable roles of lamins in the mechanoprotection of the nucleus. We uncovered that lamin loss not only alters nuclear shapes but also induces chromosomal aneuploidies (extra chromosomes) in cancer cells accompanied by altered spatial localization of chromosomal territories and transcriptional deregulation. Remarkably, loss of lamin A/C induces a transcriptional feedback response in Emerin - a LINC complex protein, along with a remarkable reorganization of actin and Nuclear Myosin I (NMI). Furthermore, Emerin - an interacting partner of lamins, transduces extraneous mechanical signals into the nucleus regulating the organization and function of chromosome territories in the interphase nucleus.

IL-12**Investigating order in chaos: Unraveling emergent mechanisms that cumulatively dictate aging and emergence of diseases**

Ullas Kolthur-Seetharam
DBS-TIFR and TIFRH

Accelerated aging and emergence of non-communicable diseases is a major cause of concern. While lifestyle and specifically dietary/metabolic inputs are known to drive these, molecular mechanisms that govern emergent properties of the system are far less understood. We are interested in unraveling molecular mechanisms that link metabolic or dietary inputs to cellular and organismal physiology with a specific emphasis on components that couple and regulate plasticity. Our research has provided a comprehensive systems level understanding of the pathways involved in metabolic-sensing and their role in metabolic and energy homeostasis at molecular, cellular and organismal levels with implications on aging, diabetes and obesity.

Investigating or identifying rules of engagement that dictate emergence of phenotypes and encompass the myriad components that make up living systems is tantalizing. Based on close to a decade's work (in our group), we are now trying to dissect out emergent properties of molecular components that dictate physiological homeostasis, which is essentially a culmination of both evolutionary history of the species and life history of the individual organism. This is exciting since metabolism is one of the biggest contributors of noise or randomness. Moreover, given the dynamic oscillation of metabolic/energetic status in all living beings, it is still unclear how response thresholds, information gating and fidelity of state reversals are achieved. Our recent work has led us to propose how molecular/metabolic oscillations (amplitudes and frequencies), which are often masked in noise, could lead to a cumulative and long-lasting consequence on phenotypes.

IL-13**Mapping Interaction Network of Human Phosphatases**

Maddika Subba Reddy

Laboratory of Cell Death & Cell Survival, Centre for DNA Fingerprinting and Diagnostics (CDFD), Hyderabad, INDIA

Phosphatases play a crucial role in biological functions and controls nearly every cellular process, including metabolism, gene transcription, translation, cell-cycle progression, protein stability, signal transduction, and apoptosis. However, the functional map of all human phosphatases and their interactome is not fully available. By using a biochemical purification followed by proteomic analysis, our lab has established the interaction network of nearly every human protein phosphatase in the cell. We found phosphatases associated with the components of varied cellular processes. Our work on some of the new functional phosphatase interactions would be discussed.

IL-14**Golgi localized small G-protein regulates cell adhesion**

Subba Rao Gangi Setty
Indian Institute of Science, Bangalore, India

Small GTPases of Arf-like (Arl) proteins regulate membrane trafficking, cytoskeleton reorganization, cell signalling and migration. Arl family consists of 21 known GTPases in which the molecular function of Arl15 is poorly defined. Genetic studies predicted a role for Arl15 in type-2 diabetes, insulin resistance, adiposity, and rheumatoid arthritis. Recent studies showed that Arl15 regulates magnesium homeostasis and insulin/TGF β signaling. Here, we have evaluated the role of Arl15 in vesicular transport using techniques to quantify cargo trafficking to mechanobiology. Fluorescence microscopy of stably expressing Arl15-GFP HeLa cells showed its localization to the Golgi and cell surface, including filopodia, and a cohort to recycling endosomes. The association of Arl15 to the membrane is independent of cytoskeletal assembly but depends on the Golgi integrity or Arf1 activation. Extensive mutagenesis analysis identified a novel V80A mutation in the GTP-binding domain that turns Arl15 into a dominant-negative form with a reduced number of filopodia. Depletion of Arl15 in HeLa cells displayed a reduced number of filopodia and mislocalization of cargo with altered endocytosis kinetics. Knockdown of Arl15 decreased cell migration and enhanced cell spreading and adhesion strength. Traction force microscopy experiments revealed that Arl15 depleted cells exert higher tractions and generate multiple focal adhesion points during the initial phase of cell adhesion compared to control cells. Collectively, these studies demonstrated a functional role for Arl15 in the Golgi, which includes regulating cargo transport to organize membrane domains at the cell surface.

IL-15**Quantitative Phase Microscopy for Clinical Diagnosis**

Renu John, Aswathy Vijay, Vikas Thapa, Ashwini S. Galande

Medical Optics and Sensors Laboratory, Department of Biomedical Engineering Indian Institute of Technology Hyderabad

Sangareddy, Telangana 502 284

e-address: renujohn@bme.iith.ac.in

Traditionally, Microscope has been one of the indispensable tools in clinical diagnostics in analyzing biological samples, cells and tissues. Biological samples like cells are Phase only objects which are sensitive to the phase of the light and therefore it's hard to visualize them under a conventional microscope with high contrast. Various techniques such as staining, fluorescence, phase contrast, and differential interference contrast has been in practice to visualize phase objects under a conventional microscope. However quantitative phase information and depth and surface morphology of biological cells and samples seems to be very important in arriving at diagnostic decisions. In recent decades, researchers have come up with a wide variety of techniques to quantify the depth and phase information in biological cells using Quantitative phase imaging (QPI) techniques. The QPI is a label-free technique that quantifies phase delay introduced by the sample [5-8] hence aiding the disease diagnosis with better accuracy. Quantitative phase microscopy has enabled researchers to quantify sub-cellular information precisely avoiding toxic dyes and laborious staining protocols. The last decade witnessed the evolution of artificial intelligence (AI) and its increasing applications in medicine including clinical treatment, diagnosis, and monitoring of diseases. The impact of AI in imaging led to its utilization in quantitative phase imaging (QPI) and microscopy (QPM) applications. This talk is intended to provide a critical overview of various methods of AI in processing QPM data such as classification, segmentation, and phase reconstruction for various medical applications. Special focus has been given to the research developments carried out in QPM at the Medical Optics and Sensors laboratory at IIT Hyderabad. We discuss a number of portable and affordable low cost quantitative microscopes and its applications in clinical imaging.

IL-16**Structure and dynamics of photosystem I supercomplex in the green alga *Chlamydomonas reinhardtii***Yuichiro TakahashiResearch Institute for Interdisciplinary Science, Okayama University
e-address: taka@cc.okayama-u.ac.jp

Oxygenic photosynthesis by plants, algae, and cyanobacteria is a complicated process that converts CO₂ and H₂O into carbohydrates using light energy. The initial step of photosynthesis is to absorb light by photosynthetic pigments in light-harvesting complexes (LHCs). The resulting excited energy is converted into redox energy in the reaction center (RC) of two photosystems (PSI and PSII). PSI complex associates with peripheral light-harvesting complexes (LHCIs) to form the PSI-LHCI supercomplex. This supercomplex generates strong reductants to reduce NADP⁺ using light energy.

The green alga *Chlamydomonas reinhardtii* is an excellent model organism for photosynthesis research because this unicellular alga is amenable to biochemical and molecular biological approaches. We determined that this algal PSI-LHCI supercomplex associates with ten copies of LHCI, which is 2.5-fold larger than that from plants¹. This result suggests that *C. reinhardtii* can grow efficiently under low light conditions. It has also been determined that the supercomplex consists of 22 protein subunits and 291 pigments, as well as three Fe-S clusters and two naphthoquinones².

It is intriguing to address how the PSI-LHCI supercomplex is synthesized in vivo. Analyzing the molecular mechanism has not been easy because the assembly includes multi-step processes and proceeds rapidly. Thus, we focused on factors assisting the assembly by characterizing mutants in which the assembly of the PSI complex is specifically compromised. So far, we have identified two chloroplast-encoded factors, Ycf3 and Ycf4^{3,4}, and three nucleus-encoded proteins, Y3IP1, CGL71/Ycf37/PYG7, and Alb3.1³⁻⁵, are directly or indirectly involved in the assembly of PSI-LHCI supercomplex. A working model for the PSI-LHCI supercomplex assembly process will be presented and discussed.

References:

1. Plant Physiol. 178 (2018) 583-595
2. Nature Plants 5 (2019) 626-636
3. The EMBO J. 16 (1997) 6095-6104
4. The Plant J. (2021)
5. Plant Cell Physiol. 63 (2022) 70-81.

IL-17**A mechanism and impact of translocal learning: A trial of international educational exchange program between India and Japan**Aki YONEHARAPh.D. Toyo University/ Indian Institute of Technology Delhi
e-address: yonehara@toyo.jp

This research is being developed based on the 2021 International Exchange Program for Primary and Secondary School Teachers of Asia-pacific Cultural Center for UNESCO (ACCU). ACCU has started this bilateral Program since 2000, and its fundamental goal is to “provide educators with a learning opportunity through international exchange and accelerate transformation of their values and behaviours” (ACCU 2020: 9). As one of possible ways to strengthen this goal, a concept of “translocal learning (TL)” (Kudo et al. 2020) was experimentally introduced into the 2021 Exchange Program between India and Japan. The purpose of this study is to analyze how the Program developed TL among the participants. Firstly, this paper introduces a concept of TL; secondly, overviews the process of program development; thirdly, explains the methods of data collection and analyses; and finally, shares the results of analyses with discussion.

Data was collected through the online pre-post surveys and one follow-up event, which was conducted a month after the Program. Likert-scaling data from the surveys were statistically analyzed, and the open-ended question and the transcript of the focus-group discussion at the follow-up event were analyzed through text-mining and contents analyses. The key findings from these analyses are as follows:

- Knowledge and interest in partner countries were statistically significantly increased after the Program.
- Teachers’ vocabulary and thoughts on some key concepts (e.g. what is a significant factor to be a “good” teacher?) became richer and substantively transformed, according to text-mining.
- From the content analyses of Indian and Japanese teachers’ focus-group discussion, the process of TL and the three stages of transformative change were observed as followed by three major codes: Code_1 Direct learning, Code_2 Reflective review, and Code_3 Translocal learning.

IL-18**Global economy and economics**Eri Ikeda

Where is the global economy heading now? Will there be a recession or recovery from COVID-19 ? This talk discusses how different schools of economics approach understanding the current state and future direction of the economy, and what would be the implication for India and Indian businesses.

IL-19**Structured light fields revolutionize materials science**Takashige Omatsu ^{a,b}^aGraduate School of Engineering, Chiba University, 1-33, Yayoi-cho, Inage-ku, Chiba, 263-8522, Japan^b Molecular chirality research center, Chiba University, 1-33, Yayoi-cho, Inage-ku, Chiba, 263-8522, Japan
e-address: omatsu@faculty.chiba-u.jp

Structured light beams with a helical wavefront, that is optical vortices¹, carry unique physical properties, including an annular spatial form, and an orbital angular momentum, and they provide us many new fundamental light-matter interactions and advanced technologies, beyond the conventional optical manipulations, and optical/quantum telecommunications. In recent years, we and our-coworkers have discovered that optical vortices twist a variety of materials (metal, silicon, polymer) to shape helical structures on a nano/micron-scale, such as helical needles, helical surface reliefs, and helical fibers, owing to orbital angular momentum transfer effects^{2,3,4}. These helical structures should enable the development of new generation metasurfaces and plasmonic/photonic crystals with the freedom of the chirality. Furthermore, going beyond the conventional nozzle jet printing technologies, optical vortices twist liquids to create a spinning fL-scale microdroplet for ultrahigh-definition printed electronics and photonics^{1,2}. In this presentation, we review the state-of-art of materials sciences and technologies with optical vortices. Also, we address recent progress of advanced optical vortex sources for materials sciences and technologies³.

Reference:

1. M. Padgett, J. Courtial, L. Allen, *Phys. Today*, 57, 35-40 (2004).
2. K. Toyoda, K. Miyamoto, N. Aoki, R. Morita, T. Omatsu, *Nano Lett.* 12, 3645-3649 (2012).
3. K. Toyoda, F. Takahashi, S. Takizawa, Y. Tokizane, K. Miyamoto, R. Morita, T. Omatsu, *Phys. Rev. Lett.*, 110, 143603/1-5 (2013).
4. T. Omatsu, K. Miyamoto, K. Toyoda, R. Morita, Y. Arita, K. Dholakia, *Adv. Opt. Mater.* 7(14), 1801672 (2019).

IL-20**Active Metamaterials**

Achanta Venugopal

Metamaterials are designed materials with sub-wavelength features made of all-dielectric or metal-dielectric combinations. The choice of materials offers active functionality as well as novel properties and applications of metamaterials. In this talk, I will present metamaterials including broadband plasmonic structures, hyperbolic metamaterial, perfect absorber, and reflectionless potential. I will present the role of different metals and dielectrics- magnetic and non-magnetic, in different functionalities ranging from single photon emission to sensors and to study light-matter interaction.

IL-21**Optical mode manipulation for quantum technologies**

Yoko Miyamoto

Department of Engineering Science, The University of Electro-Communications Institute for Advanced Science, The University of Electro-Communications e-address: yoko.miyamoto@uec.ac.jp

Spatial optical modes specifying the spatial distribution of amplitude, phase, and polarization can be a useful vehicle of information. This includes quantum technologies where entanglement and similar resources based on spatial modes can be generated and exploited. Of special interest are modes that are pure in orbital angular momentum, i.e. modes that have specific rotational symmetries around the beam axis and corresponding azimuthal mode numbers.

To make use of these modes, methods of mode manipulation that allow change in mode numbers, creation and detection of specific superpositions, and interfaces with other physical encoding schemes are key. Phase holograms have become a standard tool because they are theoretically lossless and can change the azimuthal mode number by a fixed amount regardless of input. However they do not handle superpositions very well, because to realize superpositions of spatial modes, amplitude modulation is unavoidable. To handle this we have designed a hologram to be used as a converter between azimuthal mode and path encodings, allowing us to handle superposition in the path format. The scheme was successfully used to demonstrate nonclassical correlation in spatial modes between photon pairs produced by spontaneous parametric downconversion¹.

Another area where phase holograms face limitations is in producing self-similar propagating modes, which requires modulation of radial amplitude distribution in combination with phase modulation. Self similarity is not a necessary requirement for quantum technologies, but where it is required, quasi-amplitude modulation techniques can be employed, with some practical considerations depending on how much the phase modulation can be fine-tuned. A lossless scheme using an additional hologram has also been demonstrated².

References:

- 1.Y. Miyamoto et al., J. Opt. 13, 064027 (2011).
- 2.S. Choudhary et al., Opt. Lett. 43, 6101-6104 (2018).

IL-22**A big jump from Japan joining IIT Delhi in the wake of Covid 19:
Atomic and molecular physics, higher education, and life in general**Yoshiro AZUMAe-address: yoko.miyamoto@uec.ac.jp

I will start with a simple introduction to atomic and molecular photoionization studies with synchrotron radiation. Experimental work in this area is characterized by “Small Science” (electron spectroscopy etc.) combined with “Big Science” (high energy accelerators etc.) and “user experiments”. Then, I will make some comparisons between India and Japan regarding my own research topic (Post Collision Effects upon atomic threshold photoionization), atomic and molecular physics, physics in general, science in general, and then the starkly different student cultures. Finally, I will present some thoughts about the kind of exchange of scientists and students that can be feasible and mutually beneficial.

IL-23**Many Body Localization: A Fock space perspective**Subroto Mukerjee

The approach of a physical system to thermal equilibrium is a ubiquitous phenomenon. Over the past decade and a half, systems which do not generically thermalize have been discovered and the associated phenomenon has come to be known as many-body localization. Quantum mechanics is essential to understanding the physics of these systems. In this talk, I will provide a description of many-body localization from the perspective of the Fock space of quantum mechanical systems as opposed to real space. This will have the virtue of mapping the interacting many-body system in real space to a non-interacting system on a Fock space lattice. Techniques to study localization in non-interacting systems can thus be employed to understand aspects of the more complicated problem of many-body localization.

IL-24**Living Glass: Active Matter at High Densitie**

Chandan Dasgupta

Indian Institute of Science and International Centre for Theoretical Sciences Bangalore

Active matter consists of objects that can convert internal or ambient sources of energy into systematic motion. Experimentally studied active matter includes living systems such as flocks of birds, schools of fish, swimming bacteria and migrating cells, as well as synthetic non-living examples such as vibrated granular matter, self-propelled colloids, and swimming microrobots. These systems have received a lot of attention in recent years because they exhibit various forms of self-organization and collective behaviour. After a general introduction to the nonequilibrium statistical mechanics of active systems, I will discuss some of the results of our recent studies of glassy behaviour in dense active matter. In several biological systems, such as bacterial cytoplasm, cytoskeleton-motor complexes and epithelial sheets of cells, self-propulsion or activity is found to fluidize a state that exhibits characteristic glassy features in the absence of activity. The occurrence of an active glass transition has also been observed in recent experiments on dense systems of Janus colloids. To develop a theoretical understanding of these non-equilibrium phenomena, we have studied the effects of activity in several model glass-forming liquids. Our analytic and numerical results show that dense active matter brings together the physics of glass, jamming and plasticity in an internally driven classical system.

IL-25**Strong Dynamical Heterogeneity in Active Glass-forming Liquids and its implications in the Physics of Glasses**Samarjit Karmakar

The physics of the glass transition is an age-old and important problem. 2021 Physics Nobel Prize to Prof. Giorgio Parisi for his seminal work on disordered systems certainly highlights this. Recently glassy behaviour in systems with active self-propelled particles has added a new dimension to this problem. Although it is not clear whether activity can help us in having a better understanding of the equilibrium glass transition problem, it definitely is generating a plethora of new phenomena. Activity-driven glassy dynamics is ubiquitous in collective cell migration, intracellular transport, dynamics in bacterial and ant colonies, etc. It also extends the scope and extent of the as-yet mysterious physics of glass transition. Active glasses are hitherto assumed to be qualitatively similar to their equilibrium counterparts at an effective temperature, T_{eff} . Here we combine large-scale simulations and an analytical mode-coupling theory (MCT) for such systems and show that, in fact, an active glass is inherently different from an equilibrium glass. Although the relaxation dynamics can be equilibrium-like at a T_{eff} , effects of activity on the dynamical heterogeneity (DH), which has emerged as a cornerstone of glassy dynamics, are quite nontrivial and complex. With no preexisting data, we employ three distinct methods for reliable estimates of the DH length scales. Our work shows active glasses exhibit dramatic growth of DH and systems with similar relaxation times and T_{eff} can have widely varying DH. To theoretically study DH, we extend active MCT and find excellent agreement between the theory and simulation results. Our results question the supposedly central role of DH in glassy dynamics and can have fundamental significance even in equilibrium.

IL-26**Artificial Multiferroic Heterostructures for Spin-Wave Applications**

Tomoyasu Taniyama

Department of Physics, Nagoya University

e-address: taniyama.tomo@nagoya-u.jp

Multiferroic heterostructures consisting of ferromagnetic and ferroelectric layers have attracted much attention because they enable electric-field control of magnetic properties and spin-wave propagation with very low power consumption. In this talk, we present recent progress in electric-field effect on the magnetic properties of $\text{La}_{1-x}\text{Sr}_x\text{MnO}_3/\text{BaTiO}_3$ and spin-wave propagation in Fe/BaTiO_3 . $\text{La}_{1-x}\text{Sr}_x\text{MnO}_3$ is a well-known manganite that shows a variety of magnetic phases, e.g., ferromagnetic (FM) metal, antiferromagnetic (AFM) metal, and mixed phases, etc. In the vicinity of the phase boundaries between the FM metal and AFM metal phases, electric-field-induced strain transfer, charge modulation, and ionic modulation could lead to a significant change in the magnetic properties of the epitaxial $\text{La}_{1-x}\text{Sr}_x\text{MnO}_3$ thin film in $\text{La}_{1-x}\text{Sr}_x\text{MnO}_3/\text{BaTiO}_3$. We find strain-induced saturation magnetization that is prominent close to the phase boundary at $x=0.55$ as well as the strain-induced magnetic anisotropy that appears irrespective of x value. We also demonstrate electric-field-induced switching behavior of the saturation magnetization by reversing the polarity of electric field applied across BaTiO_3 . As a second topic, we demonstrate electric-field control of spin-wave propagation in epitaxial Fe/BaTiO_3 . Since the dispersion relation of spin waves in ferromagnetic thin films depends on the direction of the magnetic easy axis, switching of the magnetic easy axis via electric-field-induced strain transfer from BaTiO_3 to Fe enables characteristic control of spin-wave propagation by an electric field. Future prospects of multiferroic heterostructures for spin-wave applications will also be discussed. This work was supported in part by JST CREST Grant No. JPMJCR18J1, JSPS Bilateral Joint Research Projects Grant No. JPJSBP120197716, and JSPS KAKENHI Grants No. 21H04614.

References:

1. T. Taniyama, J. Phys.: Condens. Matter 27, 504001 (2015).
2. H. Qin et al., Adv. Mater. 33, 2100646 (2021)
3. W. Zhu et al., Appl. Phys. Lett. 120, 112407 (2022).

IL-27**Spin chirality induced large topological Hall effect in magnetic Weyl semi-metallic $\text{Eu}_2\text{Ir}_2\text{O}_7$ (111) thin films**P. S. Anil Kumar ¹Department of Physics, Indian Institute of Science, Bangalore 560012, Karnataka, India
e-address: anil@iisc.ac.in

Rare earth pyrochlore iridates, $\text{RE}_2\text{Ir}_2\text{O}_7$, are predicted to be magnetic Weyl semi-metallic (WSM) in the presence of electron correlation (U) and spin-orbit coupling (λ). Here, we have studied the magnetotransport properties of epitaxial $\text{Eu}_2\text{Ir}_2\text{O}_7$ (111) epitaxial thin films grown on YSZ by the solid phase epitaxy technique. Low-temperature longitudinal resistivity (ρ) data shows a power-law dependence on temperature, which signifies semi-metallic charge transport. By varying the film properties, the semi-metallic charge transport is tuned to realize the predicted WSM phase. The Hall resistivity (ρ) data exhibits an anomalous Hall effect (AHE) in the temperature range of 2–25 K. The intrinsic AHE is explained in terms of momentum space Berry curvature of the Weyl nodes. In addition to the AHE, a large topological Hall effect (THE) is observed in the temperature range of 2–5 K. Due to spin chirality generated by the all-in-all-out (AIAO) non-coplanar spin structure of Ir moments, the conduction electrons acquire a real-space Berry curvature and cause a large THE. Low-temperature (2–10 K) magnetoresistance (MR) data shows a non-hysteretic large negative MR caused by a reduction in scattering by the spin canting. For the temperature of 15 K and above, MR shows hysteretic up to 90 K (metal-semimetal transition temperature). The hysteretic MR suggests magnetic field-induced domain imbalance of Ir moments. The appearance of Hysteresis above 10 K onwards suggests competition between antiferromagnetic interaction and field-induced Zeeman energy. As temperature increases, the Zeeman energy overcomes the antiferromagnetic interaction and causes domain flipping.

¹In collaboration with Mithun Ghosh and Debakanta Samal

IL-28**Review on a Mixed Anion Layered Compound (MALC)
Polycrystalline $\text{LaCu}_{1-\delta}\text{S}_{0.5}\text{Se}_{0.5}\text{O}$ ($\delta \approx 0.01$) as a Degenerate
Semiconductor**Yoichi KAMIHARA

Keio University, Japan

e-address: kamihara_yoichi@keio.jp

Mixed anion layered compounds (MACLs) demonstrate several functional electronic properties; i.e., thermoelectric conversion¹, superconductivity, and transparent semiconductivity. These functionalities strongly depend on the chemical compositions, that had been controversial on a complex mixed anion compound. Semiconducting MALC $\text{LaCu}_{1-\delta}\text{S}_{0.5}\text{Se}_{0.5}\text{O}$ are synthesized via solid state reaction. We synthesized several nominal $\text{LaCu}_{1-\delta}\text{S}_{0.5}\text{Se}_{0.5}\text{O}$ ($\delta = 0, \approx 0.01$, and ≈ 0.02). A degenerated semiconducting bulk $\text{LaCu}_{1-\delta}\text{S}_{0.5}\text{Se}_{0.5}\text{O}$ appears at $\delta \approx 0.01$. p-type carriers are doped due to Cu deficient $\text{Cu}_{1-\delta}\text{S}_{0.5}\text{Se}_{0.5}$ layers in $\text{LaCu}_{1-\delta}\text{S}_{0.5}\text{Se}_{0.5}\text{O}$. In-gap states, which dominate electrical conduction, are observed at energy ≈ 0.5 eV higher than that of the valence band in an energy band diagram for $\delta \approx 0.01$.

References:

1. Y. Liu, L. Zhao, Y. Liu, J. Lan, W. Xu, F. Li, B. Zhang, D. Berardan, N. Dragoe, Y. Lin, C. Nan, J. Li, and H. Zhu, *J. Am. Chem. Soc.* 133, 20112-20115 (2011). Remarkable enhancement in thermoelectric performance of BiCuSeO by Cu deficiencies
2. Y. Kamihara, *TEION KOGAKU (J. Cryo. Super. Soc. Jpn.)* 52, 383-388 (2017). A private story, discovery of iron-based high T_c superconductors II (in Japanese)
3. H. Hiramatsu, T. Kamiya, T. Tohei, E. Ikenaga, T. Mizoguchi, Y. Ikuhara, K. Kobayashi, and H. Hosono, *J. Am. Chem. Soc.* 132, 15060-15067 (2010). Origins of hole doping and relevant optoelectronic properties of wide gap p-type semiconductor, LaCuOSe
4. N. Azuma, T. Sawada, H. Itoh, R. Sakagami, M. Matoba, H. Usui, and Y. Kamihara, *Mater. Sci. Tech. Jpn.* 58, 64-68 (2021). In-gap-states of a mixed anion layered compound, polycrystalline $\text{LaCu}_{1-\delta}\text{S}_{0.5}\text{Se}_{0.5}\text{O}$ ($\delta \approx 0.01$) as a degenerate semiconductor (in Japanese)

IL-29**Electron spectroscopy for the physics of quantum materials**Kalobaran Maiti

Tata Institute of Fundamental Research, Homi Bhabha Road, Colaba, Mumbai 400005, India

Electronic structure evolves differently in different forms and dimensions of materials that derives their properties and can be probed directly by electron spectroscopy. Photoemission spectroscopy, a technique based on photoelectric effect, has enigmatic properties that can be exploited to probe varied faces of the electronic structure. Here, I will try to bring out how different forms of electron spectroscopy can be used to address properties such as detection of orbital selective properties of high temperature superconductors^{1, 2}, the puzzles at the Dirac point in graphene³ and properties at different depths of nanostructures⁴.

References:

- 1.G. Adhikary et al., Europhysics Letters 136, 17002 (2021).
- 2.G. Adhikary et al., Phys. Rev. B 98, 205142 (2018).
- 3.A. Pramanik et al., Phys. Rev. Letts. 128, 166401 (2022).
- 4.A. B. Dey et al., J. Phys. Condens. Mater. (Letters) 33, 42LT01 (2021).

IL-30**Using machine learning in the design and implementation of quantum algorithms**Anil Shaji

We use differentiable programming and gradient descent to find unitary matrices that can be used in the period finding algorithm to extract period information from the state of a quantum computer post application of the oracle. The standard procedure is to use the inverse quantum Fourier transform. Our findings suggest that this is not the only unitary matrix appropriate for the period finding algorithm. There exist several unitary matrices that can affect out the same transformation and they are significantly different from each other and some of these may have hardware-specific implementation advantages as well. These unitary matrices can be learned by an algorithm. Neural networks can be applied to differentiate such unitary matrices from randomly generated ones indicating that these unitaries do have characteristic features that cannot otherwise be discerned easily.

IL-31**Exploitation of topological defects in liquid crystals**

Surajit Dhara

School of Physics, University of Hyderabad, INDIA

e-address: surajit@uohyd.ac.in

Topological defects have been objects of intense studies in various disciplines starting from cosmology to condensed matter, optics and more recently in active matter. In liquid crystals (LCs) topological defects appear as a result of symmetry breaking phase transition and traditionally such defects have been considered as an undesirable feature in displays. Topological defects can also be induced by dispersing nano- and micro-particles in uniformly aligned liquid crystals. The defect-decorated particles interact via long-range anisotropic elastic forces so generated. These forces obviously have no analogues in regular colloidal systems in an isotropic dispersive medium. Another interesting manifestation of topological defects in LCs is the ability to propel and behave like steerable active particles when powered by external electric field. In this talk I will discuss these emerging and useful aspects of topological defects in liquid crystals.

IL-32**High speed nanoindentation mapping - A new paradigm in small scale mechanical testing**

P. Sudharshan Phani

International Advanced Research Centre for Powder Metallurgy & New Materials (ARCI), Hyderabad

High speed nanoindentation mapping has emerged as a powerful tool to measure the local mechanical properties with very high throughput without compromising the reliability of the measurements. A new criterion for spacing of indents has enabled high speed mapping with much higher resolution as well. These advances have now resulted in generating large indentation data sets on small volumes of materials, which can be analyzed with advanced statistical tools to quantitatively determine the properties of individual phases in a multi-phase alloy. In this talk, results of high speed nanoindentation mapping coupled with microstructural analysis using SEM/EBSD are presented to demonstrate the structure-property correlations at the micrometer length scale on different materials including coatings for aerospace applications, high strength steels for automotive applications and biomaterials. These results hold significant promise in terms of providing a potent tool to generate processing-structure-property correlations, which forms the very basis for materials research.

IL-33**OPTICS: Space borne remote sensing and beyond**

M. Senthil Kumar

Group Director Optical Systems Group & Associate Project Director – Cartography satellite (Payloads) Space Application Centre (SAC), Indian Space Research Organisation (ISRO) Ahmedabad, India, 380015

Optics is mostly seen as a branch of physics deals with the spectrum of EM radiation (light) that human eye can detect. Vast applications of light are achieved by engineering the detection/measurement of various properties of light. Observation of earth through remote space borne platforms allows a wider area coverage and more frequent visits compared to ground/near ground based platforms. Thanks to the atmospheric window, from visible to long wave infra-red spectrum form an indispensable tool/probe for optical earth observation satellites.

Introduction of remote sensing and various platform for remote sensing. Space borne earth observation basics, orbital platforms for earth observation, classification and parameters of remote sensors. Current practices on elements of remote sensors i.e. Electro Optical (EO) sensors viz., Optical elements (1inch to 1m diameter), detecting elements (low speed single pixel to high speed, low noise time delayed integration CCD), mechanical elements (metal to composite) and elements of electronics (discrete to FPGA/ASIC, low noise mixed signal-analog input to compressed digital data-package), for various applications and future direction. Advancement in configurations and manufacturing technology matching to the requirements of EO sensor that facilitated Indian earth observation missions to image ground span distance from 1 km to 1 foot: spatial, wave bands and bandwidth from single panchromatic band of 350nm to sixty plus hyperspectral channels of ± 10 nm: spectral, digitization of light intensity from 7 to 12 bits: radiometry and repetivity from 22 days to 1 day for Low earth orbit (LEO) and every $\frac{1}{2}$ hr image of Indian sub-continent from Geo-Stationary orbit (GEO): temporal. Also current trends in type of satellites viz., Large, Small, Micro and Nano for earth observation will be highlighted.

Advancement in elements of EO sensors on satellite to address the increasing application demand would generate on-board huge volume of data. Beyond the application of light for remote sensing from space, as the frequency of light is high (10^{15} Hz) in other words larger bandwidth helps in large data carrying capacity and, sources and detector for the current quantum communication research deals in near visible wavelength, it is seen as a high speed / secured data transmission media from space. Certain aspects related to the optical data reception for LEO/GEO satellites and blocks of reception terminal will be highlighted.

IL-34**The Future of Neutrino Physics**

Amitava Raychaudhuri
University of Calcutta

The neutrino is a weakly interacting uncharged particle. It is notoriously difficult to detect. Yet, many experiments around the world, notably in Japan, have made breakthroughs in this field in the past years. It is now established that the neutrinos oscillate and are therefore massive, which itself is a departure from the successful Standard Model theory of particle physics. We discuss how planned experiments will explore unknowns about neutrino mass and mixing. Moreover, these experiments will be useful for multi-messenger astronomy, testing the stability of the proton, and geophysics.

IL-35**India's contributions to the CMS Experiment and its Physics**

Brajesh C Choudhary

In this talk, in brief, I will discuss about India's contributions to the CMS detector over last quarter century and its physics program since 2010, including the discovery of the Higgs Boson and its properties.

IL-36**AstroSat, the first Indian Space Observatory**

Annapurni Subramaniam

AstroSat is the first Indian space observatory consisting of 5 major science instruments covering a large wavelength range, developed by various Indian Institutions with international collaboration. AstroSat was launched by ISRO on 28th September 2015 and is nearing completion of 7 years of successful in-orbit operations by ISRO. As the calibration scientist of the Ultra-violet Imaging telescope (UVIT), a twin telescope to observe the universe in Ultraviolet and visual pass bands, I plan to present some salient features of AstroSat, its science impact and the on-going efforts for future space telescopes.

PC-01**The Optimized Sparse Davidson Algorithm: A modern numerical approach for finding extreme eigenpairs for large Hermitian matrices**

Payal D. Solanki, M. S. Ramkarthik

Visvesvaraya National Institute of Technology, Nagpur

e-address: solankipayal2906@students.vnit.ac.in, msramkarthik@phy.vnit.ac.in

Eigenvalues and eigenvectors of matrices are central elements in science and technology. Most of the times, any problem in the natural sciences or engineering boils down to the matrix eigenvalue problem under suitable transformations. There is always a demand for methods that compute the eigenvalues and eigenvectors of Hermitian matrices because these matrices are very common in physics and engineering. In this work, several new proposals and techniques have been brought to light which improvises the popular method of numerical linear algebra called the “Davidson’s Algorithm.” The main novelty of the work lies in the fact that the algorithms proposed can be executed even on an ‘modest’ computer. In a way, we should say that the deep mathematics behind the problem under consideration helped us to simplify the problem to such an extent that we could achieve a drastic reduction in computational times in calculating the eigenpairs of huge matrices to the order of several millions just using a desktop computer. Any serious researcher who does not have an access to high-performance computing facilities and wishes to extend his computations to higher dimensions would amply benefit from our method. The technique described in this work is the “Optimized Sparse Davidson Algorithms (OSDA) ” which can be used for finding the eigenvalues and eigenvectors of sparse Hermitian matrices. The numerical evidences and detailed algorithms are also provided to prove our claims using the Hamiltonian matrices from spin chain physics. It is noteworthy that, the OSDA can be applied to the broad spectrum of problems in science and engineering including computationally intensive areas like quantum chemistry, economics, many-body physics etc.

References:

1. Ernest R. Davidson, *Journal of Computational Physics*, 17, (1975).
2. Ernest R. Davidson and William J. Thompson, *Computers in Physics*, 7, (1993).
3. Yousef Saad, *Numerical Methods for Large Eigenvalue Problems*, SIAM, (2011).
4. Sergio Pissanetzky, *Sparse Matrix Technology*, Academic Press, (1984).

PC-02**Analysis of Congestive heart failure signals using normalized entropy**

Sudhamayee Kamanoor^a, Nayan Telrandhe^b, Manimaran Palanisamy^b
^aCASEST, School of Physics, University of Hyderabad, Hyderabad -500046, Telangana, India
^bSchool of Physics, University of Hyderabad, Gachibowli, Hyderabad – 500046, India
e-address: 19phpe01@uohyd.ac.in

Analyzing the dynamics of signals obtained from human cardiovascular system at different pathological conditions using entropy has always been an inspiring area of research. In this study, we make use of the concept of Normalized Corrected Shannon Entropy (NSCE) for distinguishing the dynamical complexity and hence the functionality of healthy subjects against the Congestive Heart Failure (CHF) patients. The raw and filtered Electrocardiogram (ECG) time series is converted into symbolic time series through thresholding. This series of symbols obtained for the healthy and diseased subjects is converted into a group of code words. Later, NSCE is calculated and its mean value variation is studied by varying the word length and threshold value. The resulted entropies have shown elevated values for healthy system as compared to that of CHF subjects, in all the cases, indicating higher dynamical complexities in the former case. In conclusion, it is found that NCSE has efficiently differentiated normal data from CHF data.

PC-03**Network properties of healthy and epileptic brain signals**

Shaik Afifa Farman^a, Sudhamayee Kamanoor^a, Manimaran Palanisamy^b

^a CASEST, School of Physics, University of Hyderabad, Hyderabad -500046, Telangana, India

^bSchool of Physics, University of Hyderabad, Gachibowli, Hyderabad – 500046, India

e-address: 21phpe02@uohyd.ac.in

The complex network learning has spread to a variety of scientific disciplines, including social sciences, natural and engineering sciences. Until recently, in several areas of neuroscience, the study of brain connection has provided new theoretical and experimental avenues. Understanding network interactions among neurons to extract statistical properties is crucial for analysing the brain as a whole system. The aim of the present study is to perform statistical analysis in order to determine how closely the properties of complex network models and the epilepsy brain's network resemble each other. These network properties such as degree, node strength, transitivity, assortativity and characteristic pathlength etc. offer insight into the influence, integration, and segregation of different brain regions.

Keywords:

Epileptic network, EEG, small world.

References:

1. J.G. White, E. Southgate, J.N. Thomson, S. Brenner, The structure of the nervous system of the nematode *Caenorhabditis Elegans*, *Philos. Trans. R. Soc. Lond. B* 314 (1986) 1–340;
2. D.J. Watts, S.H. Strogatz, Collective dynamics of ‘small-world’ networks, *Nature* 393 (1998) 440–442;
3. E.T. Bullmore, D.S. Bassett, Brain graphs: graphical models of the human brain connectome, *Annu. Rev. Clin. Psychol.* 7 (2011) 113–140;
4. C.J. Stam, E.C. van Straaten, The organization of physiological brain networks, *Clin. Neurophysiol.* 123 (2012) 1067–1087;
5. C.Y. Lo, P.N. Wang, K.H. Chou, J. Wang, Y. He, C.P. Lin, Diffusion tensor tractography reveals abnormal topological organization in structural cortical networks in Alzheimer’s disease, *J. Neurosci.* 30 (2010) 16876–1688.

PC-04**Thermodynamic properties of a particle scattering by rotating trapped quantum gases**Samir Das, Shyamal Biswas

School of Physics, University of Hyderabad, Gachibowli, Hyderabad – 500046, India

e-address: dassamir579@gmail.com

We have analytically investigated the quantum phenomena of particle scattering by rotating trapped quantum gases of electrically neutral fermions and bosons for the short-range Fermi-Huang interactions between the incident particle and the scatterers. We have specifically predicted differential scattering cross-section and their angular velocity and temperature dependence for an ideal Fermi gas, an ideal Bose gas, and a weakly interacting Bose gas in rotating harmonic traps. We have used the particle scattering technique to theoretically investigate the lattice pattern of the vortices in a fast rotating Bose-Einstein condensate. We also have obtained de Haas-van Alphen-like oscillations in the differential scattering cross-section for an ideal ultracold Fermi gas in a rotating harmonic trap. Our predictions on the differential scattering cross-sections can be tested within the present-day experimental setups.

References:

1. W. J. de Haas and P. M. van Alphen, Proc. Netherlands Roy. Acad. Sci. 33, 680 (1930);
2. A. L. Fetter, Rev. Mod. Phys. 81, 647 (2009);
3. S. Stock, B. Battelier, V. Bretin, Z. Hadzibabic, and J. Dalibard, Laser Phys. Lett. 2, 275 (2005);
4. A .Bhattacharya , S. Das and S. Biswas, J. Phys. B: At. Mol. Opt. Phys. 51 075301(2015).

PC-05**Synthesis and Characterization of Sb₂Se₃ Thin Films and Numerical Simulation of p-Sb₂Se₃/n-ZnSe Heterojunction Solar Cell**Bandi Srinivas^a, Shaik Babujani^a, G. Hema Chandra^a, and Mukul Gupta^b.^aThin Film Laboratory, Department of Physics, Visvesvaraya National Institute of Technology, Nagpur - 440 010, Maharashtra, India^bUGC-DAE Consortium for Scientific Research, Khandwa Road, Indore - 452 001, Indiae-address: srinivasbandi.phy@gmail.com

Sb₂Se₃ thin films were prepared by sequential evaporation of (Sb/Se)×3 precursor stacks on the glass substrates in high vacuum using the electron beam evaporation technique followed by annealing in a tubular furnace at various temperatures in Ar atmosphere. The growth of Sb₂Se₃ films is studied by varying the annealing temperature. The XRD pattern of Sb₂Se₃ films annealed at all temperatures confirms the Sb₂Se₃ formation with the orthorhombic crystal structure. The films annealed at ≤ 250°C showed the preferred orientation along (hk0) plane, whereas films annealed at 300 ° C exhibited the (hk1) preferred orientation. Raman studies for stacked samples reveal a significant intensity peak at 191 cm⁻¹, supporting the structure of single-phase Sb₂Se₃. The morphology of Sb₂Se₃ films annealed at 300 ° C showed grain size around 500 nm. The direct optical band gap of film annealed at 300 ° C is found to be 0.86 eV. Hall effect measurement exhibited a p-type conductivity with hole concentration of 1.72×10¹¹ cm⁻³ and mobility of 36 cm²V⁻¹s⁻¹ for the film annealed at 300° C. The photovoltaic performance was studied using the SCAPS-1D (version 3.3.10) program simulator, the numerical simulation of the proposed Glass/Ni/p-Sb₂Se₃/n-ZnSe/ITO/Al heterojunction solar cell showed a power conversion efficiency of 16.95%.

Acknowledgements:

Bandi Srinivas is thankful to VNIT-Nagpur for providing institute doctoral fellowship. Authors are acknowledge to Department of Physics, VNIT Nagpur DST FIST(SR/FST/PSI/2017/5(C)) for providing X-ray characterization facility. Authors are grateful to UGC-DAE-CSR, Indore, for extending sophisticated characterization facility (SIMS).

PC-06

Electrodeposited NiO nanoflakes for electrochromic energy storage applications

Sushant B. Patil, Shivaji B. Sadale*

Department of Technology, Shivaji University, Kolhapur, Maharashtra (IN), 416004.

*Correspondance to : Dr. Shivaji B. Sadale; shivajisadale@yahoo.com; sbs_tech@unishivaji.ac.in
e-address: sushant8385@gmail.com

Electrochromic materials are known for their ability to sustain reversible and persistent changes in the optical properties when a suitable potential is applied to it. The electrochromic NiO thin film consisting of nanoflakes was electrodeposited in the potentiostatic mode onto an FTO glass substrate from an equimolar aqueous solution of nickel sulfate, sodium acetate, and sodium sulfate. The pH of the precursor solution was adjusted to 8.0 using diluted ammonia solution. and the deposition process was carried out at 1 V for 120 min. Furthermore, the electrode was annealed at 300°C for 60 min. Physicochemical properties of NiO electrode were analyzed using X-Ray Diffraction (XRD), X-ray photoelectron spectroscopy and Scanning electron microscopy (SEM). The electrochromic energy storing properties were studied in 1M KOH electrolyte using electrochemical measurements. The NiO thin film shows anodic electrochromism owing to $\text{Ni}^{2+} \leftrightarrow \text{Ni}^{3+}$ charge transition. The NiO electrode shows 8.30 F/cm² of specific capacitance at 10 mV/s along with 83.14 C/cm² of coloration efficiency at 630 nm. These results provide a new pathway for the fabrication of large-scale energy-storing smart windows, optical devices, and smart electronics.

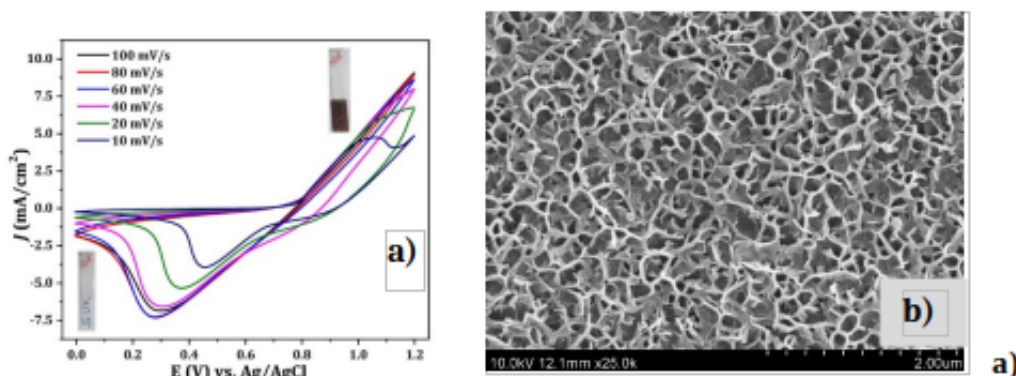


Figure 1: a) Cyclic voltammogram of NiO thin film at different scan rates with inset photographs of NiO thin films in the colored state (1.2V) and bleached state (0 V) and b) FE-SEM image of NiO thin film at 25kX magnification.

References:

1. I. Saadedin, M. Suleiman, H. Salman, K. Zrikem, G. Song, A. Rougier, Solid State Ionics, 343 (2019) 115129, <https://doi.org/10.1016/j.ssi.2019.115129> ;
2. Md Rakibuddin, Mahesh A. Shinde, Haekyoung Kim, Ceramics International, 46(7),2020, <https://doi.org/10.1016/j.ceramint.2019.12.096>.

PC-07

Photocatalytic Self-Cleaning and Stain Removing Properties of Carbon Nitride /PEDOT Composite for Smart Textile Application

Prathiba Meganathan ^a, Sounder Subbaiah ^b, Lakshmi Manokari Selvaraj ^a,
Nagarajan Srinivasan ^{c*}

^aPeriyar University, Department of Textiles and Apparel Design, Salem, Tamilnadu, India.

^bManonmaniam Sundaranar University, Department of Renewable Energy Science, Tirunelveli, Tamilnadu, India.

^c Manonmaniam Sundaranar University, Department of Chemistry, Tirunelveli, Tamilnadu, India.

e-address: prathiba@periyaruniversity.ac.in

*correspondence e-address: snagarajan@msuniv.ac.in

Photocatalyst assisted self-cleaning smart fabric technology can be consider as a budding technique for the self-removal of stain without surfactant in textile apparels. Herein, we blended a semi-conducting carbon nitride (C_3N_4) with conducting Poly(3,4-ethylenedioxythiophene) polymer and coated over cotton fabrics for photocatalytic self-cleaning and stain removing property were appraised. The C_3N_4 structure was synthesized by thermal polymerization and the carbon nitride/ Poly 3,4-ethylenedioxythiophene (C_3N_4 /PEDOT) composite were prepared using oxidative chemical polymerization method and coated over cotton fabric by using pad-dry cure method¹. The chemical structure and structural morphology were confirmed and virtuous light harvesting efficiency was observed by an intense broad UV-Visible absorption of C_3N_4 /PEDOT composite. The C_3N_4 /PEDOT composite observed photocatalytic degradation competence of 97% and enriched cyclic stability performance towards Rhodamine-B dye under solar irradiation. The photocatalytic self-cleaning and stain removing properties of C_3N_4 /PEDOT composite coated cotton fabric was achieved over various colored stain under solar irradiation.

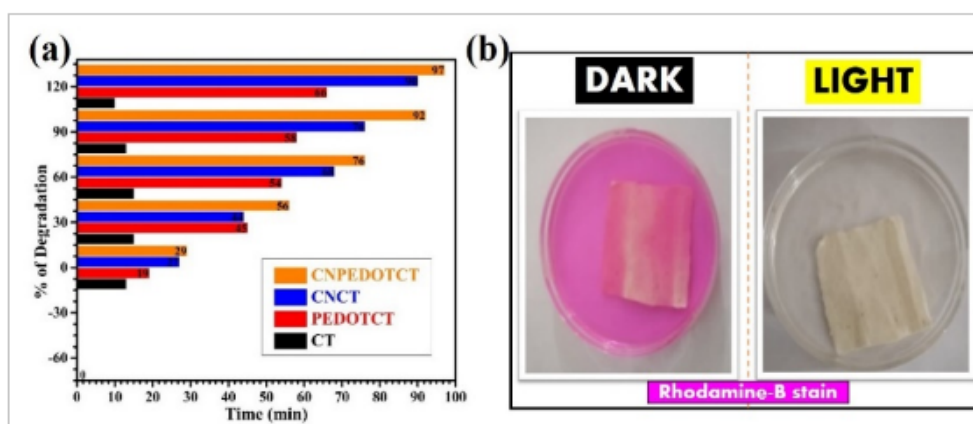


Figure 2: (a) Dye degradation percentage of C_3N_4 /PEDOT coated CT under solar irradiation, (b) Self-cleaning properties of Rhodamine-b C_3N_4 /PEDOT composite coated cotton fabric under solar irradiation.

Acknowledgements:

The author Srinivasan Nagarajan acknowledges EPSRC Impact Acceleration Account at Swansea University, UK.

References:

1. Phosphorus, Sulfur, and Silicon and the Related Elements 197.3 (2022): 244-253.

PC-08**A theorem on the generic form of the quantum cluster integral**

Soumi Dey^{a,b}, Prathyush Manchala^a, Srijit Basu^{a,c}, Debshikha Banerjee^{a,d}, and Shyamal Biswas^a

^aSchool of Physics, University of Hyderabad, Gachibowli, Hyderabad – 500046, India

^bPresent Address: Solid State and Structural Chemistry Unit, IISc, Bangalore-560012, India

^cPresent Address: Light and Matter Physics Unit, Raman Research Institute, Bangalore-560080, India

^dPresent Address: Department of Physics and Astronomy, University of Tennessee, Knoxville, USA

e-address: sbsp@uohyd.ac.in

We have obtained quantum cluster expansion of the grand free energy in a closed form for an ideal Bose or Fermi gas in both the 3-D box geometry and the harmonically trapped geometry. We have analytically obtained 1-particle density matrices for the same system in the restricted geometries. We have proposed a theorem (with a proof) about the generic form of the quantum cluster integral¹. Our Theorem: The generic form of the quantum cluster integral for a cluster of size ν of any system of ideal indistinguishable bosons (upper sign) or fermions (lower sign) in thermodynamic equilibrium would be $(\pm 1)^{(\nu-1)}$ times the canonical partition function of a single composite particle composed of ν bosons or fermions in the cluster. Our results are exact for the entire range of temperature, and are directly useful for understanding finite-size effects on a quantum gas. Our results would be relevant in the context of experimental study of spatial correlations in ultra-cold systems of dilute Bose and Fermi gases of alkali atoms.

References:

S. Dey, P. Manchala, S. Basu, D. Banerjee, and S. Biswas, Finite-size effects on the cluster expansions for quantum gases in restricted geometries, Phys. Scr. 95, 075003 (2020).

PC-09**Non-equilibrium work distribution of a 3-d harmonic oscillator with time varying angular frequency in a rotating frame**Rhitabrata Bhattacharyya^a, Saugata Bhattacharyya^b, Shyamal Biswas^c^aKrishnagar Customs Division of CC(P), 1, Cinema House Lane, Krishnagar-741101, West Bengal, India^bDepartment of Physics, Vidyasagar College, 39 Sankar Ghosh Lane, Kolkata-700006, India^cSchool of Physics, University of Hyderabad, Gachibowli, Hyderabad – 500046, Indiae-address: rhita08@gmail.com

Study of Jarzynski equality and fluctuations in the small non-equilibrium systems reflects an increasing importance both in the theoretical and experimental arena of statistical mechanics and thermodynamics¹⁻⁴. In the present work, the purpose of our study is to investigate the non-equilibrium work distribution as well as the Jarzynski equality of a non-equilibrium system in a non-inertial frame. We have considered a 3-d harmonic oscillator, oscillating with a time varying angular frequency, in a rotating frame^{5,6}. The oscillator is trapped by a trapping potential in the x-y plane, which is produced by the constant magnetic field acting along the z direction. The angular momentum produced by this magnetic field is also acting in the z direction. We have further tried to study the non-equilibrium work distribution of the time dependent harmonic oscillator for both the adiabatic and non-adiabatic processes in the limits of low and high temperatures.

References:

1. C. Jarzynski, Nonequilibrium Equality for Free Energy Differences, PHYSICAL REVIEW LETTERS, VOLUME 78, NUMBER 14, (1997);
2. C. Jarzynski, Rare events and the convergence of exponentially averaged work values, PHYSICAL REVIEW E, 73, 046105 (2006).
3. P. Talkner, E. Lutz, P. Hanggi, Fluctuation theorems: Work is not an observable. PHYSICAL REVIEW E, 75, 050102 (R) (2007);
4. H.T. Quan, C. Jarzynski, Validity of nonequilibrium work relations for the rapidly expanding quantum piston, PHYSICAL REVIEW E, 85, 031102 (2012).
5. S. Deffner, E. Lutz, Nonequilibrium work distribution of a quantum harmonic oscillator, PHYSICAL REVIEW E, 77, 021128 (2008).
6. S. Das, S. Biswas, Particle scattering by rotating trapped quantum gases at finite temperature, Physica Scripta, 96 (2021) 125037.

PC-10**Thermal Decomposition of Iron(III)citrate in Presence of Glucose
Leading to Iron Oxide Nanoparticles**

Sani Kundu^a, Maciej Zubko^{b,c}, Joachim Kusz^d, V. Raghavendra Reddy^e, Ashis Bhattacharjee^{*a}

^aDepartment of Physics, Visva-Bharati University, Santiniketan -731235, India

^bInstitute of Materials Science, University of Silesia, Chorzów, Poland

^cDepartment of Physics, University of Hradec Králové, Hradec Králové, Czech Republic.

^dInstitute of Physics, University of Silesia, Katowice, Poland

^eUGC-DAE Consortium for Scientific Research, Indore, India

e-address: sanikundu.rs@visva-bharati.ac.in

Thermal decomposition of iron-containing organic compounds in solid state is an important method to synthesize various iron oxide nanoparticles mainly due to easy control of process conditions, purity, phase, composition, microstructure, etc.¹. This method is often studied by non-isothermal thermogravimetry (TG). Analysis of the TG results leads to the understanding of the solid-state reaction by estimating the kinetic triplets (activation energy, mechanism function and reaction rate) and thermodynamic triplets (change in entropy, enthalpy and Gibb's free energy) involved in the reaction². Earlier studies have shown that the thermal decomposition of iron(III)citrate, $\text{FeC}_6\text{H}_5\text{O}_7$, as a precursor can yield ferrite, arsenite, magnetite and hematite depending upon reaction temperature and atmosphere used³. Present study attempts to find the effect of a co-precursor (glucose) on the nature of thermal decomposition of iron(III)citrate as well as the reaction product. The precursor and co-precursor are physically mixed in different weight ratios and these mixtures are thermally decomposed in furnace at 500°C for 30 mins in ambient atmosphere. The decomposed materials are used for physical characterization studies like powder XRD, SEM, TEM, magnetization measurement and ⁵⁷Fe Mössbauer spectroscopy. The results obtained indicate that only a particular combination of the precursor and co-precursor produces pure hematite nanoparticles. Solid state reaction involved has also been investigated.

References:

1. B. Das, et al., Solid State Sci (2017) 74: 62.
2. A. Dey, et al., Curr. Phys. Chem. (2018) 8: 290.
3. A. Dey, et al., Solid State Sci (2019) 95: 105932.

PC-11

Role of A-site Cationic Ordering on Structural and Magnetic Properties of Mixed-Valent Manganites

Aisha Khatun^{a,b}, Payel Aich^{a,b}, Alexander Schoekel^c, S. D. Mahanti^c, D. Topwal^{a,b}

^aInstitute of Physics, Sachivalaya Marg, Bhubaneswar 751005, India

^bHomi Bhabha National Institute, Training School Complex, Anushakti Nagar, Mumbai 400094, India

^cDESY Photon Science, Deutsches Elektronen - Synchrotron, 22603 Hamburg, Germany

^dDepartment of Physics and Astronomy, Michigan State University, East Lansing, Michigan 48824, USA

e-address: aisha.k@iopb.res.in

A-site order and disorder mixed-valent perovskites manganite, $\text{NdBaMn}_2\text{O}_6$ (NBMO) (fig.1(b)), were synthesized by the solid-state method to investigate the role of A-site cationic ordering on structural, magnetic, and magneto-transport properties of it. Temperature (T) dependent X-ray diffraction (XRD) data (fig.1(a)) reveals that the NBMO sample goes through different phase transitions, which explicitly depend on the degree of ordering of the A-site cations Nd^{3+} and Ba^{2+} . For example, the ordered NBMO undergoes multiple structural phase transitions with decreasing T, whereas the disordered compound retains its high-T crystal structure. Resistivity data confirms both order and disorder NBMO samples are insulating in nature, though their charge transport mechanism is different. Magnetization vs. temperature (M-T) data (fig.1(c)) clearly show that the cationic disorder suppresses the long-range antiferromagnetic order and enhances the ferromagnetic orders at lower T¹. Disordered NBMO exhibits larger value of magnetoresistance (MR) (fig. (d)) at low temperature than its ordered counterpart².

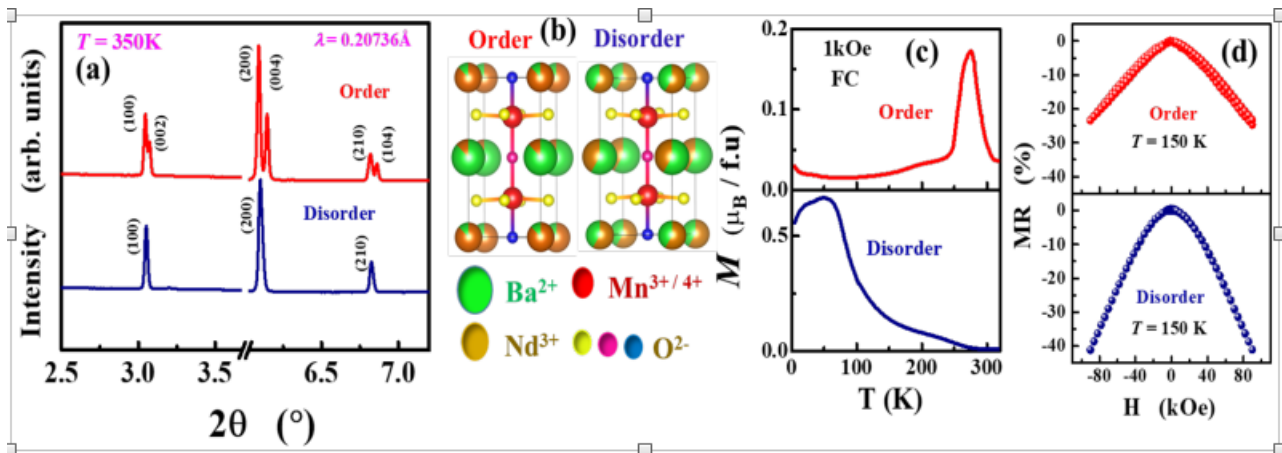


Figure 3: (a) XRD patterns, (b) crystal structure, (c) M-T data, and (d) MR data of order-disorder NBMO.

References:

1. D. Akahoshi et al. Phys. Rev. Lett. 90 (2003) 177203.
2. T. Nakajima et al. J. Phys. Soc. Jpn. 73 (2004) 2283.

PC-12

Enhanced light absorption in ultrathin CIGS solar cells using plasmonic nanoparticles

Sachin V Desarada, Nandu B Chaure

^aDepartment of Physics, Savitribai Phule Pune University, Pune, Maharashtra (IN) – 411 007
 e-address: sachind@physics.unipune.ac.in

The plasmonic effect in photovoltaics is gaining attention due to optical absorption enhancement properties in solar cells. Plasmonic structures show the wavelength selective photon scattering based on their shape, size and surrounding dielectric medium. Plasmonic enhancement is achieved through the collective oscillation of free electron cloud in the metallic materials when the size is below the wavelength of incident radiation.

The current study explores the application of plasmonic gold (Au) nanoparticles (NPs) in CuInGaSe₂ (CIGS) solar cells by using the finite element analysis method for simulation. We used COMSOL Multiphysics to simulate opto-electronic properties which solve the Poisson's and continuity equation coupled with Maxwell's equation using the below equations:

$$J_n = qn\mu_n \nabla E_c + qD_n \nabla n - qn \nabla \ln(N_c) + qnD_{n,th} \nabla \ln(T) \quad (1)$$

$$J_p = qp\mu_p \nabla E_v + qD_p \nabla p - qp \nabla \ln(N_v) + qpD_{p,th} \nabla \ln(T) \quad (2)$$

$$\nabla \times (\nabla \times E) - k_0^2 \epsilon_r E = 0 \quad (3)$$

Au NPs show different resonance frequencies in a semiconductor material, which could be used for selective wavelength absorption enhancement. Results show that the unabsorbed light in base CIGS is being absorbed in the devices with embedded Au NPs. Figure 1 shows the electric field enhancement, which shows the photon intensity enhancement after being scattered from the Au NPs. The current study reveals the effective use of plasmonic nanoparticles for efficient light absorption, which can decrease the thickness of high-efficiency thin films CIGS solar cells.

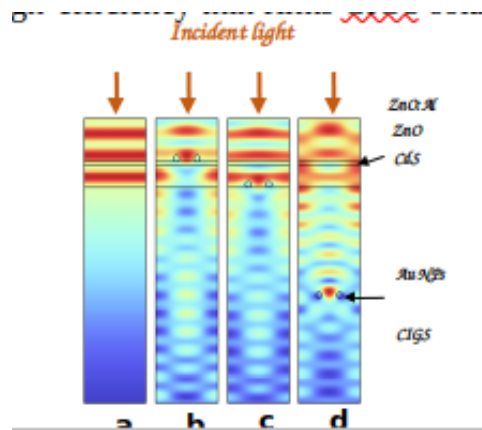


Figure 4: Electric field distribution at 600nm in a) base CIGS cell, and embedded NPs at the b) AZO, c) CdS and d) CIGS semiconductor layer.

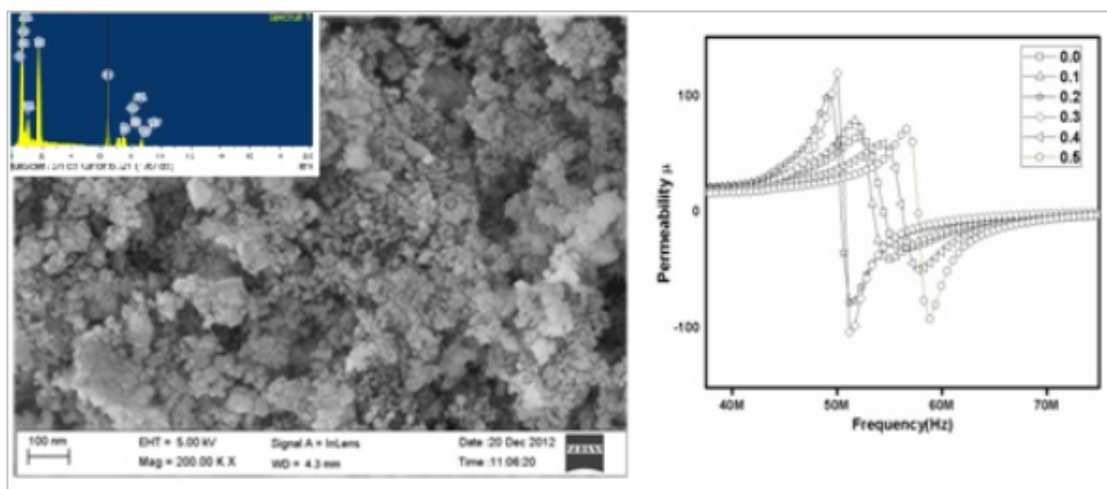
PC-13

Structural and magnetic properties of NiCuMgZn/SiO₂ nanocomposites

Ch.Sujatha

Assistant professor, Department of Physics, RGUKT Basar
 e-address: sujatha.iiit@rgukt.ac.in

The samples prepared by sol-gel method using tetraethyl ortho silicate (TEOS) as a precursor for silica effectively minimized agglomeration of magnetic nanoparticles. The magnetic nanoparticles having high surface area and modified cation distribution and increased interactions among the particles showed enhanced structural and magnetic properties compared to their bulk counter parts^{1,2}. The structural and magnetic properties of the sintered Ni_{0.5-x} Mg_x Cu_{0.05} Zn_{0.45} Fe₂ O₄ / SiO₂ samples were investigated. The crystallite size (D=15 nm - 30 nm) determined from the XRD pattern confirmed the nanocrystalline nature of the samples. The microstructures of the samples displayed ultra fine grains. The hysteresis loop of the samples demonstrated non saturation magnetization behavior indicating the particles are in the nanometer range. The magnetization showed decreasing tendency with Mg content. Non magnetic silica as a matrix successfully reduced the particle size. The samples having ultrafine particles with high resistivity, low eddy currents and high frequency stability of permeability make these materials potential candidates for high frequency electronic applications.



References:

1. Jun Wang, Wei Wu, Fan Zhao, and Guo-meng Zhao, Appl.Phys.Lett.98,083107(2011).
2. Santi Phumying, Sarawuth Labuayai, Ekaphan Swatsitang, Vittaya Amornkitbamrung, Santi Maensiri, Mater.Re. 2065,(2013)..

PC-14**Studies on aluminium and indium co-doped ZnO thin films for gas sensing application**

L.H. Kathwate, V. D. Mote*

Thin film and Material Science Research Laboratory, Department of Physics, Dayanand Science College, Latur. -413512, Maharashtra, India

corresponding author: vmote.physics@gmail.com

Nanostructured aluminium and indium co-doped ZnO thin films were prepared on a soda lime glass substrate using the spray pyrolysis method with equal variation in co-dopant concentrations. The zinc acetate dihydrate, aluminum acetate, and indium (III) acetate were used as the starting material. The microstructure and gas sensing properties of the ZnO films were studied as a function of co-dopant concentration. XRD pattern confirms that prepared films were oriented along c-axis and contained wurtzite crystalline symmetry. Further XRD result revealed that as the co-dopant concentration increased, the crystallinity of the films deteriorated dramatically. The FE-SEM images showed that the AIZO films grew like a cluster of spherical nanoparticles, which transformed into a nanosheet-like structure with an increasing co-doping percentage. The gas sensing properties of AIZO thin films were studied toward gases namely ammonia, acetone, ethanol, xylene, and methanol at room temperature. The films respond more strongly to ammonia gas suggesting that the AIZO sensor has excellent selectivity toward ammonia gas. Further, the gas sensing response of about 73%, the fast response time (~ 19 s), and recovery time (~ 17 s) towards 10 ppm ammonia gas are achieved for films when co-doped with 3 at% Al and 3 at% In. This result suggests that AIZO films are suitable candidates for ammonia gas sensor application.

Keywords:

AIZO thin films, Ammonia gas sensor, Response time, Recovery time.

PC-15**Gamma Radiation Shielding parameters of Li₂O Doped Lead Vanado Tellurite Glasses**

Mohansingh Heerasingh, T.Sankarappa*, Amarkumar Malge, Ashwini Devidas, B. Raghavendra.

Aravind Dyama, Jamadar Pallavi

Department of Physics, Gulbarga University, Kalaburagi

*Corresponding author: sankarappa@rediffmail.com

e-address: mhnaik6@gmail.com

This article presents γ -ray shielding parameters of lead-vanado-tellurite glasses doped with lithium oxide. The non-crystallinity of the samples was confirmed by XRD studies. Their room temperature density was measured by applying Archimedes principle. Using the data of density and composition, gamma ray shielding parameters were estimated with the help of Phy-X/PSD online software, for the energy range 0.015MeV - 15MeV. Mass attenuation coefficient (MAC) and linear attenuation coefficient (LAC) are found to decrease with photon energy. Obtained LAC indicated that the glass having lowest Li₂O content has the highest gamma attenuation. Tenth value layer (TVL), half value layer (HVL) and mean free path (MFP) showed increasing trend with increase of γ -ray energy. Effective atomic number (Z_{eff}) and effective electron density (N_{eff}) are found to decrease with energy. The mean free path (MFP) results revealed that present glasses are effective for shielding at lower photon energy. Based on all the obtained shielding parameters, the present glasses can be proposed for γ -ray shielding at low energy.

Keywords:

lead vanado tellurite glasses, density, Mass attenuation coefficient, Tenth value layer, half value layer, mean free path.

Acknowledgement :

Mohansingh Heerasingh acknowledges the financial assistance in the form of a research student's fellowship from the Gulbarga University.

References :

1. M. G. Dong, M. I. Sayyed, G. Lakhshminarayana, M. Celikbilek Ersundu, A. E. Ersundu, Priyanka Nayar, M. A. Mahdi, J. of Non – Cryst. Solids, <http://dx.doi.org/10.1016/j.jnoncrsol.2017.04.018>
2. Y. Al-Hadeethi, M. I. Sayyed, J. of Ceramics International, <https://doi.org/10.1016/j.ceramint.2019.10.212>.
3. K. V. Ramesh, N. Manjula Bharathi, B. Srinivasa Rao, P. Appala Naidu, International J. of Modern Physics B 23 (2009) 4833 – 4841.
4. Huseyin Ozan Tekin, Ghaida Bilal, Hesham M. H. Zakaly, Gokhan Kilic, Shams A. M. Issa, Emad M. Ahmed, Yasser Saad Rammah, Antoaneta Ene, J. of Materials, (2021) 14, 3897.
5. Erdem Sakar, Ozgur Ozpolat, Bunyamin Alim, M. I. Sayyed, Murat Kurudirek, J. of Radiation Physics and Chemistry, 166 (2020) 108496
6. Y. Al-Hadeethi, M. I. Sayyed, Hiba Mohammed, Lia Rimondini, J. of Ceramics International, 46 (2020) 251 – 257.
7. J. S. Ashwajeet, T. Sankarappa, R. Ramanna, T. Sujatha, N. Nagaraja, B. Vijaykumar, Research Journal of Material Sciences, 3(4) (2015) 1-6.
8. M. S. Al – Buriahi, V. P. Singh, Amani Alalawi, Chahkrit Sriwunkum, Baris Tonguc, J. of Ceramics

International, 46 (2020) 1564 – 15472.

9. Reza Bagheri, Alireza Khorrani Moghaddam, Seyed Pezhman Shirmardi, Bakhtiar Azadbakht, Mojtaba Salehi, J. of Non – Cryst. Solids <http://dx.doi.org/10.1016/j.jnoncrysol.2017.10.006>

10. Y. Al-Hadeethi, M. I. Sayyed, Y. S. Rammah, J. of Ceramics International, doi:10.1016/j.ceramint.2019.09.185.

11. M. I. Sayyed, H. Elhouichet, J. of Radiation Physics and Chemistry, [http : // dx . doi . org / 10 . 1016 / j . radphyschem.2016.09.019](http://dx.doi.org/10.1016/j.radphyschem.2016.09.019).

12. Shamsan S. Obaid, Dhammajyot K. Gaikwad, Pravin P. Pawar, J. of Radiation Physics and Chemistry, <http://dx.doi.org/10.1016/j.radphyschem.2017.09.022>.

13. Shamsan. S. Obaid, M. I. Sayyed, D. K. Gaikwad, Pravina, P. Pawar, J. of Radiation Physics and Chemistry, <https://doi.org/10.1016/j.radphyschem.2018.02.026>.

14. Samir Y. Marzouk, Ahmed H. Hammed, H. M. Elsaghier, W. Abbas, Nehad A. Zidan, J. of Non – Cryst. Solids, doi:10.1016/j.jnoncrysol.2017.08.031.

PC-16**Temperature-dependent dielectric relaxation and ac-conductivity of $\text{Ca}_3\text{PO}_4:\text{Tm}^{3+}/\text{Yb}^{3+}$ impedance spectroscopy**K.M. Krishna^a, K.Kumar^b^{a,b}Optical Materials and Bio-imaging Research Laboratory, Department of Applied Physics, Indian School of mines, Dhanbad-826004 (India).^aBVRIT, Narsapur, TS, Indiae-address: krishna.nano@gmail.com

Lead-free $\text{Ca}_3\text{PO}_4:\text{Tm}^{3+}/\text{Yb}^{3+}$ (CPR) polycrystalline is successfully synthesized via a high-temperature solid-state method and sinter at 1000°C temperature for 3 h. X-ray diffraction (XRD) and field emission scanning electron microscopy were employed to obtain structural information (FE-SEM). CPR has a rhombohedral phase according to the XRD pattern. The dielectric properties of all of the new phosphates were measured as a function of frequency. These new rare earth phosphates exhibit a low dielectric constant and a moderate dissipation factor. The dielectric properties of the prepared samples are measured at different temperatures up from 313 K to 373 K over a wide frequency range of 100 Hz to 5 MHz. A detailed examination of the dielectric constant (ϵ') and dielectric loss ($\tan \delta$) reveals a strong dependence on applied frequency, regardless of temperature. The impedance analysis confirms the CPR typical negative temperature coefficient of resistance (NTCR). Ca_3PO_4 with $\text{Tm}^{3+}/\text{Yb}^{3+}$ co-doping evident better insulation degradation behavior. Such material properties at low temperatures can be used in antenna applications.

References:

J. Ye, G. Wang, X. Chen, X. Dong, Effect of rare-earth doping on the dielectric property and polarization behavior of antiferroelectric sodium niobate-based ceramics, *J. Mater.* 7 (2021) 339–346. <https://doi.org/10.1016/j.jmat.2020.08.007>.

PC-17

Effect of Site Disorder on Structural and Magnetic Relaxation in $\text{Co}_2\text{Fe}_{0.5}\text{Ti}_{0.5}\text{Si}$ Quaternary Heusler Alloy Thin Film

Mainur Rahaman^a, Lanuakum A Longchar^a, M. Manivel Raja^b, Arabinda Haldar^c, S. N. Kaul^a, S. Srinath^a

^aSchool of Physics, University of Hyderabad, Hyderabad-500046, Telangana, India

^bDepartment of Physics, Indian Institute of Technology Hyderabad, Kandi 502285, Telangana, India

^cDefence Metallurgical Research Laboratory, Hyderabad-500058, Telangana, India

e-address: 18phph02@uohyd.ac.in

Motivated by an immense scientific interest in Co-based Heusler compounds¹⁻², 100 nm $\text{Co}_2\text{Fe}_{0.5}\text{Ti}_{0.5}\text{Si}$ (CFTS) thin films were grown on Si (100) by ultra-high vacuum dc magnetron sputtering at different substrate temperatures (TS) 200°C, 300°C, 450°C, 500°C, and 550°C. Energy-dispersive X-ray absorption spectroscopy yielded the actual alloy composition as $\text{Co}_{2.01}\text{Fe}_{0.51}\text{Ti}_{0.24}\text{Si}_{1.24}$. X-ray diffraction (XRD) patterns, shown in following figure (a), reveal no Bragg peaks for TS200 film, a broad fundamental peak (220) for TS350 film, and three sharp peaks (111), (220), and (422) for the remaining films. Thus, the crystalline structure gradually evolves from amorphous to an ordered $L2_1$ structure as the TS increases. In this work, broad-band and X-band FMR measurements have been carried out to investigate the effect of site disorder on magnetization (M_s), magnetic anisotropy (H_k), Landé splitting factor (g), and Gilbert damping constant (α) in CFTS Heusler alloy thin films. The film deposited at 500°C has an $L2_1$ crystal structure, a value of 2.02 for Landé splitting factor, g , maximum saturation magnetization ($M_s = 780$ G), and minimum Gilbert damping constant ($\alpha = 0.0055$)(see following figure (b)).

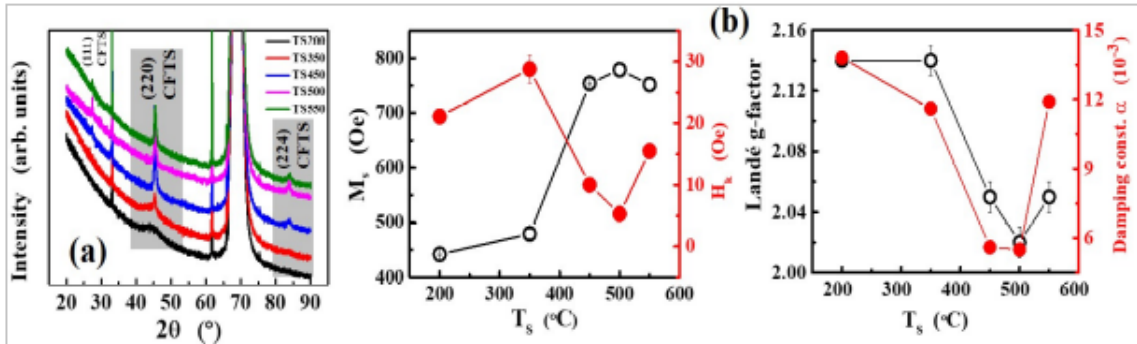


Figure 5: (a) XRD patterns (b) Variation of M_s , H_k , g , and α with respect to TS of CFTS films.

References:

1. Y. Miura, et al. J. Appl. Phys. 99, 08J112 (2006).
2. J. Chen, et al. Appl. Phys. Lett. 110 (2017) 242401.

PC-18**Nitrosamine Clusters in Water Solvent: Spectroscopy and Many-body Interactions**

Sumalya Kaluva and Mahadevappa Naganathappa*

Department of Physics, School of Science, GITAM (Deemed to be University), Hyderabad 502329 (TS) India

*Corresponding author: swamimahadev25@gmail.com

e-address: sumalyaadwi@gmail.com

The present study reports the spectroscopic and many-body interactions of nitrosamine in the water solvent. Nitrosamine is slightly soluble in water, vegetable oils, and organic solvents. The nitrosamines comprise a family of powerful carcinogenic compounds which are formed readily from various nitrogen compounds such as nitrite and their various derivatives^{1,2}. The utilization of solvent ranges between 80 to 90 % in pharmaceutical industries and other chemical operations³. Nitrosamine oligomers such as monomer to pentamer considered for the study. The different structural arrangement of nitrosamine leads to linear, ladder and cyclic forms which have been considered for the study. The spectroscopic characterization viz. geometrical parameters, infrared and electronic absorption spectra and natural transitions orbitals (NTOs) have been reported. Upon increase in number of fragments in the nitrosamine cluster there is significant change in the geometrical parameters and frequency of vibrational modes. The nitrosamine oligomers have been optimized at B3LYP-D3/6-311++G** level of theory. The electronic absorption spectra calculated using time-dependent density functional theory (TD-DFT) has been used at the same level of theory. The HOMO to LUMO gap has been reported for all the clusters of nitrosamines in water solvent. The solvation model IEFPCM has been used. The many-body interactions of nitrosamine oligomers from monomer to pentamer have been reported. To study the many-body interactions single point energy calculations performed at B3LYP-D3 (empirical dispersion=GD3) and 6-311++G** basis set. The sum of two-body interaction energies has significant contribution to the binding energies of nitrosamine oligomers. The binding energies increase from dimer to pentamer, which represents the decrease in stability of the molecule from dimer to pentamer. All calculations were performed with Gaussian 16 program package.

Keywords:

Nitrosamine clusters, Many-body interactions, Vibrational frequencies, electronic absorption spectra, quantum chemical methods, Hydrogen bonding.

References:

1. F. Murad *Angew. Chem. Int. Ed.*, 38 (1999), p. 1856.
2. P. Jiang, Q. Ximei, L. Chunhui, Q. Chunhua, W. Dianxun *Chem. Phys. Lett.*, 277 (1997), p. 508.
3. David, J. C. Constable, Conchita Jimenez-Gonzalez, and Richard K. Henderson. 'Perspective on Solvent Use in the Pharmaceutical Industry', *Organic Process Research and Development*, 11, p133-137

PC-19**Determination of natural radioactivity in some building materials**V. Thangam^a, A Chandrasekaran^{a,*}, C Gurumoorthy^b, C K Senthil Kumar^b^aDepartment of Physics, Sri Sivasubramaniya Nadar College of Engineering, Kalavakkam – 603110 Chennai.^bCentre for Applied Nuclear Research in Science and Engineering Education, Bharath institute of higher education and research, Selaiyur – 600073 Chennai.

*Corresponding author: chandrasekarana@ssn.edu.in

e-address: thangamj3@gmail.com

Building materials, rocks, and soils contain natural radionuclides such as ^{226}Ra , ^{232}Th and ^{40}K . These radionuclides continuously emits gamma rays which is harmful to living organisms. Knowledge of natural radioactivity of building materials is essential because most individuals spend 80% of their time indoor. Hence, in the present work, the activity concentrations of the radio nuclides ^{226}Ra , ^{232}Th and ^{40}K are determined using NaI(Tl) detector based Gamma ray spectrometer in some commercial building materials such as hollow block, tiles and granites from Tirunelveli District, Tamilnadu, India . The results reveal that the average activity concentrations for ^{226}Ra in hollow block, tiles and granites samples are 42.66, 88.02 and 60.39 Bq kg⁻¹ respectively and concentrations of ^{232}Th radionuclide for the same samples obtained were 13.25, 57.26 and 12.59 Bq kg⁻¹. Finally, the values of ^{40}K were 544.2, 578.04 and 587.65 Bq kg⁻¹. The effect of radiation from these building materials were assessed by radium equivalent activity (R_{eq}), indoor gamma absorbed dose rate (D_R) and annual effective dose equivalent (AEDE) by comparing them with the recommended limits prescribed by UNSCEAR. The values of annual effective dose rate were 0.25, 0.49 and 0.07 mSvy⁻¹ respectively and are much lower than the prescribed limit of unity. From the radiological point view, the above results suggest that these materials used in construction do not pose any harmful effect.

Keywords:

building materials, radionuclides, gamma ray spectrometry, AEDE.

References:

1. UNSCEAR, 2000. United Nations Scientific Committee on the Effect of Atomic Radiation. Sources and Effects of Ionizing Radiation. Report to general Assembly, with Scientific Annexes, United Nations, New York;
2. Beretka J, Matthew PJ (1985) Natural radioactivity of Australian building materials, industrial wastes and by-products. Health physics 48(1): 87-95.

PC-20

Transport Spectroscopy in a Low Phosphorous Doped Silicon Nano-Transistor

Soumya Chakraborty^a, Pooja Yadav^a, Arup Samanta^{a,b}

^aQuantum Nano-Science and Technology Lab, Physics Department, Indian Institute of Technology Roorkee, Roorkee, India-247667

^bCentre of Nanotechnology, Indian Institute of Technology Roorkee, Roorkee, India-247667
e-address: schakraborty@ph.iitr.ac.in

Dopant-atom based silicon nano-transistors and related devices have drawn immense attention in recent decades due to their vast and diverse possibilities¹⁻⁴. Individual or a few coupled dopants working as quantum dot (QD) may resonate a adverse effect in the dynamics of nano-electronic devices as their number and precise location can't be accurately controlled while fabricating by using standard diffusion doping technique, resulting in significant fluctuations in transistor characteristics for different devices.⁵

Here, we present finite-bias characterisation of electrical transport through such a device fabricated on silicon-on-insulator (SOI) wafer with low phosphorus doping ($\sim 10^{17} \text{ cm}^{-3}$) as shown in Fig. 1(a-b). One of such devices, we observe multiple Coulomb blockade oscillations having quasi-periodicity at low temperature of 5.5 K, as presented in Fig. 1(c). Such behaviour of the transport characteristics is quite unique for our device, where formation of dopant cluster is very less likely to observe such quasi-periodic feature owing to low doping concentration. Quasi-Periodic nature of the Coulomb diamonds with repetition of 4 and 5 diamonds within each group as pointed in Fig.1(c) suggests interaction of multiple dopants with a larger size quantum dot. The possible schematic device configuration, potential distribution along the channel and equivalent electrical circuit model are presented in Figs. 1(b), 1(d) and 1(e), respectively. The theoretical calculation of the transport characteristics by using Monte-Carlo methods for Orthodox theory of Coulomb blockade is presented in Fig. 1(f), which quite supports the experimental observed data.

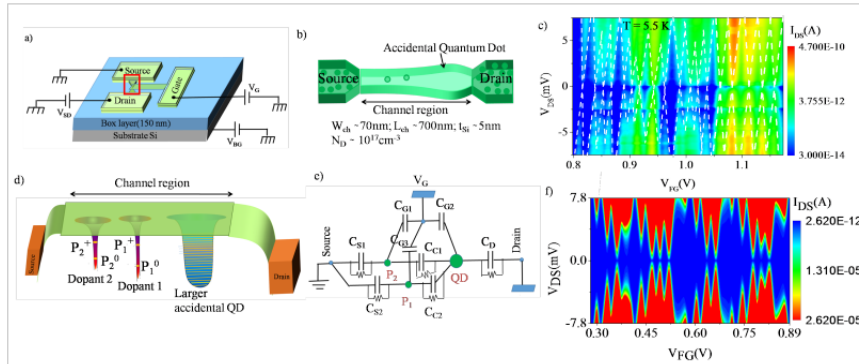


Figure 6: a) Bird's eye view of an SOI-FET. b) Schematic doping distribution in the low-doped device. c) Experimental stability diagram of the device at $T = 5.5 \text{ K}$. d) Schematic dopant potential profile in the device channel region. e) Proposed Capacitor model corresponding the device. f) Simulated stability diagram using the capacitor model shown in (e)

References:

1. Sellier H. et al.; Phys Rev Lett. 2006;97:206805;
2. Pierre, M. et al; Nature Nanotech. 5, 133–137 (2010).

3. J. J. Pla et al.; Nature 489, 541 (2012).
4. Hamid E et al.; Applied Physics Letters 97(26):262101
5. Yadav P et al.; arXiv preprint arXiv:2204.03890.Sellier H. et al.

PC-21

Correlation between structural, static and dynamic magnetic properties in $\text{Co}_2\text{FeAl}_{0.5}\text{Si}_{0.5}$ Heusler alloy thin films.

Lanuakum A Longchar^a, Mainur Rahaman^a, Manik Kuila^b, V. Raghavendra Reddy^b, M. Manivel

Raja^c, Arabinda Haldar^d, S. N. Kaul^a and S. Srinath^a

^aSchool of Physics, University of Hyderabad, Hyderabad-500046, Telangana, India,

^bUGC-DAE Consortium for Scientific Research, University Campus, Khandwa Road, Indore 452001, India

^cDefence Metallurgical Research Laboratory, Hyderabad-500058, Telangana, India

^dDepartment of Physics, Indian Institute of Technology Hyderabad, Kandi-502285, Hyderabad India.

e-address: 17paph18@uohyd.ac.in

Thermal stability of the half-metallic band gap at the Fermi energy and high spin polarization of $\text{Co}_2\text{FeAl}_{0.5}\text{Si}_{0.5}$ (CFAS) Heusler alloys have made these systems attractive for spintronic applications. CFAS thin films of thickness, $t = 12 - 75$ nm, were deposited by ultrahigh vacuum dc magnetron sputtering on $\text{SiO}_2/\text{Si}(100)$ substrates, at optimum substrate temperature of 500°C . The GIXRD patterns shows B2 structural order. Investigation of magnetocrystalline anisotropy (MCA) and magnetic reversal (MR) process using magneto-optical Kerr effect microscopy shows that, all the CFAS films exhibit in-plane uniaxial anisotropy (figure 1(a) and (b)) and the observed variations of coercive field (H_c) with field-angle, ϕ_H , is well described by the modified two-phase pinning (TP) model. Furthermore, ferromagnetic resonance (FMR) study reveals that the film with thickness, $t = 50$ nm has the highest magnetization M_s (~ 1187 Gauss), highest H_k (~ 94 Oe), lowest Gilbert damping constant α (~ 0.002) and the least ΔH_h contribution, shown in Fig.1(c).

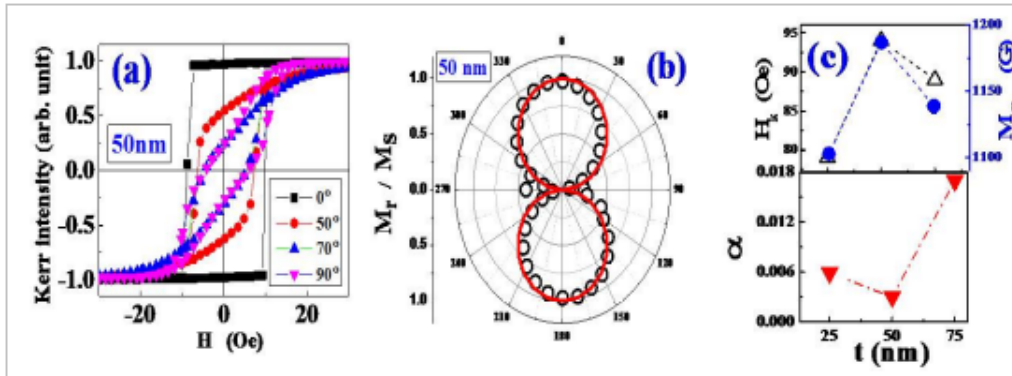


Figure 7: Static magnetic hysteresis loop at different in-plane field angles, (b) Angular variation of M_r/M_s , (c) Variation of M_s , H_k and α with t .

References:

G. H. Fecher and C. Felser, J. Phys. D. Appl. Phys. 40, 1582 (2007).

PC-22

Effect of oxygen partial pressure on the microwave tunability of the pulsed laser deposited BaO.5SrO.5TiO3 thin films

Akhil Raman T S, Shivakumar C, Andrews Joseph, K.C. James Raju

University of Hyderabad, Hyderabad, India

e-address: akhilramants@gmail.com

The dependence of microwave dielectric constant tunability of BaO.5SrO.5TiO3 (BST) thin films on the oxygen partial pressure during the pulsed laser deposition (PLD) is studied. BST thin films were deposited on Pt coated silicon substrates by PLD method. The oxygen partial pressure during the deposition were varied from 5×10^{-6} mbar to 1×10^{-1} mbar at a constant temperature of 700°C . The phase and structural properties of the BST thin films were investigated by x-ray diffraction. The dielectric properties were determined by fabricating a circular patch capacitor (CPC) structure and were measured using VNA in the frequency range from 1 GHz to 2GHz. at different external DC bias and dielectric constant and the tunability is calculated.

The X-ray diffraction studies shows that the BST thin films are polycrystalline in nature and have cubic structure (following Fig.). The tunability measurements shows that the BST thin films deposited at a higher oxygen partial pressure has a higher tunability and the tunability decreases monotonically with the decrease of the oxygen partial pressure during the deposition. The BST thin film deposited at 5×10^{-1} mbar pressure has a tunability of 78% and it decreases to 50% for the film deposited at 5×10^{-6} mbar pressure(following Fig.)

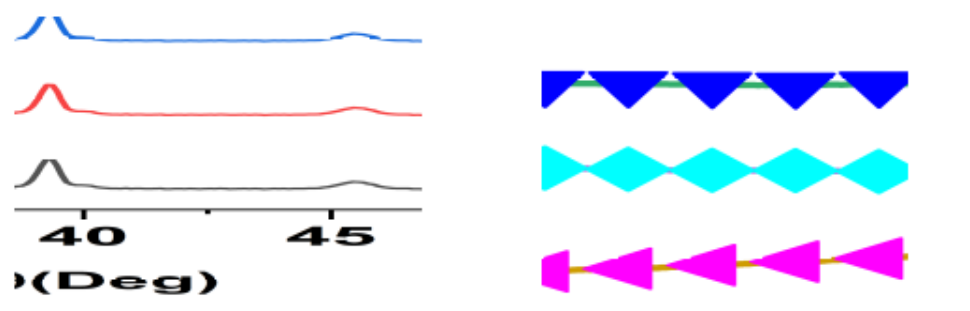


Figure 8: XRD patterns of BST5 thin films, Tunability of BST thin films at 10V DC bias

References:

1. Zhu, X. H., et al. Journal of Physics D: Applied Physics 39.10 (2006): 2282.
2. N. K. Pervez, P. J. Hansen and R. A. York, Appl. Phys. Lett. 85, 4451 (2004)

PC-23

Green Synthesis of Hematite Nanoparticles using *Tabernaemontana Divaricata* Flower Extract: Structure, Optical, Morphology and Dielectric Studies

Toton Sarkar^a, Gurupada Ghorai^b, Pratap K. Sahoo^b and Ashis Bhattacharjee^{*a}

^aDepartment of Physics, Visva-Bharati University, Santiniketan 731235, India

^bSchool of Physical Sciences, National Institute of Science Education and Research (NISER) Bhubaneswar, An OCC of Homi Bhabha National Institute, Jatni-752050, Odisha, India.

e-address: totonsarkar.rs@visva-bharati.ac.in

Iron oxide (α -Fe₂O₃, hematite) is an n-type semiconductor with wide band gap (2.2 eV) which is non-toxic and abundant-in-nature. Hematite on a nanoscale has various application potentials. Though the hematite nanoparticles are synthesized by several conventional techniques, e.g., coprecipitation, hydrothermal, combustion, and chemical, recently a significant progress has been made in producing hematite nanoparticles¹ through a new eco-friendly and safe technique called green synthesis² as an alternative. Presently, we report the synthesis of iron oxide nanoparticles by green synthesis technique using the *Tabernaemontana divaricata* (Indian name, Tagar) flower extract as a reducing/capping agent. The green synthesized iron oxide material is characterized using several physical techniques. Powder X-ray diffraction and Raman spectroscopy confirm that the synthesized material is of single crystalline phase of hematite, and the crystallites have an average size of ~ 35 nm. From the UV-Vis DRS study the direct and indirect energy band gap values have been estimated. Multiple peaks observed in the PL spectra indicate the presence of various defects in the hematite nanoparticles. SEM images are used to study the effect of the extract on the morphology of the particles and also to estimate the particle size. Dielectric constant, dielectric loss and ac conductivity of the synthesized material have been studied as a function of frequency and temperature. A considerably high dielectric constant of hematite has been observed. Observed results indicate the significant role of the extract used for the synthesis of hematite nanoparticles.

References

1. R. Vinayagam, et al., *Surfaces and Interfaces*, vol. 20, p. 100618-100626, 2020.
2. M. Huston, et al., *Nanomaterials*, vol. 11, pp. 1–29, 2021.

PC-24**Effect of Strontium Substitution on the Structural and Magnetic Properties of Barium Hexaferrite**Annarose J Palliya^a, M Thilak^a, A Das^a, J A Chelvane^b, V Gorige^a^aSchool of Physics, University of Hyderabad, Gachibowli, Hyderabad, 500046, India^bAdvanced Magnetism Laboratory, DMRL, Kanchanbagh, Hyderabad 500058, Indiae-address: annajpalliy@gmail.com

Ferrites are of great interest due to their promising device applications at room temperature (RT)¹. Mainly, hexaferrites have gained broader attention in permanent magnet applications for the past couple of years owing to their structure-property relations. In this regard, an attempt has been made to study the structural, spectroscopic, and magnetic properties and correlations among them in strontium substituted barium hexaferrite, which enable us to tune these materials for suitable applications.

A series of samples with compositional formula, $Ba_{1-x}Sr_xFe_{12}O_{19}$ ($0 \leq x \leq 1$) were synthesized by the citrate-based sol-gel auto-combustion technique. The prepared samples were structurally characterized by x-ray diffraction measurements, and the data were analyzed by the Rietveld refinement technique by assuming $P6_3/mmc$ space group². The analysis depicts the decreasing of lattice parameters with increasing Sr substitution as per the Vegard's law and is attributed to replacement of larger ion (Ba: 1.42 Å) with the smaller one (Sr: 1.25 Å)³. Field emission scanning electron microscopy images found to show a clear grain formation and their variation with Sr substitution is minimal and is attributed to the internal stress in the samples. Raman data obtained on these samples reveals the interplay between magnetic ion site-occupancies and the corresponding magnetization contributions. In view of this, magnetic field and temperature-dependent magnetic (M-H and M-T) response of these samples were measured and it has been found to have significantly hard magnetic nature (very high coercivity) at RT. As these hexaferrites are composed of lattice layers of (ferro- and antiferro-) magnetic structures, the sub-lattice magnetic contributions were estimated by fitting the M-H data using theoretical models. The obtained parameters were analyzed, and their trends were predicted for suitable permanent magnet applications.

References:

1. Kim S K, Beach G S D, Lee K J, Ono T, Rasing T and Yang H 2022 Nat. Mater. 21, 24.
2. Mahboobeh A and Ahmad G 2020 J. Phys. Chem. Solids 147, 109660.
3. Shannon R D 1976 Acta Cryst. 32, 751.

PC-25

Variation of Gilbert Damping Constant via Interface Induced Magnetic Anisotropy in LSMO/PMN-PT Heterostructures

Avisek Das^a, Mrinalini^a, Takamasa Usami^b, Satya Prakash Pati^b, Tomoyasu Taniyama^b and Venkataiah Gorige^a

^aSchool of Physics, University of Hyderabad, Gachibowli, Hyderabad 500046, India

^bDepartment of Physics, Nagoya University, Furo-cho, Chikusa-ku, Nagoya 464-8602, Japan

e-address: 20phph03@uohyd.ac.in

The field of magnonics is emerging at blistering pace in the present era due to its promising room-temperature applications in logic-based devices at low-power consumption. In view of this, the exploration of suitable ferromagnetic $\text{La}_{0.67}\text{Sr}_{0.33}\text{MnO}_3$ (LSMO) and ferroelectric $\text{Pb}(\text{Mg}_{0.33}\text{Nb}_{0.67})\text{O}_3\text{-PbTiO}_3$ (PMN-PT) magnetoelectric (ME) heterostructures is of prime interest due to their intimate interface contact¹.

In the present work, a 50 nm thick epitaxial LSMO is grown on PMN-PT single crystal oriented in [001] and [111] directions by using pulsed laser deposition. The static and dynamic magnetic response of LSMO/PMN-PT is studied by performing magnetization and ferromagnetic resonance (FMR) measurements. Due to strong ME coupling at the interface, the LSMO/PMN-PT(001) shows four-fold axes of magnetic anisotropy (MA) whereas LSMO/PMN-PT(111) shows isotropic behaviour. The observation has been interpreted on the basis of coupling between the resultant polarisations of PMN-PT and the net magnetisation vector of LSMO. With a view to understand the effect of ME-induced MA on the magneto-dynamic response along easy and hard magnetic axes of LSMO, the FMR measurements were carried. The FMR data were fitted with Kittel's equation and Gilbert damping constant (α), which is crucial parameter for spin-wave (SW) dynamics, was estimated. The calculated α values were found to be $\sim 10^{-2}$. As the LSMO/PMN-PT(001) is anisotropic in nature, α is found to be less along the hard axis compared to the easy direction. While, the LSMO/PMN-PT(111) is isotropic in nature, the α remains same in all directions. With a view to know the electric (E-) field effect on spin dynamics, the FMR data were collected on LSMO/PMN-PT poled ($E = \pm 10$ kV/cm) samples, and a significant reduction in α values was noticed. Although more investigations are required, this particular work hints that it becomes possible to realize E-field controlled spin-waves in FM/FE heterostructures to develop futuristic magnonic devices.

References:

1. D. Pesquera, E. Khestanova, M. Ghidini, S. Zhang, A. P. Rooney, F. Maccherozzi, P. Riego, S. Farokhipoor, J. Kim, X. Moya, M. E. Vickers, N. A. Stelmashenko, S. J. Haigh, S. S. Dhesi, and N. D. Mathur, Nat. Commun. 11, 3190 (2020).

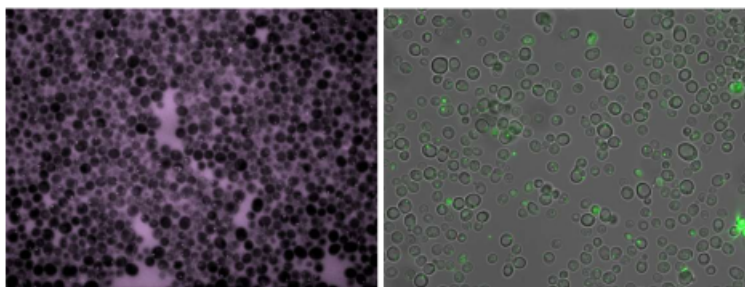
PC-26

Particle-Tracking Microrheology in Yeast

Sruthi N, Sharath Ananthamurthy

^aSchool of Physics, University of Hyderabad, Gachibowli, Hyderabad – 500046, India
e-address: sruthikd6@gmail.com

Experiments carried out earlier suggest that the reorganization of chromatin and nucleolus affects the mechanical properties like the malleability of the nucleus, leading to altered shapes. In this work we would like to measure the forces exerted on the nuclear envelope by chromatin and the nucleolus in wild type and mutant yeast cells and ask if the chromatin has any role in maintaining the shape of the nucleus. We hypothesize that in the absence of lamina, in fungi, the chromatin and chromatin-based compartments themselves provide mechanical stability and shape. The forces generated are linked to the viscoelasticity changes within the nucleus, information that is to be obtained from tweezing experiments. Particle tracking measurements would yield us information on the cellular environment near the nucleolus in cells. We plan to track fluorescent polystyrene beads of diameter 1 μm and 0.1 μm inside a yeast cell, around its organelles like Vacuole, Endoplasmic Reticulum and Nucleus, to characterize the cell environment as a preliminary method to quantify the rheology via parameters like viscosity and shear modulus, most importantly near the Nuclear membrane in mutant cells vs ‘normal’ cells. Currently we are under optimizing the internalization of these beads by cells and acquiring best images for particle tracking. Later the beads would be Plasmonically tweezed to generate forces.



Acknowledgement:

Project JRF, Institute of Eminence Grant, School Of Physics, University of Hyderabad.

References:

- (1). Gurranna Male et.al, Journal of Cell Science (2020) 133: jcs242172.
- (2). Particle tracking microrheology of complex fluids, T.G. Mason et.al, Phys. Rev. Lett., 79:3282–3285, 1997.
- (3). Diego Herráez-Aguilar et al., Scient. Rep. (2020) 10:6707.

PC-27**Effects of Gamma Irradiation on Tantalum oxide based Resistive Random access memory devices**

R. Sai Prasad Goud^{a,d}, A. Mangababu^b, Arshiya Anjum^c, K. Ravi Kumar^b, Y. Rajesh^d, A.P. Gnana Prakash^c, A. P. Pathak^b and S.V.S. Nageswara Rao^{a,b,d}

^aCentre for Advanced Studies in Electronics Science and Technology (CASEST), University of Hyderabad, Hyderabad-500046, Telangana, India

^bSchool of Physics, University of Hyderabad, Hyderabad-500046, Telangana, India

^cDepartment of Studies in Physics, University of Mysore, Manasagangothri, Mysuru-57006, Karnataka, India

^dCentre for Nanotechnology, University of Hyderabad, Hyderabad-500046, Telangana, India

e-address: 18phpe01@uohyd.ac.in

Memory has been a basic building block for information technology. Among various memory technologies, Resistive Random Access Memory (RRAM) is an important element to replace the flash memory in future generation non-volatile memory applications. Recent studies have also proven its potential in harsh radiation environment of space. In this study, we present the effects of gamma irradiation on Tantalum oxide based RRAM devices. Indium tin oxide (ITO) coated glass was taken as bottom contact, on which Tantalum oxide (TaO_x) was grown using e-beam evaporation technique at different substrate temperatures (300°C and 500°C) during deposition. The top contact silver (Ag) was deposited using Thermal evaporation method. Surface morphological and electrical characterizations were performed on Ag/TaO_x/ITO RRAM devices. These devices were subjected to a wide range (100 Gy to 40 kGy) of doses of ^{60}Co Gamma irradiation. It was observed that the fabricated devices are sustainable even for heavy dose of 40 kGy. Defects created due to irradiation and their effects on switching properties of RRAM devices will be discussed in detail.

PC-28

Structural properties, lattice dynamics, and metallization of van der Waals solid iodanil ($C_6I_4O_2$) studied using density functional theory

Subrata Mondal^{a,b}, G. Vaitheeswaran^c, Tarek Ayadi^d, Sébastien Lebègue^e, M. K. Gupta^f, R. Mittal^{f,g}

^aAdvanced Centre of Research in High Energy Materials (ACRHEM), University of Hyderabad, Prof. C. R. Rao Road, Gachibowli, Hyderabad-500046, Telangana, India,

^bInstitute of Physics, Bhubaneswar 751005, Odisha, India,

^cSchool of Physics, University of Hyderabad, Prof. C. R. Rao Road, Gachibowli, Hyderabad-500046, Telangana, India,

^dLaboratoire de la Matière Condensée et Nanosciences, Faculté des Sciences de Monastir, Université de Monastir, 5019 Monastir, Tunisia,

^eLaboratoire de Physique et Chimie Théoriques (LPCT, UMR CNRS 7019) Institut Jean Barriol, Université de Lorraine, BP 239, Boulevard des Aiguillettes, 54506, Vandoeuvre-lès-Nancy, France,

^fSolid State Physics Division, Bhabha Atomic Research Center, Mumbai 400085, India, ^gHomi Bhabha National Institute, Anushaktinagar, Mumbai, 400094, India
e-address: samphy.mondal@gmail.com

A detailed ab initio study addressing the structural, lattice dynamics and pressure induced metallization has been carried out for solid iodanil ($C_6I_4O_2$). The computed ground state structural properties reveal the crucial role of considering van der Waals correction in determining these properties. Our computed phonon dispersion confirms the dynamical stability of solid iodanil in the $P2_1/c$ symmetry without having any imaginary phonon modes. In addition, an excellent agreement can be noticed between our computed zone centered phonon frequencies and experimentally reported results. The elastic constants were also calculated to ascertain the mechanical stability of the solid iodanil in addition to lattice dynamics. Moreover, the electronic band structure has been calculated using the quasiparticle G_0W_0 approximation which results in a band gap of 2.49 eV. This value is significantly larger than the value obtained by the generalized gradient approximation, thus emphasizing the importance of quasiparticle correction to solid iodanil. This study clearly shows a reduction of the band gap under pressure and hence resulting in a band overlap eventually driving iodanil to metallize around 22 GPa. The pressure variation of the inter- and intramolecular bond lengths as well as the charge density plots explain the significant role of intermolecular I-I distance in understanding the metallization of solid iodanil.

Interactions between active rotors studied using dual optical tweezer.

Ashwini V Bhat^a, Naveena C S^b, Sharath Ananthamurthy^b

^a Department of Physics, Jnanabharathi Campus, Bangalore University, Bangalore-560056,

^bSchool of Physics, University of Hyderabad, Hyderabad-500046

e-address: sasp@uohyd.ac.in

We report the interactions between internally driven active rotors studied using a dual optical tweezer. The active rotor is *Bacillus subtilis*, a wild-type, gram- positive bacterium that uses flagellar rotation for motility. A pair of bacteria is held in dual optical tweezer at different distances and their respective flagellar rotation are studied through the durations of their approach and retreat from each other. The aim of our work is to investigate the nature of the interactions between two active optically confined rotors in their pristine form. We find, that the frequency of the rotating flagella, decreases in confined bacteria on approaching each other and increases on retreat. In other words, the flagellar rotations slow down while in the presence of a nearby neighbor and speeds up as the neighbor retreats. However, on retreat, the flagellar rotation speed of the bacterium in the retreating trap is further lowered when compared to that of the trapped bacterium held in the static trap. We investigate through this setup the hydrodynamics mediated coupling between the two active rotors.

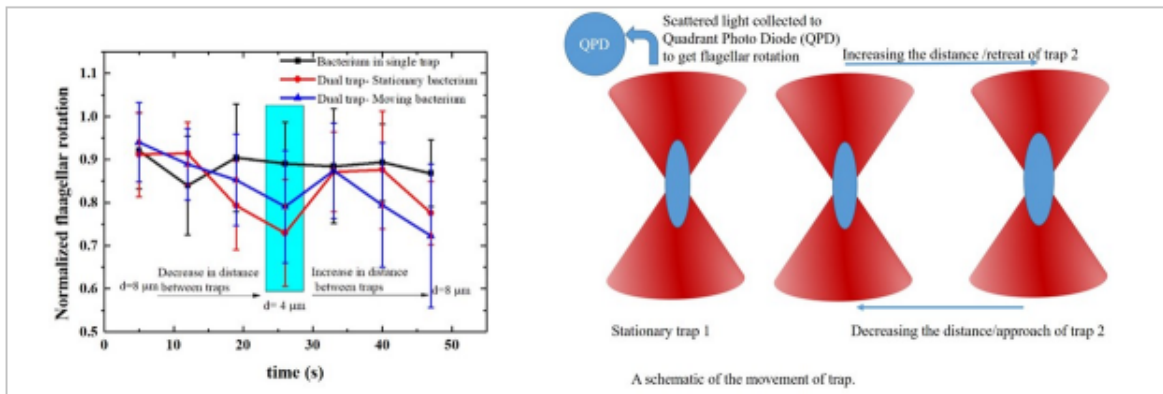


Figure 9: The graph shows the temporal variation in flagellar rotation frequency of the bacterium held at same laser power in a single optical trap (black), and in the stationary trap 1 (red) and in moving trap 2 (blue) during the approach and the retreat of bacterium in trap 2 in the dual tweezer setup. The shaded area indicates the time when the bacteria in the traps are closest to each other. The schematic of our experiment is on the right. The blue colored ellipsoids indicate the trapped bacteria.

Acknowledgements:

Ashwini V Bhat acknowledges a DST-INSPIRE fellowship. Naveena C S acknowledges CSIR-UGC-JRF.

PC-30**Effect of gallium substitution on formation of X-ferrite phase in a mixed ferrite system and its magnetic and dielectric properties**Ayushi Patel^a, Robert C. Pullar^b and Rajshree B. Jotania^{1a}.^aDepartment of Physics, School of Sciences, Gujarat University, Ahmedabad 380009, India^bDepartment of Molecular Science and Nanosystems, Università Ca' Foscari Venezia, Venice 30123, Italy.e-address: az72ze@gmail.com

Hexagonal ferrites are oxides of iron yielding applications in fields such as permanent magnets, microwave absorbers, devices in low frequency and high frequency applications, telecommunication, etc¹⁻³. The crystal structure of these hexaferrites (HFs) are characterized on the basis of stacking sequence of S, R and T blocks. The X-type HF is formed by a sequence SRS*S*R*¹ which encompasses the stacking sequence for M-type (SR) and W-type (RSS)² and thus X-type HFs are difficult to separate from W-type and M-type phase. In this study a series of HFs with gallium substitution have been synthesized by sol gel autocombustion method where the samples are sintered at 1250°C for 5 hours. The magnetic properties as well as the dielectric behaviour in the frequency region of 100 Hz to 2MHz and 200 MHz to 20 GHz have been observed. The structural investigation is done by FTIR, XRD and SEM analysis. The XRD pattern analysis reveal a very complex structure where numerable peaks of phases X-type, M-type and W-type are overlapping. To understand the phase purity better, Rietveld refinement done for pristine sample and the sample with highest gallium content reveals significant improvement in the formation of X-type phase from 5.52% to 22.39% with addition of gallium with W-type as major phase. The saturation magnetization show huge variation from 95.55 Am²kg⁻¹ to 65 Am²kg⁻¹ for pristine and gallium substituted samples. This suggests that as gallium content increases there is a better formation of desired X-type phase as low M_s values are characteristic of X-type hexaferrites. There is a significant change in the dielectric behaviour with gallium substitution. It leads to higher dielectric constant and high loss at lower frequency.

Keywords:

X-type hexaferrites, XRD, Rietveld refinement, Hysteresis loops, Electric modulus.

References:

1. R. C. Pullar, Prog. Mater. Sci., vol. 57, no. 7, pp. 1191–1334, Sep. 2012
2. J. Smit and H. P. J. Wijn, Ferrites. Philips Technical Library, 1959.
3. V. G. Harris, IEEE Trans. Magn., vol. 48, no. 3, pp. 1075–1104, 2012

PC-31**Active Material Host For Sodium-Ion Battery From Mechanically Stable Freestanding Carbon Nanotube (CNT)**

Arya Sohan^a, Poly Rose^a, P. Jeevan Kumar^a, V Seshu Bai^a, Amar Kumar^b, Preeti Yadav^b, T. N Narayanan^b, Pratap Kollu^a

^aSchool of Physics, University of Hyderabad, Prof CR Rao Road, Gachibowli, Hyderabad 500046, India

^b TATA institute of Fundamental Research -Hyderabad, Sy No 36/P Serilingampally Mandal, Telangana 500046, India
e-address: 18phph13@uohyd.ac.in

Sodium battery is emerging as a better substitute for expensive lithium-ion battery because of its low cost and abundance of sodium element in earth crust. But the major drawback of sodium battery is the diffusion difficulty of bulky sodium compared to lithium leads to low performance. Accommodating more active material to a highly porous holder can compensate this issue and can lead to higher specific capacity of sodium battery. In this work, interconnected carbon nanotubes have been synthesized using spray pyrolysis technique. Benzene boronic acid is used as a precursor to provide boron bindings that provides cross links between carbon nanotubes. These are light weight, freestanding and mesoporous in nature to act as a good active material host as well as current collector for sodium battery alloy-based anodes.

The weight of the synthesized CNT cutout of 12mm diameter is 2.2 mg whereas a traditional copper foil of same dimension is 10 mg. Moreover, the BET pore size analysis shows these ultra-light weight CNTs are highly porous (an average pore size of 0.14216 micrometers) so that diffusion of sodium ions can be easier. It must be capable enough to accommodate more active material with a low electrode weight. 12mm diameter and 0.4 mm thickness sized electrodes of CNTs are mechanically stable with the application of a static force from 3N to 18N with an increasing rate of 3N/minute at room temperature using a dynamic Mechanical Analyzer (DMA). The same experiment repeated in 100°C and 200°C are also showing the synthesized CNTs are mechanically stable and can be used for rechargeable batteries that results in exothermic reactions.

References:

1. Ummethala, R., et al., Energy Storage Materials 10 (2018) 206–215, <https://doi.org/10.1016/j.ensm.2017.04.004>
2. Daniel P Hashim., et al. (2012), Nature, Scientific reports 2, 363p <https://doi.org/10.1038/srep00363>

PC-32**Radiation tolerance of modified Ferroelectric thin films for Micro-Electro-Mechanical system applications in Nuclear Industries**Gurumoorthy Chandrasekharan^c, Sridevi Meenachisundaram^a, Naoki Wakiya^b^{a,c} Centre for Applied Nuclear Research in Science and Engineering Education
Bharath Institute of Higher Education and Research, Chennai, India^b Research Institute of Electronics, Shizuoka University, Hamamatsu, Japan.e-address: dir.cansee@bharathuniv.ac.in

Micro-Electro-Mechanical systems (MEMS) are miniature devices with beneficial applications as sensors to integrate both mechanical and electrical MEMS devices. Functional piezoelectric properties of these sensors are important for their applications as pressure sensors, Chemical sensors or inertial sensors. Advancements in fabrication of PZT, PMN-PT ferroelectric thin films with suitable composite materials are underway for their application in MEMS devices in various industries viz., Automotive, Aerospace, Biomedical and Nuclear as energy harvester, actuator, piezoelectric sensors^{1,2}. However, MEMS applications of such devices in aerospace and in nuclear industries concurrently require sustained operation with tolerance in radiation-hostile environments. Radiation tolerance levels of these devices are challenging and hence thin film fabrication by means of appropriate advanced techniques is an immense requirement to minimize the degradation of their functional responses thus rendering increased radiation tolerance. In this context, studies on radiation tolerance level of thin films under Total ionization dose (TID) more adequately simulate real-world conditions by probing material behaviour across a valuable range of exposure doses. As such, limited investigations are carried out for MEMS device applications in nuclear industries. Studies reveal that crystalline and homogeneous thin film materials can be accomplished by choosing the RF sputtering mechanism of deposition. RF sputtering deposition is a non-thermal equilibrium mechanism to retain Pb at microstructural phase. Pb retention is very crucial for persisting radiation tolerance even at high doses which is not feasible in the case of bulk and sol-gel derived PZT fabrication². Also, optimizing the microstructure and introducing the porosity are important factors to relax the epitaxial compressive strain thereby enhancing the functional responses of the ferroelectric thin films. This necessitates detailed investigations to improve device performance towards their applications in radiation environment³. Earlier studies revealed that thin films when exposed to gamma irradiation, piezoelectric properties experienced less than 5% changes up to the dose level of 5 Mrad and thereafter there will be 8% enhancement up to the dose level of 10 Mrad⁴. The main objective of the present study is to investigate radiation tolerance of PZT, PMN-PT thin films fabricated with appropriate material compositions and characterization under different deposition conditions. Enhancement of functional responses and their piezoelectric properties are discussed.

Keywords:

FE-Thin Films, MEMS devices, Radiation tolerance, piezoelectric properties

References:

1. Stevan. J. Brewer et al., Enhanced Radiation Tolerance in Mn-doped Ferroelectric Thin Films, Appl. Phys. Letts, 111, 022906, 2017
2. Isaku Kanno et al., Jpn. J. Appl. Phys., 57, 040101, 2018
3. Sridevi Meenachisundaram et al., J Alloys Compd., 787, 1128, 2019
4. Evelyn S et al., IEEE Transactions, 67, 5, 2020

PC-33**Spray deposited iron tungstate thin film memristive device for non-volatile memory application**

Amitkumar R. Patil^a, Tukaram D. Dongale^b, Keshav Y. Rajpure*^a

^aElectrochemical Materials Laboratory, Department of Physics, Shivaji University, Kolhapur, 416004, India.

^b Computational Electronics and Nanoscience Research Laboratory, School of Nanoscience and Biotechnology, Shivaji University, Kolhapur, 416004, India

e-address: patilamitkumar108@gmail.com

The Ag/FWO/FTO resistive switching (RS) device was fabricated using the chemical spray pyrolysis method. The structural, morphological, elemental, and electrical characterizations were effectively carried out to explore this study. Moreover, we report the structural refinement of the X-ray diffractograms through the Rietveld refinement method. The fabricated device exhibits bipolar resistive switching behavior with switching voltage below ± 2.5 V, good endurance of 10^3 cycles, and retention over 10^4 s. The β and $x_{63\%}$ factors of Weibull distribution suggest the good operational uniformity of the device. In addition, we investigate different memristive properties and exemplify that the fabricated device is a non-ideal memristor device using the double valued charge-flux feature. We also report the conduction mechanism of the device dominated by trap-controlled space-charge limited conduction and Ohmic conduction mechanisms. A possible filamentary RS mechanism was formulated based on experimental electrical results and charge transport fitting results. The results suggest that FeWO₄-based RRAM can be a potential candidate for non-volatile applications.

PC-34**An AFM probe of RBCs topographical structures during deformability under various physics and chemical influences.**

Bhukya Vijay Mohan, Naveena C S, Sharath Ananthamurthy

School of Physics, University of Hyderabad, Hyderabad-500046.

e-address: vijaymohan9491@gmail.com

Our study focuses on human Red Blood Cells (hRBC) exposed to various physical and chemical factors, namely hemin, zinc ions, and long-term storage. hRBCs can undergo large deformations when subjected to external forces, which allows them to pass through capillaries vessels that are narrower than the diameter of a resting RBC. The deformability of RBCs allows them to flow in small vessels while transporting oxygen and carbon dioxide. we are interested in RBC deformability and how this is affected in conditions such as in diabetes, or malaria. These aspects are investigated through cell shape geometry, internal viscoelasticity of the cell, microrheological properties of the membrane, osmotic pressure, etc. The AFM facility on the Near Field optical Microscope platform has been used to investigate the morphological, cytoskeletal, and mechanical properties of normal and hyperglycaemia hRBCs. The AFM employs an extremely fine probe with a sharp tip for force spectroscopy. Other probes with apertures are used for imaging the hRBC. Here we present initial results from these studies.

Acknowledgment:

Bhukya Vijay Mohan acknowledges a NSOM facility, School of Physics, University of Hyderabad, Naveena C S acknowledges a CSIR-UGC-JRF fellowship.

References:

1. Nagesh B V, Yogesha, Pratibha R, Praveen P, Sarbari Bhattacharya and Sharath Ananthamurthy, Optical properties of Red Blood Cells – An Optical tweezer-based analysis, SPIE Photonics West, San Francisco, California, United States of America, Vol 8947, Pages 323-335, (2014).
2. Narla Mohandas and Joel Chasis, “Red Blood Cell Deformability, Membrane Material Properties and Shape: Regulation by Transmembrane, Skeletal and Cytosolic Proteins and Lipids”, Seminars in Haematology 30(3), 171-92 (1993).
3. S. Suresh, “Mechanical Response of Human Red Blood Cells in Health and Disease: Some Structural- Property- Function Relationships”, Journal of Materials Research, 21, 1871-1877 (2006).
4. Praveen Parthasarathi, Belavadi V. Nagesh, Yogesha Lakkegowda, Shruthi S. Iyengar, Sharath Ananthamurthy, and Sarbari Bhattacharya, “Orientational dynamics of human red blood cells in an optical trap”, Journal of Biomedical Optics, 18(2), (Feb 2013).

PC-35**Bias and Frequency dependence of Metal/TaO_x/GaAs Capacitor**

M. Sravani^{a,c}, R. Sai Prasad Goud^{a,c}, A. Mangababu^b, Y. Rajesh^c, G. Rajaram^{a,b} and S.V.S. Nageswara Rao^{a,b,c}

^aCentre for Advanced Studies in Electronics Science and Technology (CASEST), University of Hyderabad, Hyderabad-500046, Telangana, India

^bSchool of Physics, University of Hyderabad, Hyderabad-500046, Telangana, India

^cCentre for Nanotechnology, University of Hyderabad, Hyderabad-500046, Telangana, India
e-address: sravani.machiboyina@uohyd.ac.in

Tantalum Oxide is a high dielectric constant material of interest in MOSFET technology. The properties of Metal-Oxide-Semiconductor (MOS) structure - high-k dielectric (TaO_x) grown on n⁺GaAs/SI GaAs substrate - were studied. Tantalum oxide films were deposited on n⁺GaAs/ SI GaAs substrate using electron beam evaporation at two different substrate temperatures of 300°C and 500 °C. Silver dots of 1mm diameter were deposited using thermal evaporation as a top contact. Current - Voltage (I-V) characteristics show that the leakage current is 4.7x10⁻⁸ A for both temperatures at -1 V and 6x10⁻⁸ A, 5.26x10⁻⁸ A at +1 V for 300 °C, 500°C respectively for a 1mm diameter structure. Capacitance-Voltage(C-V) characteristics show a systematic decrease in capacitance with increasing frequency at both substrate temperatures. Capacitance is larger at 500 °C compared to 300 °C. The substrate temperature impact on I-V and C-V characteristics will be discussed.

PC-36**Studies on the effect of Bovine serum albumin on human red blood cell membrane stiffness using an atomic force microscope**Chetana Devarakonda^a, Sharath Ananthamurthy*^b^a Department of Physics, Bangalore University, Bangalore – 560050^b School of Physics, University of Hyderabad, CUC, Gachibowli, Hyderabad, Telangana – 500046.e-address: chethana11@gmail.com

A human Red Blood Cell (hRBC) has a biconcave structure with the central crater or the dimple region having a thickness of about 1 micron and the peripheral or rim region of thickness of about 2 microns. The cell membrane of an hRBC is highly deformable. This allows it to squeeze through capillaries much smaller than itself and deliver oxygen throughout the body. Thus, studies on the mechanical properties of the RBC have garnered sufficient interest in recent times. However, there is a paucity of studies that focus on the nature and possible variation of the membrane elasticity profile across the two prominent regions of the human RBC. In this work we investigate the mechanical properties of RBC using atomic force microscopy (AFM) in order to characterize the variation of the cell membrane stiffness in different regions of the cell membrane. For this end, we change the cell membrane stiffness through the use of Bovine Serum Albumin (BSA). BSA is a serum albumin protein derived from cows. By a control in the amount of alteration in the membrane stiffness of RBCs¹ one can mimic the cell in different pathological conditions. This study aims to quantify a) the possible variation of membrane stiffness across different regions of the cell membrane and b) the changes in the membrane stiffness due to the influence of BSA.

The variation of cell stiffness of RBC at different regions of the cell is characterized by performing local force spectroscopy on the sample. Force spectroscopy studies have been carried out to obtain a radial profile of the membrane stiffness, and corresponding force-distance curves are obtained. The elasticity modulus of the sample is obtained using the Hertz model. It is observed that there is a considerable amount of variation in the stiffness of the membrane at different regions of the membrane for the same BSA concentration. This non-uniformity is found to be significantly enhanced as we go to concentrations of BSA. We are currently studying such variation in detail.

Acknowledgments:

The authors would like to thank Department of Science and Technology (DST), Government of India for a grant under PURSE project which made this work possible. One of the authors, (CD) acknowledges the Department of Science and Technology (DST) for financial assistance through the Women in Science fellowship (WOS-A).

References:

1. Selvan, Rekha, et al. "Estimation of membrane bending modulus of stiffness tuned human red blood cells from micropore filtration studies." *PloS one* 14.12 (2019): e0226640.
2. Praveen, Parthasarathi, et al. "Effect of Bovine Serum Albumin on Red Blood Cell Optical Anisotropy Probed Through the Optomechanical Response in an Optical Trap." *Macromolecular Symposia*. Vol. 376. No. 1. 2017.
3. C. C. Lien et al., "Study on the Young's Modulus of Red Blood Cells Using Atomic Force Microscope Applied Mechanics and Materials, Vol. 627, pp. 197-201, 2014
4. Musielak, M. "Red blood cell deformability measurement: review of techniques." *Clinical hemorheology and microcirculation* 42.1 (2009): 47-64

PC-37

Spin-filtering effect in a correlated single-molecular spintronics-transistor: Anderson-Holstein-Caldeira-Leggett-Rashba model

Kuntal Bhattacharyya, Debika Debnath, Ashok Chatterjee
School of Physics, University of Hyderabad, Hyderabad 500046, India
e-address: kuntalbhat22@gmail.com

The Rashba spin-orbit coupled quantum transport through a quantum dot embedded in a closed quantum loop is investigated in the presence of intra-dot electron-phonon and Hubbard interaction at a finite temperature and magnetic field. The dot at the centre is attached to the source and drain, which resembles the structure of a single molecular transistor. Also, an insulating phonon bath is placed under the dot that produces a quantum dissipation through dot-bath phonons coupling. Under the framework of the Anderson-Holstein-Caldeira-Leggett-Rashba model, the transport properties are calculated via finite temperature Keldysh non-equilibrium Green's function technique followed by successive unitary transformations that decouple the interactions present in the system. It is shown that Rashba coupling alone separates the up and down-spin currents and conductance, and the splitting gap between up and down-spin current and conductance can be tuned by changing the Rashba strength. Due to the Rashba spin-orbit coupling, the up and down-spin current through the channel behave completely opposite with respect to the spin-orbit interaction phase even when the external field is zero. The tunnelling differential conductance and spin-polarization change differently in the presence of a magnetic field with respect to polaronic interaction, spin-orbit interaction and dissipation in different temperature regimes. This study predicts that the maximum spin-polarization in a single molecular device can be obtained for a particular Rashba strength at a high magnetic field and zero temperature. The application of this study can be made in designing a tunable spin-filter.

References:

1. Qing-feng Sun, J. Wang and H. Guo, Phys. Rev. B 71, 165310 (2005).
2. R. G. Alvar, W. Lejia, D. B. Enrique, A. N. Christian, Nature. Comm. 7, 11595 (2016).
3. A. Khedri, T. A. Costi, V. Meden, Phys. Rev. B 98, 195138 (2018).
4. M. Kalla, Ch. Narasimha Raju, A. Chatterjee, Sci. Rep. 11, 10458 (2021).

PC-38

Non-equilibrium Transport In a Bi-molecular Transistor: Effect of External Magnetic Field And Temperature

Debika Debnath, Kuntal Bhattacharyya, Ashok Chatterjee

School of physics, University of Hyderabad, Hyderabad, India, 500046

e-address: debika.physics@gmail.com

Non-equilibrium quantum transport is studied in a bi-molecular transistor in the presence of the electron-electron interaction, electron-phonon interaction, phonon dissipation and an external magnetic field at finite temperature. Two quantum dots are considered to be connected in series, placed in between two metallic leads (source and drain) and the whole system is embedded on an insulating substrate which acts as a phonon bath. The tuning of the bias-voltage and the gate voltage controls the flow of electrons in the circuit. The model is described by the Anderson-Holstein-Caldeira-Leggett Hamiltonian. Incorporating suitable canonical transformations, the phonon degrees of freedom are tackled in the system and the electronic Hamiltonian is solved using the Keldysh non-equilibrium Green's function technique. The spectral function, tunnelling current and spin-polarization are calculated at finite temperature for different magnetic fields and it is found that the external magnetic field results the spin-filtering effect that separates the up-spin and down-spin tunnelling current and also causes spin polarization. The results show that the tunneling current and the spin polarization is higher for the bi-molecular transistor than the single molecular transistor, at high magnetic field and low-temperature regime.

References:

1. Chen, Z. Z., Lü, R., Zhu, B. F. Effects of electron-phonon interaction on nonequilibrium transport through a single-molecule transistor. *Phys, Rev. B.* 71, 165324 (2005).
2. Khedri, A., Costi, T. A. & Meden, V. Influence of phonon-assisted tunneling on the linear thermoelectric transport through molecular quantum dots. *Phys. Rev. B* 96, 195156 (2017).
3. Narasimha Raju, Ch., & Chatterjee, A. Quantum dissipative effects on non-equilibrium transport through a single molecular transistor: The Anderson–Holstein–Caldeira–Leggett model. *Sci. Rep.* 6, 18511 (2016).
4. Kalla, M., Narasimha Raju, Ch., Chatterjee, A. Magneto-transport properties of a single molecular transistor in the presence of electron-electron and electron-phonon interactions and quantum dissipation. *Sci. Rep.* 9, 16510 (2019).
5. Keldysh, L, Diagram technique for nonequilibrium processes, *Sov. Phys. JETP* 20, 1018 (1965).

PC-39**Dielectric and electrocaloric properties of BCTZ composite with cobalt zinc ferrite nanoparticles**

Anshu Gaur, Soumya Ranjan Parida, S. Srinath

School of Physics, University of Hyderabad, Prof. C R Rao Road, Gachibowli Hyderabad 500046

e-address: gauranshu20@gmail.com

Dielectric and electrocaloric (EC) properties of multiferroic composite of $Ba_{0.85}Ca_{0.15}Ti_{0.9}Zr_{0.1}O_3$ (BCTZ) with $Co_{0.4}Zn_{0.6}Fe_2O_4$ (CZF) nanoparticles, (1-x)BCTZ- xCZF (x=0, 0.1, 0.2, 0.3 and 0.5) calcined and sintered at 1000°C are reported. The ferroelectric BCTZ is separately synthesized by sol-gel route whereas magnetic CZF nanoparticles are obtained by co-precipitation method. Structural analysis reveals that the addition of CZF enhances the tetragonality (c/a ratio) of BCTZ crystal lattice which can be responsible for increased polarization. Room temperature dielectric data, $\epsilon^*(\omega)$, revealed that dielectric constant, ϵ' , of the composites are systematically smaller than that of the pure BCTZ due to the addition of non-ferroelectric CZF¹. The dielectric loss represented as ϵ'' is also systematic with x, but has a cross over behavior in 300 Hz-2.5 kHz frequency range: decreases in the higher range (2.5 kHz – 1 MHz) and increases in the lower range (20 Hz-300 Hz) with x. The ϵ'' -graph is characterized by a relaxation peak which shifts to lower frequencies with x. The low and higher frequency parts of $\epsilon'(\omega)$ and $\epsilon''(\omega)$ graphs are fitted with power law and Cole-Cole equations respectively. The Cole-Cole parameter, α , which is related with the distribution of relaxation time, τ , ($\alpha=0$ corresponds to the system with single τ) of 10% composite is smaller than that of BCTZ. The smaller value of α is associated with the higher density and hence more homogeneous environment of the ²composite compared to pure BCTZ sintered at the same temperature. EC aspect of the BCTZ-CZF composites are investigated by recording the temperature dependent P-E loops in the 30-130°C range at the interval of 5°C. The P of the composites plotted against the T reflects the $\epsilon'(T)$ characteristic of parent BCTZ via a broad transition peak in the range of 30-80°C. The composites with higher CZF fraction (x=0.3 and 0.5) showed stronger T-dependence than with x= 0.1 and 0.2, mainly associated with its higher density. Partial contribution of interfacial polarization is not neglected.

References:

1. M. Naveed-Ul-Haq, V. v. Shvartsman, S. Salamon, H. Wende, H. Trivedi, A. Mumtaz, and D.C. Lupascu, Scientific Reports 6, (2016).
2. Y. Bai, X. Han, and L. Qiao, Applied Physics Letters 102, 1 (2013).

PC-40**Dielectric Properties and AC Conductivity of Li₂O Doped Zinc Borophosphate Glasses**

Dawalappa B. Husenkhan, Amarkumar Malge, T.Sankarappa
Department of Physics, Gulbarga University, Kalaburagi- 585106, Karnataka, India
e-address: dawalappabh@yahoo.com

Abstract: Glass System in the composition, $(P_2O_5)_{0.65-x} (B_2O_3)_{0.1} (ZnO)_{0.25} (Li_2O)_x$; $x=0.05, 0.10, 0.15, 0.20, 0.25, 0.30, 0.35$ and 0.40 were prepared at $1473K$ by the standard conventional melt quenching method. The samples were confirmed for the amorphous nature through XRD studies. Dielectric properties were studied over the range of frequency from 50 Hz to $1MHz$ as a function of temperature. AC conductivity was determined. Data was analyzed in terms of composition, frequency, and temperature.

Keywords:

dielectric constant, dielectric loss, ac conductivity, activation energy, frequency exponent.

References:

1. Jana Mizerakova , Peter Hockicko ,Francisco Munoz, Dielectric Study Of Lithium And Sodium Borophosphate Glasses, Communications, 19 (3), 46-50, 2017.
2. V.Arun, S.Yusub, M. Venkateswarulu, A.Ramesh Babu, K.Anitha, Efficacy of copper ions on lithium ion conductivity, electron hopping, optical band gap,metallization criterion and morphology of Li₂O-B₂O₃-P₂O₅ glasses, Journal of Non-Crystalline Solids, 536, 120015, 2020.
3. Juraj Nikolic, Luka Pavic, Ana Santic, Petr Mosner , Ladislav Koudelka, Damir Pajic, Andrea Mogus-Milankovic, Novel insights into electrical transport mechanism in ionic-polaronic glasses, J Am Ceram Soc., 101, 1221–1235, 2018.
4. Soumyajyoti Kabi. Investigation on the lithium ion dynamics in the context of microscopic length scale in zinc borophosphate glass. Solid State Ionics, 334, 65-69, 2019.
5. P.Naresh, B.Kavitha, Hajeebaba K. Inamdar, D. Sreenivasu, N. Narsimlu, Ch.Srinivas, Vasant Sathe, K Sivakumar, Modifier role of ZnO on the structural and transport properties of lithium boro tellurite glasses, Journal Of Non- Crystalline Solids, 514, 35 – 45, 2019.
6. Kristina Sklepica, Radha Dilip Banhatti, Gregory Tricot, Petr Mosner, Ladislav Koudelka, and Andrea Mogus - Milankovic, Insights from Local network structures and Localized Diffusion on the Ease of Lithium-Ion Transport in Two Mixed Glass - Former Systems, The Journal of Physical Chemistry C, 1-58, 2017. DOI: 10.1021/acs.jpcc.7b05108.
7. Sanjib Bhattacharya, Amrtya Acharya, Anindya Sundar Das, Koyel Bhattacharya, Chandan Kumar Ghosh, Lithium ion conductivity in Li₂O-P₂O₅-ZnO, glass ceramics, Journal of Alloys and Compounds, 786, 707-716, 2019.
8. M.M.El-Desoky and Ahmed E. Hannora, Dielectric Relaxation and Impedance Spectroscopy of 30V₂O₅- 20Bi₂O₃-50P₂O₅ Glass, Glass Physics and Chemistry, 46(6) , 487-496, 2020.

PC-41

Synthesis, Characterization and STM study of Single QD Fe:CdS Rectifying Diode

Anup K Ghosh^a, Piyali Maity^a, Sandip Chatterjee^b, Bhola Nath Pal^c

^aDepartment of Physics, Banaras Hindu University, Varanasi, India,

^bDepartment of Physics, Indian Institute of Technology (BHU), Varanasi, India,

^cSchool of Materials Science and Technology, Indian Institute of Technology (BHU), Varanasi, India.

e-address: akghosh@bhu.ac.in

The field of single dot electronics is growing remarkably high since the last decade by improving device fabrication techniques. TiO_2 and CdS:Fe quantum dots (QDs) have been synthesized by hot-injection method. Samples are characterized by X-ray diffraction (XRD), Transmission electron microscopy (TEM). The optical absorption and band gap have been estimated from UV-V is spectra. The photoluminescence spectra have been measured to study the luminescence properties, defect states, and oxygen vacancy present in samples. The ITO/ TiO_2 /CdS:Fe quantum dot heterostructures rectifying diodes were grown by spin coating and are studied by scanning tunneling microscopy (STM) at ambient temperature. Scanning tunneling spectroscopy (STS) has been used for investigation of rectification properties of single-dot diodes. The images reveal individual CdS QDs having a spherical shape with maximum diameter of 4 nm. The threshold voltage has been tuned from 1.62 eV to 0.33 eV which makes the diode useful for daily life electronics with low power consume.

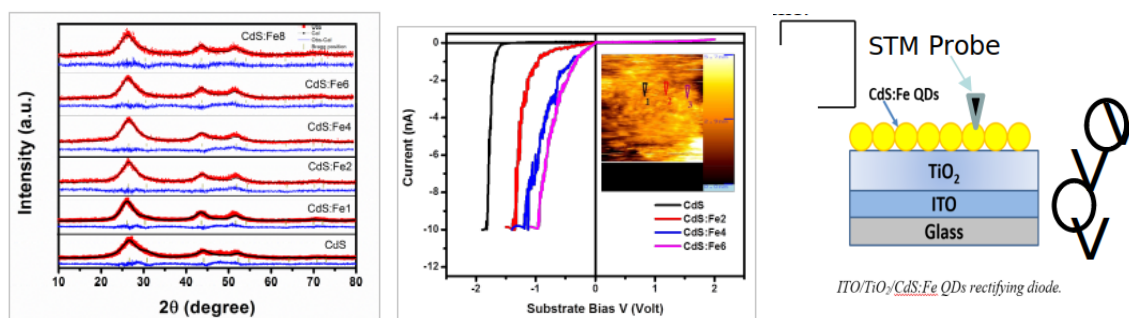


Figure 10: XRD pattern and Rectifying behavior

Acknowledgments:

PM is thankful to the Department of Science and Technology, India for INSPIRE Fellowship. AKG is thankful to DST-SERB, India and IoE Program (Grant no. CRG/2019/000896 and Scheme No: 6031 respectively) for financial support.

References:

1. M. Y. Li, S. K. Su, H. S. P. Wong and L. J. Li, Nature, 2019, 567, 169–170.
2. B. Capozzi, J. Xia, O. Adak, E. J. Dell, Z.-F. Liu, J. C. Taylor, J. B. Neaton, L. M. Campos and L. Venkataraman, Nat. Nanotechnol., 2015, 10, 522–527.

PC-42

Study of Thermo Optics Coefficients and Thermo Polarizable Coefficients in LiNbO₃ Open Type Optical Waveguide using Point Dipole Approximation

Velagapudi Suhasini^a I.V. Subbareddy^b^aResearch Scholar, Department of Electronics, GITAM, Hyderabad, Telangana, India.^bDepartment of Physics, GITAM (Deemed to be University), Hyderabad, Telangana, India.e-address: suhasini2508@gmail.com

The Thermo Optic Coefficients (TOCs), $(dn_o/dT, dn_e/dT)$ in LiNbO₃ open-type optical waveguide are calculated using Point Dipole Approximation and Sellmeier equations. These values are used to find the possible set of polarizabilities of Li⁺, Nb⁵⁺ and O²⁻ ions at different temperatures from 298K to 772K for the wavelengths 0.4545 μ m, 0.6328 μ m, and 1.0642 μ m from which Thermo Polarizable Coefficients (TPCs) $(d\alpha_{Li^+}/dT, d\alpha_{Nb^{5+}}/dT, d\alpha_{O^{2-}}/dT)$ were calculated.

The results indicate that 1) As temperature increases, n_o and n_e increase, 2) As wavelength increases, n_o and n_e decrease 3) The magnitude of TOC for extraordinary index (dn_e/dT) is about two times the ordinary index TOC (dn_o/dT) . 4) With the increase of temperature, the Polarizability of Nb⁵⁺ ion decreases and the polarizability O²⁻ ion increases for a given wavelength. 5) As wavelength increases the Polarizabilities of Nb⁵⁺ and O²⁻ decrease for a given temperature. 6) TPCs of O²⁻ ions increase and Nb⁵⁺ ions decrease with temperature. At a given temperature TPC of O²⁻ ion decreases and Nb⁵⁺ ions increase with wavelength. TPCs of O²⁻ ion is lower than that of Nb⁵⁺.

Keywords:

Polarizability, Thermo Optic Coefficients, Point Dipole Approximation, Sellmeier Equations, LiNbO₃.

References:

1. Jian J, Xu M, Liu L, et al 2019 Opt Express, 27 (2019), p. 18731.
2. Rao A and Fathpour S 2018 IEEE Journal of Selected Topics in Quantum Electronics, vol. 24, no.6.
3. Manohar P, Sathyanarayan R B and R Ethiraj 2015 IJTT Vol 5 No 4 pp 306-310.
4. Sathyanarayan R B, Manohar P, R Ethiraj and Ch Gopal Reddy 2016 IJCET Vol 6 No 1 pp 112-116.

PC-43

Structural Stabilization and Optical, Electrical analysis of $\text{Al}_{1-x}\text{Ga}_x\text{O}_3$ at different Ga- compositions prepared by Mechanical alloying method

Collin B Nettar, R. N Bhowmik

Department of Physics, Pondicherry University, Puducherry, India

e-address: collinbnettar@gmail.com

The mechanically alloyed sample demonstrated a structural phase change of Ga- doped Al_2O_3 (GaAlO) sample from β - phase to α - phase under varied Ga- compositions. The analysis of X-ray diffractometer patterns and X-ray photoelectron spectra bands indicated the chemical stability of GaAlO structure for Ga at Al sites. The interplanar spacing of Al_2O_3 (104) reduces after Ga- doping, as seen by the (104) plane location at approximately $2\theta = 35.20^\circ$ greater than the value indicated by conventional spectra ($2\theta \sim 35.14^\circ$) for $\alpha\text{-Al}_2\text{O}_3$ ¹. The decrease in the interplanar spacing of Al_2O_3 (104) suggests that some Ga in Ga^{3+} states incorporated into Al_2O_3 lattice by substituting for Al sites because the ionic radii of Ga^{3+} and Al^{3+} are 0.62\AA and 0.53\AA respectively². R.N Bhowmik et. al found that the lattice parameter (a, c) has been decreased from that of the pure $\alpha\text{-Fe}_2\text{O}_3$ sample by doping Ga (x=0.2-0.4) compositions³. A similar kind of result was observed in GaAlO samples, the dopant concentration reduces the lattice parameters of the GaAlO sample while increasing the Ga content. The particle size increases with the Ga-dopant. The agglomeration process is happened between Al_2O_3 and Ga_2O_3 in the nanocomposite and results in the increase of grain size. The microstrain values increased with an increase in Ga content, developing comprehensive stress in the GaAlO sample. The dislocation density (dislocation lines per unit area) decreases with an increase in average crystalline size⁴. UV-Visible spectra showed two optical bandgaps at the lower energy side (4.25-4.55) eV and the higher energy side at (4.75-5.02) eV, both energy bandgaps were less than the optical bandgap of defect-free Al_2O_3 ¹. The reduction in the optical bandgap may be due to the defect-induced electronic transition from the valence band to the conduction band⁵. The electrical conductivity measurement in the temperature range 300K-573K showed a transformation from a metal-like behavior (low-temperature region) to a semiconductor-like (high-temperature region) behavior⁶. The electrical conductivity at room temperature (300K, $\sigma \sim 2.06 \times 10^{-3} \text{ Simen/m}$) decreased while the electrical conductivity increases at 573K ($\sigma \sim 4.82 \times 10^{-7} \text{ Simen/m}$) with the increase of Ga composition. The present work shows that the crystal structure, optical bandgap, and electrical conductivity of the pure Al_2O_3 are modified by Ga with different dopant concentrations.

References:

1. J. Gangwar, B. K Gupta, S.K Tripathi, A. K Srivastava, *Nanoscale* 7 (2015) 13313-13334.
2. L. Lin, R. Miao, W. Xie, J. Chen, Y. Zhao, Z. Wu, J. Qiu, H. Yu, S. Zhou, *iScience* 24 (2021) 101984.
3. R. N Bhowmik, R. J Choudhary, P. Mitra, V. R Reddy, A. K Sinha, *J. Appl. Surf. Sci.* 573 (2022) 151609.
4. E. F. A Zeid, I. A. Ibrahim, A. M Ali, W. A. A Mohamed, *Results Phys.* 12 (2019) 562-570.
5. C. B Nettar, R. N Bhowmik, A. K Sinha, *J. Ceram. Inter.* 48 (2022) 10677- 10687.
6. R. N Bhowmik, A. G Lone, *J. Alloys Compd.* 680 (2016) 31-42.

PC-44**Temperature Dependence of Electrical conductivity of ZnO-V₂O₅-B₂O₃-MnO Glass nano composites**

Ashwini Devidas, T.Sankarappa*, Amarkumar Malge, Mohansingh Heerasingh, Raghavendra. B and Jamadar Pallavi

Department of physics, Gulbarga University, Kalaburagi 585106, Karnataka, India

*Corresponding author: sankarappa@rediffmail.com

e-address: ashwininilange06@gmail.com

The glasses with composition, (ZnO)_{0.3} - (V₂O₅)_{0.6-x} - (B₂O₃)_{0.1} - (MnO)_x; x=0.05 to 0.2 were synthesized by following the standard melt quenching method. From the powder XRD studies, the samples were confirmed to be nano crystalline glass composites. Room temperature density was measured by applying Archimedes principle. Density is found to be in the range 3.0163gm/cm³ - 3.3102gm/cm³ and it increased with increase of MnO concentration. DC conductivity has been measured by two probe method in the temperature range from 303K to 523K. Conductivity increased with increase of temperature revealing semiconducting behavior of the samples and decreased with increase of MnO content. High temperature conductivity was found to vary as per Mott's Small Polaron hopping (SPH) model. This lead to the determination of the activation energy for conduction and it was found to decrease with increase of MnO content. The data deviated from Mott's SPH model has been looked at in the light of Variable range hopping (VRH) models due to Mott and Greaves. Density of states at Fermi level has been derived from the VRH model analysis. It was confirmed that Greaves VRH model explain adequately the behavior of low temperature conductivity. It is for the time that zinc-boro-vanadate glass nano composites mixed with MnO have been investigated for electrical conductivity and data analyzed thoroughly.

Keywords:

Glass nano composites, density, conductivity, Small polaron hopping, Variable range hopping.

Acknowledgement:

One of the authors Ashwini Devidas acknowledges the financial assistance received from the Gulbarga University in the form of merit fellowship for her PhD studies.

References:

1. Anindya Sundar Das, Madhab Roy, Debasish Roy, Sanjib Bhattacharya, Indian J. Pure and Appl. Physics, 57 (2019) 803-811.
2. S. Dalal, S. Khasa, M.S. Dahiya, A. Yadav, A. Agarwal, S. Dahiya, J. As. Cer. S. 3 (2015) 234-239.
3. Muhammad Faris Syazwan Mohd Shofri, Mohd Hafiz Mohd Zaida, Rabiatal Adawiyah Abdul Wahab, Khamirul Amin Matori, Sidek Hj. Ab Aziz, Yap Wing Fen, J. Mater. Res. Technol. 9, 4, 6987 (2020).
4. M. Jerroudi, L. Bih, E. Haily et al., "Optical and electrical properties of manganese doped-alkali metaphosphate glasses," Materials Today: Proceedings, 30 (2019) 1052-1055.
5. Wafaa Ahmina, Mouloud El Moudane, Mohammed Zriouil, M'hamed Taibi, J. Phase Transitions, 89, 11, 1051-1061 (2016).
6. A. L. Patterson, The Scherrer Formula for X-Ray Particle Size Determination, Phys. Rev. 56 (1939) 978-982.
7. Sanjib Bhattacharya, Anindya Sunder Das, Madhab Roy, Debasish Roy J. Non-Crystalline Solids 460 (2017) 29-35.
8. C. F. Drake, J. A. Stephan, and B. Yates, J. Non-Cryst. Solids 28 (1978) 61.

9. J. S. Ashwajeet, T. Sankarappa, T. Sujata, R. Ramanna, J. of Non-Cryst. Solids 486 (2018) 52-57.
10. M. M. El-Desoky, H. S. S. Zayed, F. A. Ibrahim, H. S. Ragab, J. Physica B, 404 (2009) 4125-4131.
11. Aloka Ghosh, S. Bhattacharya, D. P. Bhattacharya, A. Ghosh, J. Appl. Physics, 103 (2008) 083703.
12. Amartya Acharya , Koyel Bhattacharya, Chandan Kumar Ghosh , Achintesh Narayan Biswas, Sanjib Bhattacharya, J. Materials Science & Engineering B, 260 (2020) 114612.
13. M. Amarkumar, T. Sankarappa, J.S. Ashwajeet and T. Sujata J. Of Physics Conference Series, 1172 (2019) 012012.
14. Anindya Sundar Das, Dipankar Biswas, Madhab Roy, Debasish Roy, Sanjib Bhattacharya, Indian J. Pure and Appl. Physics, 2018.
15. A. Ghosh, D. Chakravorty, J. Phys. Condens. Matter, 2 (1990) 931-938.

PC-45

Microwave Characterization of PVDF-TrFE-Nafion blended films

P. Nikhil Mohan^a, C. Thirimal^b, Andrews Joseph^a, *K.C. JamesRaju^a

^a School of Physics, University of Hyderabad, Gachibowli, Hyderabad, Telangana, India-500046,

^b Centre for Nanoscience and Technology, VNR Vignana Jyothi Institute of Engineering and Technology, Bachupally, Hyderabad, Telangana, India-500090

e-address: *kcjrsp@uohyd.ac.in

The free-standing pure PVDF-TrFE and PVDF-TrFE-Nafion blended films are fabricated by the casting method and tested for structural, morphological and microwave studies. The X-ray diffraction pattern and FTIR spectrum confirmed the formation of ferroelectric β -phase of PVDF-TrFE. The surface morphology of blended films is studied by scanning electron microscope (SEM). The morphological changes observed in the blended films clearly indicate the change in the nucleation process of the films during their formation with a strong interaction between them. The microwave dielectric measurements are carried out in the X band frequency range using a vector network analyzer (VNA). The microwave absorption properties of the blends are also studied in the same frequency range.

Keywords:

PVDF-TrFE, Nafion, Blends, dielectric, microwave absorption, VNA

PC-46

Detection of milk adulteration based on principal component analysis of absorption and transmission spectra

Ravinder Tirupati , Samrat L Sabat, M Ghanashyam Krishna

Centre for Advanced Studies in Electronic Sciences and Technology (CASEST), School of Physics, University of Hyderabad,
Hyderabad, Telangana 500046, India
e-address: 19phpe06@uohyd.ac.in

Milk is an excellent source of many essential nutrients, including calcium, protein, and vitamin A and D. In everyday life, milk and other products are part of our balanced diet. Milk adulteration leading to lower nutritional value and several health hazards is one of the major challenges in modern day life. Milk adulteration due to mixing of milks from different sources is a common problem. The detection and monitoring of these adulterants is, therefore, very important. There are many different techniques to detect adulterants in milk of which UV-Visible-Near Infrared (NIR) spectrophotometry is a simple and cost-effective method which can also become portable. However, the challenge is to detect adulterants in a noisy spectrum. To achieve this, the principal component analysis (PCA) method is adopted. The absorption and transmission spectra of raw milk, different brands of commercially available milk with varying fat contents (from 3 to 6 %) as well as skimmed milk were recorded in the 200-2500 nm wavelength range. Around 200 spectra were obtained from these milk samples at regular intervals of time. From the recorded spectra, the principal components were extracted. K-means clustering was applied on the PCA features to separate the milk samples into different clusters based on, its adulteration constituents and source of origin. The obtained results indicate promise for the development of a portable prototype device for the detection of adulterants in milk.

PC-47

Highly Enhanced SQ Efficiency in ZnS/CdSe Core/Shell nanowire: An Ab-Initio Study

Rishit S. Shukla^a, Vidit B. Zala^a, Sanjeev K. Gupta^b, P. N. Gajjar^a^aDepartment of Physics, University School of Sciences, Gujarat University, Ahmedabad – 380 009, India.^b Computational Materials and Nanoscience Group, Department of Physics, St. Xavier's College, Ahmedabad – 380 009, India.e-address: rishitshukla@gujaratuniversity.ac.in

An ab-initio study using SIESTA package was carried out to structurally optimize and subsequently, compute the electronic band structures and density of states (DOS) for ZnS and CdSe nanowires (NWs) in their hexagonal Wurtzite (WZ) phase. The lattice parameters of the fully optimized ZnS and CdSe NWs were 6.32\AA and 7.14\AA , respectively with their respective diameters of 11.85\AA and 13.62\AA . Vacuums of 10\AA each were left along the X- and Y- axes, to avoid the interactions between adjoining NW images. The ZnS and CdSe both show direct bandgaps of 2.89 eV and 2.14 eV, respectively along the Γ point. Based on the calculated bandgaps, the Shockley-Quisser (SQ) efficiencies for the bare ZnS and CdSe NWs were evaluated. The calculated SQ efficiencies of ZnS and CdSe NWs were 6.24% and 20.38%, respectively. However, previous studies have shown that incorporating such semiconducting NWs into the core/shell (c/s) formation, could significantly fine tune the electronic bandgaps which could also enhance the SQ efficiencies. Motivated by this, the study of the structural and electronic properties for ZnS/CdSe core/shell (c/s) NW was taken up. The fully optimized ZnS/CdSe c/s NW has $c = 5.73\text{\AA}$ and a diameter of 13.83\AA , with a vacuum of 10\AA along the X- and Y- directions. The ZnS/CdSe c/s NW shows an indirect bandgap of 1.48 eV^1 . The calculated SQ efficiency was revealed to be 32.97%, which is a significant improvement over the bare ZnS and CdSe NWs. Also, this value of SQ efficiency is precariously close to the maximum possible theoretical SQ efficiency of 33.7%. Hence, our study showed that there is a transition of bandgap from direct to indirect, upon the incorporation of the ZnS and CdSe NWs into the ZnS/CdSe c/s NW configuration. Also, this strategy significantly shrunk the electronic bandgap, which in turn, greatly escalated the SQ efficiency.

Reference:

Shukla, R. S., Zala, V. B., Gupta, S. K. and Gajjar, P. N. ZnS/CdX (X = S, Se, Te) core/shell nanowires: an attempt at tuning the electronic bandgaps and SQ efficiencies. *Journal of Materials Chemistry C* 9, 6605–6617 (2021).

PC-48

Mixed-valence iron phosphate: Superhydrophilic multi-plated microflakes towards symmetric supercapacitor

Tushar B. Deshmukh , Babasaheb R. Sankapal

Department of Physics, Nanomaterial and Device Laboratory, Visvesvaraya National Institute of Technology, South Ambazari Road, Nagpur, Maharashtra 440010 India.

Mixed valence state iron phosphate microflakes have been grown using binder-free simple, and low-cost chemical bath deposition (CBD) method. Interestingly, grown microflakes embedded with layered flakes platelets are responsible for capillary action to exhibit a superhydrophilic nature. Iron Phosphate includes two-oxidation (Fe^{+2} and Fe^{+3}) state of cation and unique surface architecture that will play important role in the charge storage by providing more redox-active centres which motivated to employ as liquid configured supercapacitive electrode. To get insight, structural, valence state, surface morphological, and contact angle investigations have been performed through XRD, XPS, SEM, HR-TEM, and contact angle measurements. Multilayer hierarchical iron phosphate pseudocapacitive electrode exhibited specific capacitance of 927 F/g at a 3 mV/s scan rate through cyclic voltammetry and excellent coulombic efficiency through galvanostatic charge-discharge with 96.7% stability at 4000 cycles in KOH electrolyte. First-ever fabricated liquid configured symmetric supercapacitor device based on iron phosphate electrode yield capacitance of 80 F/g at the scan rate of 10 mV/s with cycling stability of 80% after 2500 cycles opening up-its practical ability.

PC-49

Electrical Transport Mechanism Studies in Borotellurite Glasses

Amarkumar Malge^a, T. Sankarappa^{a*}, Sujatha T^a, Devidas G.B^b, Ashwajeet J.S^c, Ashwini Devidas^a and Mohansingh Heerasingh^a

^aDepartment of Physics, Gulbarga University, Kalaburagi 585106, Karnataka, India.

^bDepartment of Physics, Kuvempu University, Shankaraghatta, Shimoga 577451, Karnataka, India.

^cDepartment of Physics, Davangere University, Davangere 577007, Karnataka, India.

* Corresponding author: sankarappa@rediffmail.com ; Tel.: +91 9449663636

e-address: amarmalge1992@gmail.com

By adopting melt quenching technique, a series of borotellurite glasses in the composition $(B_2O_3)_{0.2} - (TeO_2)_{0.3-x} - (ZnO)_{0.28} - (Li_2CO_3)_{0.2} - (Dy_2O_3)_{0.02} - (WO_3)_x$; $x = 0.02, 0.04, 0.06, 0.08$ and 0.10 were synthesized. Their non-crystalline nature was confirmed from the measured powder XRD patterns. The room temperature density was found to increase with increase of WO_3 content. This has been understood to be due to substitution of high dense WO_3 to low dense TeO_2 . Molar volume is also increased with increase of WO_3 revealing the formation of additional BO_4 and WO_6 units in the glass network. DC conductivity has been measured using two-probe method for the temperature range 300K-640K. Conductivity increased with temperature of WO_3 concentration. Variation of conductivity at high temperature obeyed Mott's small polaron hopping (SPH) model and Mott's variable range model (VRH) model at low temperature. SPH model based analysis yielded activation energy for conduction which is found to increase off with increase of tungsten oxide content. Variations in conductivity and activation energy with changes in WO_3 are in agreement with changes noted in the estimated average polaron hopping distance and polaron radius. The derived density of states at Fermi level from VRH model based analysis of the conductivity data at low temperature are in close agreement with literature quoted values for similar glasses.

Keywords:

Borotellurite glasses; electrical conductivity; small polaron hopping, variable range hopping, activation energy.

Acknowledgement:

Authors acknowledge financial assistance received from the DST (SERB), Government of India, New Delhi in the form of a major research project sanctioned to Prof. T. Sankarappa, Principal Investigator.

Reference:

1. S. Selvi, K. Marimuthu, G. Muralidharan, *Journal of Luminescence*, 159 (2014) 207-218.
2. G. Lakshminarayana, Kawa M. Kaky, S.O. Baki, A. Lira, Priyanka Nayar, I.V. Kityk, M.A. Mahdi, *Journal of Alloys and Compounds* 690 (2017) 799–816.
3. T. Sasikala, L. Rama Moorthy, A. Mohan Babu, *Spectrochimica Acta Part A: Molecular and Biomolecular Spectroscopy* 104 (2013) 445–450.
4. Nimitha S. Prabhu, Vinod Hegde, Akshatha Wagh, M.I. Sayyed, O. Agar, Sudha D. Kamath, *Journal of Non-Crystalline Solids* 515 (2019) 116–124.
5. D.D. Ramteke, H.C. Swart, R.S. Gedam, *Journal of Rare earths*, vol. 35, 5 (2017) 480.
6. J.S. Ashwajeet, T. Sankarappa, T. Sujatha, R. Ramanna, *Journal of Non-Crystalline Solids* 486 (2018) 52–57.
7. C. Madhukar Reddy, B.Deva Prasad Raju, N.John Sushma, N.S.Dhoble, S.J.Dhoble, *Renewable and Sustainable Energy Reviews* 51(2015)566–584.
8. O. Ravi, C. Madhukar Reddy, L. Manoj, B. Deva Prasad Raju, *Journal of Molecular Structure*

1029 (2012) 53–59.

9. J.S Ashwajeet, T Sankarappa, T Sujatha, R.Ramanna, J. Non-Cryst. Solids 486 (2018) 52.

10. G. Upender, Ch. Sameera Devi, V. Chandra Mouli, Materials Research Bulletin 47 (2012) 3764–3769.

11. Dhankhar Sunil, R S Kundu, R Parmar, S Murugavel, R Punia and N Kishore, Solid State Sci. 48 (2015) 230.

12. Seema Thakur, Vanita Thakur, Anumeet Kaur, Lakhwant Singh, Journal of Non-Crystalline Solids 512 (2019) 60–71.

13. B. V. R. Chowdari, P. Pramoda Kumari, Journal of Materials Science 33 (1998) 3591–3599.

14. Amarjot Kaur, Atul Khanna, AIP Conference Proceedings 2115, (2019) 030253.

15. Dipankar Biswas, R.K. Nanao Ningthemcha, Anindya Sundar Das, Loithongbam Surajkumar Singh, Journal of Non-Crystalline Solids 515 (2019) 21–33.

PC-50

Synthesis of Self Assembled Poly (methyl Methacrylate) layers for Resistive Random Access Memory Application on Flexible Substrate

Midde Rahul^a, Y Rajesh^b, M Ghanashyam Krishna^a

^aCentre for Advanced Studies in Electronic Sciences and Technology (CASEST), School of Physics, University of Hyderabad, Hyderabad, Telangana 500046, India.

^bCentre for Nanotechnology, University of Hyderabad, Hyderabad, Telangana 500046, India
e-address: 18phpe05@uohyd.ac.in

Poly (methyl Methacrylate)PMMA is a polymer of interest across a broad range of disciplines from biological, chemical to electronics. PMMA, which is e-beam sensitive material is extensively utilized as a resist material for electron beam lithographic patterning in electronic devices layers. Since it is intrinsically insulating, PMMA films are also being investigated for application as the active switching layer in resistive switching and resistive random access memory (RRAM) applications. A challenge in this field is to develop RRAMs on flexible substrates. In this study the synthesis of PMMA films by spin coating, with chloroform as the solvent, on silver coated flexible substrates is presented. PMMA films with thicknesses ranging from a few microns to sub-micron range are obtained. It is observed that the process leads to self-assembled arrays of PMMA particles which extend over a few mm. The particle sizes within the arrays range from a few nms to several hundreds of nm. These self assembled structures could be employed for a pattern free devices which could lower the cost of device fabrication. It is proposed that the the obtained self assembled structures can also find applications in optoelectronic devices.

PC-51

The electronic and adsorption properties of tyramine neurotransmitter based on fullerene nanocage- A DFT approach

A. K. Vishwkarma*, T. Yadav, A. Pathak

Department of Physics, Institute of Science, Banaras Hindu University, Varanasi- India

*corresponding author: akv1993.au@gmail.com

We report ab-initio results that explore the ability of C_{24} and $B_{12}N_{12}$ fullerene to interact with tyramine at the DFT-B3LYP/6-31G (d, p) level of theory. The interaction of tyramine with doped (BC_{23} and $CB_{11}N_{12}$) fullerene is also studied. The results suggest that the most favourable interaction of the fullerene is with tyramine that may be utilized for drug delivery applications. We have analysed the adsorption energies, HOMO-LUMO gaps, molecular electrostatic potential and thermodynamical properties in gas as well as aqueous media.

Keywords:

DFT, HOMO-LUMO, adsorption properties.

PC-52

Mesoporous and Phase Pure Anatase TiO₂ Nanospheres for Enhanced Photocatalysis

Praveen kumar L^a, Harita Pant^b, Avijith^c, Vadali V. S. S. Srikanth^b, Rajanikanth Ammanabrolu^{a*}

^a School of Physics, ^b School of Engineering Sciences and Technology, University of Hyderabad, Gachibowli, Hyderabad 500 046, Telangana, India

*Corresponding author: ammanabrolu@uohyd.ac.in

e-address: 19phph05@uohyd.ac.in

An easy microwave-assisted hydrothermal method is used to prepare phase pure anatase TiO₂ nanospheres with an average crystallite size of ~10 nm. Titanium butoxide and methanol are used as the precursor and solvent to prepare the TiO₂ nanospheres. Methanol has a moderate-loss tangent value of ~0.659. Therefore, it aided efficient absorption of microwaves and rapid local heating for the reaction to complete quickly, leading to the formation of TiO₂ nanospheres with microporosity, a high specific surface area of 60.46 m²/g, and high N₂ adsorption capacity indicating the possibility of enhancing the intrinsic photocatalytic activity of anatase TiO₂. As anticipated, the anatase TiO₂ nanospheres, when tested in the typical photodegradation of methylene blue dye, exhibited an efficiency as high as 98%.

References:

1. A. Fujishima, K. Honda, Electrochemical photolysis of water at a semiconductor electrode. *Nature* 238 (1972) 37–38. <https://doi.org/10.1038/238037a0>.
2. B. Bakbolat, C. Daulbayev, F. Sultanov, R. Beissenov, A. Umirzakov, A. Mereke, A. Bekbaev, I. Chuprakov, Recent developments of TiO₂-based photocatalysis in the hydrogen evolution and photodegradation: A review. *Nanomaterials* 10 (2020) 1790. <https://doi.org/10.3390/nano10091790>.
3. R. Katal, S. Masudy-Panah, M. Tanhaei, M. H. Farahani, H. Jiangyong, A review on the synthesis of the various types of anatase TiO₂ facets and their applications for photocatalysis. *Chem. Eng. J.* 384 (2020) 123384. <https://doi.org/10.1016/j.cej.2019.123384>

PC-53**DFT Investigation of Adsorption of NH₃ by Sensing Arrays of PtAs₂ Monolayer**Vidit B. Zala^a Rishit S. Shukla^a Sanjeev K. Gupta^b P. N. Gajjar^a^aDepartment of Physics, University School of Sciences, Gujarat University, Ahmedabad – 380 009, India^bComputational Materials and Nanoscience Group, Department of Physics, St. Xavier's College, Ahmedabad – 380 009, India.
e-address: viditz@gujaratuniversity.ac.in

The continuous increase in the population has lead to elevated demands of dairy as well as agricultural products. To match the supply, the animal husbandry and usage of artificial fertilizers have increased dramatically, which has resulted in high proliferation of ammonia (NH₃) gas. The hazards of excess NH₃ in the atmosphere can be avoided with the help of NH₃ sensors. A density functional theory (DFT) based study has been conducted to inspect the NH₃ adsorption on PtAs₂ monolayer. With high surface to volume ratio, the atomically thin PtAs₂ monolayer possesses a direct electronic band gap of 0.37 eV, bearing semiconducting nature. For NH₃ gas, the adsorption energy of PtAs₂ monolayer is -0.51 eV. Moreover, the charge density difference and projected density of states suggest physical adsorption of NH₃ by PtAs₂ monolayer. The desorption time of 0.43 millisecond is evocative of excellent reversibility of PtAs₂ monolayer towards NH₃ gas, i.e. the possibility of reusing sensing arrays of PtAs₂ monolayer for NH₃ detection. The computed current-voltage (I-V) relation can aid to correlate with the experimental studies. Observing the I-V characteristics, it is clear that PtAs₂ monolayer becomes extremely sensitive towards NH₃ at a bias voltage of 1.0 V. Our results predict use of PtAs₂ monolayer as sensing arrays in NH₃ gas sensor.

References:

Zala, V. B., Shukla, R. S., Bhuyan, P. D., Gupta, S. K., & Gajjar, P. N. (2021). Highly Selective and Reversible 2D PtX₂ (X= P, As) Hazardous Gas Sensors: Ab-initio Study. *Applied Surface Science*, 150391.

PC-54

Nontrivial Electrophoresis of Silica Nano and Microrods in a Nematic Liquid Crystal

Muhammed Rasi M^a, Archana S^a, Ravi Kumar Pujala^b and Surajit Dhara^a

^aSchool of Physics, University of Hyderabad, Gachibowli, Hyderabad-500046, India

^b Department of Physics, Indian Institute of Science Education and Research (IISER) Tirupati, Tirupati, Andhra Pradesh, 517507, India

e-address: 20phph01@uohyd.ac.in

We study DC and AC electrophoresis of silica nano and microrods in a thin film of a nematic liquid crystal. These particles induce virtual topological defects and demonstrate nontrivial electrophoresis. We measure several electrophoretic mobility coefficients and compare with those calculated theoretically. We demonstrate a competing effect of elastic and electrostatic torques that arises due to tilting of the rods in the liquid crystal. A simple theory describing this effect allows us to measure the effective polarisability of the rods. Our approach is simple and applicable to a wide variety of asymmetric and polarisable particles.

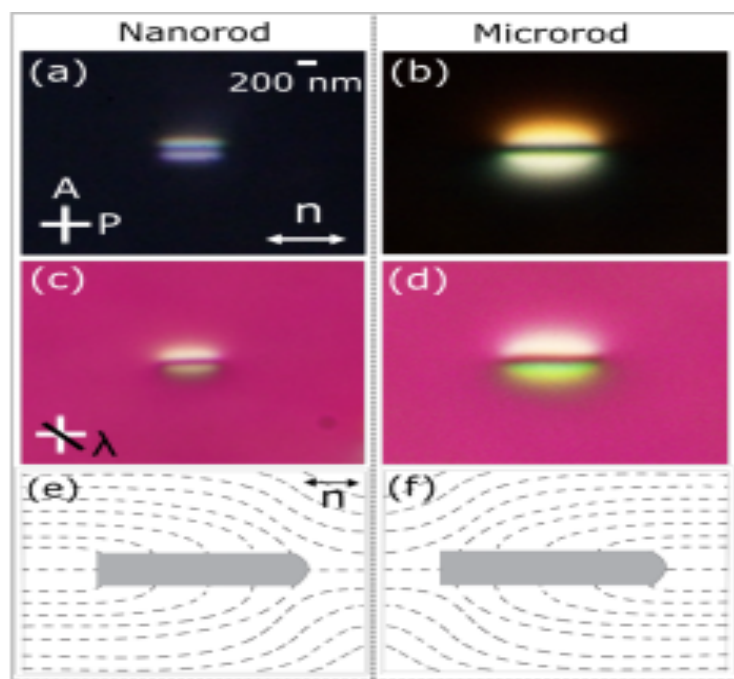


Figure 11: virtual topological defects induced by particles in a nematic liquid crystal

Reference:

Muhammed Rasi M, Archana S, Ravi Kumar Pujala, Surajit Dhara, Nontrivial electrophoresis of silica nano and microrods in a nematic liquid crystal, *Soft Matter*, 2022,18, 6043-6050

PC-55

Enhanced Electrochemical and Photocatalysis Using CZTS-MWCNT Nanocomposites

Ravi Mudike^a, Sardar Tathagata^a, Kunal Roy^a, Shiva Kumar Swamy^a, Jagadeesh Babu

Sriramoju^b, Prasanna D. Shivaramu^{a*}, Dinesh Rangappa^{a*}

^aDepartment of Applied Sciences (Nanotechnology), Visvesvaraya Technological University, Center for Postgraduate Studies, Muddenahalli, Chikkaballapur-562 101, India.

^bDepartment of Physics, Malla Reddy Engineering College (A), Secunderabad- 500 100, T.S., India.

e-address: prasuds@gmail.com; dineshrangappa@gmail.com

The electrochemical and photocatalytic properties of hydrothermally synthesized copper zinc tin sulfide-multiwalled carbon nanotubes (CZTS-MWCNT) hetero-structured nanocomposites (NCs) were investigated. The structural and optical properties of the CZTS nanoparticles (NPs) and CZTS-6 wt% MWCNT were characterized by XRD, SEM, TEM, Raman, XPS, BET, FTIR and UV-Vis spectroscopy. The TEM image confirmed that the CZTS NPs are anchored to MWCNTs. The BET surface area of CZTS NPs was 12.59 m² /g, which is slightly lower than the 13.94 m² /g observed for CZTS-6 wt% MWCNT NCs, indicating that MWCNTs increase surface area due to enhanced pore size distribution and pore volume. The bandgaps of CZTS NPs and CZTS-6 wt% MWCNT NCs are 1.65 eV and 1.4 eV, respectively. It shows that the CZTS-6 wt% MWCNT NCs with an optimum bandgap (1.4 eV) can absorb more photons when exposed to solar radiation, leading to an increase in photoresponse activities. Under visible light radiation, photocatalytic dye degradation of methylene orange studies revealed a 14% higher photodegradation efficiency for CZTS-6 wt% MWCNT NCs than CZTS NPs. The photocurrent responses are 74 $\mu\text{A}/\text{cm}^2$ and 164 $\mu\text{A}/\text{cm}^2$ for CZTS NPs and CZTS-6 wt% MWCNT NCs, respectively. The photocurrent response of CZTS-6 wt% MWCNT NCs is more than twofold higher than that of CZTS NPs. CZTS-MWCNT NCs enhance photocatalytic and photoresponse activity over CZTS NPs due to their optimal bandgap and rapid charge carrier mobility.

Keywords:

CZTS, MWCNT, photoelectrochemical, photocurrent response, methylene orange, photocatalytic dye degradation.

PC-56**Indigenous Development of Laser Diffraction Setup for Characterizing the Structure of Photonic Crystals**Saranya Narayanan^{*a}, Nishant Shankhwar^a and B.V.R Tata^{a,b}^aSchool of Physics, University of Hyderabad, Gachibowli, Hyderabad – 500046, India^b Centre for Interdisciplinary Research, GITAM Deemed to be University, Visakhapatnam, 530045, Indiae-address: 17phph30@uohyd.ac.in

Photonic crystals (PCs) grown in bulk, as well as in thin film form, need to be characterized for structural ordering and symmetry. Since the photonic crystal length scales are in the order of visible light, laser light diffraction is well suited for characterizing the structure of different photonic crystal systems where the diffracted intensity is related to the structure factor. Here we report the indigenous development of Laser diffraction setup for the characterization of structural ordering and symmetry of photonic crystals. The diffraction setup contains a He-Ne laser source of wavelength 633nm with a power of 20 mW. The incident light intensity falling on the sample is adjustable using a set of neutral density filters. The laser light is focused on to the sample by a convex lens. We have grown photonic crystals in one millimeter path length quartz cells having rectangular cross-section. In order to maintain the sample at constant temperature and minimize scattering from reflections arising from walls of the sample container we place the sample cells in a vat filled with index matching fluid. The Bragg diffraction/scattering pattern from samples are captured on a translucent screen placed at distance that maximizes the q - range, where q is the scattering wavevector. The scattering pattern is captured using a CMOS camera with the help of a fixed focal length lens. The captured digital images are stored in a computer. The recorded diffraction images are analyzed by developing a computer program in python language. Using this program we convert the 2D-digital image data into scattering profile viz., scattered/diffraction intensity $I(q)$ versus q . Using the information of particle size and shape, we extract the structure factor $S(q)$ information as function of q . Apart from presenting the structure factor obtained for different photonic crystals, the paper also discusses the details involved in designing the laser diffraction set-up and its advantages and limitations. The lattice constant measured using present laser diffraction set-up is compared with that obtained from Bragg diffraction recorded from UV-visible spectrum from same samples.

Acknowledgements:

The authors gratefully acknowledge the support of DST-SERB vide Sanction order No. CRG/2019/003714 with BVR Tata as PI and S. Venugopal Rao as Co-PI

References:

1. B.V.R. Tata, R.G. Joshi, D.K. Gupta, J. Brijitta and Baldev Raj, *Current Sci.*, 103, 1175 (2012)
2. D. Karthickeyan, R. G. Joshi, and B. V. R. Tata, *J. Chem. Phys.* 146, 224503 (2017)
3. A. Haldar and V. Ramarao, *IEEE Photonics Journal*, 12, 1 (2020)
4. A.V. Petukhov, J.M Meijer, G. J. Vroege, *Current Opinion in Colloid and Interface Science*, 20, 272(2015)

PC-57

One-Step Synthesis of Bismuth Ferrite by Microwave Assisted Solvothermal Method

Mahima Ann Paul^a, Pravallika Banoth^a, Pratap Kollu^{a,b}

^aSchool of Physics, University of Hyderabad, Gachibowli, Hyderabad – 500046, India

^bCASEST, School of Physics, University of Hyderabad, India.

e-address: 18ipmp15@uohyd.ac.in

The simultaneous exhibition of ferroelectric and ferromagnetic properties at room temperature and strong magnetoelectric coupling makes Bismuth Ferrite, BiFeO₃ (BFO) one of the most extensively studied multiferroic materials. It has promising applications in photovoltaics, photocatalysis, spintronic devices, electro-optics, and energy-efficient data storage. Optimization of microwave synthesis of BFO, in the shortest possible duration, by varying microwave power and concentration of mineralizer (Potassium Hydroxide-KOH) has been studied. Pure phase BFO without any impurities, aggregations or secondary phases has been synthesized by the microwave-assisted solvothermal (MWAST) method in 3-minutes. X-ray diffraction (XRD) results verify the successful synthesis of single-phase rhombohedral BFO, further confirmed by the Fourier transform infrared spectrum. Unsaturated polarization-electric field loops of BFO samples indicate a high leakage current, which could be minimized by doping with suitable transition elements like chromium. Microstructural analysis by field-emission scanning electron microscopy revealed the formation of spherical BFO micro-flowers with nano-petals. The sample shows a single-phase crystalline structure with soft ferromagnetic behavior and acts as a promising dielectric material at high temperatures, suggesting that the synthesis of BFO by MWAST might be suitable for multiferroic applications.

Reference:

Microwave-Assisted Solvothermal Route for One-Step Synthesis of Pure Phase Bismuth Ferrite Micro flowers with Improved Magnetic and Dielectric Properties, Pravallika Banoth, Arya Sohan, Chinna Kandula, Ravi Kumar Kanaka, and Pratap Kollu, ACS Omega 2022 7 (15), 12910-12921, DOI: 10.1021/acsomega.2c0021.

PC-58

Finite element method simulation studies on Photonic Crystal templates with and without defects with emphasis on Q-modes

Nishant Shankhwar^a, Saranya Narayanan^a, B. V. R. Tata^{a,c} and S. Venugopal Rao^b

^aSchool of Physics, University of Hyderabad,

^bAdvanced Centre of Research in High Energy Materials, University of Hyderabad,

^cCentre for Interdisciplinary Research, GITAM (Deemed to be University), Visakhapatnam, 530045, India

e-address: nishant.shankhwar@gmail.com

In this work, different types of photonic crystals (PhCs) varying in terms of structural arrangement (rectangular or hexagonal) of particles, as well as, in terms of the refractive index contrast have been studied. The PhC structures considered for simulation were monolayers of periodically arranged particles on a silica substrate with and without a point-defect. The finite element method simulations have been performed with an aim to (a) determine the PhC structure that enables maximum electric field confinement, hence enhancement in Q-factor; and (b) to compare the electric field enhancement in the near-field region around a gold nanoparticle present inside the point-defect with that of a nanoparticle present on the surface of the silica substrate without the PhC. The results of the simulations reveal the following: i) light is confined more efficiently by the hexagonal lattice than the rectangular lattice owing to more closely packed structure of the former; ii) PhC with higher refractive index contrast gives better enhancement in Q-factor. It has been observed that point-defect in a 5x5 supercell of the hexagonal TiO₂ PhC with particle size $a=253$ nm and refractive index $n=2.67$, exhibits Q-factor ~ 100 . Simulations with plasmonic nanoparticle at the defect site in PhC of high refractive index contrast showed further enhancement (about one order in magnitude) in Q-factor as compared to the PhC structure with bare point-defect. It has been observed that the electric field at the distance of 5 nm (near-field region) from the surface of a 40 nm gold nanoparticle present inside the point-defect was enhanced approximately 7 times compared to the nanoparticle without PhC. The above-mentioned computational results are relevant to applications like Surface Enhanced Raman Spectroscopy.

Acknowledgements:

The authors gratefully acknowledge the support of DST-SERB vide Sanction Order No. CRG/2019/003714 with B. V. R. Tata as PI and S. Venugopal Rao as Co-PI.

References:

1. Liu, Bing, et al. "Recent advances in merging photonic crystals and plasmonics for bioanalytical applications." *Analyst* 143.11 (2018): 2448-2458
2. Narayanan, Saranya, and B. V. R. Tata. "Effect of doping on defect modes of 2D photonic band gap crystals." *AIP Conference Proceedings*. Vol. 2269. No. 1. AIP Publishing LLC, 2020.
3. Akahane, Yoshihiro, et al. "High-Q photonic nanocavity in a two-dimensional photonic crystal." *nature* 425.6961 (2003): 944-947.
4. Mu, Zhongde, et al. "Photonic crystal hydrogel enhanced plasmonic staining for multiplexed protein analysis." *Small* 11.45 (2015): 6036-6043.

PC-59**Rheology of lyotropic chromonic liquid crystals**

M.V. Saisavadas^{a*}, M. Praveen Kumar^a, B.V.R. Tata^{a,b} and Surajit Dhara^a

^aSchool of Physics, University of Hyderabad, Gachibowli, Hyderabad – 500046, India

e-address: dssaisav@gmail.com

We investigate the shear induced flow behaviour of the nematic phase of a lyotropic chromonic liquid crystal (LCLC) formed by dissolving 32 wt% of Sunset Yellow (SSY) using a rheometer. We observed flow curves to exhibit three dynamic regimes viz., R1, R2 and R3 for a certain ranges of shear rate, $\dot{\gamma}$ and temperature, T. Regimes R1 and R3 exhibited Newtonian flow behaviour with stress $\sigma \propto \dot{\gamma}$, whereas the regime R2 showed a near plateau stress region characterised by a power law $\sigma \propto \dot{\gamma}^\beta$, where β is found to be in the range of 0.31-0.36. Upon increasing shear rate, interestingly we observed SSY LC to undergo a continuous transition from region R1 to R2 and a discontinuous transition with a hysteresis from region R2 to R3. Further, we observe the flow behaviour in the regimes R2 and R3 to be qualitatively similar to the behaviour reported in worm-like micellar systems and twist bend nematic liquid crystals. The time dependence of stress under steady shear recorded for the near-plateau regime show dynamic stress fluctuations, exhibiting periodic and quasi periodic oscillations. Further, the non-monotonic flow behaviour and stress dynamics in this system is discussed in the context of shear banding.

Acknowledgements:

The authors gratefully acknowledge the support of DST-SERB vide Sanction Order No. CRG/2019/003714 with B. V. R. Tata as PI and S. Venugopal Rao as Co-PI.

References:

- 1) M. Praveen Kumar, et al. Phys. Rev. Materials 5, 115605 (2021)
- 2) R. Bandyopadhyay et al. Phys. Rev. Lett. 84, 2022 (2000)
- 3) R. Bandyopadhyay and A. K. Sood, EPL 56, 447 (2001)
- 4) A. K. Sood and R. Ganapathy, Pramana J. Phys. 67,33 (2006)

PC-60

Power spectral analysis on colloidal suspensions of thermo-responsive poly(N-isopropyl acrylamide) PNIPAM microgels

Sivaram vintha^{*a}, Manimaran Palanisamy^a, B.V. R. Tata^{a,b}^aSchool of Physics, University of Hyderabad, Gachibowli, Hyderabad – 500046, India^bCentre for Interdisciplinary Research, GITAM Deemed to be University, Visakhapatnam, 530045, Indiae-address: siva25271@gmail.com

Mathematical modeling plays a vital role in studying experimental systems through simulations such as Monte-Carlo (MC) and molecular dynamics (MD) simulations. Here we adopt MC simulations based on the Metropolis algorithm to study the aqueous suspension of poly(N-isopropyl acrylamide) (PNIPAM) microgel suspensions interacting via Multi-Hertzian (MH) pair potential. Constant NVT MC Simulations have been carried out over a wide volume fraction range (volume fraction, $\phi = 0.3$ to 0.85) and a temperature range ($T = 15^\circ\text{C}$ to 40°C) for PNIPAM microgel suspensions at various temperatures (i.e at $T=15^\circ\text{C}$ to 26°C). In this work, we characterize the fluctuation behavior of the total energy of the N particle system at temperatures below, at, and above a critical temperature T_c (around the melting point of PNIPAM microgel crystal) through Fourier power spectral analysis. we found from the analysis that the energy fluctuations show uncorrelated random (Brownian type) behavior below and above T_c , and fractional Brownian motion at the critical temperature. In addition to presenting the energy behavior, we also discuss the ordering and phase behavior of suspensions analyzed by computing quantities such as pair-correlation functions and mean-square displacement behavior as a function of volume fraction and temperature.

References:

1. B.V.R. Tata, J. Brijitta and R.G. Joshi, Int. J. Eng. Sci. and Applied Maths. 5, 240 (2013)
2. P. Manimaran et al. Physica A. 389, 3703-3710 (2010)
3. Maxime J. Bergeman et al Nature Commun. 9, 5039 (2018).
4. R.G. Joshi, B.V.R. Tata, Colloid Polym Sci. 295, 1671 (2017)

PC-61**Investigation of Room Temperature Structural and Electrical properties of Ti doped CuO Nano particles**

N.S. Maruthi^a, Hanamanta Badiger^b, B.G.Hegde^b, B.Gobinath^c, Shaila Umesh Durgasimi^d, Shidaling Matteppanavar^{*e}

^aDepartment of Physics, Annamalai university, India.

^b Department of Physics, Rani Channamma University Belagavi, India.

^cThiru Vi Ka Govt Arts college, Thiruvarur, India

^dBagalkote Engineering College Bagalkote, India.

^eDepartment of Physics KLE society's Basavaprabhu kore Arts cience and commerce college Chikkodi, India.

*Corresponding Author email: siddutifr@gmail.com

e-address: vamaruna@gmail.com

Copper oxide (CuO) has attracted much attention in the applications of electrochemical cells, gas sensors, magnetic storage media, photovoltaic cells, light emitters and thermoelectric materials. In this present work the synthesis of Ti doped CuO ($\text{Cu}_{1-x}\text{Ti}_x\text{O}$, where $x=0.1, 0.2, 0.3, 0.4$ and 0.5) nano particle by modified auto combustion method with urea as a fuel. The detailed room temperature structural and electrical properties of Ti doped CuO nanoparticles were systematically characterized through X-ray diffraction studies (XRD), FT-IR spectra, Field-emission scanning electron microscope (FE-SEM) and electrical properties by impedance analyzer. The average crystal size and micro-strain of pure Ti doped CuO nanoparticles were calculated using Debye-Scherrer equation and Rietveld Refinement carried out for obtaining lattice parameter and bond distance from VESTA programming for all the samples. The XRD pattern reveals that confirmation of monoclinic structure with C2/c space group and well matched with JCPDS No. 02-1225 without formation of second phase, FT-IR spectra confirms the presence of Cu-o bond and slight change in vibrational peak from 520 to 529cm^{-1} . The morphology of Ti doped CuO nanoparticle was observed in FE-SEM and shows the particle size is $1-2\mu\text{m}$. The complex impedance measurement at room temperature, with frequency range $1\text{KHz}-1\text{MHz}$, this implies the dielectric constants and dissipation factor are gradually decreases with increasing in frequency and Z' versus Z'' plot suggest the presence of electrical process occurring and relaxation in the system.

PC-62**Electronic structure and magnetic properties of Ruthenium based full Heusler alloy Ru_2CrX ($\text{X} = \text{Si}, \text{Ge}$)**

Mainak Dey sarkar, G Vaitheeswaran*

School of Physics, University of Hyderabad, Gachibowli, Hyderabad – 500046, India

*Corresponding author: vaithee@uohyd.ac.in e-address: dsmainak238@gmail.com

We have investigated the electronic structure and magnetic properties of full-Heusler alloy Ru_2CrX ($\text{X}=\text{Si},\text{Ge}$) using density functional theory implemented within Vienna Ab initio Simulation Package (VASP) with the generalized gradient approximation (GGA) for the exchange-correlation energy. The magnetic configurations of the alloy were examined by simulating different initial magnetic (NM, FM, AFM1,AFM2) arrangements. We have found that the compound is stable for AFM2 state which agrees quite well with the available experimental results. The role of strong correlation effect is vivid from the standard GGA results where the above compounds are found to be semi-metallic in contrast to experimental semiconducting nature. In order to overcome this we have performed GGA+U calculations to account for the on-site correlation at the transition metal sites:(Cr:3d) and (Ru:4d) atoms. This has considerably improved the electronic structure resulting in a narrow band gap which is close to the experimental results. The above results emphasis the importance of strong coulomb correlation effect in intermetallic Heusler compounds.

Acknowledgements:

Mainak Dey Sarkar is thankful for the financial assistance granted by DST-SERB. Authors are thankful to CMSD and University of Hyderabad,for providing computational facilities.

References:

1. H.Okada et al : App. Phys.Lett. 92, (2008) 062502.
2. H.Okada et al.: Journal of Physics: Conference Series 150, (2009) 042153.
3. T. Kanomata, T. Awano , T. Eto: Solid State Communications 340 (2021) 114525

PC-63

2TBA functionalized silver clusters as active SERS substrates for D-glucose detection and metering

Ingilala Venkataramanaiah, Chandrahas Bansal, Amnanabrolu Rajanikanth

School of Physics, University of Hyderabad, Gachibowli, Hyderabad – 500046, India

e-address: ivr5326@gmail.com

Quantitative detection of D-Glucose in body fluids is important for management of diabetes mellitus. In this work we present a novel and inexpensive method for synthesis of silver nanocluster films on a substrate by a physio chemical extension of the Tollens reaction method for silver mirror test that is commonly employed to detect the presence of aldehydes in aqueous solutions. Our method consists of arresting the silver film formation on a glass surface. Glucose does not directly attach on the silver surface and therefore it is required to functionalize the silver substrate for attachment of D-glucose for use as substrates for surface enhanced Raman Scattering. We use 2-Thienyl Boronic Acid (2-TBA) to functionalize the Ag cluster film so that it serves as a linker molecule which attaches to silver at the thienyl site and to the D-Glucose molecule at the B(OH)₂' site of the 2-TBA molecule¹. The 2-TBA functionalized SERS substrate gives good Raman signal and the intensity of one of the Raman lines appearing at 990 cm⁻¹ was used to quantify the D-Glucose amount concentration in the range 5 micro mole/liter to 1 milli mole/liter in aqueous solutions. This range is suitable to measure D-glucose levels in saliva for application in diabetes.

Key Words:

cluster film, functionalization, SERS

References:

1. Raju Botta, A. Rajanikanth, C.Bansal, Sensing and Bio-Sensing Research 9 (2016) 13–16.

PC-64**Reddish-orange emissions from Sm³⁺ doped Sm₂Si₂O₇ -based glass ceramics for solid-state lighting applications**

M. Monisha and Sudha D Kamath

Department of Physics, Manipal Institute of Technology, Manipal Academy of Higher Education, Manipal, Karnataka -576 104, India.

e-address: monisham2013@gmail.com

The present work reports on the structural and luminescence behaviour of Sm³⁺ doped glass ceramics prepared via melt-quenching and heat-treatment process. The XRD studies on the heat-treated glasses revealed the formation of Sm₂Si₂O₇ crystalline phase. FESEM studies showed the morphological change in the glass ceramics subjected to higher heating temperature. The absorption spectra showed the lower bandgap values for the glass ceramic obtained at higher temperature. Excitation and emission studies on heat-treated samples showed improvement in their intensities compared to the unheated base glass. The thermal quenching is observed at higher temperatures (540° C and 580° C for 3 hours) of heat-treated samples. Calculations based on luminescence spectra including radiative transition probability, stimulated emission cross-section and branching ratio showed good results for glass ceramics prior to precursor glass. Longer lifetimes of Sm³⁺ ions (milliseconds) in the level ⁴G_{5/2} are seen for glass ceramics. Color coordinates and correlated color temperature (CCT, K) values suggested the reddish-orange emissions from the glass ceramics. Thus, Sm³⁺ doped Sm₂Si₂O₇ glass ceramics are favorable materials for solid-state lighting and laser applications.

References:

1. Siying Wang, Hongbo Zhang, Tong Wang, Huimin Lv, Xiangyu Zou, Yulin Wei, et al. Synthesis and luminescence properties of Sm³⁺ doped molybdate glass ceramic. *J. Alloys Compd.* 2020;823:153822.
2. Weihuan Zhang, Yuepin Zhang, Shaoye Ouyang, Zhixiong Zhang, Haiping Xia. Enhanced luminescent properties of Sm³⁺ doped glass ceramics -as potential red-orange phosphor for white light-emitting diodes. *Mater. Lett.* 2015;160:459-462.
3. Fangfang Hu, Yuncheng Jiang, Yihang Chen, Rongfei Wei, Hai Guo, Changkui Duan. Optical thermometry based on the thermal coupling of low-lying levels of Sm³⁺ in highly stable NaGdF₄ glass ceramics. *J. Alloys Compd.* 2021;67:159160.
4. Sherin Thomas, Jithesh Kavil, Achamma Mathew Malayali. Dielectric properties of PTFE loaded with micro and nano-Sm₂SiO₇ ceramics. *J. Mater. Sci. Mater. Elec.* 2016;27:9780-9788.
5. W. T. Carnall, P. R. Fields, K. Rajnak. Electronic Energy Levels in the Trivalent Lanthanide Aquo Ions. I. Pr³⁺, Nd³⁺, Pm³⁺, Sm³⁺, Dy³⁺, Ho³⁺, Er³⁺, and Tm³⁺. *J. Chem. Phys.* 1968;49:4424.

PC-65

Lattice Dynamics of 5-ATZN predicted from first principle studies

Supratik Mukherjee^a, Prathap Kumar Jharapla^a, and G Vaitheeswaran^b^aAdvanced Centre of Research in High Energy Materials (ACRHEM), University of Hyderabad, Telangana, 500046, India^bSchool of Physics, University of Hyderabad, Telangana, 500046, Indiae-address: 19acpp06@uohyd.ac.in

We present a density functional based computational study of oxygen rich 5-Aminotetrazolium nitrate (5-ATZN), which is a promising gas-generating propellant. 5-ATZN¹ is an oxygen-rich compound, and found to have better burning rates and increased temperature stability which are highly desirable for gas-generating propellants. Considering these features, a detailed theoretical investigation is necessary to investigate the sensitivity and mechanical stability by computing structural, elastic and electronic band structure properties of 5-ATZN. In the present work, we employed Plane wave pseudopotential method (PW/PP) implemented in CASTEP is used to calculate structural properties and elastic constants. The electronic bandgap calculations were carried out using WIEN2k package using full potential linear augmented plane wave method (FP-LAPW). 5-ATZN (CH₄N₆O₃) crystallizes in monoclinic space group P21/c, with 56 atoms in unit cell. Ordering of these elastic constants along the principal directions are as follows: $C_{22} < C_{11} < C_{33}$.

C_{11}	C_{22}	C_{33}	C_{12}	C_{13}	C_{23}	C_{44}	C_{55}	C_{66}	C_{15}	C_{25}	C_{35}	C_{46}	B
36.86	8.86	66.21	4.02	26.59	11.54	9.01	16.94	3.03	-1.84	0.14	-1.92	-0.55	7.58

Figure 12: Table -Elastic constants and Bulk Modulus of 5-ATZN.

The study of the elastic constants reveals that b-axis is more sensitive and c-axis is less sensitive to shock initiation. The TB-mbJ bandgap of this material is found to be 4.5 eV.

References:

1. A.H.S. Ruediger, S.H. Hermann, US Patent 3,898,112 (1975)

PC-66

Topological study of nonsymmorphic Dirac semimetal phase in layered Matlockites ACdSb (A = Rb, Cs)

Aiswarya T, G Vaitheeswaran

School of Physics , University of Hyderabad, Gachibowli, Hyderabad-500046, India

Corresponding author: vaithee@uohyd.ac.ine-address: aiswaryat95@gmail.com

Due to their extraordinary physical characteristics, such as ultra-high mobility and very high magnetoresistances, materials containing exotic quasiparticles, such as massless Dirac and Weyl fermions, have attracted considerable interest from physics and material science communities. Here, we demonstrate that the very stable ACdSb has an electronic band structure that has several Dirac cones that combine to produce a Fermi surface with a line of Dirac nodes that resembles a diamond. We theoretically studied three-dimensional Dirac semimetal with nodal lines protected by crystalline symmetries. We discuss about the nodal lines that are shielded by the union of time reversal and inversion symmetry. In the lack and presence of the spin-orbit coupling, we suggested several class of nodal lines. Because of this, ACdSb is a particularly interesting candidate for research on Dirac electrons and Dirac node features. We calculated the Z_2 invariants for ACdSb and found them weak topological materials.

Acknowledgment:

Aiswarya T is thankful to Prime Ministers Research Fellowship (PMRF) for the funding support. The authors thank CMSD, University of Hyderabad for the computational facility.

References:

1. B. Owens-Baird, L.-L. Wang, S. Lee, and K. Kovnir, *Zeitschrift fur anorganische und allgemeine Chemie* 646, 1079 (2020).
2.] S. M. Young and C. L. Kane, *Physical review letters* 115, 126803 (2015).

PC-67

Role of annealing ambience on the electrical properties of Ge MOS Capacitors with HfO₂/Ge₃N₄ as gate dielectric

S.V. Jagadeesh Chandra

Department of Physics, GITAM School of Science, GITAM (Deemed to be) University, Visakhapatnam-530045
e-address: jsangara@gitam.edu

Investigations on post deposition annealing (PDA) ambience, including oxygen (O₂) and forming gas (FG), on interfacial and electrical properties of a HfO₂ gate dielectric on nitrided Ge are analyzed. Experiments to study the interface quality, and chemical composition of HfO₂/Ge₃N₄/Ge devices were carried out using, high-resolution transmission electron microscopy (HRTEM) imaging, and X-ray photoelectron spectroscopy (XPS) measurements, respectively. The XPS study confirmed that O₂ PDA effectively improves the HfO₂ film stoichiometry, and the stability of the interface between HfO₂/Ge₃N₄/Ge stacks is enhanced. Further, HRTEM images showed that the interface between HfO₂/Ge₃N₄/Ge stacks for O₂-annealed devices was smooth, uniform, and flat. The experimental results for devices annealed in O₂ at 500°C exhibited improved interfacial and electrical characteristics, such as a high dielectric constant of ~19; high capacitance, 1.2 nF, low equivalent oxide thickness, 1.5 nm; interface trap density, $2.18 \times 10^{11} \text{ cm}^{-2} \text{ eV}^{-1}$; and gate leakage currents in the order of nA, $0.5 \times 10^{-9} \text{ A/cm}^2$, as compared with FG annealing devices. The Fowler-Nordheim tunneling current conduction mechanism was also verified. Therefore, these results are evidence that the O₂ PDA process improves the interfacial and electrical properties of HfO₂/Ge₃N₄/Ge metal-oxide-semiconductor (MOS) devices as compared with FG annealing.

PC-68

Flexible PVDF-HFP based SERS active substrates with biosynthesized Au nanoparticles

Saloni Sharma^{*a,b}, M Ghanashyam Krishna^{b,c,d}, S. V. S. Nageswara Rao^{b,d}, and Ram Manohar Yadav^{a,e*}

^aDepartment of Physics, V.S.S.D. College, CSJM University, Nawabganj, Kanpur, 208002, Uttar Pradesh India

^bCenter for Nanotechnology University of Hyderabad, Prof. CR Rao Road, Gachibowli, Hyderabad, 500046, Telangana, India

^cSchool of Physics, University of Hyderabad, Prof. CR Rao Road, Gachibowli, Hyderabad, 500046, Telangana, India

^dCentre for Advanced Studies in Electronics Science and Technology (CASEST), University of Hyderabad, Hyderabad 500046, Telangana, India

^eDepartment of Physics, University of Allahabad, Prayagraj-211002 Uttar Pradesh, India

*e-address: saloni.nano@uohyd.ac.in, rmanohar28@gmail.com

Pollutant detection in water has always been a challenge and flexible thin polymer membranes can be used to overcome this problem. Here free standing transparent composite films of Poly(vinylidene fluoride-hexafluoropropylene) (PVDF-HFP) embedded with Au nanoparticles were prepared for Methylene blue (MB) detection. MB is an organic dye and due to frequent use in various industries, it became most abundant pollutant in aquatic medium. Because of its toxicity: detecting and removing MB from water resources is now a matter of necessity. Au nanoparticles were synthesized by dropping the AuCl₃ solution on Neem(Meliaceae) leaves and further PVDF-HFP films were mimicked on those leaves. These freestanding films were used as Surface Enhanced Raman Spectroscopy (SERS) substrates for the detection of Methylene blue. A significant enhancement in intensity (10⁴) has been noticed in SERS signal as compare to pristine polymer samples. Another characteristic of these polymer-based SERS substrates is that these can be molded into any form. The data will be presented in conference.

Keywords:

PVDF-HFP, Methylene Blue, SERS.

PC-69

Enhanced photocatalytic hydrogen evolution from reduced graphene oxide-defect rich TiO_{2-x} nanocomposites

Jagadeesh Babu^{S. a,b}, Murthy Muniyappa^{a,c}, Navakoteswara Rao^{V^d}, Ravi Mudike^a,
MaheshShastri^{a,c}, SardarTathagata^a, Prasanna D.Shivaramu^a, ShankarM.V. ^d,
Anand Kumar C.S.^a DineshRangappa^a
e-address: dineshrangappa@gmail.com

Solar-driven photocatalytic hydrogen generation by splitting water molecules requires an efficient visible light active photocatalyst. This work reports an improved hydrogen evolution activity of visible light active TiO_{2-x} photocatalyst by introducing reduced graphene oxide via an eco-friendly and cost-effective hydrothermal method. This process facilitates graphene oxide reduction and incorporates intrinsic defects in TiO_2 lattice at a one-pot reaction process. The characteristic studies reveal that RGO/ TiO_{2-x} nanocomposites were sufficiently durable and efficient for photocatalytic hydrogen generation under the visible light spectrum. The altered band gap of TiO_{2-x} rationally promotes the visible light absorption, and the RGO sheets present in the composites suppresses the electron-hole recombination, which accelerates the charge transfer. Hence, the noble metal-free RGO/ TiO_{2-x} photocatalyst exhibited hydrogen production with a rate of $13.6 \text{ mmol h}^{-1} \text{ g}_{cat}^{-1}$ under solar illumination. The appreciable photocatalytic hydrogen generation activity of $947.2 \mu\text{mol h}^{-1} \text{ g}^{-1} \text{ cat}$ with $117 \mu\text{Acm}^{-2}$ photocurrent density was observed under visible light ($>450 \text{ nm}$).

Keywords:

TiO_{2-x} RGO/ TiO_{2-x} Defect rich TiO_2 Photocatalyst Photo anode Solar hydrogen generation

PC-70

Defect - Polymorphism - Controlled Electrophoretic Propulsion of Anisometric Microparticles in a Nematic Liquid Crystal

Devika V.S^a, Dinesh Kumar Sahu^a, Ravi Kumar Pujala^b, and Surajit Dhara^a

^aSchool of Physics, University of Hyderabad, Gachibowli, Hyderabad – 500046, India

^bSoft and Active Matter Group, Department of Physics, Indian Institute of Science Education and Research (IISER), Tirupati, Andhra Pradesh 517507, India
e-address: devikavs2@gmail.com

The nontrivial shape of colloidal particles creates complex elastic distortions and topological defects in liquid crystals and plays a key role in governing their electrophoretic propulsion through the medium^{1,2}. Here, we report experimental results on defects and the electrophoretic transport of anisometric (snowman shaped) polystyrene particles subjected to an alternating electric field perpendicular to the director in a nematic liquid crystal. We demonstrate that the shape asymmetry gives rise to defect polymorphism by nucleating point or ring defects at multiple locations on the particle and controls the direction as well as the magnitude of the electrophoretic propulsion. Unlike spherical particles, quadrupolar anisometric particles can be transported in multiple directions in the plane perpendicular to the applied field. Our findings provide an alternative degree of freedom in translocating microparticles in liquid crystals for applications in microfluidics, controlled transport, and directed assembly.

References:

1. T. M. Squires and M. Z. Bazant, Induced-charge electroosmosis, *J. Fluid Mech.* 509, 217 (2004).
2. O. D. Lavrentovich, Active colloids in liquid crystals, *Curr.Opin. Colloid Interface Sci.* 21, 97 (2016).

PC-71

Investigating The Effect Of Morphology Of Titanium Dioxide Nanostructures On The Electronic Properties Of A Diode Device

Avijit Tudu, Praveen K. Lavudya, Rajanikanth Ammanabrolu
School of Physics, University of Hyderabad, Gachibowli, Hyderabad – 500046, India
e-address: 21phph13@uohyd.ac.in

Titanium dioxide nanostructures has been synthesized successfully by hydrothermal method. The hydrothermal growth period was for 12 hours at 180°C. The effect of Titanium Dioxide nanostructures on electronic properties a diode device has been investigated. From XRD (X-Ray Diffraction) analysis we confirmed the preparation of Titanium Dioxide nanostructures. The FESEM (Field Emission Scanning Electron Microscopy) images show nanowires morphology obtained hydrothermally. The nanowire formation was confirmed by Raman analysis. Our main aim of this work is to fabricate a diode device. In this work, a sandwich type diode device is fabricated, in which Indium Tin Oxide (ITO) coated glass and Silver are used as front electrode and back electrode, respectively. Current-Voltage (I-V) characteristics of the fabricated diode device has been measured to estimate the ideality factor of the device. Diode devices were prepared with Titanium Dioxide nanowires and the other with Titanium Dioxide nanoparticles (P25). From the I-V characteristics curve we see that the diode device with Titanium Dioxide nanowires shows better performance in comparison to Titanium Dioxide (P25) nanoparticles. The present report gives us an idea that the electronic properties of diode device depend on the morphology of the synthesized material and we can study other nanostructures and study their effect on these diode devices.

References:

1. Fehmi Aslan, Hihmet Esen, FahrettinYakuphanoglu, Silicon, December (2019)
2. M. Yilmaz, A. Kocyigit, S. Aydogan, U. Incekara, A. Tursucu, and H. Kacus, Journal of Mater Science: Mater Electron, October (2020)
3. Pallab Kumar Das, Sudipta Sen, Nabin Maran Manik, Journal of Nano Research, (2021)
4. G.S. Falk, M.Borlaf, M.J. Lopez-Munoz, J.C. Farinas, J.B. Rodrigues Neto, R. Moreno, Journal of Nanoparticle Research (2018).
5. Erman Erdogan, Mehmet Yilmaz, Sakir Aydogan, Umit Incekara and HaticeKacus, Semiconductor Science and Technology (2021).
6. B. Coskun, K. M. Dwarka, M. Soylyu, A.G.Al-Sehemi, A. Dere, Ahmed Al-Ghamdi, R.K. Gupta, F. Yakuphanoglu, Thin Solid Films (2018).

PC-72**Vertical distribution of natural radionuclides and health assessment in sediment samples of the northeast coast of Tamil Nadu**V Sathish^a, A Chandrasekaran^{a*}, C Gurumoorthy^b, C K Senthil Kumar^b^aDepartment of Physics, Sri Sivasubramaniya Nadar College of Engineering, Kalavakkam – 603110 Chennai.^bCentre for Applied Nuclear Research in Science and Engineering Education, Bharath institute of higher education and research, Selaiyur – 600073 Chennai.¹Corresponding author: chandrasekarana@ssn.edu.ine-address: sathishv@ssn.edu.in

In this study, nearly 63 shoreline sediment samples were collected from twenty-one locations at three different depths (0 – 20 cm, 20 – 40 cm, and 40 – 60 cm) along the northeast coast of Tamil Nadu. The collected samples were examined to estimate the activity concentration of natural radionuclides (²³⁸U, ²³²Th, and ⁴⁰K) using a NaI(Tl) γ -ray detector. The radiological parameters such as annual effective dose equivalent (AEDE), external hazards (H_{ex}), γ -index (I_γ), and activity utilization index (AUI) are estimated and compared with recommended levels provided by united nations scientific committee on the effects of atomic radiation (UNSCEAR). The radiological data were processed by different multivariate statistical parameters to determine the similarities and correlations among the different depths of the samples. the average concentrations of radiological parameters (for top(0-20cm), middle(20-40cm), and bottom(40-60cm)): AEDE (0.12, 0.08, and 0.08 mSvy⁻¹), H_{ex} (0.55, 0.37, and 0.38), I_γ (0.74, 0.51, and 0.52), and AUI (1.45, 0.89, and 0.90), are below permissible limits. Our findings reveal that shoreline sediment does not significantly pose a radiological concern to human health and this study gives baseline data for radioactivity in shoreline sediment samples for northeast coast of Tamil Nadu.

Keywords:Beach sediment; NaI(Tl) γ -ray detector; Natural radioactivity; Dose assessment.**References:**

UNSCEAR, 2000. Sources and Effects of Ionizing Radiation, United Nations Scientific Committee on the Effects of Atomic Radiation UNSCEAR 2000 Report to the General Assembly, with Scientific Annexes, UNSCEAR 2000 Report.

PC-73**Mineral and thermal analysis of ancient potteries of Tami Nadu**

A.Tamilarasi, A. Chandrasekaran

Department of Physics, Sri Sivasubramaniya Nadar College of Engineering, Kalavakkam-603110, Chennai.

e-address: tamilarasia@ssn.edu.in; chandrasekarana@ssn.edu.in

The characterization of the ancient potteries provides information about the technical and cultural activities of the past humans. For this, 19 pottery samples were recently excavated from archaeological site Vikravadi, Tamilnadu. These collected samples were subjected by Fourier Transform Infrared Spectroscopy (FTIR) and Thermogravimetry and Differential Thermal analysis (TG-DTA) for estimate the firing atmosphere, firing temperature and the nature of the raw material used to make pottery by ancient artisans at the time of manufacturing. From FT-IR technique minerals such as quartz, albite, orthoclase, microcline, and hematite were identified. TG-DTA analysis reveals that the pottery samples are fired at oxidizing atmosphere temperature range between 800°C and 900°.

Keywords:

Archaeological pottery, Firing temperature, FT-IR, TG-DTA, Oxidizing atmorpere

References:

1. Palanivel, R., and U. Rajesh Kumar. "Thermal and spectroscopic analysis of ancient potteries." *Romanian Journal of Physics* 56.1-2 (2011): 195-208;
2. Gomathy, Y., et al. "A preliminary study of ancient potteries collected from Kundureddiyur, Tamil Nadu, India." *Microchemical Journal* 165 (2021): 106100.

PC-74

Analysis of Heavy metal Contamination of sediments of Kovalam, Tamilnadu using X-ray Fluorescence Spectroscopic Technique

S. Karthikayini, A. Chandrasekaran

^aDepartment of Physics, Sri Sivasubramaniya Nadar College of Engineering, Kalavakkam, Chennai-603110
e-address: karthikaphy171199@gmail.com; chandrasekarana@ssn.edu.in

The analysis of heavy metal contamination in the sediment of Kovalam beach was examined by the pollution indices which describe the potential environmental and human health risks posed due to natural or anthropogenic activities. The fifteen sediment samples were collected and heavy metal (Si, K, Ca, Ti, Fe, Cu, Ni, Pb, and Zn) concentrations were determined by X-Ray fluorescence Spectroscopy. In order to assess the pollution status of the samples geo-accumulation index (I_{geo}), contamination factor (CF), pollution load index (PLI), and enrichment factor (EF) were evaluated. Based on the average concentration, K, Ca, Ti, Fe, Cu and Pb exceeded than their corresponding background value. The result of pollution indices reveals that the samples are contaminated by heavy metals Ti and Fe. The contamination may have occurred due to natural or anthropogenic activities.

Keywords:

Heavy metals, Pollution Indices, XRF, Kovalam beach

References:

1. Wedepohl, K. Hans. "The composition of the continental crust." *Geochimica et cosmochimica Acta* 59.7 (1995): 1217-1232.
2. Salem, Dalia MS Aly, et al. "Comprehensive risk assessment of heavy metals in surface sediments along the Egyptian Red Sea coast." *The Egyptian Journal of Aquatic Research* 40.4 (2014): 349-362.

PC-75

Investigation of molecular interaction studies of ethylene glycol /sulfolane binary mixtures at different temperatures using volumetric, dielectric relaxation, and DFT methods

V Manjula ^{ab}, T. Vamshi Prasad ^c, K. C. James Raju ^d, T. Vishwam ^a

^aDepartment of Physics, GITAM (Deemed to be University) -Hyderabad, Patancheru (M), TS- 502329, India

^bDepartment of Physics, Geethanjali College of Engineering and Technology, Hyderabad, Telangana, 501301, India

^cDepartment of Physics, B. V. Raju Institute of Technology Vishnupur, Narsapur, Medak District – 502313. Telangana, India, India.

^dSchool of Physics, University of Hyderabad, Hyderabad, Telangana 500046, India

*Corresponding author: vtalloju@gitam.edu, kcjrsp@uohyd.ac.in

The complex permittivity spectra of ethylene glycol/sulfolane mixtures in the complete concentration range have been determined as a function of frequency between $0.02 < \nu/\text{GHz} < 20$ in the temperature range 298.15K-323.15K at intervals of 5K. The dielectric relaxation parameters were retrieved by using Havriliak-Negami equation to determine excess permittivity, excess Gibbs activation energies, Kirkwood correlation factors, and Bruggeman factors of the ethylene glycol/sulfolane binary mixtures. The excess volumetric and dielectric parameters such as permittivity, refractive index, and relaxation times are fitted with the Redlich-Kister polynomial equation. The obtained data can be interpreted by different microscopic processes, including the association and dissociation of hydrogen-bound networks under molecular interaction and the parallel or antiparallel orientational rearrangement between heterogeneous dipoles in the system. The stability and single-point energy calculations are also performed using DFT (B3LYP), MP2 methods with 6-311G++ (d, p), and cc-pVDZ basis sets. The evaluated results are correlated with the orientation of the dipoles, Gibbs's free energy of activation (ΔG^*) parameter and strength of the hydrogen bond.

Keywords:

Dielectric relaxation, Excess parameters, Kirkwood (geff) factor, DFT, Gibbs's free energy

PC-76

Effect of Reaction Atmosphere on the Solid State Reaction of 1-Ferrocenyl Ethanol

Manisha Chakraborty, Ashis Bhattacharjee*

Department of Physics, Visva-Bharati University, Santiniketan - 731235

e-address: Manishachakraborty.rs@visva-bharati.ac.in

Solid state thermal decomposition is a process of redistribution of bonds in the solid upon heating and subsequent formation of new products different from the reactant(s)¹. Thermal decomposition of solid organometallic complexes is a popular way to prepare metal oxide nanoparticles. Further, a kinetic modelling for a solid state thermal decomposition is a pertinent way to investigate the thermal conversion of solid precursors into materials with application potential². Presently, the non-isothermal decomposition of 1-ferrocenyl ethanol (say, FcEtOH) has been carried out under N₂ and O₂ atmospheres in 300 K - 800 K range.

The thermogravimetry profiles (following Figure) show that the decompositions are multistep complex processes. The peak deconvolution method is used to separate the peaks. The thermal decomposition of FcEtOH follows 4 steps for N₂ atmosphere, while for O₂ atmosphere, 3 steps are observed. Model-free isoconversional methods are used for kinetic analysis³. Thermodynamic parameters (ΔS , ΔH and ΔG) are calculated for each step. Powder XRD study of the decomposed materials has been done. Present study describes the solid-state synthesis of hematite nanoparticles using organoiron precursor as well as estimates the associated reaction kinetic and thermodynamic parameters as well as their dependence on the reaction environment.

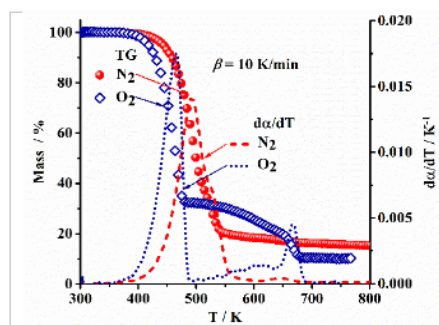


Figure 13: TG and $d\alpha/dT$ profiles under N₂ and O₂ atmospheres

References:

1. Brown M E 2001 Introduction to Thermal Analysis: Techniques and Applications, Vol 1 (Springer Science and Business Media).
2. Hayoune F, et al. 2020 Thermochim. Acta 690 178700.
3. Vyazovkin S, et al. 2011 Thermochim. Acta 520 1.

PC-77

An Electronically Tunable Metal-Insulator-Metal (MIM) varactors with and without floating metal

Shivakumar Chedurupalli^a, Akhil Raman T S^b, Surajit Kumar Nath^c, and James Raju K.C^{a, b}

^aCentre for Advanced Studies in Electronics Science and Technology,

^bSchool of Physics, University of Hyderabad, Gachibowli, Hyderabad-500046, India

^cInternational College of Semiconductor Technology, NYCU, Hsinchu 300, Taiwan

e-address: 19phpe05@uohyd.ac.in^a, akhilramants@gmail.com^b, skn.st06@nycu.edu.tw^c, kcjrsp@uohyd.ac.in

Tunable varactors are realized on Coplanar Waveguide (CPW) structure with $Ba_{0.5}Sr_{0.5}TiO_3$ (BST) sandwiched between gold (Au) and platinum (Pt) electrodes on the sapphire substrate¹⁻³. BST is deposited using Pulsed laser deposition technique and metals are deposited with RF sputtering system. The proposed MIM varactors with and without floating metal is shown in following Fig. 15. MIM capacitor is formed when the top metal and bottom metal have an overlap with BST dielectric between the top and bottom metals. In case of without floating metal, BST etching is done by wet chemical etching and the etch rate achieved for the BST film with the mixture of the HF: HNO₃:H₂O₂:H₂O in the ratio of 1:25:50:20⁴ and patterned top electrode are realized by lift off process.

S_{11} parameters are measured using VNA, Capacitance values are extracted from measured S_{11} values shown in following figure 16. The with and without floating metal devices shows 20% and 34% capacitance tunability over 1–5 GHz for a control voltage of 0–20 V. In case of no-floating metal structure, found better tunability and quality factor than the with floating metal varactor due to via connections, a series capacitance minimized.

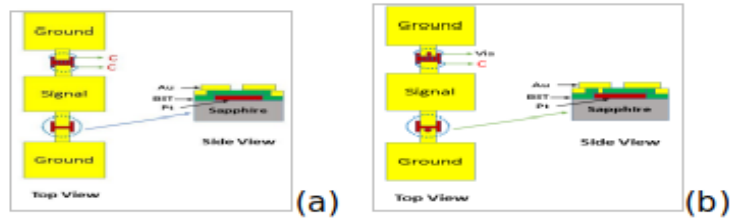


Figure 14: BST thin film MIM varactor (a) with and (b) without floating metal

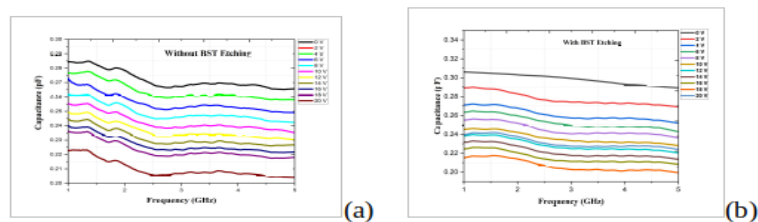


Figure 15: Extracted capacitance (C) from one-port S-parameter results over control voltage

References:

1. G. Subramanyam et al., “Challenges and opportunities for multi-functional oxide thin films for voltage tunable radio frequency/microwave components,” J. Appl. Phys., vol. 114, no. 19, Nov. 2013,

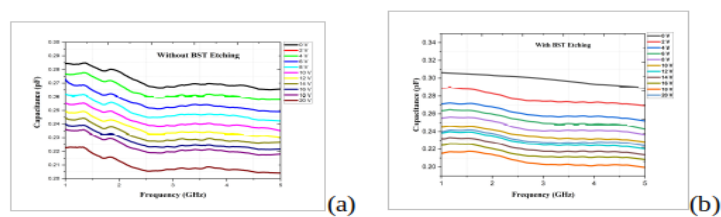


Figure 16: Extracted capacitance (C) from one-port S-parameter results over control voltage

Art. no. 191301.

2. B. Ouagague et al., "BST tunability study at DC and microwave frequencies by using IDC and MIM capacitors," in Proc. Asia-Pacific Microw. Conf., Dec. 2010, pp. 1837–1840.
3. S. K. Nath, J. P. Goud, S. S. Kongbrailatpam, G. Rajaram and K. C. J. Raju, "A Highly Tunable Barium Strontium Titanate Thin Film MIM Varactor With Floating Metal," in IEEE Microwave and Wireless Components Letters, vol. 31, no. 12, pp. 1283-1286, Dec. 2021, doi: 10.1109/LMWC.2021.3110981.
4. Tianjin Zhang, et. al.. Wet Chemical Etching Process of BST Thin Films for Pyroelectric Infrared Detectors, Ferroelectrics, 410:1, 137-144.

PC-78**Aliovalent (Sr, Zr) co-doping on BiFeO₃ for improved multiferroic characteristics**

Teneti Pullarao^{a,b}, G Nagaraju^a, Pittala Suresh^c

^a Department of Physics, Acharya Nagarjuna University, Nagarjuna Nagar, Guntur-522510.

^b Department of Freshman Engineering, PVP Siddhardha Institute of Technology, Kanur, Vijayawada – 520007.

^c Department of Physics, School of Engineering, Dayananda Sagar University, Bengaluru, Karnataka, India.

Corresponding author's e-address: spittala.phy@gmail.com,

Tel: +919848868798.

BiFeO₃ and Bi_{1-x}Sr_xFe_{1-y}Zr_yO₃ (x=0.1, y=0.1, 0.2) polycrystalline materials were synthesized by sol-gel method. The effect of co-doping of (Sr, Zr) ions on the structural and magnetic properties of BiFeO₃ were systematically investigated. Rietveld analysis from XRD revealed the structural formation of BiFeO₃. BiFeO₃ and Bi_{1-x}Sr_xFe_{1-y}Zr_yO₃ (x = 0.1, y = 0.1, 0.2) exhibits rhombohedral structure with R3c space group. All the M-H curves of Bi_{1-x}Sr_xFe_{1-y}Zr_yO₃ exhibit finite coercivity suggesting room temperature ferromagnetic nature of the compound. With increasing Zr concentration. the ferromagnetic nature in the compound gets enhanced obtaining a maximum coercivity for the 10% substitution of Zr and 20% substitution of Sr. Interestingly, for fixed Zr concentration (y = 0.1) ferromagnetic order improves drastically with increasing Sr concentration. Therefore, B-site substitution is more effective in inducing ferromagnetism in the compound.

Keywords:

Bi_{1-x}Sr_xFe_{1-y}Zr_yO₃, sol-gel, Structural and Magnetic properties.

PH-01**Characterization of Atmospheric Aerosols at an urban site:
Hyderabad**

Nagaraju Guthikonda^a, Anasibnu Basheer^b, Sakshi Jain^a, Pradeep Attri^b, P Prem Kiran^a,
Ashok Vudayagiri^a, Devleena Mani Tiwari^b, Vijay P Kanawade^b

^aSchool of Physics, University of Hyderabad, India

^bCentre for Earth, Ocean and Atmospheric Sciences, School of Physics, University of Hyderabad, India

e-address: vijaykanawade@uohyd.ac.in

correspondence e-address: prem@uohyd.ac.in, ashok_vs@uohyd.ac.in

Atmospheric aerosols are liquid or solid particles suspended in the air. Characterization of aerosols is of fundamental and practical significance in various fields such as medical, industrial and scientific research. Aerosols have been widely studied due to their effects on human health, air quality, weather, and climate. Optical properties associated with scattering and absorption of radiation by aerosols in the visible and infrared region (450-1100 nm) are of fundamental importance not only in scientific research but also industrial applications. Particle size, chemical composition, morphology plays a key role in the absorbance and scattering of radiation (or laser light). The low intensity laser beam scattering from aerosols either follows Rayleigh scattering or Mie scattering depending on the particle size. The fact that aerosols have strong spatio-temporal heterogeneity due to uneven distribution of sources, sinks, and meteorological effect. We have collected aerosol samples during winter using high volume sampler on the University of Hyderabad campus (urban environment). We have performed optical characterization on the aerosol-coated quartz filters using Raman Scattering, Field-Emission Scanning Electron Microscopy (FESEM) and Energy Dispersive X-Ray Spectroscopy (EDS). Our preliminary analyses revealed that aerosol mass ranged from 112 – 178 $\mu\text{g}/\text{m}^3$ consisting of mostly SiO_2 (50- 75 %) as a major element and Al, Ca, K, S as minor elements. The aerosol radius is varying from 200 nm to 10 μm . Furthermore, from the scattering experiments revealed the dominant Raman modes of the silica (980 cm^{-1}), carbon D- band (1350 cm^{-1}) and carbon G - band (1580 cm^{-1}). The observations confirmed the dominant role of silica on the urban aerosol environment.

PH-02

Magnetic reconnection in the wakes of cosmic strings

Dilip Kumar, Soma Sanyal

^a University of Hyderabad, Hyderabad, India

e-address: 21phph03@uohyd.ac.in

The motion of cosmic strings in the universe leads to the generation of wakes behind them. We study magnetized wakes of cosmic strings moving in the post recombination plasma. We show that magnetic reconnection can occur in the post shock region. The reconnection leads to a large amount of kinetic energy being released in the post shock region. The release of the kinetic energy can lead to a fast radio burst. Since fast radio bursts have been detected by several radio telescopes, we predict that this could be a probable signature for a magnetized cosmic string wake.

Keywords:

cosmic strings, shocks, magnetic reconnection.

PH-03**Maximal Acceleration in DFR space-time**E. Harikumar, Suman Kumar Panja and Vishnu Rajagopal^aSchool of Physics, University of Hyderabad, Gachibowli, Hyderabad – 500046, Indiae-address: sumanpanja19@gmail.com

Quantum gravity has been studied using various approaches, and all of these approaches introduce a fundamental minimum length scale in the theory. Non-commutative geometry is an approach which incorporates minimum length scale naturally. Minimum length scale implies the existence of an upper limit on the proper acceleration, known as maximal acceleration. In this study, we investigate the non-commutative corrections to the maximum acceleration in the Doplicher-Fredenhagen-Roberts (DFR) space-time and demonstrate that the non-commutativity decreases the magnitude of the maximum acceleration value in the commutative limit. From the positive semi-definiteness of the magnitude of the maximum acceleration, we get an upper bound on the acceleration along the extra spatial coordinates. From non-relativistic limit of geodesic equations in DFR space-time and weak field approximation of Einstein's field equation, we obtain the explicit form of Newtonian potential. We derive a lower bound on the radial distance between two particles by expressing the non-commutative correction term of the maximum acceleration in terms of Newton's potential and employing positivity condition.

References:

1. S. Doplicher, K. Fredenhagen and J. E. Roberts, Phys. Lett. B 331 (1994) 29 .
2. C. E. Carlson, C. D. Carone and N. Zobin, Phys. Rev. D 66 (2002) 075001.
3. R. Amorim, Phys. Rev. D 78 (2008) 105003.
4. E. R. Caianiello, Lett. Nuovo Cimento 32 (1981) 65.
5. H. E. Brandt, Lett. Nuovo Cimento 38 (1983) 15.
6. A. D. Sakharov, JETP Lett. 3 (1966) 288.
7. E. Harikumar and V. Rajagopal, Ann. Phys. 423 (2020) 168332.
8. E. Harikumar, S. K. Panja and V. Rajagopal, arXiv:2202.06591v1 [hep-th] (2022).

PH-04**A Study of Photoionized Gas in Two HII Regions of the N44 Complex in the LMC Using MUSE Observations.**

Susmita Barman^a, Naslim Neelamkodan^b, Suzanne C. Madden^c, Marta Sewilo^{d,e}, Francisca Kemper^{f,g}, Kazuki Tokuda^{h,i,j}, Soma Sanyal^a, and Toshikazu Onishi^h

^aSchool of Physics, University of Hyderabad, Gachibowli, Hyderabad – 500046, India

^bDepartment of Physics, College of Science, United Arab Emirates University (UAEU), Al-Ain, 15551, UAE,

^cLaboratoire AIM, CEA/DSM - CEA Saclay, F-91191 Gif-sur-Yvette, France ,

^dCRESST II and Exoplanets and Stellar Astrophysics Laboratory, NASA Goddard Space Flight Center, Greenbelt, MD 20771, USA,

^eDepartment of Astronomy, University of Maryland, College Park, MD 20742, USA,

^fEuropean Southern Observatory, Karl-Schwarzschild-Str. 2, D-85748, Garching b. München, German

^gInstitute of Astronomy and Astrophysics, Academia Sinica, 11F of Astronomy-Mathematics Building, AS/NTU, No.1, Sec. 4, Roosevelt Rd., Taipei 10617, Taiwan ,

^hDepartment of Physical Science, Graduate School of Science, Osaka Prefecture University, 1-1 Gakuen-cho, Sakai, Osaka 599-8531, Japan,

ⁱDepartment of Physics, Graduate School of Science, Osaka Metropolitan University, 1-1 Gakuen-cho, Naka-ku, Sakai, Osaka 599-8531, Japan,

^jDepartment of Earth and Planetary Sciences, Faculty of Sciences, Kyushu University, Nishi-ku, Fukuoka 819-0395, Japan
e-address: barmansusmita147@gmail.com

We studied the ionization structure and physical conditions of two luminous H II regions in the N44 star-forming complex of the Large Magellanic Cloud using the spectral synthesis code CLOUDY, and the observation was done by the Multi-Unit Spectroscopic Explorer (MUSE) on the Very Large Telescope. The spectral maps of various emission lines reveal a stratified ionization geometry in N44 D1. The spatial distribution of [O I] λ 6300 emission in N44 D1 indicates a partially covered ionization front at the outer boundary of the H II region, while in N44 C, the patches of [S II] λ 6717 and [O I] λ 6300 emission bars are found in the interior. The results of spatially resolved MUSE spectra are tested with the photoionization models for the first time in these H II regions. A spherically symmetric ionization-bounded model with a partial covering factor can reproduce the observed geometry and most of the diagnostic line ratios in N44 D1. Similarly, in N44C, we apply a low-density and optically thin model based on the observational signatures. Our modelling results show that the ionization structure and physical conditions of N44 D1 are mainly determined by the radiation from an O5 V star. However, local X-rays, possibly from supernovae or stellar wind, play a crucial role. In N44 C, the main contribution of the radiation is from three ionizing stars, O8V, O5III and O9.5V.

PH-05**Magnetic field evolution in the wakes of cosmic string.**

Soumen Nayak, Sovan Sau, Soma Sanyal

School of Physics, University of Hyderabad, Gachibowli, Hyderabad – 500046, India

e-address: soumennayak@uohyd.ac.in

We study the evolution of magnetic fields in cosmic string wakes in a plasma with a low resistivity. The initial magnetic field in the wake is modelled on the magnetic fields that are generated by the motion of particles around cosmic strings. The plasma is characterized by a high β value. We find multiple shock like structures developing in the wake of the string. We study the detailed structure of the shocks formed and the evolution of the magnetic field in the shock using a 2-D magnetohydrodynamic simulation. Our results show that instead of a single uniform shock forming behind the cosmic string we have multiple shocks forming at short time intervals behind the string. The presence of multiple shocks will definitely affect the observational signatures of cosmic string wakes as these signatures depend upon the temperature fluctuations generated by the shock. We also find that as the shock moves away, the residual magnetic field left behind reconnects and dissipates rapidly. The magnetic field around the string is thus very localized. We find that magnetic field reconnections take place in cosmic string wakes. This leads to the decrease of the magnetic field in the post shock region.

References:

1. S. Sau, S. Sanyal, Eur. Phys. J. C 80, 152 (2020)
2. S. Zenitani, T. Miyoshi, Phys. Plasmas 18, 022105 (2011).
3. S. Nayak, S. Sau, S. Sanyal, arXiv:2204.13303[astro-ph.CO]

PH-06

The CMS Level-1 Calorimeter Trigger for the HL-LHC

Piyush Kumar and Bhawna Gomber

On behalf of the CMS collaboration CASEST, University of Hyderabad, Prof C R Rao Road, Gachibowli, Hyderabad, Telangana, India

e-address: piyush.kumar@uohyd.ac.in

The High-Luminosity LHC will open an unprecedented window on the weak-scale nature of the universe, providing high-precision measurements of the standard model as well as searches for new physics beyond the standard model. Such precision measurements and searches require information-rich datasets with a statistical power that matches the high-luminosity provided by the Phase-2 upgrade of the LHC. Efficiently collecting those datasets will be challenging, given the harsh environment of 200 proton-proton interactions per LHC bunch crossing. For this purpose, CMS is designing an efficient data-processing hardware trigger (Level-1) that will include tracking and high-granularity calorimeter information. The current conceptual system design is expected to take full advantage of the present-day large FPGAs and link technologies (28 Gbps) over the coming years. Therefore, providing a high-performance, low-latency computing platform for a large throughput and sophisticated data correlation across diverse sources. The envisaged L1 trigger algorithms for the barrel calorimeter have been developed and implemented over the Xilinx XCVU9P FPGA. The expected performance and physics implications of trigger algorithms are studied using Monte Carlo samples with a high pile-up, simulating the harsh conditions of the HL-LHC. The proposed design and expected performance of the upgraded CMS L1 calorimeter trigger are summarised in the poster.

Reference:

The Phase-2 Upgrade of the CMS Level-1 Trigger. Technical Report CERN-LHCC- 2020-004. CMS-TDR-021, CERN, Geneva, Apr 2020. URL <http://cds.cern.ch/record/2714892>

PH-07**Deviations from isotropic turbulence of heavy-ion collision plasma**

Abhisek Saha and Soma Sanyal
University of Hyderabad, Hyderabad, India
e-address: 17phph12@uohyd.ac.in

Signs of turbulence have been observed at the relativistic heavy-ion collision at high collision energies. We study the signatures of turbulence in this system and find that there are significant departures from isotropic turbulence in the initial and the pre-equilibrium stages of the collision. As the anisotropic fluctuations are subleading to the isotropic fluctuations, the Kolmogorov spectrum can usually be obtained even for the initial stages. However, the energy spectrum and the temperature fluctuations indicate deviations from isotropic turbulence. Since a strong momentum anisotropy exists between the transverse and the longitudinal plane, we study the energy density spectrum in these two planes by slicing the sphere into different planes. The geometrical anisotropy is reflected in the anisotropic turbulence generated in the rotating plasma and we find that the scaling exponent is different in the two planes. We also obtain the temperature spectrum in the pre-equilibrium stages. The spectrum deviates from the Gaussian spectra expected for an isotropic turbulence. All these seem to indicate that the large-scale momentum anisotropy persists in the smaller length scales for the relativistic heavy-ion collisions.

PH-08**A search for dark matter in Higgs to $\tau\tau + E T^{miss}$ final state by using p-p collision data of CMS detector at $\sqrt{S} = 13$ TeV**

Bisnupriya Sahu, Dr. Bhawna Gomber

(For the CMS Collaboration)

University of Hyderabad, Hyderabad, India

e-address: bisnupriya.sahu@cern.ch, bhawna.gomber@cern.ch

The undetected dark matter search is performed in the final state of Higgs decaying to a pair of tau leptons and large missing transverse energy (MET) with the proton-proton collision data of CMS detector at CERN LHC, at center of mass, $\sqrt{S} = 13$ TeV. The benchmark for this particular search is performed with two simplified models of DM+h productions. First one is Z' -two-Higgs-Doublet(Z' -2HDM) model, where Z' will decay into standard model like Higgs boson and an intermediate heavy pseudoscalar particle (A), which further decays into a Dirac fermionic dark matter particle. Another one is Z' baryonic model, where a new massive vector mediator Z' emits a Higgs boson and then decays to a pair of Dirac fermionic DM particles. In Z' - 2HDM model the mass of Z' , $m_{Z'}$ up to 1265 GeV, mass of DM, $m_{DM} = 100$ GeV and mass of the heavy pseudoscalar A, $m_A = 300$ GeV are excluded. Also, in Z' baryonic model, mass of DM, $m_{DM} = 1$ GeV, Z' mass up to 615 GeV are excluded using only 2016 data set of CMS detector.

References:

CMS Collaboration, “ Search for dark matter produced in association with a Higgs boson decaying to $\gamma\gamma$ or $\tau^+\tau^-$ at $\sqrt{s} = 13$ TeV ”, JHEP 09 (2018) 046 , doi:10.1007/JHEP09(2018)046, arXiv: 1806.04771 .

PH-09**Abstracts for 12th India-Japan Science and Technology seminar**

Jaydeb Das

Department of Physics and Astrophysics, University of Delhi. Delhi-110007, India
e-address: akv1993.au@gmail.com**Abstract-1**

We explore the possibility of CP violation in baryonic $\Lambda_b \rightarrow (\Lambda_c, p)\pi^+\mu^+\mu^-$ decays which are mediated by two Majorana sterile neutrino and are $|\Delta L| = 2$ lepton number violating processes. Appreciable CP asymmetry can be obtained if there are two on-shell Majorana neutrinos that are quasi-degenerate in mass with the mass difference of the order of average decay widths. We find that given the present constraints on the heavy to light mixing element $|V_{\mu N}|$, the $\Lambda_b \rightarrow p^+\pi^+\mu^+\mu^-$ and $\Lambda_b \rightarrow \Lambda_c^+\pi^+\mu^+\mu^-$ decay rates are suppressed but could be within the experimental reach at the LHC. If searches of the modes are performed, then experimental limits on the rates can be translated to constraints on the Majorana neutrino mass m_N and heavy to light mixing element squared $|V_{\mu N}|^2$. We show that the constraints on the $(m_N, |V_{\mu N}|^2)$ parameter space coming from the $|\Delta L| = 2$ baryonic decays are complementary to the bounds coming from other processes.

Abstract-2

One major motivation for extending the present Standard Model (SM) is its inefficiency in providing enough of Charge-parity violation (CPV) required which is one of the Sakharov conditions for explaining the disappearance of antimatter from the Universe. However, every CPV phenomenon seen so far in laboratory-based experiments has been consistent with the Cabibbo-Kobayashi-Maskawa (CKM) mechanism of the SM. Therefore it is imperative to continue looking for observables that are not only experimentally measurable but also at the same time- for exceptional sensitivity to NP with CPV. The penguin-induced flavor-changing neutral current (FCNC) transitions $b \rightarrow s$ and $b \rightarrow d$ are among the most valuable probes of flavor physics. In this work, we study CP-violation in angular observables in the SM framework as well as in a new physics scenario for the process of $\Lambda_b \rightarrow \Lambda\mu^+\mu^-$. One important result of our studies is that new CP-violating phases will produce clean signals in CP-violating asymmetries.

Abstract-3

In this work we consider the simple Z_2 symmetric extension to the Standard Model (SM) and proceed to study the nature of electroweak phase transition (EWPT) in the early universe. We show that the nature of the phase transition changes from a smooth crossover in the SM to a strong first order with this addition of the real scalar. Furthermore, we show the entropy release in this scenario is higher than that of the SM. This can lead to a strong dilution of frozen out dark matter particles and baryon asymmetry, if something existed before the onset of the phase transition.

PH-10**Neutrino Phenomenology in A_4 Modular Symmetry with Type-III Seesaw and Leptogenesis**

Priya Mishra, Mitesh Kumar Behera, Papia Panda, Rukmani Mohanta.
School of Physics, University of Hyderabad, Gachibowli, Hyderabad – 500046, India.
e-address: mishpriya99@gmail.com

In this work, we implement A_4 modular invariance approach with $U(1)_{B-L}$ as an additional gauge symmetry to the standard model (SM) within the framework of type-III seesaw mechanism. The model includes SM particle content with extra $SU(2)_L$ triplet, hyperchargeless fermion Σ and a scalar singlet ρ which breaks the $U(1)_{B-L}$ symmetry. Fermionic triplet participates in the seesaw mechanism to give tiny mass to neutrinos and the mass of lightest one is contributing in the CP violating parameter to explain matter-antimatter asymmetry in the Universe. Hence, we are able to explain neutrino phenomenology, to name a few, sum of neutrino masses, reactor mixing angle, effective electron neutrino mass parameter in neutrinoless double beta decay etc. satisfying their present experimental 3σ bound respectively. Also we are successful in explaining leptogenesis.

References:

Type-III seesaw under A_4 modular symmetry with leptogenesis and muon (g-2), Priya Mishra, Mitesh Kumar Behera, Papia Panda, Rukmani Mohanta, e-print: 2204.08338 [hep-ph].

PH-11**Superdense star in kappa-deformed space-time**

Vishnu Rajagopal , E. Harikumar, S. Bhanu Kiran

School of Physics, University of Hyderabad, P.O. Central University, Hyderabad, 500046, Telangana, India

e-address: vishnurajagopal.anayath@gmail.com

The effects of the non-commutativity are expected to be more strong in an extremely strong gravitational background. Astrophysical objects such as superdense star is a suitable candidate for studying the non-commutative effects. We study the superdense star in non-commutative space-time by generalising the anisotropic core-envelope model to the kappa-deformed space-time. We construct the kappa-deformed Einstein's field equation and by solving this, derive the expressions for kappa-density and kappa-pressure in the isotropic core and anisotropic envelope respectively. Using the positivity condition of the density and pressure in the kappa-deformed space-time, we obtain bounds on the deformation parameter.

References:

S. B. Kiran, E. Harikumar and V. Rajagopal, Mod. Phys. Lett. A 34 (2019) 1950116.

PH-12**3+1 sterile neutrino study of Super-ORCA**

Dinesh Kumar Singha^a, Monojit Ghosh^a, Rudra Majhi^a, Rukmani Mohanta^a

^aSchool of Physics, University of Hyderabad, Gachibowli, Hyderabad – 500046, India

e-address: dinesh.sin.187@gmail.com

In this work, we have explored the hierarchy, octant and CP violation sensitivity of DUNE and P2O experiment in its three proposed configurations in standard three flavor scenario and in the presence of an extra light sterile neutrino. We have shown that the near detectors are crucial for the study of the sterile neutrinos, as for the far detectors, the oscillation frequency is averaged out due to the rapid oscillation of the sterile mass squared difference. We found that water cherenkov type near detectors are pretty insensitive to sterile oscillation parameters like θ_{14} , that is why we preferred to use liquid argon time projection chamber (LArTPC) type near detector (DUNE like ND) for all three configurations of P2O. Super-ORCA detector configuration of P2O is better at probing 10 eV^2 sterile neutrinos, whereas DUNE is better at investigating 1 eV^2 sterile neutrinos. We found that the Super-ORCA configuration gives the best sensitivity to hierarchy, octant and CP violation studies.

Acknowledgment:

DKS acknowledges Prime Ministers Research Fellowship, Govt. of India.

References:

1. Letter of Interest for a Neutrino Beam from Protvino to KM3NeT/ORCA, Eur.Phys.J.C 79 (2019) 9, 758 e-Print: 1902.06083 [physics.ins-det];
2. Sensitivity to light sterile neutrinos at ESSnuSB, JHEP 03 (2020) 026 e-Print: 1912.10010 [hep-ph]

PH-13**Rational Extension of Quantum Theories**Bhabani Prasad Mandal^a^aDepartment of Physics, Institute of Science, Banaras Hindu University, Varanasi-221005, INDIA
e-address: bhabani@bhu.ac.in

In 2009 new families of orthogonal polynomials (related to some of the old sets) which arise as solutions of second order eigenvalue differential equations with rational coefficients have been discovered¹. These polynomials have remarkable properties that even after removing of 1st few polynomials from the set of orthonormal polynomials, these still form an orthonormal set with respect to a different weight function. These are known as exceptional orthogonal polynomials (EOP). So far only two EOPs have been discovered corresponding to Jacobi and Laguerre COPs. This discovery has boosted largely the quantum mechanical study of various systems as new ES systems whose solutions are written in terms EOPs are found². Such systems are strictly isospectral to some of the usual ES systems and are called the rational extension (RE) of usual ES systems. The study of EOPs have been extended to bound and scattering state solutions in ES quantum theories, diffusion equations, random process, quantum information entropies, etc³. However, there are still many open problems related to EOPs which need serious attention. In this article we would like to investigate some of the open problems and extend the quantum theory accordingly. In particular, we like to explore the cause of strict isospectrality in RE systems and to extend the results beyond one particle one dimensional systems.

References:

1. D. Gomez-Ullate, N. Kamran and R. Milson, J. Math. Anal. Appl. 359 (2009) 352.
2. N. Kumari, R. K. Yadav, A. Khare, B. P. Mandal, Annals of Physics 385 (2017) 57–69.
3. C.-L. Ho, J.-C. Lee, R. Sasaki Ann. Phys. 343 (2014) 115

PH-14**Extracting the best physics sensitivity from T2HKK: a study on optimal detector volume at Japan and Korea**

Papia Panda, Monojit Ghosh, Priya Mishra, Rukmani Mohanta
^aSchool of Physics, University of Hyderabad, Gachibowli, Hyderabad – 500046, India
e-address: ppapia93@gmail.com

T2HK is an upcoming long-baseline experiment which will have two water Cherenkov detector tanks of 187 kt volume each at distance of 295 km from the source. An alternative project, T2HKK is also under consideration where one of the water tanks will be moved to Korea at a distance of 1100 km. The flux at 295 km will cover the first oscillation maximum and the flux at 1100 km will mainly cover the second oscillation maximum. As physics sensitivity at the dual baseline rely on variation in statistics, dependence of systematic uncertainty, effect of second oscillation maximum and matter density, 187 kt detector volume at 295 km and 187 kt detector volume at 1100 km may not be the optimal configuration of T2HKK. In this work we have tried to optimize the ratio of the detector volume at both the locations by studying the interplay between the above mentioned parameters. For the analysis of neutrino mass hierarchy, octant of θ_{23} and CP precision, we have considered two values of δ_{CP} as 270° and 0° and for CP violation we have considered the value of $\delta_{CP} = 270^\circ$. These values are motivated by the current best-fit values of this parameter as obtained from the experiments T2K and NO ν A. Interestingly we find that if the systematic uncertainty is negligible then the T2HK setup i.e., when both the detector tanks are placed at 295 km gives the best results in terms of hierarchy sensitivity at $\delta_{CP} = 270^\circ$, octant sensitivity, CP violation sensitivity and CP precision sensitivity at $\delta_{CP} = 0^\circ$. For current values of systematic errors, we find that neither T2HK, nor T2HKK setup is giving better results for hierarchy, CP violation and CP precision sensitivity. The optimal detector volume which is of the range between 255 kt to 345 kt at 1100 km gives better results in those above mentioned parameters.

PH-15**Exploring astronomical PAHs in the epoch of JWST**

Mridusmita Buragohain^a, Takashi Onaka^b, Amit Pathak^c, and Itsuki Sakon^d

^aSchool of Physics, University of Hyderabad, Gachibowli, Hyderabad – 500046, India

^bDepartment of Physics, Faculty of Science and Engineering, Meisei University, Tokyo 191-8506, Japan

^cDepartment of Physics, Banaras Hindu University, Varanasi 221 005, India

^dDepartment of Astronomy, Graduate School of Science, The University of Tokyo, Tokyo 113-0033, Japan

e-address: ms.mridusmita@uohyd.ac.in

Polycyclic Aromatic Hydrocarbons (PAHs) have found a noteworthy place in the family of possible interstellar organics as revealed by their spectral footprints, particularly observed in the mid infrared wavelength range starting from 3 to 20 μm (Tielens, 2008). The observed emission bands in these wavelengths are popularly known as “Aromatic Infrared Bands (AIBs)” as suggested by nature of the carriers. PAHs are mostly apolar or weakly polar, hence rotational spectroscopy, which is the usual method of identification of a molecule, is rather difficult. The nearest comparable confirmed species to PAH is benzonitrile (*c*-C₆H₅CN), which was detected through rotational transitions, and may be considered as a precursor for PAH formation in the ISM (McGuire et al., 2018). A recent detection of two isomers of small PAHs (naphthalene) with a CN group by McGuire et al. (2021) have encouraged the community to search for more varieties of PAHs. Previous observations made by ISO, Spitzer, AKARI, SOFIA etc. have revealed various characteristics of PAH bands, although a higher resolution and sensitivity is required in order to probe any possible presence/absence of these organics. The recently launched James Webb Space Telescope (JWST) offers higher sensitivity as well as resolution compared to previous observations and thus opens prospects to study astronomical PAHs. In this presentation, we highlight the capability of JWST in order to study various characteristics of PAH bands, which will further lead to identification of PAH family, if present.

References:

1. McGuire B. A., et al., 2018, *Science*, 359, 202
2. McGuire B. A., et al., 2021, *Science*, 371, 1265
3. Tielens A. G. G. M., 2008, *ARA and A*, 46, 289

PH-16

Complex dynamical properties of coupled Van der Pol-Duffing oscillators with balanced loss and gain.

Puspendu Roy and Pijush K. Ghosh

Department of Physics, Siksha-Bhavana, Visva-Bharati University, Santiniketan, PIN 731 235, India.

e-address: puspenduroy716@gmail.com

We consider a Hamiltonian system of coupled Van der Pol-Duffing(VdPD) oscillators with balanced loss and gain[1,2]. The system is analyzed perturbatively by using Renormalization Group(RG) techniques as well as Multiple Scale Analysis(MSA). Both the methods produce identical results in the leading order of the perturbation. The RG flow equation is exactly solvable and the slow variation of amplitudes and phases in time can be computed analytically. The system is analyzed numerically and shown to admit periodic solutions in regions of parameter-space, confirming the results of the linear stability analysis and perturbation methods. The complex dynamical behavior of the system is studied in detail by using time-series, Poincaré-sections, power-spectra, auto-correlation function and bifurcation diagrams. The Lyapunov exponents are computed numerically. The numerical analysis reveals chaotic behavior in the system beyond a critical value of the parameter that couples the two VdPD oscillators through linear coupling, thereby providing yet another example of Hamiltonian chaos in a system with balanced loss and gain.

References:

1. Pijush k. Ghosh and P Roy, J.Phys. A: Math. Theor. 53 (2020) 475202 (27pp); Pijush K Ghosh, J .Phys: Conf. Ser. 2038 012012(2021) ; P Roy and Pijush k. Ghosh J.Phys. A: Math. Theor. 55 (2022) 315701(26pp).
2. B. Peng, S. K. Ozdemir, F. Lei, F. Monifi, M. Gianfreda, G. L. Long, S. Fan, F. Nori, C. M. Bender, and L. Yang, Nature Physics 10, 394 (2014); C. M. Bender, M. Gianfreda, S. K. Ozdemir, B. Peng, and L. Yang, Phys.Rev. A 88, 062111 (2013).

PH-17

Non-linear Schrödinger equation with time-dependent balanced loss-gain and space-time modulated non-linear interaction

Supriyo Ghosh and Pijush K. Ghosh

Department of Physics, Siksha-Bhavana, Visva-Bharati, Santiniketan, PIN 731235, India
e-address: supriyoghosh.rs@visva-bharati.ac.in

We consider a class of one dimensional vector Non-linear Schrödinger Equation(NLSE) in an external complex potential with Balanced Loss-Gain(BLG) and Linear Coupling(LC) among the components of the Schrödinger field. The solvability of the generic system is investigated for various combinations of time modulated LC and BLG terms, space-time dependent strength of the nonlinear interaction and complex potential. We use a non-unitary transformation followed by a reformulation of the differential equation in a new coordinate system to map the NLSE to solvable equations. Several physically motivated examples of exactly solvable systems are presented for various combinations of LC and BLG, external complex potential and nonlinear interaction. Exact localized nonlinear modes with spatially constant phase may be obtained for any real potential for which the corresponding linear Schrödinger equation is solvable. A method based on supersymmetric quantum mechanics is devised to construct exact localized nonlinear modes for a class of complex potentials. The real superpotential corresponding to any exactly solved linear Schrödinger equation may be used to find a complex-potential for which exact localized nonlinear modes for the NLSE can be obtained. The solutions with singular phases are obtained for a few complex potentials. We have extended this work for the Non-local NLSE introduced by Ablowitz and Musslimani.

References:

M.J. Ablowitz and Z.H. Musslimani, Integrable nonlocal nonlinear Schrödinger equation, Phys. Rev. Lett. 110, 064105 (2013).

PH-18

Sulfate Reducing Bacteria based Bio-electrochemical system: Towards Sustainable Landfill Leachate and Solid Waste Treatment

K. Sushma Varma , Rajesh Singh^a

^aSchool of Environment and Sustainable Development, Central University of Gujarat,
Gandhinagar, Gujarat

e-address: k.sushma@cug.ac.in

The economic and demographic growth, urbanization, and changing lifestyles have increased solid waste generation at an explosive rate, posing a global waste disposal concern^{1,2}. Landfilling treatment technology of waste, though globally prevalent, is resource intensive and not effective from the economic, environmental, and sustainable standpoints³ as it causes serious environmental damage. The present study assesses the potential of the bioelectrochemical system (BES) integrated with sulfate-reducing bacteria (SRB) in the sustainable treatment and decontamination of landfill wastes. The SRB constitute an integral part of the metabolism responsible for organic matter anaerobic degradation in anoxic marine sediments⁴. Solid waste and landfill leachate collected from a matured landfill site were evaluated for long-term treatment using the integrated SRB-BES anaerobic designed bioreactors after pre-treatment. Based on periodic gas composition analysis, physico-chemical characterization of the leachate and solid waste and metal concentration determination, the present system demonstrated significant improvement in volumetric hydrogen production by suppressing methanogenesis. The high reduction percentages of metals Be (90.35), Cd (BDL), Sb (93.14), Ni (99.93), Cr (87.81), COD (88.74) and sTOC (36.11) removal were observed. This mineralization can be attributed to the synergistic effect of ammonia-assisted pre-treatment complexation and microbial sulfide formation. Despite being amended with 0.1N ammonia, the treated leachate level of NO₃ - (2.350 ± 1.077 mg/L) reduced by 5.3 times- a potential and feasible solution for groundwater pollution from landfill leaching⁵. The BES-treated solid waste was evidently more stabilized as shown by a five-fold increase in surface area and potentially useful for leachate immobilization and bio-fortification of agricultural fields. The vector arrangement and magnitude showed similar treatment with differences in magnitudes for both leachate and solid waste. These findings support the efficacy of SRB-BES in the treatment of landfill leachate and solid waste sustainably. It utilizes low cost treatment conditions and anaerobic SRB adapted to landfill sites. This technology may prove to be a sustainable treatment strategy upon scaling up as its outcomes are two-pronged: landfill waste treatment and energy recovery.

References:

1. Z. Zhu, Y. Zhao, Y. Zhu, M. Zhang, Y. Yu, Y. Guo and T. Zhou, "Efficient treatment of mature landfill leachate with a novel composite biological trickle reactor developed using refractory domestic waste and aged refuse, *Journal of Cleaner Production*, vol. 305, p. 127194, 2021;
2. W. Tan, B. Xi, X. Zhao and Q. Dang, "Emerging Views on the Overall Process Treatment of Municipal Domestic Waste for the Sustainable Use of Landfills in China," *Engineering*, vol. 6, pp. 733-735, 2020.
3. P. Wijekoon, P. A. Koliyabandara, A. T. Cooray, S. S. Lam, B. C. Athapattu and M. Vithanage, "Progress and prospects in mitigation of landfill leachate pollution: Risk, pollution potential, treatment and challenges," *Journal of Hazardous Materials*, vol. 421, p. 126627, 2022.
4. J. Song, J. Hwang, I. Kang and J. Cho, "A sulfate reducing bacterial genus, *Desulfosediminicola* gen. nov., comprising two novel species cultivated from tidal flat sediments.," *Scientific Reports*, no. 11, p. 19978, 2021.
5. R. J. Stoklosa, . A. P. Orjuela, L. Sousa, N. Uppugundla, D. Williams, B. Dale, D. Hodge and V. Balan, "Techno-economic comparison of centralized versus decentralized biorefineries for two alkaline pretreatment processes," *Bioresource Technology*, vol. 226, pp. 9-17, 2017.

PH-19

Search for Dark Matter (DM) using monophoton final state data at LHC using CMS detector

Shriniketan Acharya, Dr. Bhawna Gomber

School of Physics, University of Hyderabad, Gachibowli, Hyderabad – 500046, India

e-address: shriniketan.acharya@cern.ch

We report on the results of new physics searches in a final state containing a photon and missing transverse energy called “monophoton searches” in a p-p collision at $\sqrt{S} = 13$ TeV. The data correspond to an integrated luminosity of 138 fb^{-1} . In the Standard Model, the only process that results in the genuine signature of a single photon and large MET is $Z + \gamma$ production, in which the Z boson decays into a neutrino (ν) and an antineutrino ($\bar{\nu}$). The rate of $Z + \gamma$ production can be precisely calculated in the SM, and therefore a deviation of the observation from the prediction in this signature is a robust indicator of the physics beyond the standard model. This process, in which the Z boson decays to 2 neutrinos, is known as the irreducible process, as the signal and background look exactly the same in the detector. In practice, multiple other collision and non-collision processes mimic the signature and thus constitute the additional background to this search. Our aim is to reduce the contributions from such non- $Z+\gamma$ backgrounds and other remaining backgrounds using the data-driven techniques and Monte Carlo (MC) simulations. Results are interpreted in the context of dark matter using simplified models and large extra dimension using ADD model.

References:

1. C.M.S. Collaboration, Search for new physics in final states with a single photon plus missing transverse momentum in proton-proton collisions at 13 TeV using 2016 data. JHEP 1902, 074 (2019).
2. Search for Dark Matter and Large Extra Dimensions in pp Collisions Yielding a Photon and Missing Transverse Energy. (Phys. Rev. Lett. 108, 261803(2012)).

PO-01

Resonating Photonic Nanostructures and its Applications

Shereena Joseph, Joby Joseph

Optics and Photonics Centre, Indian Institute of Technology Delhi (IITD), New Delhi, 110016 India.

e-address: sherin5462@gmail.com

In recent times the nano dimensional photonic structures are gaining immense attention for developing various devices in the field of biosensing and energy harvesting. In this work we are demonstrating the high-sensitive photonic and plasmonic modes involved in photonic and plasmonic structures for biosensing. Moreover, the nanostructures are explored for its light trapping capabilities and confinement in energy harvesting. The confined light in such plasmonic devices can also be used for the production of hydrogen through water splitting process.

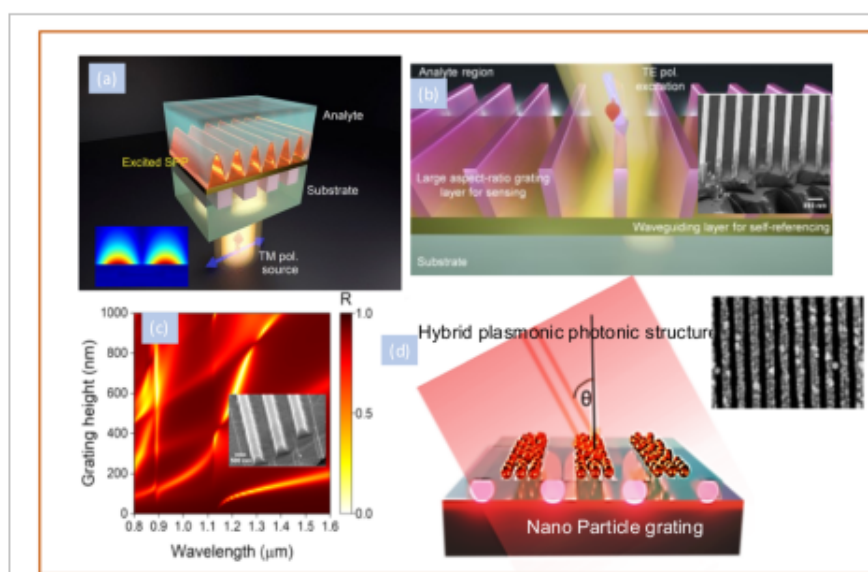


Figure 17: (a) A plasmonic grating based sensor, (b) High Aspect ratio dielectric guided mode resonance sensor, (c) Photonic- plasmonic hybrid structure, (d) Plasmonic light trapping structure.

Acknowledgement:

The Authors Acknowledge the funding from Ministry of Electronics and Information Technology (MeitY) India, and Toyo University through Collaborative Education & Research Program of IITD-BNERC, Toyo University-Japan.

References:

1. High-Sensitivity Resonant Cavity Modes Excited in a Low Contrast Grating Layer with Large Aspect-Ratio” S. Joseph, S. Sarkar, J. Joseph accepted for publication in IEEE Sensors Journal (July 2022).
2. Exploring the Optical Bound State in the Continuum in a Dielectric Grating Coupled Plasmonic Hybrid System, S. Joseph, S. Sarkar, S. Khan, J. Joseph, Advanced Optical Materials, 9 (8), 2001895 (2021).

3. Grating-Coupled Surface Plasmon-Polariton Sensing at a Flat Metal–Analyte Interface in a Hybrid-Configuration, S. Joseph, S. Sarkar, J. Joseph ACS Applied Materials and Interfaces 12 (41), 46519-46529(2020).
4. Direct and Broadband Plasmonic Charge Transfer to Enhance Water Oxidation on a Gold Electrode M. Graf, G. B. Vonbun-Feldbauer, M. T. M. Koper, ACS Nano, 15, 3188 (2021).

PO-02**Three photon transition in a four-level atomic system**Amitava Bandyopadhyay^a, Suman Mondal^b^aDepartment of Physics, Visva-Bharati, Santiniketan, PIN 731235, West Bengal, India^bNational Institute of Science Education and Research (NISER) Bhubaneswar, Jatni, PIN 752050, Khurda, Odisha, Indiae-address: amitava.bandyopadhyay@visva-bharati.ac.in

A four-level atomic system^{1,2}, consisting of one ground energy level, two intermediate energy levels and one uppermost energy level, are subjected to coherent radiation fields. A weak probe field is applied between the ground energy level and the first excited state whereas a strong control field is used to couple the second excited state with the first excited state. A third coherent radiation field, which is termed as the switching field, is applied between the second excited state and the uppermost energy level. The interaction of the three radiation fields with the atomic system is studied by using the density operator method. The optical Bloch equations^{1,3} for this four-level system are derived from the Liouville equation^{1,3} by adding the decay terms phenomenologically and by using the rotating wave approximation^{1,3} and dipole approximation^{1,3}. A set of sixteen Optical Bloch equations are solved analytically under population conservation to derive an expression for the probe coherence term which is used to simulate the probe absorption features. It is shown that under Doppler free condition a two-photon EIT¹⁻² window is transformed into enhanced probe absorption peak as the switching field is introduced. Under Doppler broadened condition the appearance of the enhanced absorption peak is found to depend on certain combinations of the Control and switching Rabi frequency¹⁻³. A very narrow bandwidth optical band stop filter can be conceptualized by using the outcome of this study. The time evolution of the system is also studied in order to examine the transient response of the system.

References:

1. Suman Mondal, Dipanwita Das, Parantap Dey, Dipankar Bhattacharyy and Amitava Bandyopadhyay, *Optik*, 265 (2022) 169410.
2. O. Lahad, R. Finkelstein, O. Davidson, O. Michel, E. Poem, O. Firstenberg, *Phys. Rev. Lett.* 123 (2019), 173203.
3. S. E. Harris, *Phys. Rev. Lett.* 62 (1989) 1033.

PO-03**Optical switching in probe field propagation through microwave driven inverted-Y type atomic system**

Kalan Mal^a, Suman Mondal^b, Amitava Bandyopadhyay^c

^aDept. of Physics, Suri Vidyasagar College, Suri, Birbhum, West Bengal, India PIN-731101

^bNational Institute of Science Education and Research (NISER) Bhubaneswar, Jatni, Khurda, Odisha, India PIN 752050

^cDept. of Physics, Visva- Bharati, Santiniketan, Birbhum, West Bengal, India PIN-731235

e-address: kmsvc08@gmail.com

Interaction of a four-level inverted-Y type system^{1,2} with four electromagnetic fields is considered in this present study. The system has two ground energy levels, one intermediate energy level and one uppermost energy level. A weak probe field is applied between one of the two ground states and the intermediate state whereas a microwave field couples the two ground energy levels. A repump field connects the intermediate energy level with the other ground level. The high power control field acts between the intermediate energy level and the uppermost energy level. Dipole approximation^{3,4} and rotating wave approximation^{3,4} are used to derive the optical Bloch equations from the Master equation³. The steady state behavior of the atomic system is studied for both Doppler free and Doppler broadened conditions. In presence of the microwave field, the simulated probe response shows electromagnetically induced gain for stationary atoms as well as under Doppler broadened condition. The power of the applied microwave field is found to play a crucial role in switching the probe field propagation from subluminal to superluminal. The band width and sharpness also depends on the power of the microwave field.

References:

1. A. Ghosh, K. Islam, D. Bhattacharyya and A. Bandyopadhyay J. Phys. B: At. Mol. Opt. Phys. 49 (2016) 195401
2. A. Ghosh, K. Islam, Suman Mondal, D. Bhattacharyya, Nikhil Pal and A. Bandyopadhyay J. Phys. B: At. Mol. Opt. Phys. 51 (2018) 145501.
3. M. O. Scully and M. S. Zubairy, "Quantum Optics", Cambridge University Press: London (1997).
4. S. C. Rand, "Lectures on Light: Nonlinear and Quantum Optics using the Density Matrix" Oxford University Press: New York (2010).

PO-04

Probe response characteristics of a twelve-level atomic system under cascade configuration

Surajit Golder^a, Suman Mondal^b, Kalan Mal^c, Amitava Bandyopadhyay^a

^aDepartment of Physics, Visva-Bharati, Santiniketan, PIN 731235, West Bengal, India

^bNational Institute of Science Education and Research (NISER) Bhubaneswar, Jatni, PIN 752050, Khurda, Odisha, India

^cDepartment of Physics, Suri Vidyasagar College, Suri, PIN 731101, West Bengal, India

e-address: surajitgolder@gmail.com

A twelve-level atomic system under cascade configuration 1 is studied numerically to find out the probe response under different physical conditions. Density operator method^{1,2} is used in this work to derive a set of one hundred and forty four Optical Bloch equations (OBEs) from the Liouville equation or the master equation with the phenomenological decay terms added. These OBEs are solved numerically under steady state condition to determine the probe absorption and probe dispersion features under different values of control and probe Rabi frequencies as well as their detunings. A comparative study between the ^{133}Cs $6S_{1/2} \rightarrow 6P_{3/2} \rightarrow 6d_{5/2}$ and ^{87}Rb $5S_{1/2} \rightarrow 5P_{3/2} \rightarrow 5d_{5/2}$ multi-level cascade type transitions is done based on this model and it is shown how the electromagnetically induced transparency (EIT)^{3,4} peaks differ in the two cases. It is further interesting to find out from this study that by playing with the detuning of the applied coherent fields the transparency windows can be converted into enhanced absorption⁵ of the probe field. The corresponding dispersion profiles are also examined.

References:

1. S. Mondal, S. S. Sahoo, A. K. Mohapatra and A. Bandyopadhyay, Opt. Commun. 472 (2020) 126036.
2. H. S. Moon and H. R. Nho, J. Opt. Soc. Am. B 31 (2014) 1217.
3. S. E. Harris, Phys. Rev. Lett. 62 (1989) 1033.
4. D. J. Fulton, S. Shepherd, R. R. Moseley, B. D. Sinclair and M. H. Dunn, Phys. Rev. A 52 (1995) 2302.
5. "Lectures on Light: Nonlinear and Quantum Optics using the Density Matrix" by S. C. Rand, Oxford University Press, New York, 2010.

PO-05

Ultrafast Nonlinear Optical Switching and Sensing Response of Bimetallic Nanoparticles Produced Using Bessel Beam

Dipanjan Banerjee^a, Akkanaboina Mangababu^b, Ravi Kumar Kanaka^b, Venugopal Rao Soma^{a,1}.

^aAdvanced Centre of Research in High Energy Materials (ACRHEM),

^bSchool of Physics, University of Hyderabad, Hyderabad 500046, Telangana, India

¹Corresponding author: soma.venu@uohyd.ac.in

e-address: dipanjan.banerjee22@gmail.com

In this study, we have generated bimetallic (BM) nanoparticles (NPs)¹ using femtosecond Bessel beam (BB) ablation technique. The NPs displayed prominent ultrafast optical switching. Subsequently, the plasmonic nanoparticles were utilized in trace-level sensing of real-time explosives using surface-enhanced Raman scattering (SERS) technique. The major advantage of Bessel beams is its unchanged intensity profile and a higher depth of focus, making it pertinent for laser ablation². Following figure depicts the schematic of the ablation experiment, TEM data, EDS data. The absorption peak of the ablated BM NPs was observed at 449 nm. The ultrafast nonlinear response has been assessed through the Z-scan technique. The NPs (~ 22 nm average size) have unveiled fascinating mixed nonlinear absorption curves. The SERS data was obtained by detecting real-time explosives such as RDX ($100 \mu\text{M}$), TETRYL ($5 \mu\text{M}$) at the trace levels.

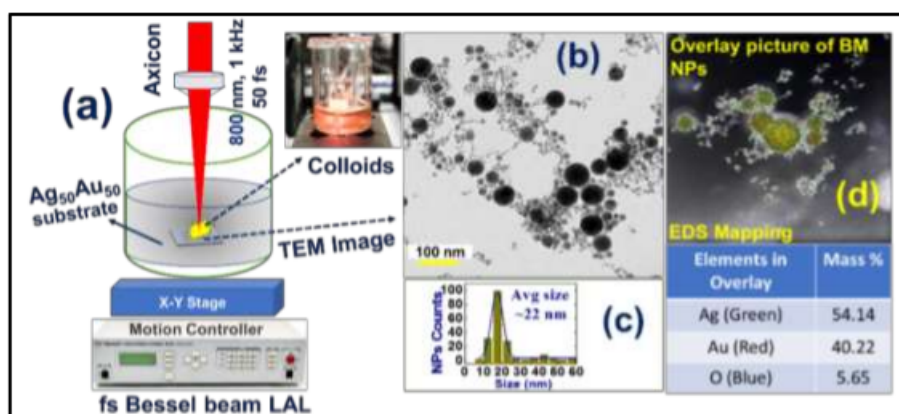


Figure 18: (a) Schematic of 800 nm, 1 kHz, 50 fs BB LAL experiments using an axicon (b) TEM image of BM alloy NPs (c) Size distribution data of the NPs (average ~ 22 nm) (d) EDS mapping data revealing the formation of BM alloy NPs, along with mass percentage data presented.

References:

1. R. J. White, R. Luque, V. L. Budarin, J. H. Clark and D. J. Macquarrie, Chem. Soc. Rev. 38, 481–494 (2009).
2. J. Durnin, J.J. Miceli and J.H. Eberly, “Diffraction-free beams,” Phys. Rev. Lett. 58, 1499 (1987).

PO-06

Understanding the Laser-Aerosol Interaction: Simulation of the Laser Beam Propagation through Optical System and Aerosol clouds

Sakshi Jain^a, Nagaraju G^a, Anasibnu Basheer^b, D. P. S. L. Kameswari^a, Vijay P. Kanawade^b, P. Prem Kiran^a, Ashok Vudayagiri^a

^aSchool of Physics, University of Hyderabad, Gachibowli, Hyderabad – 500046, India

^bCentre for Earth, Ocean and Atmospheric Sciences, University of Hyderabad, India

e-address: ashok_vs@uohyd.ac.in, prem@uohyd.ac.in

Aerosols are ubiquitous in the atmosphere that can scatter or absorb sunlight (laser beam) depending on their composition. Understanding interaction of atmospheric aerosols with electromagnetic field will help in understanding of nature of aerosols and about propagation of light through them. We study light scattering by aerosol particles by simulation, using Mie scattering theory and compare it with experiments within a laboratory setup. The underlying principle is that aerosols/aerosol clouds with various refractive indices and absorption characteristics can be represented by corresponding optical elements with different refractive indices, shapes, and focusing conditions. Gaussian beams and a combination of optical systems were used to mimic the modifications experienced by the He-Ne laser beam propagating through the atmosphere via our initial ABCD matrix approach. The evolution of the spot size and radius of curvature were obtained from simulations of the laser beam propagation through optical systems (coupled with spherical and cylindrical lenses). At several points along the beam propagation path, He-Ne laser beam profiles were measured to validate the simulated results. The experimental and simulated data are observed to match closely. The important and fundamental consideration to incorporate the effect of aerosols on the laser beam propagation through atmosphere is via the radial distribution of the aerosol particles $n(r)=n_0 \frac{l(r)}{l_0}$ where $n(r)$ is the radially varying refractive index due to the aerosol clouds, n_0 is the refractive index of the aerosols, $l(r)$ is the size of the aerosol cloud along the laser propagation direction, and l_0 is the average thickness of the aerosol cloud. The evolution of phase(wave) front of the He-Ne laser beam through a set of aerosols obtained from the Urban environment is investigated.

PO-07

Real Time Terahertz Imaging of Organic and Inorganic materials

P. Naveen Kumar, Nagaraju Menchu, A. K. Chaudhary

Advanced Centre of Research in High Energy Materials (ACRHEM), University of Hyderabad Prof. C.R. Rao Road, Gachibowli, Hyderabad, Telangana 500046, India.

e-address: naveenperiketi@gmail.com

Terahertz (THz) radiation compensates the gap between the microwave and infrared region of the electromagnetic spectrum which is extended between 100 GHz to 10 THz frequency or 3 mm to 30 μm wavelength region. Its low photon energy is good enough for samples to avoid radiation damage and makes it a non-destructive technique to study the optical properties of materials. THz imaging is positioned to play a key role in both industrial and academic research applications, as most of the organic and inorganic materials are either transparent or semi-transparent to THz radiation which makes it capable of imaging the material. THz radiation acts as a perfect tool to investigate and image the biological tissues and growing cancer in human body without any harmful side-effects. As THz radiation is capable of penetrating through the materials, THz imaging systems can be used in detection of concealed objects which can be of potential threat, thus making THz imaging suitable for defence and Security applications. We report the real time pulsed terahertz imaging of both organic and inorganic objects in reflection mode geometry. The images generated are represented in both time-domain and frequency-domain.

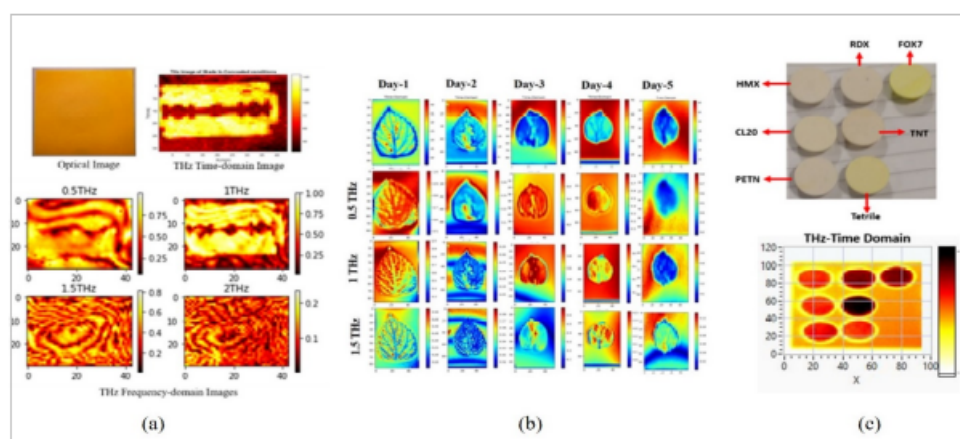


Figure 19: a) THz imaging of metallic object in concealed condition. b) THz imaging of plant leaf for water dynamic studies. c) THz imaging of primary and secondary explosive molecules.

Reference:

Jepsen, P. U., Cooke, D., and Koch, M. (2011). Terahertz spectroscopy and imaging – Modern techniques and applications. *Laser and Photonics Reviews*, 5(1), 124-166.

PO-08

Study of PEDOT polymer based charge transfer mechanisms for the demonstration of photons- electron interaction in the green line fluorescence spectra of plant leaves

Nikhitha Kuppathi^a, Kandi Suryaprakash^a, Arjun V.S^b, A K Chaudhary^b

^a School of Physics, University of Hyderabad, Gachibowli, Hyderabad 500046, India

^b ACRHEM, University of Hyderabad, Gachibowli, Hyderabad 500046, India

e-address: nikhithadermal@gmail.com

The study reports the visible radiation, i.e., (532 nm) induced red chlorophyll fluorescence spectra of green leaves from two different plants¹. We have used PEDOT polymer as a host quenching medium for the recording of red chlorophyll fluorescence in Giloy and Spinach². Since chlorophyll possesses very weak absorption at 532 nm, therefore, recording of fluorescence spectra is a challenging task. However, adding a few milligrams of PEDOT in an 80% aqueous acetone solution of plant leaf extract resulted in a drastic enhancement in the fluorescence signal. The extract of Giloy and Spinach leaf show ten and two times enhancement in their respective fluorescence signals. We have used a 532 nm wavelength of 1.5 nanosecond pulse received at a 10kHz repetition rate from the DPSS laser system. The fluorescence spectra were detected using fibre coupled spectrophotometer. The charge transfer mechanism between chlorophyll and PEDOT initiated due to photon-electron interaction³. We have provided the charge transfer mechanism to explain the fluorescence signal enhancement process. In the final step, we attempted to record the fluorescence spectra directly from leaves. The leaves were cut into 8mm×6mm size and mixed with 80% aqueous acetone solution of PEDOT. We used a dichroic mirror as a filter which helped us to filtered out the residual incident 532 nm wavelength and record the pure fluorescence signal.

References:

1. Lang, M., Stober, F., and Lichtenthaler, H. K. (1991). Fluorescence emission spectra of plant leaves and plant constituents. *Radiation and environmental biophysics*, 30(4), 333-347.
2. Kumari, Archana, A. K. Chaudhary, and K. Rajasekhar. "Study of charge transfer mechanism of PEDOT polymer for detection of solid TEX and CL-20 explosives using pulsed photoacoustic technique." *Spectrochimica Acta Part A: Molecular and Biomolecular Spectroscopy* 241 (2020): 118597.
3. Shanmugam S, Xu J, Boyer C. Utilizing the electron transfer mechanism of chlorophyll a under light for controlled radical polymerization. *Chemical science*. 2015;6(2):1341-9.

PO-09

Growth and Photoluminescence Properties of α -MoO₃ Nanoneedles

Chinthapudi Srinivasulu^a, Santanu Kumar Padhi^b, K L Naidu^c, Ashok Vudayagiri^a^aSchool of Physics, University of Hyderabad, Hyderabad-500046, India^bPhysics Department, University of Turin, Via P. Giuria 1-7, 10125 Turin, Italy.^cDepartment of Physics, GITAM (Deemed to be University), Visakhapatnam-530045, Indiae-address: 19phph24@uohyd.ac.in

Single-crystalline α -MoO₃ nanoneedles (NNs) were grown via a facile one-step hydrothermal method¹. The synthesized α -MoO₃ NNs are characterized for their structural, morphological, vibrational, and optical properties. The X-ray diffraction (XRD) indicates the orthorhombic α -MoO₃ phase with minor impurities. These NNs growth mechanisms with various processing parameters (viz., the volume of precipitant HNO₃, temperature, and time) in detail were investigated by transmission electron microscopy (TEM) in combination with high-resolution transmission electron microscopy (HR-TEM). These TEM studies imply a novel particle-based orientational- attachment (OA, non-classical approach) scheme². The field emission scanning electron microscopy (FESEM) micrographs show that the average width of these NNs is about 81 nm and length of 2.14 μ m. The Raman investigation shows mainly the presence of stretching and wagging modes of Mo-O bonds. The photoluminescence (PL) at room temperature; NNs exhibit an intervalence charge transfer (IVCT) shoulder at 460 nm, in addition to an intense band-to-band deep-level emission (DLE) at 438 nm, respectively³. Hence, PL studies shed light on the electronic structure and vacancy defects in the synthesized α -MoO₃ NNs.

Acknowledgments:

Ch.Srinivasulu acknowledges of a CSIR-UGC-JRF fellowship. School of Physics and Chemistry instrumental facilities support is acknowledged.

References:

1. A. Chithambararaj, N. Rajeswari Yogamalar, and A. C. Bose, *Crystal Growth and Design* 16, 1984 (2016).
2. B. B. V. Salzmann, M. M. van der Sluijs, G. Soligno, and D. Vanmaekelbergh, *Acc. Chem. Res.* 54, 787 (2021).
3. E. Ghaleghafi and M. B. Rahmani, *Solid State Sciences* 94, 85 (2019).

PO-10

Bound State of Solitons

Dheerendra Singh, Prasanta K. Panigrahi

Department of Physical Sciences, Indian Institute of Science, Education and Research Kolkata, Mohanpur, West Bengal 741246, India.

e-address: ds17ip010@iiserkol.ac.in

The bound state (BS) of solitons was predicted by Malomed in the context of the nonlinear Schrodinger equation (NLSE) for coherent and incoherent nonlinear couplings¹. Further studies reveal that two temporal solitons with opposite phase attract to each other in the nonlinear medium till a certain distance, after which the attraction turns into repulsion thus restituting their initial separation. One can call these entities as soliton molecules, due to their resemblance with both the constituents of the diatomic molecule^{2,3}. The array of compound states of temporal solitons can be studied in the bimodal optical fiber with the three-level Λ type system⁴. For this purpose, we propose the cnoidal wave-like ultrashort pulses and delineate the parameter regimes for the occurrence of the array of compound states. Particularly, it is found that cn and sn type of waves represent compound states by increasing the strength of the atomic coherence. We also numerically studied their respective frequency spectra, which reveals the phase information between the two pulses.

References:

1. Boris A Malomed. "Bound solitons in coupled nonlinear Schrodinger equations". In: Physical Review A 45.12 (1992), R8321.
2. M Stratmann, T Pagel, and F Mitschke. "Experimental observation of temporal soliton molecules". In: Physical review letters 95.14 (2005), p. 143902.
3. A Hause et al. "Binding mechanism of temporal soliton molecules". In: Physical Review A 78.6 (2008), p. 063817.
4. Manali Verma et al. "Ultrashort pulse train in rare earth doped bimodal optical fiber". In: JOSA B 39.5 (2022), pp. 1429–1437.

PO-11

Modelling Spin-to-Orbital Angular Momentum Conversion of in Tightly-focused Circularly-polarized Light

Nitish Kumar, Nirmal K. Viswanathan

School of Physics, University of Hyderabad, Gachibowli, Hyderabad – 500046, India

e-address: nitish.phy1@gmail.com

Based on the vectorial Debye theory we investigate optical effects related to spin-orbit interaction of light, arising due to high-NA focusing of circularly polarized Gaussian beam of light. The conversion of spin angular momentum (SAM) to the orbital angular momentum (OAM) arising due to partial conversion of circularly polarized light beam and the generation of an optical vortex beam is investigated in detail in the focal region. Tight focusing of a Gaussian beam is known to generate vortex beam of charge ± 1 in the Z-component of the electric field. We on the other hand retro-reflect circularly-polarized focused Gaussian beam to generate a ± 2 charge optical vortex beam in the Fourier plane. By using a mirror as the reflecting surface, we were able to achieve high conversion efficiency of $> 30\%$. In addition to the polarization-dependent vortex beam generation we also study its polarization dynamics.

PO-12

Bifurcation of complex singular points due to circular birefringence in a uniaxial crystal plate

Anagha Sreedharan, Nirmal K Viswanathan

School of Physics, University of Hyderabad, Gachibowli, Hyderabad, 500046, India
e-address: anaghakandoth@gmail.com

The appearance of bifurcation in a complex optical field is accompanied by the appearance of critical points (complex singularities) that rearrange the topological features. This can be achieved via variation of the optical field parameters and / or the medium parameters. The branching of complex critical points into isolated points appear in pairs to conserve the total topological charge of the optical field¹. Here, we investigate the bifurcation in the dark fringe of an interference pattern, simulated in the output beam of a paraxial beam propagating through a twisted elliptically birefringent crystal plate². The dark-fringe bifurcation in the intensity map of the output optical beam-field accompanies a complex singularity dynamics in the phase map that splits into a pair of vortex-saddle type phase singularities, which is realized by varying the circular birefringence of the crystal plate.

References:

1. Novitsky, A.V. and Barkovsky, L.M., 2009. Poynting singularities in optical dynamic systems. *Physical Review A*, 79(3), p.033821.
2. Sreedharan, A. and Viswanathan, N.K., 2022. Spin-orbit coupling mediated transverse spin mode rotation in a uniaxial crystal. *Optics Letters*, 47(15), pp.3768-3771.

PO-13**Picosecond Laser Ablated GaAs Surface Structures for Antireflective and SERS Applications**

A. Mangababu^a, Kanaka Ravi Kumar^a, Dipanjan Banerjee^b, R. Sai Prasad Goud^c, Venugopal Rao Soma^b, S.V.S. Nageswara Rao^{a,c}

^aSchool of Physics, University of Hyderabad, Gachibowli, Hyderabad – 500046, India

^bAdvanced Centre of Research in High Energy Materials (ACRHEM), DRDO Industry Academia – Centre of Excellence (DIA-COE), University of Hyderabad, Hyderabad 500046, Telangana, India

^cCentre for Advanced Studies in Electronics Science and Technology (CASEST), University of Hyderabad, Hyderabad 500046, Telangana, India

e-address: mangababuind@gmail.com

Surface structuring of semiconductors have promising applications in various fields such as photonics, electronics, optoelectronics, solar cells etc. In this study, GaAs, one of the high potential candidates for the above mentioned applications is exposed to picosecond laser pulses for tuning its surface properties thereby attaining novel aspects of the GaAs periodic surface structures. Laser ablation has been carried out utilizing an Nd:YAG, EKSPLA, PL2351 laser [30 ps, 532 nm, 10 Hz] in different surrounding media such as air, distilled water, ethanol, and PVA. There is a significant effect of the ablation medium on the morphology of GaAs quasi-periodic surface structures. Further, these structures are studied for antireflective and SERS properties. Details about the role of surrounding medium on the morphology and properties of the ablation products will be discussed.

PO-14**A study of the spin-Hall effect of light at different incident angle**

Upasana Baishya , Nirmal K. Viswanathan

School of Physics, University of Hyderabad, Gachibowli, Hyderabad – 500046, India

e-address: upasanabaishya@gmail.com

The study of the spin-Hall effect of light (SHEL) and the consequent transverse spin-shifts (SS) as a manifestation of the spin-orbit interaction is an area of emerging interest. Following the Richards & Wolf treatment of focussing of light and vectorial angular spectrum method we investigate the SHEL at an air-glass interface by characterising the spin shift at different off-axis region in the cross-section of the light beam at the Fourier plane. The measurements are directly related to the incident angle of the light beam whose range starts from the normal incidence up to the angle dependent on the NA of the focusing lens. The simulation and the experimental transverse shifts from the cross-polarisation components due to the light-matter interaction of the reflected focused light for linear input polarisation is measured via the weak measurement method.

PO-15**Electron-atom scattering in Ultracold Plasma**

Satyam Prakash, Dr. Ashok Vudayagiri

School of Physics, University of Hyderabad, Gachibowli, Hyderabad – 500046, India

e-address: dassamir579@gmail.com

The recent developments in deriving the effective potential for electron-atom scattering in a dense semiclassical plasma is relevant to understanding the plasma conductivity and correlation functions. For this, electron-atom momentum transfer cross-section(MTCS) using effective optical potential including Hartree-Fock, Polarisation potentials, and the exchange effects is calculated. At low screening strength(κ) and coupling strength(Γ), High energy density plasma(HEDP) and Ultracold Neutral plasma(UNP) characteristics overlap. The ionisation efficiency and the velocity distribution at ultracold temperature can be determined using the scattering theory. Moreover the bound state formation as per the Levinson's theorem sheds light on thermalisation of electrons at microsecond timescale.

We derive the appropriate potential for the partially ionised Ultracold Plasma system to explain the experimental observations (i) The long range coulomb interactions shift the zero energy of isolated atoms. (ii) The ionisation process of rydberg atoms placed in a plasma medium doesn't depend strongly, upto 100 cm^{-1} , on the plasma electron energy. We also investigate on the potential parameters leading to the formation of bound states in Ultracold plasma medium. The bound state formation of Li^- in Lithium ultracold plasma could provide novel insights into the ionisation processes at temperatures as low as 1mK.

References:

1. "Contribution of electron-atom collisions to the plasma conductivity of noble gases" -S. Rosmej, H. Reinholz, and G. Röpke, Phys. Rev. E 95, 063208 –(2017);
2. "Exploring the crossover between high-energy-density plasma and ultracold neutral plasma physics", Phys. Plasmas 26, 100501 (2019); <https://doi.org/10.1063/1.5119144>;
3. Ionization of Rydberg atoms embedded in an ultracold plasma- Nicolas Vanhaecke, Daniel Comparat, Duncan A. Tate, and Pierre Pillet; Phys. Rev. A 71, 013416 -(2005)

PO-16

Unravelling the intraband ultrafast carrier dynamics in few layer MoS₂ by probing with mid IR pulses

Vinod k Rajput^a, Prasenjit Jana^a, Deepak Maity^b, T N Narayanan^b, Sri Ram G Naraharisetty^a

^aSchool of Physics, University of Hyderabad, Gachibowli, Hyderabad – 500046, India

^bTata Institute of Fundamental Research, Hyderabad-500046.

e-address: vinodrajput1989@gmail.com

Like graphene, two dimension metal dichalcogenides (TMDCs) are currently emerging research field with several range of applications. In this, Molybdenum disulphide MoS₂ is the most important TMDCs due to its direct band gap in mono layer (1.8 eV) and this band gap is tunable with number of layers. This band gap variability is needed for several industrial and scientific applications, which is not feasible in the graphene. It is important to have the fundamental understanding of the charge carrier dynamics of these materials, we used pump probe technique to investigate the non-equilibrium carrier dynamics in MoS₂. We pumped the few layer system above the band gap or to the continuum states using 500 nm (2.48 eV) optical pulses. This non equilibrium system is probed with an energy much less than the band gap of the material falling in the mid-IR region i.e. 2000 nm (0.62 eV) and 4000 nm (0.31 eV) and observed different phenomena as shown in following figures, We also studied pump power dependent dynamics of carriers, which revealed different carrier relaxation time dynamics and variable carrier density. These experiments gave insights about the extremely short lived Pauli blocking, ground state bleach, different excited state dynamics and anisotropic dynamics. These unique studies of probing the 2D materials near and below bandgap are necessary to give insights for effective use in the applications of optoelectronic and photonic devices such as photo detector and modulators.

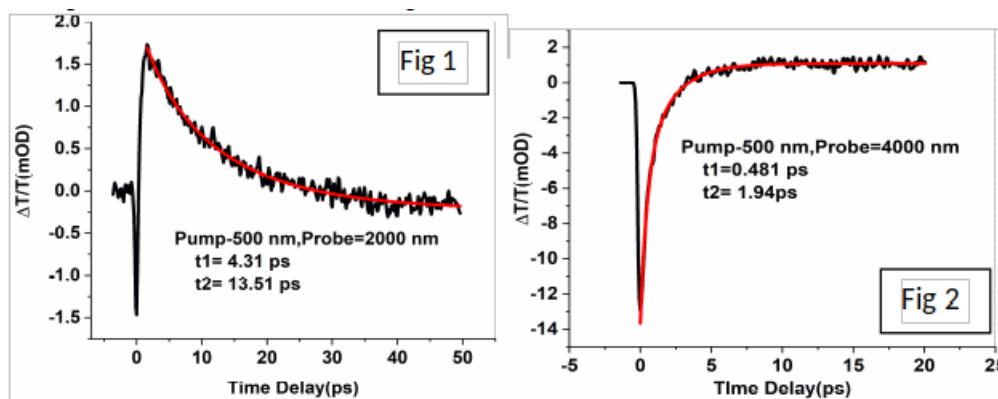


Figure 20:

References:

1. Cha, S., Sung, J., Sim, S. et al. 1s-intraexcitonic dynamics in monolayer MoS₂ probed by Ultrafast mid-infrared spectroscopy. *Nat Commun* 7, 10768 (2016).
2. Chen, H., Wen, X., Zhang, J. et al. Ultrafast formation of interlayer hot excitons in atomically thin MoS₂/WS₂ heterostructures. *Nat Commun* 7, 12512 (2016).
3. Poellmann, C., Steinleitner, P., Leierseder, U. et al. Resonant internal quantum transitions and femtosecond radiative decay of excitons in monolayer WSe₂. *Nature Mater* 14, 889–893

PO-17

Excited state relaxation dynamics study of IR-780 dye using home-built broadband multicolour transient absorption spectrometer

Sajin Ponnann, D Narayana Rao, Sri Ram G Naraharisetty
School of Physics, University of Hyderabad, Gachibowli, Hyderabad – 500046, India
e-address: 17phph25@uohyd.ac.in

A transient absorption spectroscopy (TAS) using ultrafast laser pulses is very commonly used to probe non-equilibrium excited dynamics on various molecular systems. This often needs expensive spectrometers and multichannel detectors, in this work we demonstrated a cost-effective home-built TAS with an inexpensive fiber optic-based spectrometer detection, with a broadband white light continuum as the probe. We used this system to investigate the broad band transient dynamics on IR-780 dye, with pump excitation at 780 nm. We measured the decay dynamics of stimulated emission peak (812 nm) and ground state bleach (803 nm) S0 to S1. Also, we observed a unique long-lived new vibrational state (670 nm-760 nm) and two excited-state absorptions (530 nm and 569 nm S1 to Sn). This infrared dye is extensively used in the in vivo imaging and photo therapy treatment, this work unravels the nonequilibrium fast dynamics of the dye.

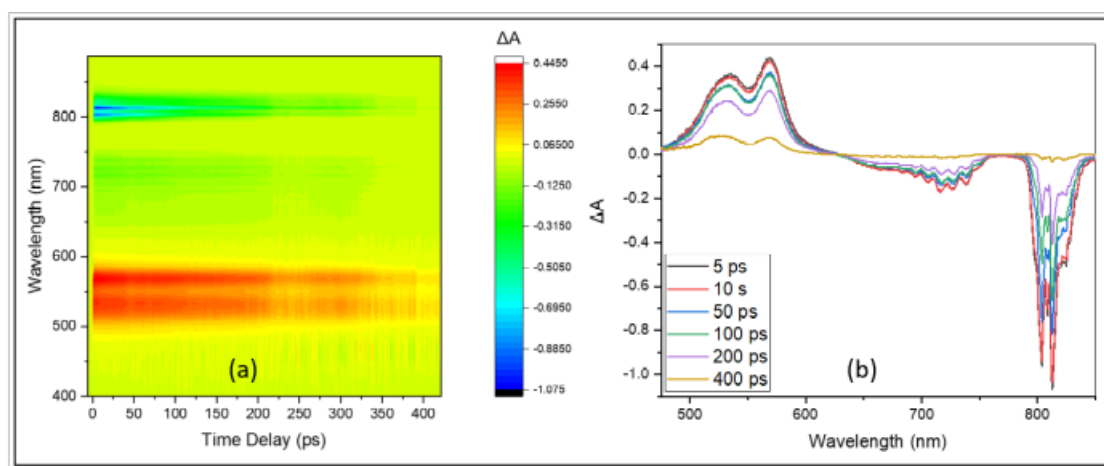


Figure 21: (a) Transient absorption spectra of IR-780, excited with 780nm and probed with white light continuum (b) Change in ΔA spectrum with respect to the delay time.

References:

1. C. Sahoo, M. Sethupathy, N. A. Saad, D. N. Rao, and S. R. G. Naraharisetty, "Ultrafast pump-probe signal detection using a data acquisition card," *Journal of Instrumentation*, vol. 13, no. 10, Oct. 2018, doi: 10.1088/1748-0221/13/10/P10027;
2. D. Kumar Das, K. Makhal, and D. Goswami, "Observing ground state vibrational coherence and excited state relaxation dynamics of a cyanine dye in pure solvents," *Physical Chemistry Chemical Physics*, vol. 20, no. 19, pp. 13400–13411, 2018, doi: 10.1039/c7cp08605a.

PO-18

Plasmonics on optical nanofibers: a versatile platform for strong light-matter interaction

Bratati Das, Elaganuru Bashaiah, Resmi M, Ramachandrarao Yalla
 School of Physics, University of Hyderabad, Gachibowli, Hyderabad – 500046, India
 e-address: bratatidas418@gmail.com

Fibers with a particular sharp structure at the end (Nano-tip) can be used for optical sensing, beam shaping, biomedicine, and many other sensing purposes due to the efficient channeling of light¹. Finite-difference time-domain (FDTD) method has become one of the useful numerical tools for the demonstration of the electromagnetic field. So here, we have performed Finite-difference Time-Domain Method (FDTD) simulations for Nanofiber, nanofiber tip, and dipole source to find the channeling efficiency (η) for different positions of dipole source and to study the effect of gold nanoparticle (AuNP) on channeling efficiency in the single-mode regime. A dipole is placed at the end of the Nano-tip and after that, an AuNP is placed inside the FDTD region [following Fig:(a)], and a frequency domain and power monitor measure the coupling. We have fabricated the nanofiber [following Fig:(c)] using the chemical etching method². In this work, the effect of the radius and effect in the presence of an AuNP for the optimization of the fiber coupling is studied using the finite-difference time-domain (FDTD) method. By using gold nanoparticles, we can achieve up to 43.5% coupling efficiency [following Fig:(b)] for Silica Nano-tip.

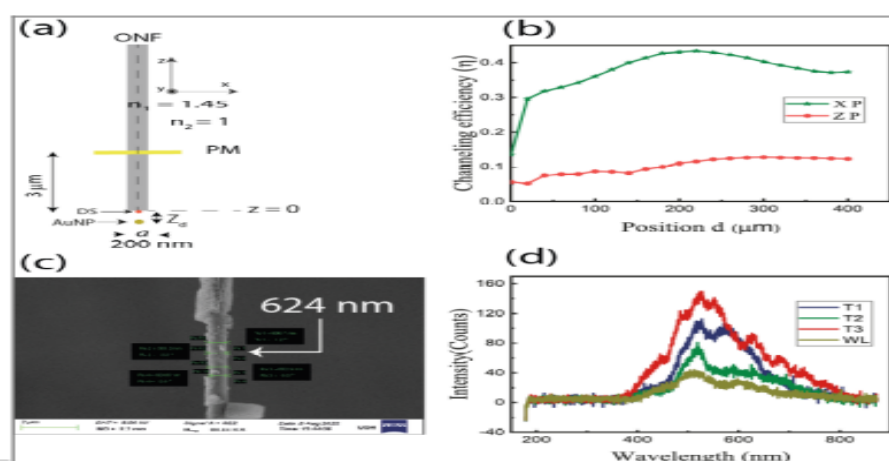


Figure 22: (a) is the schematic for dipole nano-tip simulation (b) is the result of the simulation (c) is the fesem image of the fabricated nano-fiber (d) is the scattering of AuNP .

References:

1. Tuniz, A., and Schmidt, M. A. (2018). Interfacing optical fibers with plasmonic nanoconcentrators. *Nanophotonics*, 7(7), 1279-1298.
2. Khashi, H. J. (2012). Fabrication of submicron-diameter and taper fibers using chemical etching. *Journal of Materials Science and Technology*, 28(4), 308-312.

PO-19

Compact Optical Scheme for mid-IR Spectrum Generation

Prasenjit Jana, Vinod K Rajput, Sri Ram G Naraharisetty
 School of Physics, University of Hyderabad, Gachibowli, Hyderabad – 500046, India
 e-address: 20phph06@uohyd.ac.in

Lab-based Optical techniques often employed to generate mid-IR pulses are discussed. These constructions follow a different frequency generation process for mixing signal and idlers pulses from optical parametric oscillators synchronously pumped by Ti: Sapphire laser (75fs, 1KHz repetition rate). Here, we proposed a new optical scheme that improves the day-to-day operation stability and ease of tuning spectrum anywhere in the 2 to 10 μm mid-IR region. Instead of using multiple dichroic mirrors, which are very expensive, we used only one. A dichroic mirror separates the signal and the idler coming from OPA; meanwhile, they are retraced back to the same dichroic mirror on a different spot using retro mirrors without making any angle. Because of the retro-reflector configuration, the delay change does not disturb the spatial overlap of signal and idler. This is the key to easily tuning the spectrum of the specified mid-IR region. The demonstrated scheme is very compact and cost-effective, with extreme stability.

Keywords:

Silver Thiogallate (AgGaS₂ or AGS), Optical parametric amplifier (OPA), Signal and Idler, Difference Frequency Generation process, Mid-IR generation, collinear DFG mixing.

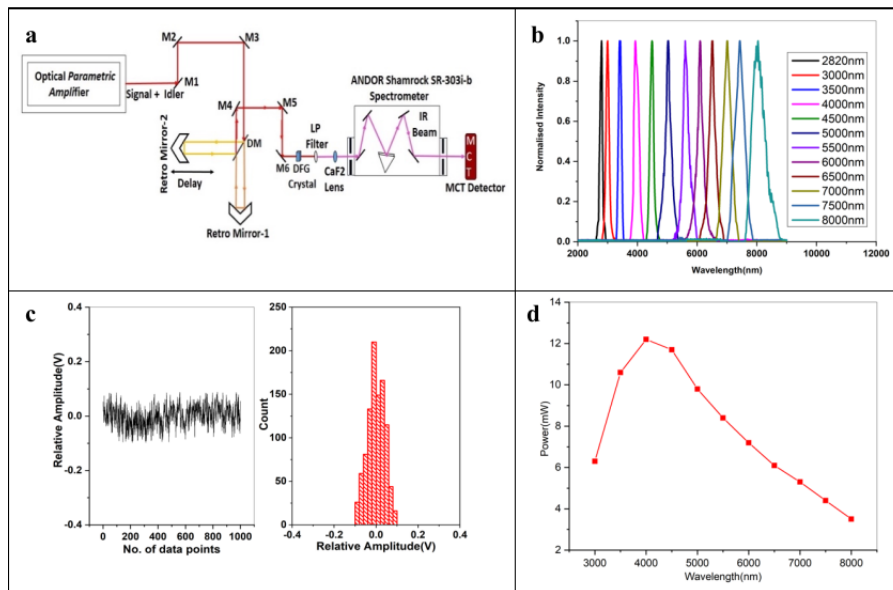


Figure 23: a) Optical layout of a home-built DFG setup using the retro mirror. b) Spectral tuning of the IR pulses over 2-8 μm using a home-built setup. c) Home-built signal to noise ratio. d) Experimentally obtained IR power curve with 1.1 W fundamental OPA input.

References:

1. F. Rotermund, V. Petrov, and F. Noack, *Opt. Commun.* 185, 177 (2000).
2. O. Isaienko and E. Borguet, *Opt. Express* 16, 3949 (2008).
3. M. Beutler, I. Rimke, E. Büttner, P. Farinello, A. Agnesi, V. Badikov, D. Badikov, and V. Petrov, *Opt. Express* 23, 2730 (2015)

PO-20

Z-Scan technique for measurement of nonlinear refractive index in Ag-nano particles

Niloofer Sulthana, Sajin Ponnan, D. Narayana Rao, Sri Ram G Naraharisetty
School of Physics, University of Hyderabad, Gachibowli, Hyderabad – 500046, India
e-address: 19ipmp17@uohyd.ac.in

Ag nanoparticle synthesized by laser ablation exhibits many interesting linear and nonlinear properties. The major reason for this is due to the surface plasmon modes residing on the nanoparticles resulting in coupling with the irradiate electromagnetic wave, thereby creating a stronger electric field. It contributes to increased absorption because of the surface plasmon resonance effect in comparison with bulk materials. We adopt the Z scanning technique to study the degenerate optical non-linearities of material using a single high intense laser beam. In the open-aperture Z-scan method, one can inspect the property of the reverse saturable absorption originating from multi-photon absorption, where the excitation source is a Gaussian beam. Theoretical study of a reflected gaussian beam from a single interface having spatial modification with intensity-dependent refractive index and absorption coefficient has been done. A nonlinear phase front distortion gets induced in the sample as the focused beam passes through it and this can be represented as an optical transmittance variation through an aperture placed in the transmitted beam path. The analytic expressions of the Z-scan traces for a femtosecond-laser (Ti-sapphire, 75 fs-1KHz) are included and the data was collected using a Lock-in amplifier and a DAQ and the sample showed unique spectra for the absorption as the size and morphology of nanoparticles vary together with the intensity of light.

Keywords:

Laser ablation, Z-scan, silver nanoparticles, two-photon absorption, Gaussian beam.

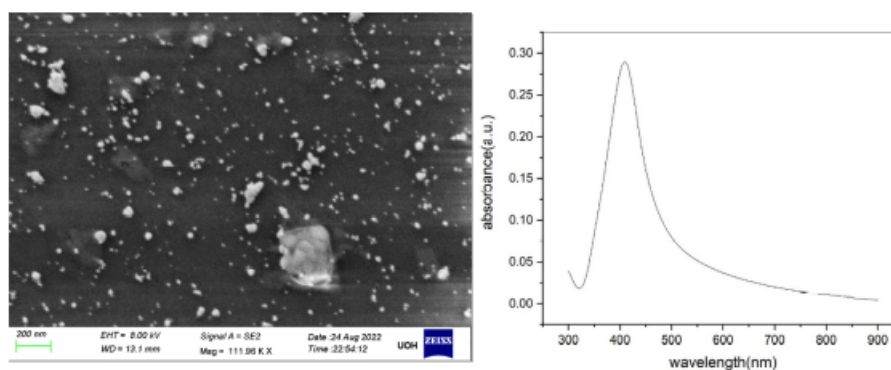


Figure 24: FESM image of laser ablated silver nanoparticle and its UV spectrum.

References:

1. A. Alesnikov, J. Pilipavičius, A. Beganskienė, R. Sirutkaitis, and V. Sirutkaitis, Lithuanian Journal of Physics, Vol. 55, No. 2, pp. 100–109 (2015) ;
2. Bing Gu, Ya-Xian Fan, Jing Chen, J. Appl. Phys. 102, 083101 (2007) ;
3. Characterization Techniques and Tabulations for Organic Nonlinear Materials, M. G. Kuzyk and C. W. Dirk, Eds., page 655-692, Marcel Dekker, Inc., 1998.

PO-21

Does Surface Roughness Affect Contact Angle?

Namitha L S, Md Abu Taher, D. Narayana Rao, Sri Ram G Naraharisetty
 School of Physics, University of Hyderabad, Gachibowli, Hyderabad – 500046, India
 e-address: 18ilmb20@uohyd.ac.in

Anisotropic surface structures on copper and stainless steel (SS) surfaces are fabricated by femtosecond fiber laser writing. These structures show hydrophilic to superhydrophobic properties as they evolve. Ellipsoidal water droplets with anisotropic contact angles (CAs) are formed on these surfaces, and their dependence on line spacing between laser scanning is discussed. The ellipsoidal volume of droplets on hydrophilic to hydrophobic surfaces is quantified experimentally. The wide range of anisotropic CAs produced on the copper, and SS surfaces are measured. The transition of anisotropic CAs and dynamics of droplet spreading on both surfaces are studied. The triple contact line (TCL) theory states that CAs are defined by the TCL boundary between air, water and the surface rather than the surface roughness. Along with a mathematical framework for the theory, the experimental confirmation of the TCL theory on ellipsoidal droplets over a wide range of CAs is provided. This work experimentally verified the TCL theory across a wide range of CAs.

Keywords:

laser direct writing, hydrophilic, superhydrophobic, anisotropic contact angles, ellipsoidal droplet, triple contact line (TCL) theory

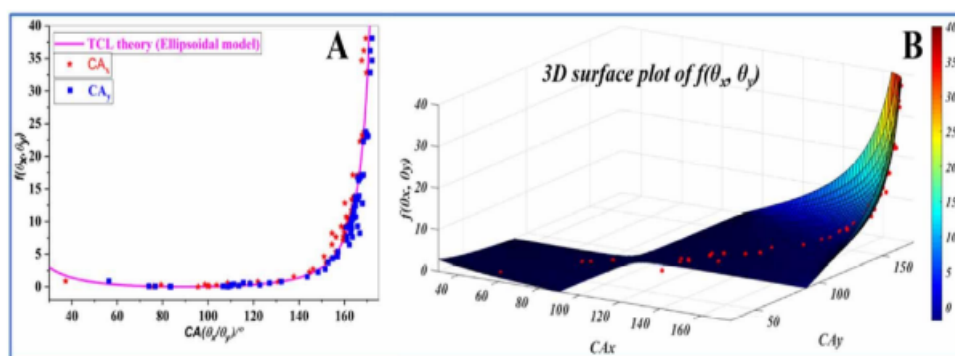


Figure 25: Combined data from Cu and SS substrates are presented in these figures. (A) Two-dimensional plot of the volume function $f(\theta_x, \theta_y)$ vs CAs. (B) Three-dimensional plot of the $f(\theta_x, \theta_y)$ vs θ_x and θ_y . The red-coloured symbols represent the experimental value of the $f(\theta_x, \theta_y)$.

References:

1. Md Abu Taher, Hitheswar Prasad, Navanith Krishnan P K, Narayana Rao Desai and Sri Ram G Naraharisetty, Surf. Topogr.: Metrol. Prop. 7 035001 (2019);
2. Md Abu Taher, Vinod K Rajput, Navanith Krishnan P K and Sri Ram G Naraharisetty, J. Phys. D: Appl. Phys. 55 055305 (2022)

PO-22

Ultrafast Pump-Probe Signal Detection using a Box-car and Lock-in Amplifier

Vinay Gudala , Vinod Rajput, Prasenjit Jana, Sri Ram G Naraharisetty

School of Physics, University of Hyderabad

e-address: 18ipmp17@uohyd.ac.in

This study consists of the data collection from a home-built pump-probe setup using two different amplification (Box-car and Lock-in) processes with the help of the National Instrumentation Data Acquisition Card (NI-DAQ). Box-car and Lock-in amplify the detector's collected probe pulse (MCT, Si-detector). The difference in the results of these methods is shown here. The advantage of using Box-car with NI-DAQ is visible in the quality of data collected, with very little noise compared to others. This result can be attributed to its fast- sampling rate, pulse-to-pulse noise suppression technique, and MCT detector detection scheme. The other approach includes a Lock-in amplifier along with a DAQ card. In this method, the signal is amplified before DAQ processes it, and in the process, the signal accumulates some amount of noise, which can be seen in the output. The usage of DAQ in both cases functions as a synchronizer that acquires the signal from the amplifier and is shown as output. In this method, only a single DAQ card is used for detection. Data Acquisition done by a NI-DAQ along with Box-car is much more effective than the other methods.

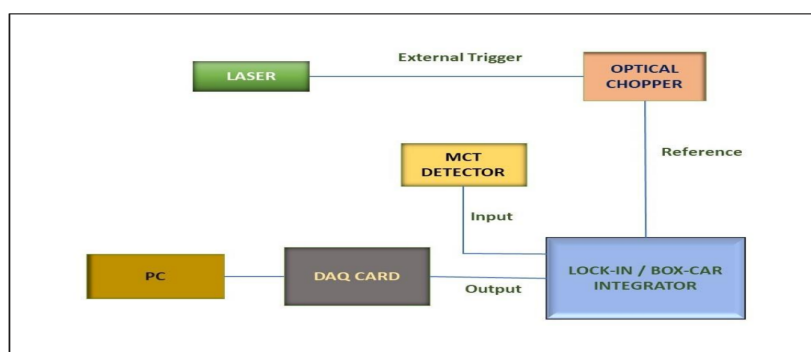


Figure 26: Schematic diagram of signal detection using Lock-in / Box-car integrator.

Keywords:

Data acquisition, NI-DAQ, MCT-detector, Box-car Integrator, Lock-in Amplifier

References:

1. C. Sahoo, M. Sethupathy, Nabil A. Saad, D. Narayana Rao, Sri Ram G. Naraharisetty. JINST 13 P10027 (2018)
2. Bhagyajyothi, Immanuel J., P. Bhaskar, Parvathi C.S. Sensors and Transducers. 153. 22-28 (2013)
3. J L Collier, B J Goddard, D C Goode, S Marka, H H Telle. Meas. Sci. Technol. 7. 1204-1211 (1996)

PO-23

In situ Fiber Diameter Measurement Using Whispering Gallery Modes

Elaganuru Bashaiah, Resmi M, Bratati Das, Ramachandrarao Yalla

School of Physics, University of Hyderabad, Gachibowli, Hyderabad – 500046, India

e-address: basha.elaganuru30@gmail.com

We report Whispering Gallery Mode (WGM) of optical microfiber when overlapped with optical nanofiber (ONF) and fabrication of ONF using the chemical etching method. Where optical microfiber acts as WGM resonators¹. 600 to 800 nm wavelength source is used to excite the optical microfiber, where the evanescent field of ONF couples with optical microfiber. Transmitted spectra recorded by Frequency Domain Field and Power monitor through ONF. A finite Difference Time Domain simulation has performed to get the results. For fabricating (ONF), Hydrofluoric (HF)² acid and U shape aluminum metal holders are used. Here, HF is used to etch the fiber in two steps. WGM resonators are produced at different wavelengths/frequencies. These wavelengths can estimate the diameter of ONF without damaging the ONF which is fabricated using chemical etching.

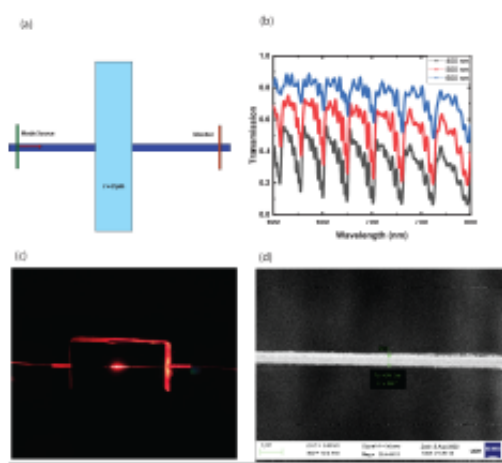


Figure 27: a) Schematic of WGM. b) Simulation results of WGM with the function of wavelength. (c) Scattering image of ONF. (d) FESEM image of a fabricated nanofiber ($d = 540$ nm).

References:

1. Kaur, J., Minz, R. A., Vairagi, K., Gupta, P., and Mondal, S. K. (2021). Excitation of Whispering Gallery Modes of a Microresonator Integrated in an Optical Fiber Axicon. *IEEE Photonics Technology Letters*, 33(24), 1495-1498.
2. Khashi, H. J. (2012). Fabrication of submicron-diameter and taper fibers using chemical etching. *Journal of Materials Science and Technology*, 28(4), 308-312.

PO-25

Fiber-Coupled Single Photon Source Using Optical Nanofiber Tip

Resmi M, Elaganuru Bashaiah, Bratati Das, Ramachandrarao Yalla
 School of Physics, University of Hyderabad, Gachibowli, Hyderabad – 500046, India
 e-address: resmi712010@gmail.com

Optical nanofibers (ONF) are optical fibers having a diameter of a few hundred nanometers. The challenging aspect of Quantum Information Science is the efficient channeling of single photons from a single photon emitter into a single mode fiber. It has been shown that up to 38% of photons from an emitter can be directly coupled to the single-mode optical fiber by utilizing the flat tip of a silica ONF¹. Theoretical study to enhance the efficiency is done by performing simulations using an optical nanofiber tip (ONFT) and single dipole source (SDS) by numerical simulations. Experimental realization of the results is being carried out by fabricating an ONFT using two-step chemical etching using HF acid² and then depositing a quantum dot (QD) on it. The maximum coupling efficiency is obtained when the SDS is placed on the face of the ONFT. The experimental feasibility of the simulations is shown by observing the spectrum.

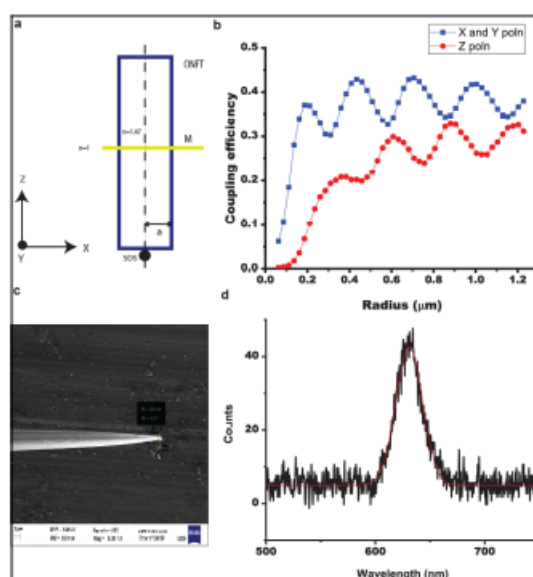


Figure 29: a) Schematic of the performed simulation. b) Radius v/s Coupling efficiency for the particular case. c) Typical image of an ONFT fabricated of 820 nm. d) Fluorescence spectrum of the QD deposited on the ONFT.

References:

1. Chonan, Sho, Shinya Kato, and Takao Aoki. "Efficient single-mode photon-coupling device utilizing a nanofiber tip," *Scientific reports* 4.1 (2014): 1-7.
2. Hani J. Kbashi. "Fabrication of Submicron-Diameter and Taper Fibers Using Chemical Etching," *J. Mater. Sci. Technol.*, 2012, 28(4), 308-312.

PO-26

Near perfect ultra-broad band absorbing surfaces fabricated by ultrafast lasers

Nitin Chaudhary, Thirunaukkarasu K, Sri Ram G Naraharisetty
 School of Physics, University of Hyderabad, Gachibowli, Hyderabad – 500046, India
 e-address: 20paph04@uohyd.ac.in

Fabrication of hierarchical micro/ nano structures on the thin stainless steel (SS304) surface provides the fabulous antireflection properties that can be used in various application such as photovoltaic detectors, efficient solar energy harvesting systems, national defence, low light imaging systems etc. Due to their wide range of potential uses, antireflective surfaces have garnered a lot of interest and have been the focus of in-depth study in recent years. However, obtaining ultralow reflectance on a metal surface is still a challenging problem because of the high optical impedance mismatch between a metal surface and air. Ultrafast laser fabrication can enable the manufacturing of micro and nano structures via the one step ablation processing. To further reduce the footprint of the laser on substrate we used the ultrafast direct laser interference patterning (DLIP) method. As a result, it significantly increased the antireflection property of the laser treated surfaces by efficiently trapping the incident photons incident on these micro/nano modulated structures. We optimized the ultrafast femtosecond laser parameters and we achieved the average total reflectivity for the broad band (250 nm to 2000 nm) range is 1.19%, and for the UV-Vis-NIR (300 nm to 2000 nm) is <0.05%. Further the average total reflectivity in the visible range is as low as 1.05% in the spectral region of 400 to 700nm. These ultra-antireflective SS surfaces are insensitive to incident polarization and has a wide incident cone angle of acceptance. This novel fabrication method is simple and adaptable to a variety of materials, which offers up new avenues for the development of broad-band ultra-low-reflectivity materials.

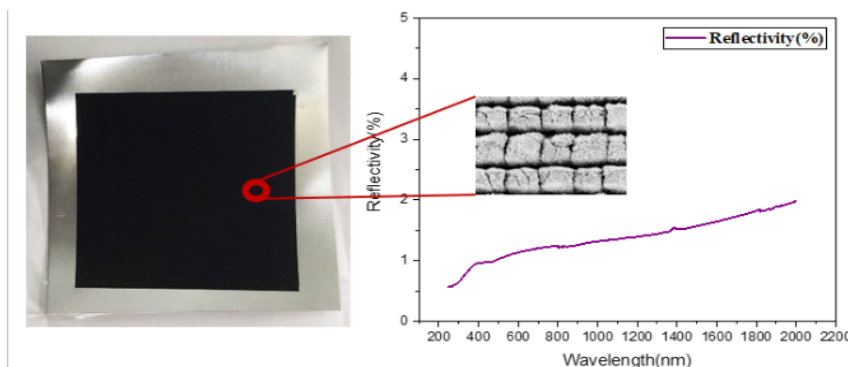


Figure 30: Diffused reflectance and inset micro/nano structure of super black surface

Keywords:

Ultrafast laser, Interference patterning, broad band antireflective surface, specular and diffused reflectivity.

References:

1. T. Chen, W. Wang, T. Tao, A. Pan, and X. Mei, "Broad-Band Ultra-Low-Reflectivity Multiscale Micro-Nano Structures by the Combination of Femtosecond Laser Ablation and in Situ Deposition," *ACS Appl. Mater. Interfaces*, vol. 12, no. 43, pp. 49265–49274, 2020 ;
2. R. Lou, G. Zhang, G. Li, X. Li, Q. Liu, and G. Cheng, "Design and fabrication of dual-scale broadband antireflective structures on metal surfaces by using nanosecond and femtosecond lasers," *Micromachines*, vol. 11, no. 1, 2020 ;

3. K. Thirunaukkarasu, Nitin Chaudhary et al., “Mechanically and thermally stable thin sheets of broadband antireflection surfaces fabricated by femtosecond lasers,” *Opt. Laser Technol.*, vol. 150, no. January, p. 107935, 2022 ;
4. M. Du et al., “Fabrication of antireflection micro/nanostructures on the surface of aluminum alloy by femtosecond laser,” *Micromachines*, vol. 12, no. 11, 2021

PO-27**Ultrashort pulse compression and pulse measurement**

Shamna, Shilpa M, D. Narayana Rao, Sri Ram G Naraharisetty
School of Physics, University of Hyderabad, Gachibowli, Hyderabad – 500046, India
e-address: 19ipmp11@uohyd.ac.in

Ultrashort laser pulses have very Fourier transform limited spectral width and perfect phase relation among the frequencies. Ultrashort laser beam experiences group velocity dispersion (GVD) when travels through dispersive materials. This results in a temporally longer laser pulses and gives positive chirp to it. Prism compression technique counteract the material dispersion caused when the laser travels through the optical components and shorten the pulse for various experimental applications. Dispersion phenomenon of the prism causes a continuously increasing temporal delay across the beam and automatically eliminate the positive chirp by overlapping the wavelength components with each other, causing compression of ultrashort pulse. We successfully compressed the pulse from 102 fs to back to 87 fs using the double prism compression technique. This is quantified by our home built auto correlator.

Keyword:

Group Velocity Dispersion (GVD), Mode locked, Autocorrelation, Prism compression, Michelson Interferometer.

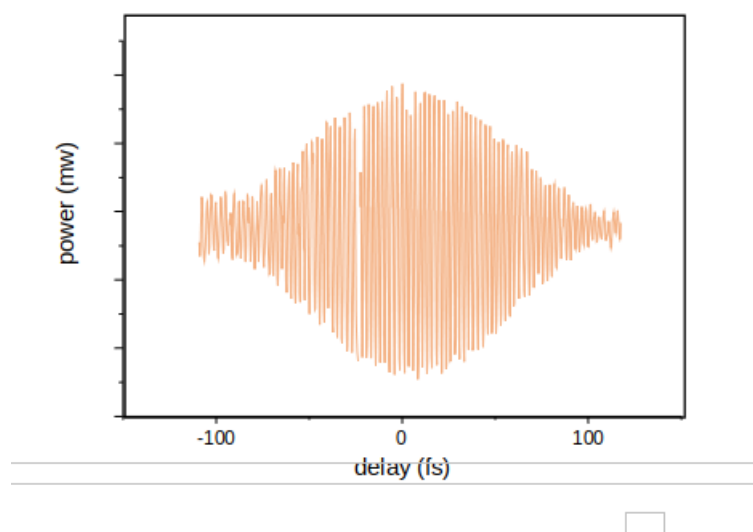


Figure 31: Autocorrelation of compressed pulse

References:

1. J. Diels and W. Rudolf, Ultrashort Laser Pulse Phenomena, Second Edition (Massachusetts, Academic Press, 2006).
2. E. Oran Brigham, The Fast Fourier Transform: An Introduction to Its Theory and Application (New Jersey, Prentice Hall, 1973).
3. Weiner AM. Ultrafast optics. Hoboken (NJ): John Wiley and Sons; 2009.
4. Rullière C. Femtosecond laser pulses: principles and experiments. New York (NY): Springer; 2005. p. 426.

PO-28**Thermodynamic properties of a particle scattering by rotating trapped quantum gases**

Kanaka Ravi Kumar^a, Chandu Byram^b, Jagannath Rathod^b, Dipanjan Banerjee^b, A.Mangababu^a,
R. Sai Prasad Goud^c, Venugopal Rao Soma^b, S.V.S. Nageswara Rao^{a,c}

^aSchool of Physics, University of Hyderabad, Gachibowli, Hyderabad – 500046, India

^b Advanced Centre of Research in High Energy Materials (ACRHEM), DRDO Industry Academia – Centre of Excellence (DIA-COE), University of Hyderabad, Hyderabad 500046, Telangana, India

^cCentre for Advanced Studies in Electronics Science and Technology (CASEST), University of Hyderabad, Hyderabad 500046, Telangana, India

e-address: ravikumarkanaka001@gmail.com

In this work, we prepare titanium nanoparticles (Ti NPs) by using picosecond (ps) laser irradiation of titanium nitride (TiN) powder suspended in DMF solvent. Under continuous magnetic stirring, the micron-sized particles of TiN are irradiated with ps laser pulses at different laser irradiation times (15, 30, 45, 60 minutes). The formation of Ti NPs is observed upon the interaction of laser pulses with TiN in DMF. The experiment is carried out by utilizing Nd:YAG laser [EKSPLA, PL2351] having a pulse duration of 30 ps, wavelength of 1064 nm, and repetition rate of 10 Hz. The yield of Ti NPs has increased with laser irradiation time. The optical and structural properties of Ti NPs are characterized by UV-Vis-NIR spectroscopy, and FESEM respectively. Details of all the characterizations and results will be discussed.

ES-01**Applicability of Fitts' Law to the Interaction of Young Adults with Touchscreen**

Pinaki Chakraborty , Savita Yadav, Lokesh Meena, Deepanshu Yadav

Department of Computer Science and Engineering, Netaji Subhas University of Technology, New Delhi 110078

e-address: pinaki.chakraborty@nsut.ac.in

Fitts' law is widely used to predict the time required to acquire targets when human beings use various physical and digital gadgets. However, there is no consensus on whether Fitts' law can be applied to the interaction with touchscreens. We conducted an experiment with 100 young adults (mean age: 19.80 years, S.D.: 0.67) who are expert in using digital technologies. We asked the participants to acquire targets of different size and at different distance displayed on a touchscreen using the tap gesture and the drag and drop gesture and measured the time they took for the same. We observed that Fitts' law was not applicable to the interaction of the young adults with touchscreen for either of the gestures. We also observed that the participants required 36 – 40% lesser time to acquire targets with the tap gesture than with the drag and drop gesture. The interaction with touchscreens is inherently different from the interaction with other input devices. New models to predict the time required for acquiring targets may be developed for touchscreens.

ES-02**Multi-class cancers classification using neural networks from non-invasive factors**

Brindha Senthil Kumar^a, Manimaran Palanisamy^b, Lal Himglina^a

^a Department of Computer Engineering, Mizoram University, Aizawl, India,

^b School of Physics, University of Hyderabad, Hyderabad, India

e-address: brindhamzu@gmail.com

The present cohort study focuses on classifying three cancer types: gastric, breast, and head & neck cancers from lifestyle features using a well-generalized neural network classifier. A set of five well-studied features: kuhva (paan), tuibur (aqueous tobacco extract), smoking, alcohol, snuff (smokeless tobacco products) and smoked food data are collected from gastric, breast cancer, head & neck and healthy controls. There are 200 observations for healthy controls, 173 for gastric cancer, 117 for breast cancer and 100 for head and neck cancer cases. The missing values are replaced by median. The class imbalance is handled by upsampling all the cancer cases observations to 200 each using SMOTE. Neural network model is able to generalize well the test data with accuracy of 75% and accuracy of 73% on training data. The accuracy is achieved using two hidden layers with 16 and 8 neurons, respectively, which has greatly reduce the computation cost during training the model. The random state is not altered for all four different hidden layers architectures: [24,16,8], [16,8,6], [16,8,4], [16,8] to achieve training - test accuracy of 71-75, 74-75, 75-75, 73-75, respectively. The above model is optimized with learning rate of 0.01, and momentum of 0.98, maximum iteration was set to 500, 'lbfgs' is used as optimizer and relu as the activation function. This multi- class cancer classification model has given a satisfactory accuracy of 75% only from the non-invasive features. The neural network model is generalized under four different hidden layer architectures without altering the random state during train and test split. Kuhva, tuibur, smoking, alcohol, snuff and smoked food can be cause of these cancers from lifestyle perspective apart from the genetic burden of this disease. The accuracy of the presented model can be further improved by doing more sampling in the near future. Furthermore, appropriate etiology of these cancers insight can be extracted when these features are integrated with cancer variants.

ES-03**Role of Artificial Intelligence in Cyber Security: Pros and Cons**

Sai Hima Harshini Easankarala, Pradeepthi K.V

C.R.Rao Advanced Institute of Mathematics, Statistics and Computer Science (AIMSCS), University of Hyderabad Campus,
Hyderabad, India

e-address: harshinieasankarla@gmail.com,

Tremendous growth in computation and automation has led to the expansion of cyberspace and its invasion into the various aspects of our lives. The major drawback of this is the surge in more targeted and sophisticated cyber attacks. Security and privacy are always a major concern which ushers researchers to discover new mitigation techniques. Though use of cryptographic algorithms on the data in transit and rest is being practised, it is not able to provide robust security as attackers are able to capitalise on other vulnerabilities present in the various attack surfaces. Emerging technologies like Artificial Intelligence(AI), specifically Machine Learning(ML) and Deep Learning(DL) techniques are being advocated and applied vigorously in research and in pragmatics as well. In this work,

- We highlight the recent work in AI and ML which make a huge impact in mitigating attacks.
- We also ponder on the pros and cons that AI/ML based security systems have and
- Whether they are suitable for real-world implementations.

For example, during the recent pandemic, attackers sent malicious messages to users with a keyword ‘COVID-19’, leading to an attack called mobile threat. ML was used to combat Short Messaging Service(SMS) scams by extraction and selection of features, learning the patterns and training the models using a ML use-case called Mobile Threat Defence(MTD)¹ system based upon string information. It includes ML algorithms such as Support Vector Machine(SVM), K-Nearest Neighbour(KNN), Naive Bayes(NB). The challenges AI cyber systems should go through are using large representative datasets during training phase so that models can learn all test cases. Further there is a need for consistent re-training of the models to keep them updated with the latest versions of malware. It is observed that anomaly based techniques where ML algorithms try to match the patterns are more accurate and preferable than signature based techniques. Apparently maintaining the rate of false positives extremely low and detecting the threats timely should be the major goals of the trained cyber systems².

References:

1. K. Shaukat, S. Luo, V. Varadharajan, I. A. Hameed and M. Xu, "A Survey on Machine Learning Techniques for Cyber Security in the Last Decade," in *IEEE Access*, vol. 8, pp. 222310-222354, 2020, doi: 10.1109/ACCESS.2020.3041951.
2. F. Liang, W. G. Hatcher, W. Liao, W. Gao and W. Yu, "Machine Learning for Security and the Internet of Things: The Good, the Bad, and the Ugly," in *IEEE Access*, vol. 7, pp. 158126-158147, 2019, doi: 10.1109/ACCESS.2019.2948912.

CI-01

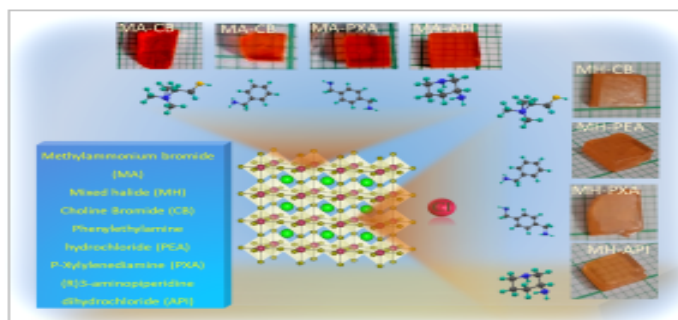
Additive engineering in MAPbBr₃ single crystals for tunable high order harmonics

Sarvani Jowhar Khanam, Murali Banavoth

Solar Cells and Photonics Research Laboratory, School of Chemistry, University of Hyderabad, Hyderabad 500046, Telangana, India

e-address: khanam.sarvani@gmail.com

In recent years, organic-inorganic hybrid halide perovskite single crystals (OIHPSCs) have emerged as a promising material for higher energy radiation detection due to their large stopping power and outstanding charge transport properties leading to a high mobility-lifetime product, tunable bandgap, and low-cost solution-processed method of material preparation. However, deformity and phase segregation in OIHPSCs and mixed halide perovskite materials significantly affect stability and optical properties¹. Additive engineering in 3D perovskite single crystal (PSC) synthesis has proved feasible and costs effective². Using various aliphatic, aromatic, and chiral additives has a pronounced effect on morphology and optical properties. A Series of experiments have been conducted to correlate the structure-property-performance of these single crystals. The outcomes indicated that additives increased the stability of engineered SCs and possessed a significant bluer shift in their harmonics compared to pristine MAPbBr₃ and current research is anticipated to open new avenues in perovskite crystal growth.



--

References:

1. Z. Lian, Q. Yan, T. Gao, J. Ding, Q. Lv, C. Ning, Q. Li and J. L. Sun, Journal of the American Chemical Society, 2016, 138, 9409–9412.
2. Y. Feng, L. Pan, H. Wei, Y. Liu, Z. Ni, J. Zhao, P. N. Rudd, L. R. Cao and J. Huang, Journal of Materials Chemistry C, 2020, 8, 11360–11368.

CI-02**Facile synthesis of Ni-Cr bimetallic oxide grafted with ethylenediamine for sequestration of Malachite Green from aqueous solution**

Md Atif Qaiyum, Dr Soumen Dey
e-address: maqaiyum94@gmail.com

A batch study was conducted to test the potential of detoxifying malachite green dye from waste water by the phenomenon of adsorption of malachite green onto ethylenediamine—mixed metal oxide composite (MMC). The co-precipitation-induced grafting approach was used to create MMC, which was then characterised using FTIR spectroscopy, scanning electron microscopy, BET surface area analysis, and point of zero charge (pHzpc). The adsorption of malachite dye was adjusted by varying key physio-chemical parameters such as contact duration, pH, concentration, and temperature. The procedure is controlled by a pseudo-second-order kinetics ($R^2 = 0.999$) and Freundlich isotherm ($R^2 = 0.996$) model. The maximum adsorption capacity was reported to be 574.21 mg/g. Adsorption of dye onto MMC was discovered to be spontaneous ($\Delta G^\circ = -4.84$ kJ/mol) and endothermic ($\Delta H^\circ = 15.72$ kJ/mol). The adsorbent could be regenerated using methanol/water solution. Under ambient circumstances, MMC was shown to be a superior and more promising adsorbent when compared to similar adsorbents. Thus, an energy-efficient and atom-cost-effective technique for the production of ethylenediamine-fabricated bimetallic oxide with outstanding dye removal capability from water has been developed.

CI-03**Dissolution of soft magnetic FeSiAl alloy cores from spent printed circuit boards and synthesis of α -Fe₂O₃ nanoparticles for methylene blue dye degradation**

Dinesh Patil, M. B. Sridhara, J. Manjanna

Department of Chemistry, Rani Channamma University, Belagavi 591 156, Karnataka, India

e-address: sridhara.mb@gmail.com, Tel.: 99 1658 4954;Correspondence e-address: jmanjanna@rediffmail.com, Tel.: 96 6398 3459

This study aims 3R recovery, reuse and recycle of metals from spent printed circuit boards (PCBs). Here, soft magnetic FeSiAl alloy cores of spent PCBs were used to synthesize α -Fe₂O₃ nanoparticles (NPs) for visible-light-driven degradation of methylene blue (MB) dye. The spent FeSiAl alloy cores were dissolved completely in 100 mM citric acid and 10 mM ascorbic acid mixture at 80°C. The dissolved Fe stabilized as Fe^{II}-citrate or Fe^{III}-citrate and/ or Fe^{II}-ascorbate in the solution. Then, the α -Fe₂O₃ NPs were synthesized from the above Fe dissolved solution using NaOH solution and characterized by powder XRD, TG-DSC, FESEM-EDX, TEM, UV-Vis DRS, and BET isotherm. The synthesized α -Fe₂O₃ NPs were flat spindle shaped and few were oval with particle size between 20 and 30 nm range. Further, the band gap of α -Fe₂O₃ NPs was calculated by Tauc's equation and found to be 1.84 eV and BET specific surface area was about 64.2 m²g⁻¹. Under visible light irradiation, the α -Fe₂O₃ NPs showed high efficiency for the degradation of MB dye in the presence of H₂O₂. To get optimum conditions, various experiments such as α -Fe₂O₃ NPs dosage, volume of H₂O₂, [MB] and nature of light were studied. Thus, it can be proposed that the present study is simple, environmentally benign and highly efficient for the synthesis of α -Fe₂O₃ NPs and subsequent degradation of MB dye.

References:

1. Lee et al., Hydrometallurgy 68 (2003) 5
2. Li et al., J. Hazard. Mater. 176 (2010) 288
3. Nayaka et al., Hydrometallurgy 151 (2015) 73; Nayaka et al.,
4. Waste Manage. 78 (2018) 51;
5. Patil et al., J. Environ. Manage. 256 (2020) 109935
6. Patil et al., J. Haz. Mat. Adv. 4 (2021) 100032.

CI-04

Synthesis, Structural Design and Effect of Substituents on Acylhydrazones: Evaluation of Cytotoxicity, Cytocompatibility and Hemolytic Activity: Structure-Activity Relationship Using DFT and in silico Molecular Docking Studies

Vinodkumar P. Sajjana , Prabhudeyara M. Gurubasavaraaj

Department of Chemistry, Rani Channamma University, Vidyasangama, PBNH-4, Belagavi-591156.

e-address: vinodkumarsjjn@gmail.com

Acylhydrazone compounds have been synthesized effectively by condensation of aldehyde and hydrazide at a 1:1 molar ratio. Compounds 1-3 were characterized by FT-IR, ^1H NMR, ^{13}C NMR, and single-crystal X-ray diffraction. The crystal structure of compound 1 shows a trans configuration around the C=N bond and a monoclinic system with C 2/c. All compounds exhibited good anti-cancer activity against 4 cell lines such as A375 (human malignant melanoma), A549 (human lung adenocarcinoma), HT-29 (human epithelial intestinal) and MDA-MB-232 (human metastatic breast). In addition, the non-toxic action was verified using the cytocompatibility assay on the L929 normal cell line and the hemolysis assay on human red blood cells. Various parameters such as HOMO-LUMO energies, Hirshfeld surface analysis, and Molecular Electrostatic Potential (MEP) surface have been calculated using DFT and compared to experimental values. Compounds 1, 2, and 3 were subjected to molecular docking on the active sites of the protein structures to observe the binding energy. The binding affinity of 1 with the EGFR, HER2 and VEGF from molecular docking was -7.2, -6.3 and -5.1 Kcal/mol, respectively, showing the greatest activity as predicted with AutoDoc.

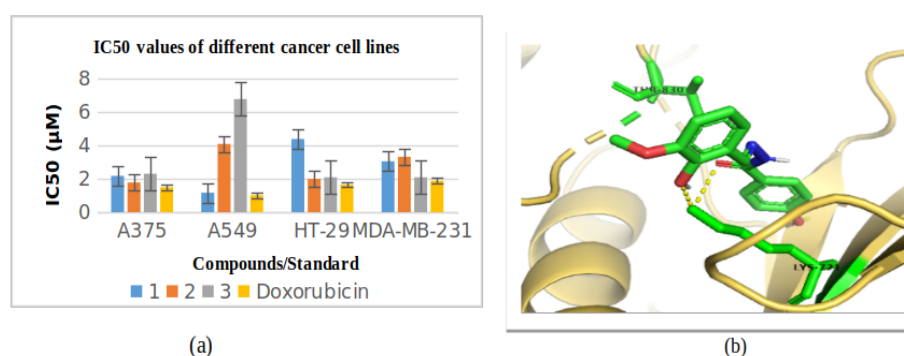


Figure 32: (a) IC₅₀ values of compounds 1-3 against 4 cell lines; (b) 3D docking visualization with VEGF receptor.

Reference:

V. P. Sajjan, L. B. Anigol, P. M. Gurubasavaraaj, D. Kotresha, S. S. Pradhan, S. Venkatesh, D. Patil. Journal of Molecular Structure, 2022, 1265, 133457.

CI-05

Synthesis and electrical properties of Nanocrystalline CuTiO₃ for fuel cell applications

Mubeen H Jakati, Naeemakhtar Momin, J. Manjanna

Dept. of Chemistry, Rani Channamma University, Belagavi 591156, Karnataka, India.

e-address: mubeenjakati3@gmail.com

Perovskites have been explored for their catalytic and electrical properties related to ionic and electronic migration for the development of high efficient energy devices including SOFC¹. The lanthanum gallate (LaGaO₃) materials like La_{1-x}Sr_xGa_{1-y}Mg_yO_{3-δ} (LSGM) have shown high oxide ion conductivity (σ). On doping of transition metal in LSGM is expected to improve σ similar to that of YSZ and doped ceria. The perovskites are considered as alternatives to conventional electrolyte materials of SOFCs².

In this study, the synthesis and electrical properties of CuTiO₃ is reported. It was prepared by using titanium tetraisopropoxide and copper acetate by sol-gel method. The XRD, XPS, FTIR, UV-VIS DRS, FESEM - EDX and EIS techniques were used for its characterization. The ionic transference (t_{ion}) and electronic transference (t_{ele}) numbers have been computed by chronoamperometric technique. The CuTiO₃ showed the high oxide ion conductivity of 2.88×10^{-6} S cm⁻¹, 4.98×10^{-6} S cm⁻¹, 9.57×10^{-6} S cm⁻¹, 1.81×10^{-5} S cm⁻¹, 3.31×10^{-5} S cm⁻¹ at 823 K, 873 K, 923 K, 973 K and 1023 K, respectively with a lower Ea of 0.90 eV, 1.12 eV, and 0.88 eV for grain, grain boundary and total conduction, respectively. The t_{ion} (0.97, 0.88, and 0.85) and t_{ele} (0.03, 0.12, and 0.15) at 873 K, 973 K and 1023 K, respectively. The suppressed Nyquist plots and transport numbers here suggest that the ionic conduction in CuTiO₃. Thus, CuTiO₃ as economically viable single-layer electrolytes for fuel cells has been explored here.

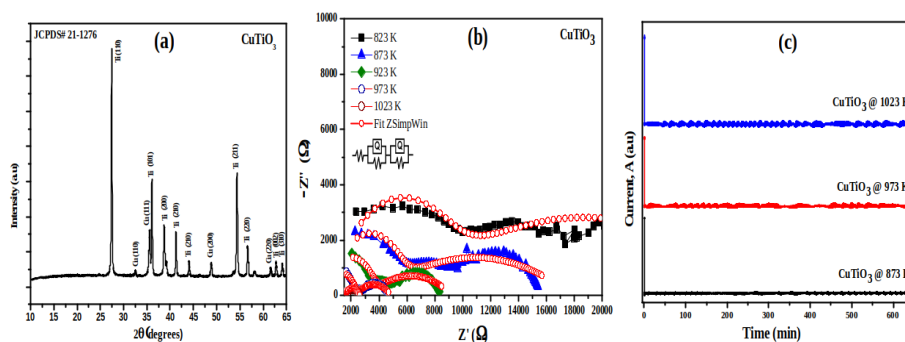


Figure 33: (a) XRD pattern of CuTiO₃ (b) Nyquist Plots of CuTiO₃ (c) Chronoamperometric curves of CuTiO₃

Reference:

1. S. Safari, et al, Journal of Photochemistry and Photobiology A: Chemistry. 394 (2020) 112461.
2. J. Sunarso, et al. Prog. Energy Combust. Sc. 61 (2017) 57.

CO-01

A Unified Radical Sulfonation-Cyclization of 1,6-Enynes with Sodium Sulfinates: A General Access for the Synthesis of Sulfonated Benzofurans and its analogues

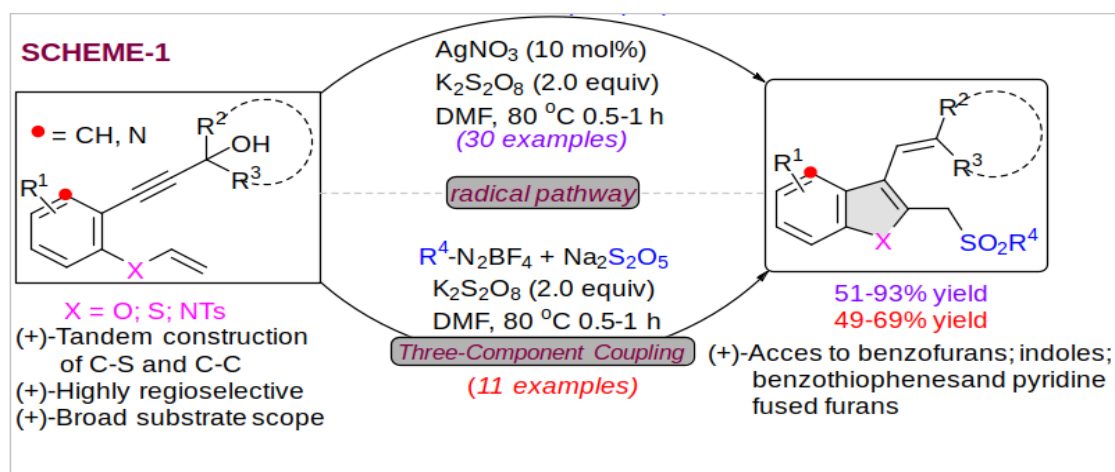
Arram Haritha Kumari, Raju Jannapu Reddy

Department of Chemistry, UCS, Osmania University, Hyderabad 500 007, India.

e-address: harithapamu@gmail.com, rajuchem77@osmania.ac.in

webpages: <https://www.rjreddyresearchgroup.com/>

Among the various benzofuran derivatives, the 2,3-disubstituted benzofurans are widely distributed in numerous natural products¹ and pharmaceutical chemistry.² On the other hand, the sulfone derived organic compounds are extremely useful in organic synthesis³ and especially in medicinal chemistry.⁴ Therefore, incorporation of the sulfone functionality into benzofuran frameworks may nurture their biological properties extensively. In this poster presentation, we will demonstrate a novel and highly efficient Ag-catalyzed sulfonyl radical triggered cyclization of 1,6-enynes with sodium sulfinates in the presence of $K_2S_2O_8$ in DMF at 80°C (Scheme-1)⁵. The method allows the tandem construction of C-S and C-C bonds to access a wide range of sulfonated benzofurans and its corresponding analogs in good to high yields. Moreover, we have successfully developed a three component reaction of 1,6-enynes, aryldiazonium salts and $Na_2S_2O_5$ as a SO_2 surrogate under the influence of $K_2S_2O_8$ to furnish the corresponding 2,3-disubstituted benzofuran derivatives.



Acknowledgments:

We thank SERB-CRG [CRG/2021/003544] and WOSA [SR/WOS-A/CS-14/2019], New Delhi for financial assistance.

References:

- Keay, B. A.; Dibble, P. W. Furans and their Benzo Derivatives: Applications, In Comprehensive Heterocyclic Chemistry II, Vol. 2; Katritzky, A. R.; Rees, C. W.; Scriven, E. F. V., Eds.; Pergamon: Oxford, 1996, 395. b) Goel, A.; Kumar, A.; Raghuvanshi, A. Chem. Rev. 2013, 113, 1614.
- Nevagi, R. J.; Dighe, S. N.; Dighe, S. N. Eur. J. Med. Chem. 2015, 97, 561 and references herein.
- P. F. Schnellhammer, Expert Opin. Pharmacother. 2002, 3, 1313-1328
- R. J. Reddy, A. H. Kumari, RSC Adv. 2021, 11, 9130-9221; b) R. J. Reddy, A. H. Kumari, J. J. Kumar, Org. Biomol. Chem. 2021, 19, 3087-3118.
- R. J. Reddy, A. H. Kumari, G. R. Krishna, To be Communicated.

CO-02

Design, Synthesis, Optimization and In-vivo Validation of New Imidazopyridine Scaffold as Dual hTLR7 and hTLR9 Antagonists

Nirmal Das^{a,c}, Purbita Bandopadhyay^{b,c}, Swarnali Roy^a, Bishnu Prasad Sinha^{b,c}, Uddipta Ghosh Dastidar^{a,c}, Oindrila Rahaman^b, Sourav Pal^{a,c}, Dipyaman Ganguly^{b,c}, Arindam Talukdar^{a,c}

^aDepartment of Organic and Medicinal Chemistry, CSIR-IICB, 4, Raja S.C. Mullick Road, Jadavpur, Kolkata - 32, India

^bDepartment of Cancer Biology and Inflammatory Disorder; CSIR-IICB, 4, Raja S.C. Mullick Road, Jadavpur, Kolkata -32, India

^c Academy of Scientific and Innovative Research, Ghaziabad-201002, India

e-address: nirmaldas549@gmail.com

Aberrant expression of endosomal toll-like receptors (TLRs) TLR7 and TLR9 which are the sub-family of Pattern Recognition Receptor (PRRs), present in distinct immune cells in response to body's own ligands which are coming from dead cell are involved in several autoimmune diseases. Thus, these TLR7 and TLR9 became a widely accepted therapeutic targets. In this study we were focused on development of a new chemotype, i.e., imidazo-pyridine core (is a 'drug prejudice'¹ scaffold) in the field of antagonist designing targeting hTLR7/9². Extensive structure activity relationship (SAR) studies over the imidazopyridine core give us the key information of minimal pharmacophoric features to get antagonism against hTLR7/9. The importance of C2, C3, and C7 position in imidazopyridine core and proper installation of a specific group at these positions were illustrated in this study through SAR. We identified 42 as the lead which showed very good selectivity profile against hTLR8 with an IC₅₀ values 8.32 μ M. Isothermal titration calorimetric (ITC) experiment excluded the direct agonist binding for the observed antagonistic activity with the ligands CL264 and CpGb which are the ligands of TLR7 and TLR9, respectively. In vitro pharmacokinetic (PK) studies and in vivo pharmacodynamic (PD) study in mice depict the lead 42 is ideal for oral absorption and efficacious having IC₅₀ values of 0.04 μ M and 0.47 μ M against TLR9 and TLR7, respectively. Imidazopyridines core is established as very promising chemotypes to explore potential therapeutic candidates in relevant clinical contexts.

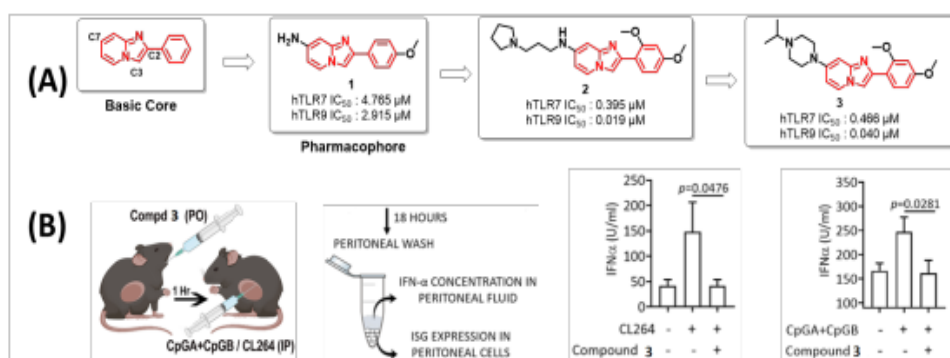


Figure 34: (A) Our designed new class of potent hTLR7 and hTLR9 antagonist. (B) In-Vivo efficacy study of the lead compound 3 against both TLR7 and TLR9.²

The goal of the study was to develop a new scaffold, i.e., imidazo-pyridine as potent hTLR7/9 antagonist with a very good PK and PD data. As the endosomal pH is acidic and hTLR3/7/8/9 are endosomal TLRs, in the design of molecule we strategically incorporated weakly basic amine group in the molecule. The SAR showed the aromatic group at C-2 position have a very crucial role to get optimum potency. C-3 position is very sensitive as on addition of heterocyclic aliphatic chain at this position compounds antagonistic activity improve significantly but the PK profile of these compounds became poor. At C-7 position the basicity of the piperazine ring is playing a crucial role for hTLR7/9 antagonism as the antagonism diminished as soon as the donatable lone pair is unavailable on the

piperazine ring. Thus, our newly designed imidazo-pyridine derivatives being very potent as well as stable in human and mice plasma, moderate Caco-2 permeable, along with stable in human and mice liver microsome, could open a new horizon for the development a new drug for autoimmune disorder based on imidazo-pyridine chemotype.

References:

1. Current Topics in Medicinal Chemistry. 2017; 17(2).
2. Journal of Medicinal Chemistry. 2022; Article ASAP. <https://doi.org/10.1021/acs.jmedchem.2c00386>

CO-03

Target Based Design Synthesis and Development of Small Molecules for Treatment of Non-Alcoholic Fatty Liver Disease (NAFLD)

Sunny Goon ^{a,c}, Dipayan Sarkar ^a, Saheli Chowdhuri ^b, Abhishek Sen ^b, Uddipta Ghosh Dastidar

^a, Mohabul Alam Mondal ^c, Partha Chakrabarty ^b, Arindam Talukdara ^a

^aDepartment of Organic and Medicinal Chemistry, CSIR-IICB, 4, Raja S.C. Mullick Road, Jadavpur, Kolkata - 700032, India

^b Cell Biology & Physiology Division, CSIR-IICB, 4, Raja S.C. Mullick Road, Jadavpur, Kolkata - 700032, India

^c The Department of Chemistry, Jadavpur University, Kolkata, West Bengal, 700032, India

e-address: sunny.chem416@gmail.com

The term “nonalcoholic fatty liver disease” (NAFLD) refers to a variety of liver disorders that can afflict persons who use little to no alcohol. Some individuals with NAFLD can develop non-alcoholic steatohepatitis (NASH), an aggressive form of fatty liver disease, which is characterized by liver inflammation and may progress to advanced scarring (cirrhosis) and liver failure (Hepatocellular carcinoma). These hepatocellular damages are mostly similar to the impairment caused by heavy alcohol consumption. NAFLD results from excessive accumulation and deposition of Triacylglycerol (TAG) in hepatocytes and therefore deregulation of enzymes responsible for controlling intracellular lipid turnover and homeostasis may play an important role in NAFLD¹. Adipose triglyceride lipase (ATGL) also known as patatin-like phospholipase domain-containing protein 2 (PNPLA2) is one such vital enzyme associated with the intracellular degradation of TAG. Constitutive photomorphogenic 1 (COP1) is an E3 ubiquitin ligase that regulates phototropism in plants and target transcription factors for degradation in mammals. Also it serves as a crucial regulator in mammalian embryonic development, cellular processes and the DNA damage response. Recent study suggested that, COP1 recognize and bind with ATGL via ‘V-P’ motif and degrade it via Ubiquitin Proteasomal System². Thus, targeting COP1 and modulating its activity can help us to increase the proportion of ATGL in hepatic cells which in turn may lower the TAG content in liver.

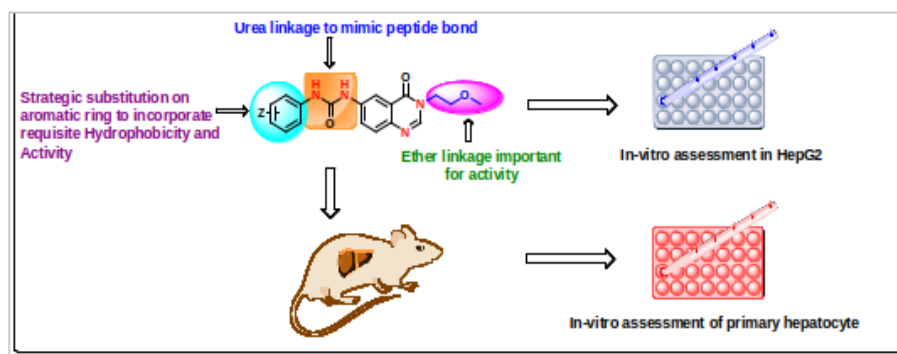


Figure 35: Prototype of Design and Validation of new class of Quinazolinone scaffold

In our recent research work we are aiming to develop some new chemical entities which behave as COP1 modulators and thereby can lower proteasomal degradation of ATGL. Our designed pharmacophore is based on quinazolinone core with urea linkage to mimic ‘V-P’ motif of ATGL. The step-by-step SAR modification helped us to understand the role of different substitutions across the quinazolinone core to get better interaction with COP1. The promising biological results have showed us that our newly designed quinazolinone derivatives can improve activities of ATGL by modulating COP1 enzyme and can be used as a new therapeutic avenue for the treatment of NAFLD³.

References:

1. J. C. Cohen, J. D. Horton, H. H. Hobbs, *Science*, 2011, 332(6037), 1519-23
2. M. Ghosh, S. Niyogi, M. Bhattacharyya, M. Adak, D. K. Nayak, S. Chakrabarti, P. Chakrabarti,

Diabetes, 2016, 65, 3561–3572

3. Quinazolinones derivatives for treatment of non-alcoholic fatty liver disease, preparation and use thereof WO2022003712 (A1).

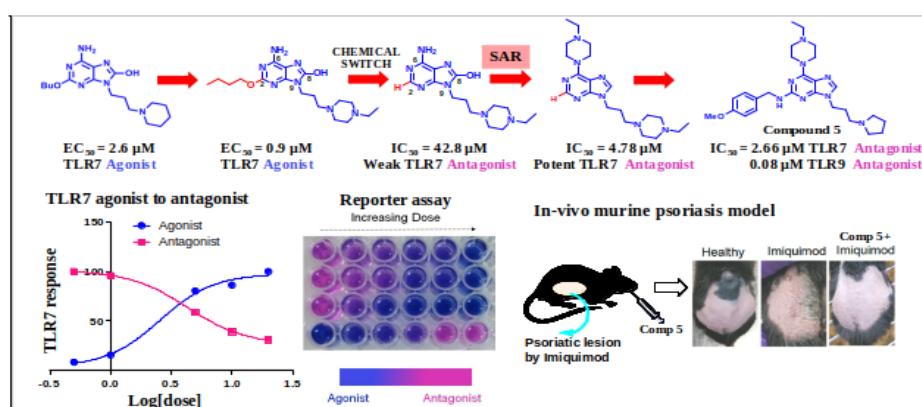
CO-04

A “chemical switch” to convert a TLR7 agonist into an antagonist and structural optimization leading to dual TLR7/9 antagonist relevant to psoriasis model

Dipika Sarkar, Deblina Raychaudhuri, Ayan Mukherjee, Biswajit Kundu, Bishnu Prasad Sinha, Dipyaman Ganguly, Arindam Talukdar
 Indian Institute of Chemical Biology, Jadavpur, Kolkata- 700032, India
 e-address: dipikasarkar.0123@gmail.com

Toll-like receptors (TLRs), mostly expressed on antigen-presenting cells such as dendritic cells, are a class of pathogen-encoded pattern recognition proteins, which provide the first line of defense against the invasion of pathogenic microorganisms by regulating innate immune system of the host. Endosomal TLRs (pH = 4.5 – 6.5) play vital roles as “double edged sword” in identifying nucleic acid derived from the pathogens as well as the extracellular nucleic acid of the host. When self-originated DNA and RNA molecules get access to endosome, they abruptly trigger TLR7/8/9 and kick off critical innate immune events which lead to the development of autoimmune disorders. Hence, suppressing the stimulation of TLR7/9 with appropriate antagonists could serve as novel pathogenic node in these disease contexts.

During the designing of suitable TLR7 antagonists, a known purine TLR7 agonist was chosen as prototype and eventually with nominal structural modification at C2 position, we came across a singular “chemical switch” which can convert a potent agonist into a novel antagonist. Incorporation of a basic center at C6 position further increased the potency of the antagonist and we wound up with a clinically relevant TLR7 antagonist [$IC_{50}(\text{TLR7}) = 4.7 \mu\text{M}$] having good selectivity over TLR8 and encouraging pharmacokinetics with 70.8% oral bioavailability in mice¹. Further literature analysis suggested that, the dual TLR7/9 antagonists could be more appropriate clinically. Therefore, we expanded our strategy to design dual TLR7/9 antagonists through SAR development and modulated the chemical features at C2, C6 and N9 position in the purine scaffold which furnish a robust dual TLR7/9 antagonist with tremendous ADME profile and promising in vivo pharmacokinetics². The therapeutic potential of the selected lead compound 5 [$IC_{50}(\text{TLR9}) = 0.08 \mu\text{M}$ and $IC_{50}(\text{TLR7}) = 2.16 \mu\text{M}$] in a preclinical murine model of psoriasis advocate 5 as a compelling descendant for future development into a clinically significant therapeutic molecule.



References:

1. J. Med. Chem. 2020, 63, 4776-4789
2. J. Med. Chem. 2021, 64, 9279-9301

CO-05

Development of a chemical biology tool enabling reversible optical control of protein labeling: A promising new direction in photopharmacology

Himadri Sekhar Sarkar,^{a,d} Takato Mashita,^b Toshiyuki Kowada,^{a,b,c} Satoshi Hamaguchi,^c
Toshitaka Matsui,^{a,b,c} Shin Mizukami^{a,b,c}

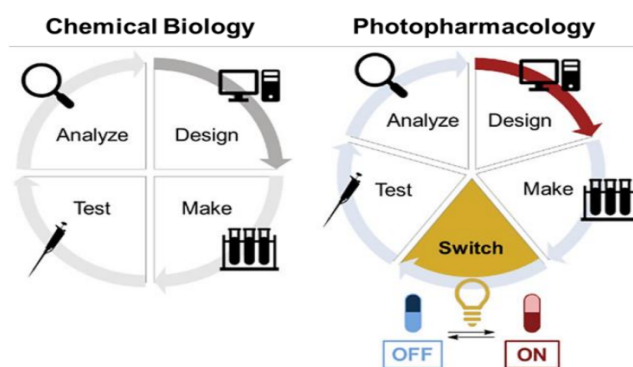
^aInstitute of Multidisciplinary Research for Advanced Materials, Tohoku University, 2-1-1, Katahira, Aoba-ku, Sendai, Miyagi 980-8577, Japan,

^b Department of Chemistry, Graduate School of Science, Tohoku University, Miyagi 980-8578, Japan,

^cDepartment of Molecular and Chemical Life Sciences, Graduate School of Life Sciences, Tohoku University, 2-1-1, Katahira, Aoba-ku, Sendai, Miyagi 980-8577, Japan,

^dPresent affiliation: CSIR-Indian Institute of Chemical Biology, Kolkata-700032, India
e-address: himadrisarkar@csiricb.res.in

Proteins account for the most important molecules in living organism by functioning through interaction with numerous biomolecules. Thus, understanding the structure, distribution, trafficking and functions of protein of interests (POIs) in living cells is one of the fundamental goals of chemical biology research. Protein labeling systems that specifically label a tag-fused POI with a functional small-molecule have been proven to be versatile methods for elucidating protein functions in living cells. However, it is difficult to apply them to repetitive control of the protein functions because of their irreversibility. As the emerging technology, photopharmacology provides a uniquely powerful means to enable the optical control of biological processes in living cells with high spatiotemporal resolution¹. To overcome the limitation of irreversibility, a new chemical biology tool, incorporating the primary concept of photopharmacology, for reversible optical control of protein labeling is of utmost importance. Aiming to develop the desired photoswitchable protein labeling system, we have developed novel ligands that can reversibly bound to a selective protein on the basis of photochromism.



Escherichia coli dihydrofolate reductase (eDHFR), a key enzyme in the folate metabolism, has been established as a promising tag protein. Recently, we have reported a photoswitchable ligand, azoMTX, that can efficiently bind with eDHFR and can switch its enzyme activity.² However, azoMTX also binds to human DHFR (hDHFR) and inhibits the activity.³ This property would hinder the application of azoMTX as a chemical tool in human cells. Therefore, a new set of photoreversible molecules capable of selective binding to eDHFR, will be presented in this conference. The newly synthesized compounds reversibly isomerize upon UV light (394 nm) and green light (560 nm) irradiation and offer high thermal stability of the active Z-isomers. The new compounds also show reversible optical control of eDHFR enzyme activity inhibition, while almost no activity change in case of hDHFR⁴. One of the compounds in its active Z-isomeric form exhibits more than 21 times higher affinity to eDHFR than hDHFR, indicating the selectivity of binding to eDHFR. Thus, our newly developed eDHFR-selective photoswitchable inhibitors will be useful as a next-generation chemical biology tool in developing photoreversible protein labeling systems.

References:

1. P. Kobauri et al. *J. Med. Chem.* 2022, 65, 4798–4817.
2. T. Mashita et al. *ChemBioChem* 2019, 20, 1382–1386.
3. C. Matera et al. *J. Am. Chem. Soc.* 2018, 140, 15764–15773.
4. H. S. Sarkar et al. submitted.

CO-06

Design, synthesis, and antimicrobial evaluation of novel 10-undecenoic acid based lipidic triazoles against plant pathogens

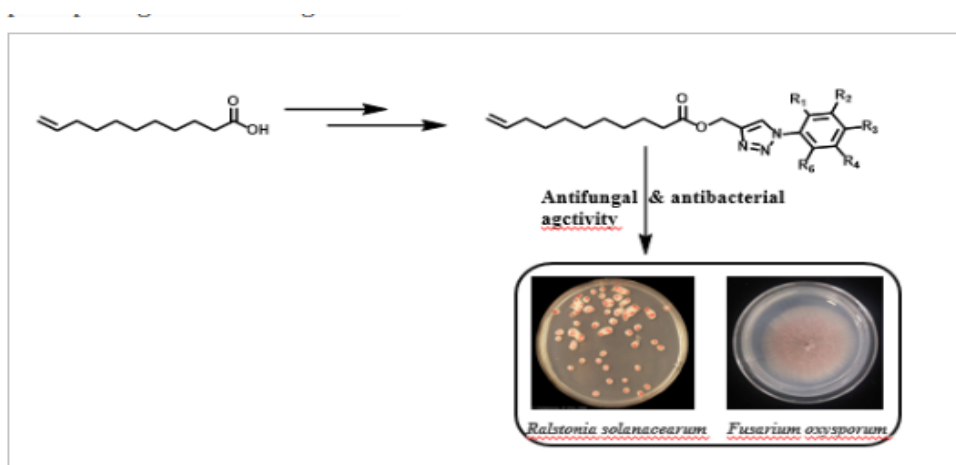
Gandhi B,^a Greeshma K,^b Durga Prasad Ruvulapalli,^b Shiva ShankerKaki^a

^a Centre for Lipid Science & Technology, CSIR-Indian Institute of Chemical Technology.

^b Crop Protection Section, ICAR-Indian Institute of Oilseeds Research, Hyderabad.

e-address: gandhi.indra13@gmail.com.

10-Undecenoic acid (UA) a pyrolysis by-product of castor oil is a well-known nonspecific topical antifungal agent which is aimed at treating superficial infections. Of all the available saturated and unsaturated fatty acids, UA was reported to be the most potent antifungal compound with a double bond at 10th position which plays a key role in its activity. Different UA-based products were reported to show antiviral and antibiotic activities as well as UA is a key component in the synthesis of many insecticides, mosquito repellents, and plant growth regulators. Desenex is a commercially available UA-based ointment the key benefit of this UA-based ointment is its potent antifungal activity coupled with a non-irritating impact. Another class of compounds with potential chemotherapeutic, antiviral, and fungicidal properties are heterocyclic compounds which have inspired a fervent interest in them. Among heterocyclics, triazoles are a crucial component of all cells and living matter, making them one of the most important heterocyclic substances with outstanding pharmacological action. Due to their diverse biological, agrochemical, and chemical properties, more than 0.2 million triazole derivatives were reported in the literature. In the present work, we report a series of novel 10-Undecenoic acid-based triazole derivatives using click reaction. The synthesized lipidic triazole compounds were studied for the antibacterial and antifungal activities against *Ralstonia solanacearum* and *Fusarium oxysporum*, respectively. Among all the compounds, it was found that compounds with iodo substituent and tert-butyl substituent displayed the highest antibacterial and antifungal activity respectively. The results of the present study suggest that the synthesized novel lipidic triazole derivatives of 10-Undecenoic acid could be potential antimicrobial compounds. The present work is the first report on the design, synthesis, and antimicrobial assessment of 10-Undecenoic acid-based triazole against plant pathogenic microorganisms.



CO-07

Design, synthesis, and antimicrobial evaluation of novel 10-undecenoic acid based lipidic triazoles against plant pathogens

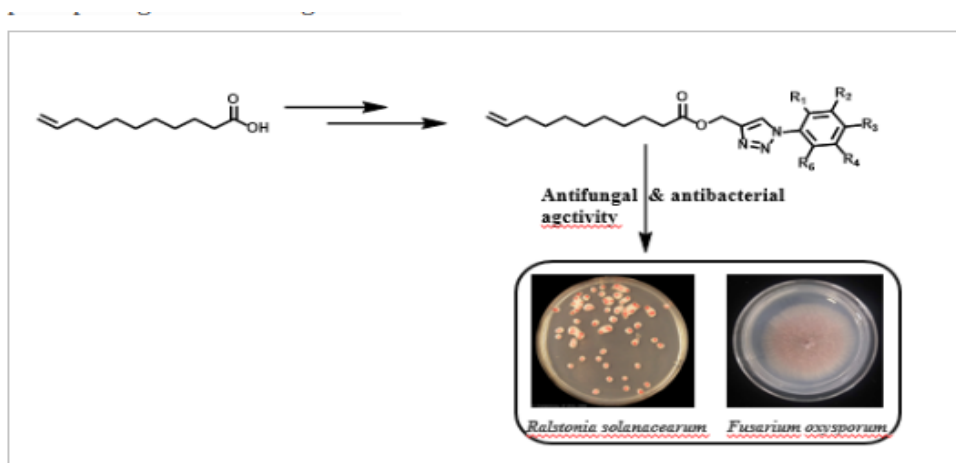
Gandhi B,^a Greeshma K,^b Durga Prasad Ruvulapalli,^b Shiva ShankerKaki^a

^a Centre for Lipid Science & Technology, CSIR-Indian Institute of Chemical Technology.

^b Crop Protection Section, ICAR-Indian Institute of Oilseeds Research, Hyderabad.

e-address: gandhi.indra13@gmail.com.

11-Undecenoic acid (UA) a pyrolysis by-product of castor oil is a well-known nonspecific topical antifungal agent which is aimed at treating superficial infections. Of all the available saturated and unsaturated fatty acids, UA was reported to be the most potent antifungal compound with a double bond at 10th position which plays a key role in its activity. Different UA-based products were reported to show antiviral and antibiotic activities as well as UA is a key component in the synthesis of many insecticides, mosquito repellents, and plant growth regulators. Desenex is a commercially available UA-based ointment the key benefit of this UA-based ointment is its potent antifungal activity coupled with a non-irritating impact. Another class of compounds with potential chemotherapeutic, antiviral, and fungicidal properties are heterocyclic compounds which have inspired a fervent interest in them. Among heterocyclics, triazoles are a crucial component of all cells and living matter, making them one of the most important heterocyclic substances with outstanding pharmacological action. Due to their diverse biological, agrochemical, and chemical properties, more than 0.2 million triazole derivatives were reported in the literature. In the present work, we report a series of novel 10-Undecenoic acid-based triazole derivatives using click reaction. The synthesized lipidic triazole compounds were studied for the antibacterial and antifungal activities against *Ralstonia solanacearum* and *Fusarium oxysporum*, respectively. Among all the compounds, it was found that compounds with iodo substituent and tert-butyl substituent displayed the highest antibacterial and antifungal activity respectively. The results of the present study suggest that the synthesized novel lipidic triazole derivatives of 10-Undecenoic acid could be potential antimicrobial compounds. The present work is the first report on the design, synthesis, and antimicrobial assessment of 10-Undecenoic acid-based triazole against plant pathogenic microorganisms.



CO-08**Synthesis of Novel Indolizine Derivatives with Biological Activity**

Tairabi Khanadal, Pramod N Patil, Basavaraj Padmashali
Rani Channamma University, Department of Chemistry, Belagavi-591156, India.
e-address: basavarajpadmashali@yahoo.com

¹In pharmacology field synthesis of new Indolizine derivatives plays vital role which is Eco friendly in nature. All newly consolidated ²Indolizine derivatives are spectroscopically authenticated which were relayed by FTIR, H¹NMR and C¹³NMR. ²Heterocyclic substituted compounds are preeminent and adequately scrutinized classes of organic substituted molecules ³Heteroaromatic structures formed due to superseded of one carbon with another different atom.^{4,5}Indolizine is a heterocyclic N-bridged aromatized compound. A tremendous kind of synthesis of Substituted indolizine derivatives played a very dominant role in pursuits of biological which have a wide verity of applications in medicinal, pharmaceutical, the ability to inhibit⁵ anti-inflammatory⁶ actively and glowingly investigated as indolizine substituted derivatives which also acting as regulation of ion channel^{7,8}. The derivatives of Indolizine substituents play a vital role in the fields of antibacterial,⁹ antiviral and anti-inflammatory.

Keywords:

2-aminopyridine, Indolizine, Phenacyl bromide, antibacterial.

References:

1. Microwave induced synthesis, and pharmacological properties of novel 1- benzoyl-4-bromopyrrolo[1,2-a] quinoline-3-carboxylate analogues
2. Mechanism of cycloaddition to indolizines
3. DABCO catalysed highly regioselective synthesis of fused imidazo-heterocycles in aqueous medium
4. Highly Efficient Synthesis of Functionalized Indolizines and Indolizinones by Copper-Catalyzed Cycloisomerizations of Propargylic Pyridines
5. Copper(II)-Catalyzed Indolizines Formation Followed by Dehydrogenative Functionalization Cascade to Synthesize 1-Bromoindolizines
6. One-Pot Synthesis of 2-Phenylimidazo[1,2- α]pyridines from Acetophenone, [Bmim]Br₃ and 2-Aminopyridine under Solvent-Free Conditions
7. Microwave-Assisted Convenient Syntheses of 2-Indolizine Derivatives from Morita-Baylis-Hillman Adducts: New in silico Potential Ion Channel Modulators
8. Crystal, molecular and electron structure of (2R,3R,4aS,5S,7R,10aS,10bS)-5-ethyl-2,3-dimethoxy-2,3,7-trimethyl-decahydro-2H- [1,4]dioxino[2,3-g]indolizin-7-ium iodide hydrate.
9. Synthesis, antibacterial, and antioxidant studies of 7-amino-3-(4-fluorobenzoyl)indolizine-1-carboxylate derivatives.

CO-09

Efficient Synthesis of Functionalized pyrrolo[1,2-a]quinolines and their biological profile

Pramod N Patil, Tairabi Khanadal, Basavaraj Padmashali
Rani Channamma University, Department of Chemistry, Belagavi-591156, India.
e-address: basavarajpadmashali@yahoo.com

Pyrrolo[1,2-a]quinoline is one of the five isomers of indole and it serves as a precursor for widespread pyrroloquinoline. A pyrroloquinoline skeleton is found to be plenty and highly in bioactive natural alkaloids¹. The easiness of accessibility of the starting materials and the generality of the reaction sequences make it a highly attractive strategy to synthesize a wide range of pyrrolo[1,2-a]quinoline derivatives²⁻⁴. 6-Bromoquinoline was reacted with donor-acceptor(D-A) substituted phenacyl bromide to form quinolinium salts, which were then treated with electron-deficient alkynyl such as dimethyl acetylene dicarboxylate [DMAD] which is used as dipolarophile in presence of a base undergo [1+3] cycloaddition reaction to form novel pyrrolo[1,2-a]quinoline derivatives to form good yield. The selected compounds have been screened for biological potency and spectral analyser⁵.

Keywords:

Pyrroloquinoline; alkaloids; bioactive; quinolinium.

References:

- 1.N. Asano, R. J. Nash, R. J. Molyneux, G. W. Fleet, *Tetrahedron: Asymmetry* 2000, 11, 1645.
- 2.D. L. Comins, S. Huang, C. L. McArdle, C. L. Ingalls, *Org. Lett.* 2001, 3, 469.
3. D. L. Comins, Y. M. Zhang, *J. Am. Chem. Soc.* 1996, 118, 12248.
- 4.D. Srirani, P. Yogeewari, R. Thirumurugan, T. R. Bal, *Nat. Prod. Res.* 2005, 19, 393.
- 5.Synthesis of Some New Indolizine and Pyrrolo[1,2-a]quinoline Derivatives via Nitrogen Ylides *Z. Naturforsch.* 2009, 64b, 434 – 438

CO-10

Biodegradable-Biocompatible Renewable Amino Acid Derived Polyhydroxyurethanes

Bantumelli Prasannatha,^a Billa Narasimha Rao,^a Chiranjeevi Padala,^b Bramanandam Manavathi,^b Tushar Jana^a

^aSchool of Chemistry,

^bMolecular and Cellular Oncology Laboratory, Department of Biochemistry, School of Life Sciences, University of Hyderabad, Hyderabad, India.

e-address: manuprasannatha@gmail.com

The versatile nature of the polyurethanes, made a hallmark in the various fields viz., automobiles, textiles, military, medical devices, agriculture etc¹. But the usage of phosgene and diisocyanates in the synthesis of polyurethanes shows a negative impact on the environment. Polyhydroxyurethanes (PHUs)² synthesized by the polyaddition of bicyclic carbonates like sebacic acid and diglycerol based bicyclic carbonates with diamines are found to be one of the best approach to address these issues. The diamines used are prepared by the renewable amino acids in order to reduce toxicity of the degraded products. These PHUs show remarkable biodegradable and cell viability in comparison with commercial diamine based PHUs. The PHUs and its degradable products have shown excellent cell viability studies in HEK cells, studied in nanogram to milligram concentration range. Due to the presence of hydrophobic and hydrophilic components in these PHUs shows excellent nanofiber like self-assembly in THF:Water (1:1) mixture was observed. The drug loading and releasing studies were done by CLSM imaging and spectroscopic studies.

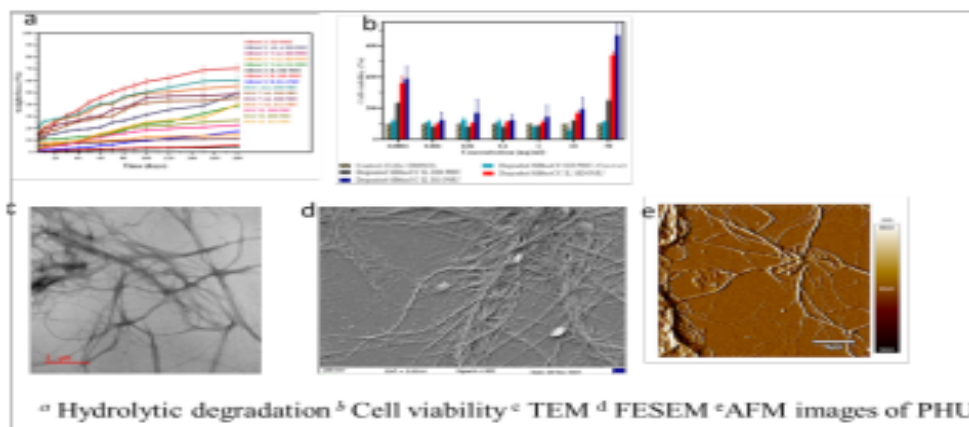
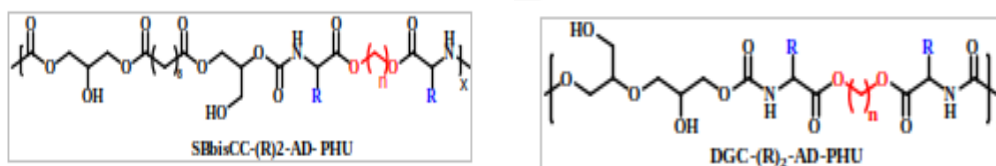


Figure 36: Amino acid based PHU



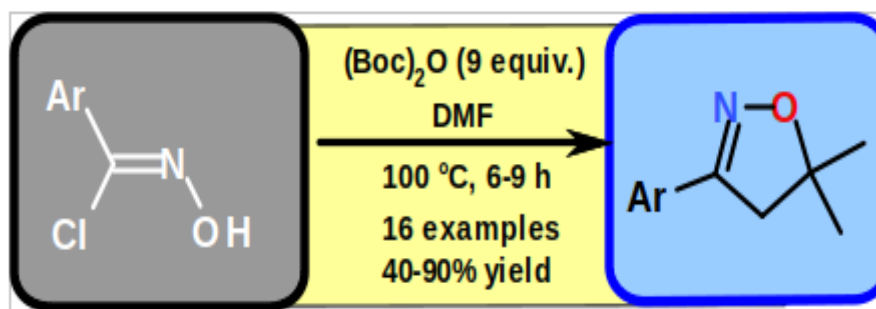
References:

1. D.K. Chattopadhyay, K.V.S.N. Raju Prog. Polym. Sci. 2007, 32, 352–418
2. Maisonneuve, L.; Lamarzelle, O.; Rix, E.; Grau, E.; Cramail, H. Chem. Rev, 2015, 115, 12407-12439.

CO-11

Additive-Free Efficient and Regioselective Construction of Functionalised Isoxazolines from Chloro-Oxime and Boc-AnhydrideRaghuramaiah Mandadapu,^{a,b} Mangala Phadte^b^aSyngenta Biosciences Pvt. Ltd., Santa Monica Works, Corlim, Ilhas, Goa, India-403110^bDepartment of Chemistry, Mangalore University, Mangalagangothri, India-576119e-address: mangala.phadte@syngenta.com

Isoxazoline derivatives are a significant family of five-membered heterocyclic compounds that are present in a variety of biologically active compounds as well as a wide range of natural products^{1,2}. There are only a few synthetic methods known for the synthesis of 5,5-dimethyl isoxazolines (Scheme-1). However, those methods suffer from several limitations such as low yields, need for costly catalysts and oxidising agents or bases.^{3,4} Therefore, development of simple and high yielding Methodology for the synthesis of isoxazolines are highly desirable. Herein, we report an additive/base-free synthesis of 5,5-dimethyl isoxazolines using boc-anhydride and chloro-oxime. This Methodology provides an access to functionalized isoxazolines in moderate to high yields.

**References:**

1. Encarnacion, R. D.; Sandoval, E.; Mamstrom, J.; Christophersen, C. J. *Nat. Prod.* 2000, 63, 874-875.
2. Makoto Fujinami.; Yuki Takahashi.; Yoshitaka Tanetani.; Minoru Ito.; Mina Nasu. *J. Pestic. Sci.* 2019, 44, 282-289.
3. X. Zhu, Y.-F. Wang, W. Ren, F.-L. Zhang, S. hiba. *Org.Lett.* 2013,15, 3214.
4. Di Shi.; Hai-Tao Qin.,Chen Zhu.; Fng Liu. *Eur. J. Org. Chem.* 2015, 5084-5088.

CO-12

Hydrogen Bond Assisted Reactivity of Ylideneketonitriles with 1° Amines: A Chemo Selective Synthesis of 2-Pyridone and 2-Aminopyridine Derivatives.

Damodar Karuturi,^{a,b} Mahesh Kalbagh,^{a,b} Prashantha Kamath,^a Venunath Hapse,^a Alok Kumar Pandey,^a Mukul Lala^b

^aSyngenta Biosciences Pvt. Ltd. Santa Monica Works, Corlim, Ilhas, Goa, 403110, India.

^bDept. of Chemistry, Mangalore University, Mangalagangothri, 574199, Karnataka, India. e-address: mukul.lal@syngenta.com

Ylideneketonitrile 2e with chlorodifluoromethyl demonstrated a strong solvent dependence chemoselective reaction with primary amines to form either 1-N-alkylated-3,5-disubstituted-2-pyridones or 2-N-alkylated-3,5-trisubstituted pyridines in decent to good yields (26-91%). The mechanistic aspects of the reaction were investigated by ReactIR and the reactivity switch from apolar-aprotic and polar-protic-nucleophilic solvents to polar-protic-non-nucleophilic solvents could be explained by interplay of hydrogen bonding and nucleophilicity of solvents.

The chemo selectivity further demonstrates the synthetic utility of the Methodology i.e. “diversity on demand” allowing access to various pyridine or pyridone derivatives from push-pull system.

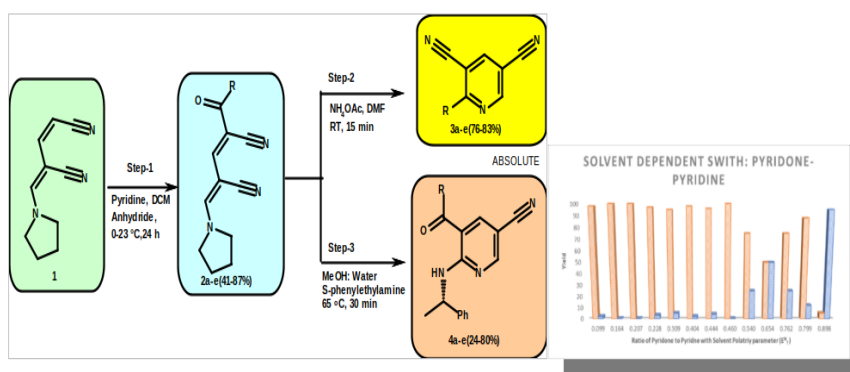


Figure 37: Solvent dependence Chemo selective reaction of push pull system (2e) with primary amines.

CO-13

Reagent-Based Diversity-Oriented Synthesis Approach to Fused 1,4-Dihydropyrimidines, Dihydroisoxazolines, 2,3-Dihydrofurans, Substituted 4H-pyran and Cyclohexane-1,3-diones from 2-(2,2,2-trifluoro-1-aryl-ethylidene)cyclohexane-1,3-diones as Scaffold

Mahesh R Kalbagh,^a Meguovilie Sachu,^{a,b} Damodar Karuturi,^{a,b} Prashantha Kamath,^a Mark Montgomery,^c Mukul Lal^{a,b}

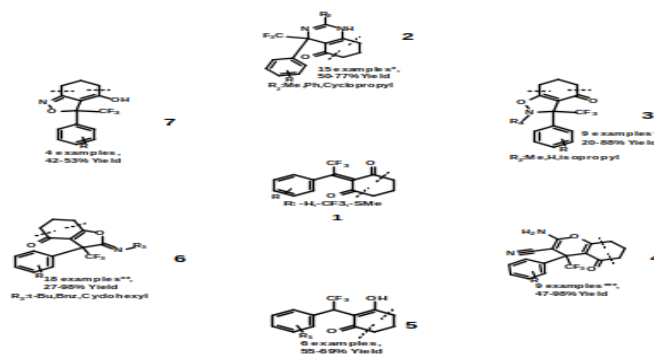
^a Syngenta Biosciences Pvt. Ltd. Santa Monica Works, Corlim, Ilhas, Goa, 403110, India.

^b Dept. of Chemistry, Mangalore University, Mangalagangothri, 574199, Karnataka, India.

^c Syngenta Jealott's Hill International Research Centre, Bracknell, Berkshire RG42 6EY, UK.

e-address: mahesh.kalbagh@syngenta.com

The present work outlines the reagent-based diversity-oriented synthetic strategy to access fused heterocycles from 1,3-cyclohexadienenones. Recently, we had reported the synthesis of a variety of ene-diones from cyclohexadiones with a variety of trifluoromethyl ketones, these ene-diones were utilized in the current work for preparing variety of fused heterocycles. The ene-diones when treated with aminoimidines, hydroxylamine, isocyanides and malononitrile gave corresponding 1,4-dihydropyrimidines (2), regio selective dihydroisoxazolines (3,7), 2,3-dihydrofurans (6) and 4h-pyrans (4) with quaternary trifluoromethyl group. 61 Novel CF₃ containing fused heterocyclics were synthe-



sized by varying the reagents. Structures were confirmed by ¹H, ¹³C, ¹⁹F NMR, HR-MS & X-Ray crystallography. All the compounds were tested for their potential as lead molecules in agro-chemistry.

References:

1. Fujiwara T., O'Hagan D., J. of Flu. Chem., 2014, 167, 16
2. Vijay V. D., Faisal Y. A., J. Serb. Chem. Soc., 2009, 74(11), 1219
3. Mahesh R. K., Damodar K., Shashidhara K., Mark M., Prashantha K., Mukul L., Syn. Comm., 2020, 50, 3062.

CO-14

Dual Metallation in a Two-Dimensional Covalent Organic Framework for Photocatalytic C–N Cross-Coupling Reactions

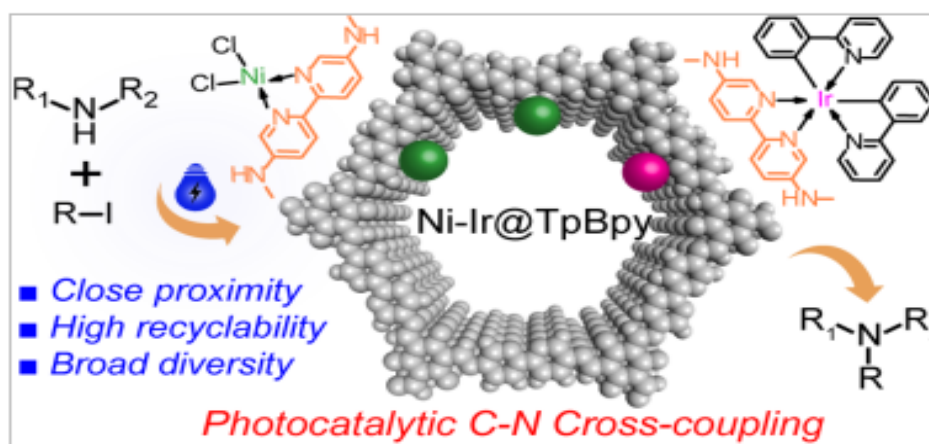
Ayan Jati,^a Kaushik Dey,^{a,b} Maryam Nurhuda,^c Matthew A. Addicoat,^c Rahul Banerjee,^{a,b} Biplab Maji^a

^a Department of Chemical Sciences, Indian Institute of Science Education and Research Kolkata, Mohanpur 741246, India.

^b Centre for Advanced Functional Materials, Indian Institute of Science Education and Research Kolkata, Mohanpur 741246, India.

^c School of Science and Technology, Nottingham Trent University, Clifton Lane, NG11 8NS Nottingham, United Kingdom
e-address: aj19rs@35@iiserkol.ac.in

Covalent organic frameworks (COFs) are a promising toolbox in the field of heterogeneous catalysis¹. Herein, we report a dual metallation (iridium and nickel) strategy in a single 2D-COF TpBpy to perform a variety of C–N cross-coupling reactions². Moving from the traditional approach³, we focus on the COF-backbone as a host for metal-catalyzed photosensitive C–N coupling reactions. The controlled metallation and recyclability without deactivation of both catalytic centers are unique with respect to previously reported coupling strategies. We performed various photoluminescence and electrochemical studies with Hammett correlations to understand the mechanism. The developed protocol enables selective and reproducible coupling of a diverse range of amines (aryl, heteroaryl, alkyl), carbamide, and sulfonamide with electron-rich, -neutral, and -poor (hetero)aryl iodides. Keeping this strategy in perspective, we explored the activity to produce non-steroidal anti-inflammatory drug Fulfenamic acid, strong pharmacophore N,5-diphenyloxazol-2-amine, Food and Drug Administration (FDA) approved drugs Flibenserin, Tripelennamine and did late-stage diversification of the derivatives of ibuprofen, naproxen, gemfibrozil, helional, glycine, and ϵ -aminocaproic acid.



References:

1. Cote, A. P.; Benin, A. I.; Ockwig, N. W.; O’Keeffe, M.; Matzger, A. J.; Yaghi, O. M., *Science* 2005, 310, 1166-70
2. Jati, A.; Dey, K.; Nurhuda, M.; Addicoat, M. A.; Banerjee, R.; Maji, B., *J. Am. Chem. Soc.* 2022, 144, 7822-7833.
3. Gisbertz, S.; Reischauer, S.; Pieber, B., *Nat. Catal.* 2020, 3, 611-620

CO-15

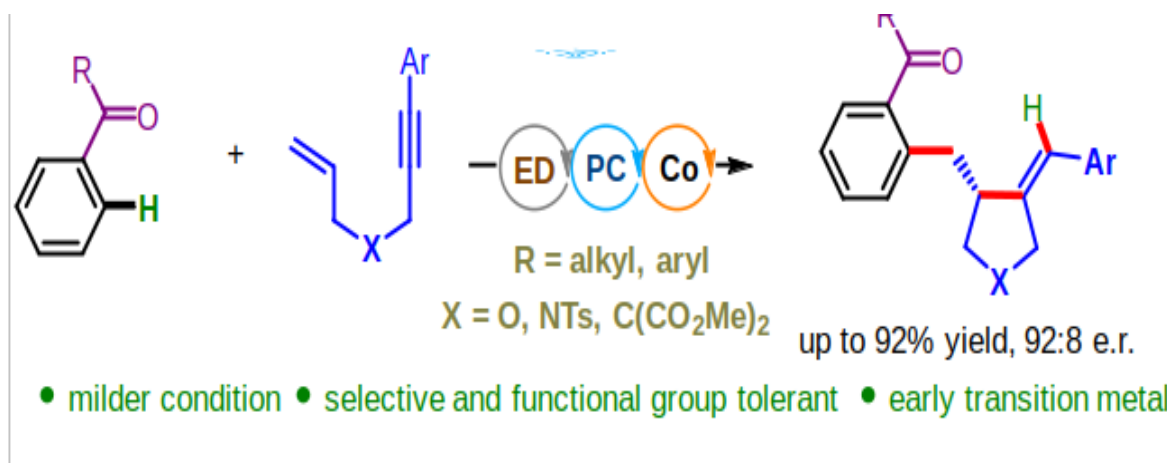
Enantioselective C–H bond functionalization of aromatic ketones with 1,6-enynes via photoredox/cobalt dual catalysis

Kakoli Maji, Pradip Ramdas Thorve, Pramod Rai, Biplab Maji

Department of Chemical Sciences Indian Institute of Science Education and Research Kolkata

e-address: km16ip015@iiserkol.ac.in

Directing group-enabled C–H functionalization reactions have emerged as a powerful tool in organic synthesis¹. In the evolution of such a process, heavy metals are gradually being replaced by the earth's abundant transition metals utilizing both strongly and weakly coordinated directing groups. Recently, visible-light photocatalysis has been coupled with the transition metal-catalyzed C–H bond activation reactions enabling the replacement of stoichiometric metal oxidants and thereby reducing waste. However, light-mediated generation of a low-valent first-row transition metal complex and its applications in these reactions, particularly with the aid of a weakly coordinating group, is lagging. Herein, we report the Enantioselective C–H bond functionalization of aromatic ketones with 1,6-enynes via photoredox/cobalt dual catalysis.² For this initial study, 1,6-enyne was used as the coupling partner. This reaction proceeds at an exceptionally mild condition at room temperature utilizing cobalt and chiral diphosphine ligand. This cascade reaction featured the formation of two new C–C and one C–H bond in a highly chemo- and regioselective manner. A large number of substrates were isolated in high yields and selectivities. Our protocol can be applied for the late-stage diversification of biologically active molecules and natural products. Mechanistic studies, including kinetic, deuterium labeling, cross-over experiment, luminescence quenching, cyclic voltammetry, and control experiments, were conducted to validate the proposed mechanistic hypothesis.



References:

1. K. Tsuchikama, Y. Kuwata, Y.-k. Tahara, Y. Yoshinami and T. Shibata, *Org. Lett.*, 2007, 9, 3097-3099; (b) R. Santhoshkumar, S. Mannathan and C.-H. Cheng, *Org. Lett.*, 2014, 16, 4208-4211; (c) R. Santhoshkumar, S. Mannathan and C.-H. Cheng, *J. Am. Chem. Soc.*, 2015, 137, 16116-16120; (d) A. Whyte, A. Torelli, B. Mirabi, L. Prieto, J. F. Rodríguez and M. Lautens, *J. Am. Chem. Soc.*, 2020, 142, 9510-9517.
2. K. Maji, P. R. Thorve, P. Rai and B. Maji, *Chem. Commun.*, 2022, DOI: 10.1039/D2CC03595B.

CO-16**A Biogenic Cu₂O/Cu Nanocatalyst for Sonogashira and Chan-Lam Cross Coupling**

Dr. Utpal Bora

Department of Chemical Sciences, Tezpur University, Napam, Sonitpur, Assam

e-address: ubora@tezu.ernet.in

A mesoporous Cu₂O/Cu nanomaterial was prepared by in situ gas phase H₂O/O₂ stimulating approach via the deposition of Cu₂O on the surface of Cu nanoparticles in the presence of water extract of papaya peel as the reducing agent. The hybrid Cu₂O/Cu nano catalyst obtained as such offers an efficient Methodology for the Sonogashira cross coupling of aryl iodides with aryl acetylenes under Palladium free conditions and for the Chan-Lam amination of imidazoles and benzimidazoles with arylboronic acids under base free conditions. The electron microscopic characterization of the nanomaterial reveals the nanomaterial to have Cu₂O and Cu phases stacked one above other like lamellar sheets. The presence of Cu₂O phase in hybrid nano catalyst provides an attractive advantage highlighting a Cu (I)-Cu (0) synergistic interaction in the respective cross-coupling reaction.

References:

1. Sarmah, M., Sarmah, D., Dewan, A., Bora, P., Boruah, P.K., Das, M.R., Bharali, P. and Bora, U., Catal. Lett., 2022, (accepted for publication)
2. Chakraborty, D., Nandi, S., Mullangi, D., Haldar, S., Vinod, C.P., Vaidhyanathan, R., ACS Appl. Mater Interfaces, 2019, 11(17), 15670-15679.
3. Kou, J., Saha, A., Bennett-Stamper, C., Varma, R.S., Chem. Commun., 2012, 48(47), 5862-5864.

CO-17

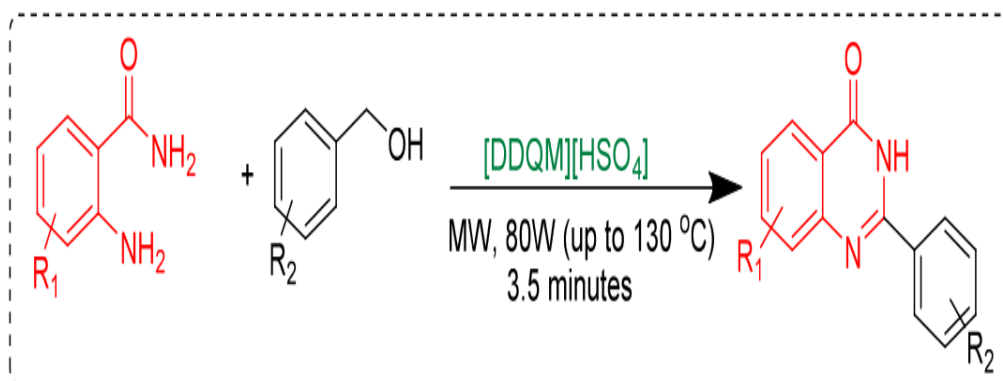
[DDQM][HSO₄] Ionic liquid as a Bifunctional Catalyst for the Synthesis of 2-Phenylquinazolin-4(3H)-ones under Microwave Irradiation

Diganta Sarma

Dibrugarh University, Dibrugarh-786004, Assam, India

e-address: dsarma22@dibru.ac.in

A new acidic ionic liquid 1-dodecylquinolin-1-ium bromide ([DDQM][HSO₄]) has been designed and explored as a bifunctional catalyst for the tandem oxidative synthesis of 2-phenylquinazolin-4(3H)-ones. Starting from anthranilamide and benzyl alcohol derivatives; the prepared ionic liquid was found to be an efficient catalyst as well as solvent for the desired transformation providing quantitative yield under continuous microwave irradiation of 80 W up to 130 °C for 3.50 minutes. Further metal/external acid-base/ligand free protocol for the rapid oxidative synthesis of medicinally important 2-phenylquinazolin-4(3H)-ones via in situ oxidation of benzyl alcohol derivatives using the designed ionic liquid adds a golden touch to the task-specificity of the ionic liquid.



References:

1. Dutta, B.; Dutta, N.; Dutta, A.; Gogoi, M.; Mehra, S.; Kumar, A.; Deori, K.; Sarma
2. Dutta, A.; Damarla, K.; Kumar, A.; Saikia, P.J.; Sarma, D.; *Tetrahedron Lett.*, 2020, 61, 151587
3. Dutta, B.; Garg, A.; Phukan, P.; Kulshrestha, A.; Kumar, A.; Sarma, D.; *New J. Chem.*, 2021, 45, 12792.
4. Dutta, A., Damarla, K., Bordoloi, A., Kumar, A., Sarma, D.; *Tetrahedron Lett.*, 2019, 60, 1614-1619.

CO-18

Mn(OAc)₃-Promoted Cycloannulative-Sulfonyl Migration of (E)- β -Iodovinyl Sulfones with 2-(arylethynyl)phenols for the Synthesis of Chromene Derivatives.

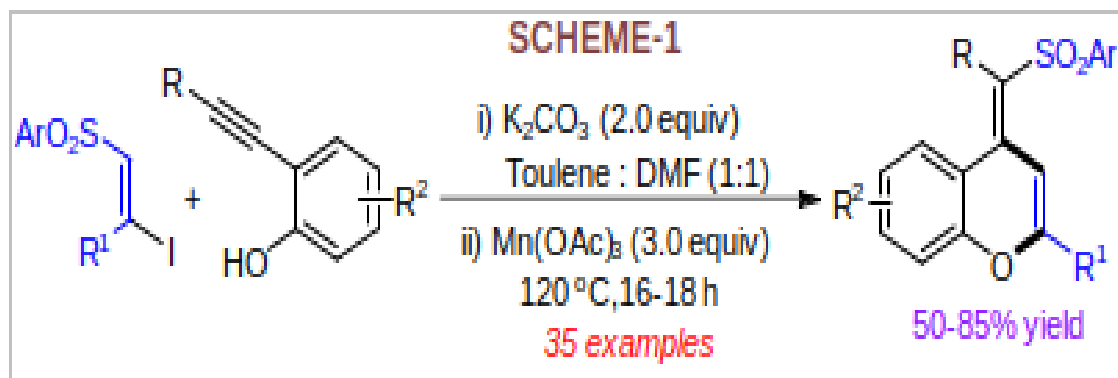
Jangam Jagadesh Kumar, Raju Jannapu Reddy
 Department of Chemistry, UCS, Osmania University, Hyderabad 500 007, India.
 e-address: jagadeeshou@gmail.com, rajuchem77@osmania.ac.in
 Webpage: <https://www.rjreddyresearchgroup.com/>

Chromenes are widely distributed in naturally occurring alkaloids¹, many of these scaffolds possess a broad spectrum of pharmacological activities² and exhibit photochromic properties in the crystalline state³. Among various organosulfur functionalities, sulfones are versatile building blocks in organic synthesis⁴ and constitute widespread applications in medicinal chemistry.⁵ Considering distinguished biological activities both of these skeletons, yet exploring the new methods for the synthesis of sulfone-derived chromene derivatives remains a goal.

In this poster presentation, we present an efficient base-mediated oxa-Michael addition of (E)- β -iodovinyl sulfones with 2-(arylethynyl)phenols and subsequent Mn(OAc)₃-promoted cycloannulative-sulfonyl migration is realized in a one-pot operation (Scheme-1).⁶ Notably, this process features a broad substrate scope and easy elaboration into numerous multifaceted chromene analogues in good to high yields.

Acknowledgments:

We thank SERB-CRG [CRG/2021/003544], New Delhi for financial assistance.



References:

- (a) G. P. Ellis, *Chromenes, Chromanones, and Chromones (Chemistry of Heterocyclic Compounds)*, Wiley, New York, 1977, vol. 31, pp. 11-141; b) G. A. Iacobucci, J. G. Sweeny, *Tetrahedron* 1983, 39, 3005-3038.
- A review article, see: M. Costa, T. Dias, A. Brito, F. Proença, *Eur. J. Med. Chem.* 2016, 123, 487-507.
- P. Kumar, P. Kumar, S. Venkataramani, S. S. V. Ramasastry, *ACS Catal.* 2022, 12, 963-970.
- (a) R. J. Reddy, A. H. Kumari, *RSC Adv.* 2021, 11, 9130-9221; b) R. J. Reddy, A. H. Kumari, J. J. Kumar, *Org. Biomol. Chem.* 2021, 19, 3087-3118.
- P. F. Schnellhammer, *Expert Opin. Pharmacother.* 2002, 3, 1313-1328.
- R. J. Reddy, J. J. Kumar, G. R. Krishna, Manuscript under preparation.

CO-19

Pd-Catalyzed Interrupted Benzofuran-Vinylation of 2-(Arylethynyl)-phenols/anilines with (E)- β -Iodovinyl Sulfones to Access 2,3-Disubstituted Benzofuran Derivatives

Nunavath Sharadha, Raju Jannapu Reddy

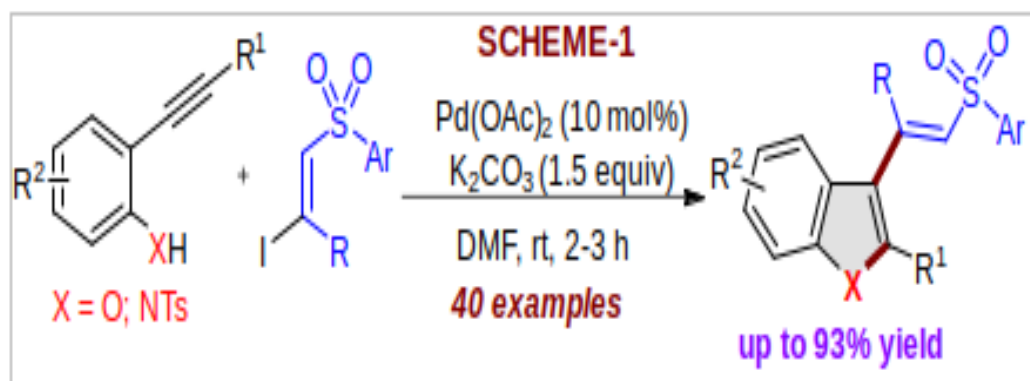
Department of Chemistry, UCS, Osmania University, Hyderabad 500 007, India.

e-address: nunavath.sharadha0631@gmail.com

correspondence e-address: rajuchem77@osmania.ac.in

Webpage: <https://www.rjreddyresearchgroup.com/>

Benzofurans and indoles are privileged class of compounds with a great deal of attention due to their wide pharmacological properties, such as, anti-ulcer, antimicrobial, anti-inflammatory, antioxidant, antitumor, antiplatelet, antimalarial, antidepressant and anticonvulsant activities.¹ In contrast, the sulfones², in particular vinyl sulfones are yet important class of functional group due to their widespread applications in medicinal chemistry³. On account of the biological significance of these skeletons, yet exploring the new methodologies for the synthesis of vinyl sulfone-derived benzofuran and indole analogues is highly desirable. In this poster presentation, we report a simple and highly efficient Pd(OAc)₂-catalyzed cyclization of 2-(arylethynyl)phenol/anilines followed by interrupted vinylation using (E)- β -iodovinyl sulfones under mild reaction conditions (Scheme-1)⁴. This cascade method allows a quick construction of C-O/N and C-C bonds to access a wide range of 2,3-substituted benzofuran and indole derivatives. The present unified benzofuran-vinylation exhibits significant features, such as mild reaction conditions, broad substrate scope, and excellent functional group compatibility.



Acknowledgements:

Acknowledgments: We thank SERB-CRG [CRG/2021/003544] and DST-INSPIRE FELLOWSHIP [IF180732], New Delhi for financial assistance.

References:

1. D. Goyal, A. Kaur, B. Goyal, *ChemMedChem*, 2018, 13, 1275-1299.
2. R. J. Reddy, A. H. Kumari, *RSC Adv.* 2021, 11, 9130-9221; b) R. J. Reddy, A. H. Kumari, J. J. Kumar, *Org. Biomol. Chem.* 2021, 19, 3087-3118.
3. D. C. Meadows, J. Gervay-Hague, *Med. Res. Rev.* 2006, 26, 793-814
4. R. J. Reddy, N. Sharadha, G. R. Krishna, To be submitted.

CP-01**Insights into the Cren7 mediated structural stabilization of DNA in Crenarchaea**

Geethika K., Angel Rose Thomas, T. Srividya Vyjayanthi, Soumit S. Mandal

Department of Chemistry, Indian Institute of Science Education and Research (IISER) Tirupati, Tirupati, Andhra Pradesh India,
e-address: geethika@students.iisertirupati.ac.in

Crenarchaea have several chromatin proteins which organize DNA into a compact form. Cren7 is one such protein which performs this function and enables crenarchaeal organisms to survive in extreme climates. In our study, we have attempted to examine the compaction mechanism. Cren7 was treated with Calf thymus DNA (CTD, 58% AT content), polynucleotides and representative spectroscopic signals characterize their structural changes. The dissociation constant (K_D) was estimated from the data and its value indicates that Cren7 formed a stable complex with CTD and poly(dA-dT) · poly(dA-dT). A combination of electrostatic and non-electrostatic interactions stabilizes this complex. From the low binding enthalpy it was concluded that the complexation was entropy driven. While the nature of anions did not have any role on the Cren7-DNA complexation, but it involved 3 pairs of ions at the interface. The variation in pH of the solution (between pH 6 and 8) led to a change in affinity and binding site size but temperature did not result in any such effects. Cren7 bound to ~10 bp's, of DNA, increasing its flexibility and thermal stability by more than ~30. Cren7 induces a cooperative structural transitions in DNAs but the protein remains structurally intact in this process. The salt dependent spectroscopic measurements allowed the estimation of energy stabilization parameters at extreme solution conditions. All these analysis deciphers the mystery of Cren7 mediated DNA organization in crenarchaeota.

Reference:

Geethika K., Angel Rose Thomas, T. Srividya Vyjayanthi, and Soumit S. Mandal Phys. Chem. Chem. Phys. 2022. Advance Article (DOI: 10.1039/D2CP02190K)

CP-02**A Minimum Energy Path Exploration of Chemical Reaction Mechanisms Through the FFoRCE Method**Dudam Praveen, K. V. Jovan Jose

School of Chemistry, University of Hyderabad, Telangana, India, 500046.

e-address: 17chph54@uohyd.ac.in

The reaction path prediction and locating the transition state on the potential energy surface is a tedious task. It is computationally expensive to calculate the higher-order derivatives and maintain the accuracy and reliability of the results. In developed methods that can predict the reaction path and locate the transition state, prior knowledge provided from a user like a reactant and product for the reaction path searching the existing methods is nudged elastic band (NEB)¹ and growing string method (GSM)². Another approach applied constant force between the reactants, then reduced the minimal distance to reach a transition state in the artificial force-induced reaction (AFIR) method³. We developed a new novel method, Feature Vector Force Reaction Coordinate through Minimum Energy (FFoRCE), to generate the reaction path between the reactant and product. The advantage of the technique is on the fly generating the transition state. A constrained bond algorithm minimizes the entire reaction path in an Iterative manner. The poster presents the method and benchmark studies on elementary organic reactions.

References:

1. Henkelman, G.; Jónsson, H. Improved Tangent Estimate in the Nudged Elastic Band Method for Finding Minimum Energy Paths and Saddle Points, *J. Chem. Phys.* 2000, 113 (22), 9978–9985.
2. Zimmerman, P. M. Automated Discovery of Chemically Reasonable Elementary Reaction Steps, *J. Comput. Chem.* 2013, 34 (16), 1385–1392.
3. Maeda, S.; Taketsugu, T.; Morokuma, K. Exploring Transition State Structures for Intramolecular Pathways by the Artificial Force Induced Reaction Method, *J. Comput. Chem.* 2014, 35, 166–173.

CP-03**A New Recurrent Neural Network (RNN)-Based Method for Designing Onsite Druglikeness Molecules**

Srinivasarao Mande, K.V. Jovan Jose

School of Chemistry, University of Hyderabad, Hyderabad – 500046, INDIA.

e-address: 17chph28@uohyd.ac.in

Over the last few decades, we have witnessed many advances in developing computational models to predict a wide span of physicochemical properties that are beneficial for screening promising drug-likeness molecules. The computational method is sustainable for designing drug molecules by avoiding laboratory synthesis of chemicals and enabling potential screening of many drug candidates based on the physicochemical or Lipinski's rule of five (RO5)¹ and ADMET properties.² We have developed a novel method to construct potential drug-likeness molecules with properties employing artificial neural networks (ANN).³ The current oral and poster present the development of a novel recurrent neural networks (RNN) algorithm and benchmark studies to develop potential drug-likeness molecules to treat diseases such as Alzheimer's, COVID-19, HIV, Parkinson's, Tuberculosis, Breast cancer, and many more diseases.

References:

1. Lipinski C.A., Rule of five in 2015 and beyond: Target and ligand structural limitations, ligand chemistry structure and drug discovery project decisions, *Adv. Drug Deliv. Rev.* 2016, 101, 34-41.
2. Daina A., Michielin O. and Zoete V., SwissADME: A free web tool to evaluate pharmacokinetics, drug-likeness and medicinal chemistry friendliness of small molecules, *Sci. rep.* 2017, 7, 1-3.
3. Amabilino S., Pogány P., Pickett S.D., and Green D.V., Guidelines for recurrent neural network transfer learning-based molecular generation of focused libraries, *J. Chem. Inf. Model.* 2020, 60, 5699-5713.

CP-04

A Rapid Deep-Learning Algorithm to Predict Systematic Growth Patterns of Atomic Clusters

Sridatri Nandy , K.V. Jovan Jose,

School of Chemistry, University of Hyderabad, Hyderabad 500046

e-address: 18chph01@uohyd.ac.in

Homoatomic metal clusters have been studied for several decades due to their wide range of applications¹. However, the potential construction and applications of larger metal clusters and nanoparticles remain unexplored. The electronic stability is described through the spherical jellium model². On the other hand, the geometrical stability of the high-symmetry systems relies on the number of atoms on the shell of the clusters. In the present work, we have developed a deep-learning algorithm to predict the electrostatic potential topographical (ESP) minima of metal clusters for assisting in the systematic growth of atomic clusters. This method incorporates a symmetry hierarchy accounting for both geometric and electronic effects in the growth pattern of the metal cluster. Preliminary benchmark studies prove that this algorithm efficiently builds atomic clusters of up to 15 nm and illustrates the minimum number of atoms required to preserve the spherical symmetry of the atomic cluster. The poster details our work and the benchmark studies on the Magnesium prototype nanoclusters.

References:

1. Liu. L. and Corma. A., Metal Catalysts for Heterogeneous Catalysis: From single Atoms to Nanoclusters and Nanoparticles, Chem. Rev. 2018, 118, 10, 4981-5079.
2. de Heer. Walt A. The physics of simple metal clusters: experimental aspects and simple models, Rev. Mod. Phys. 1993, 65,611

CP-05**Feature Vector Driven Global Optimization of Molecular Cluster**

Gunjan Rajendra Ramteke , K. V. Jovan Jose

School of Chemistry, University of Hyderabad, India

e-address: gunjanrramteke@gmail.com

Molecular clusters are investigated for its structure, electronic and thermochemical properties¹. The interaction energy, enthalpies and entropies of gas phase clusters have been studied previously employing DFT and higher level of theories². The restrictions appear in investigating higher order of aggregate size in both theoretical and experimental field due to the exponential increment in possible minima on potential energy surface. The current article presents an approach to overcome such restrictions by applying a local optimization procedure and less expensive energy evaluation supported by deep learning based techniques³. Molecular aggregates are generated by adopting a systematic procedure followed by geometry optimization. The geometry optimization is carried out by employing several mutation operations in feature space governed by molecular electrostatic potential and minimizes the energy of initial geometry. Deep learning-based techniques enable the estimation of a candidate structure's machine-learned energy. The approach mentioned in this poster enables a trade-off between computational expense and chemical precision. The algorithm produced architecturally unique molecular aggregates of (CO₂)_n, n = 30, 32, 34, 36, 38, 40 and minimized the geometry to the global minimum state.

References:

1. Marques J. M. C. ; Pereira F. B.; Llanio-Trujillo J. L.; Abreu P. E.; Albertí M.; Aguilar A.; Pirani F.; Bartolomei M. A global optimization perspective on molecular clusters. *Phil. Trans. R.Soc A* 375, 2016.
2. Yañez, O.; Báez-Grez, R.; Inostroza, D; Walter A.; Ricardo Pino-Rios, R.; Jorge Garza,J; Tiznado W. AUTOMATON: A Program That Combines a Probabilistic Cellular Automata and a Genetic Algorithm for Global Minimum Search of Clusters and Molecules. *J. Chem. Theory Comput.* 2019, 15, 1463-1475.
3. Behler, J. Constructing high-dimensional neural network potentials: A tutorial review. *International Journal of Quantum Chemistry.* 2015, 16, 1032-105.
Biocatalysis, Hydroxynitrile lyase, stereocomplementary, asymmetrization, aliphatic aldehydes, β -nitroalcohols.

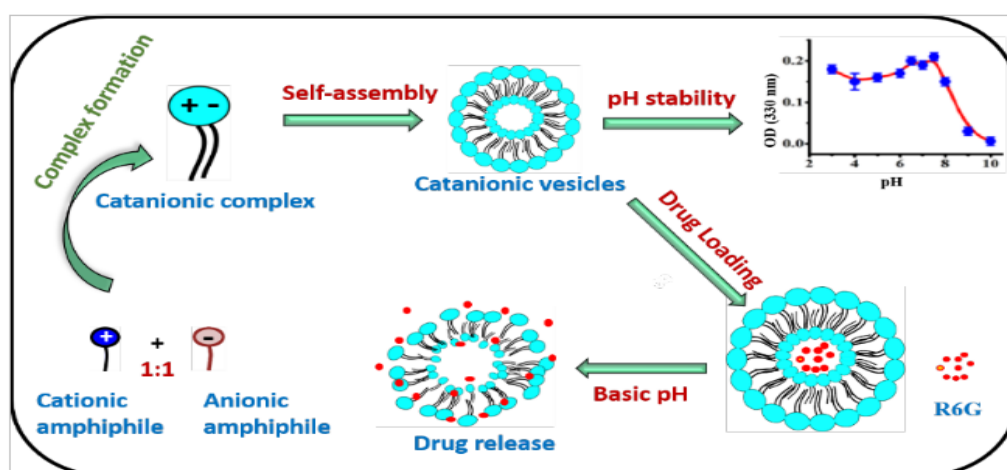
CP-06

Base-triggerable lauryl sarcosinate-dodecyl sulfate catanionic liposomes. Structure, biophysical characterization, and drug entrapment/release studies

Chinapaka Ravindar , S.Thirupathi Reddy, Dokku Sivaramakrishna, Deepthi Priyanka Damera, Musti J. Swamy

School of Chemistry, University of Hyderabad, Hyderabad, 500046
e-address: ravindrachem32@gmail.com, mjswamy@uohyd.ac.in

Equimolar mixtures of oppositely charged single-chain amphiphiles form a variety of phases, including vesicles. Such catanionic mixed lipid systems show high stability and exhibit versatile physicochemical properties^{1,2}. In the present study we have investigated the aggregation behaviour of lauryl sarcosinate hydrochloride (LS.HCl) in aqueous dispersion as well as its interaction with the anionic surfactant, sodium dodecyl sulfate (SDS). The CMC of LS.HCl was estimated to be 5 mM by isothermal titration calorimetry (ITC) and fluorescence spectroscopy using pyrene as the fluorescence probe. Turbidimetric and ITC studies on the interaction of LS.HCl with SDS established that the two surfactants form an equimolar catanionic complex. Crystal structure of lauryl sarcosinate-dodecyl sulfate (LS-DS) complex revealed that the complex is stabilized by classical N-H...O as well as C-H...O hydrogen bonds, besides electrostatic attraction between LS (cation) and DS (anion) and dispersion interactions between the hydrocarbon chains. Differential scanning calorimetric studies revealed that phase transition of equimolar LS-DS complex is significantly reduced compared to the analogous LG-DS and LA-DS complexes in the fully hydrated state. Dynamic light scattering, atomic force microscopic and transmission electron microscopic studies established that the LS-DS catanionic complex forms stable medium-sized vesicles (diameter 300-500 nm). In vitro studies demonstrated that the vesicles can entrap Rhodamine 6G (R6G), a representative anti-cancer drug, with an efficient release profile in the physiologically relevant pH range of 7.0-8.0, suggesting that the LS-DS catanionic vesicles can potentially be used in drug delivery applications.



References:

1. Y. Deng, J. Ling, M. H. Li, *Nanoscale*, 2018, 10, 6781–6800.
2. P. K. Tarafdar, S. T. Reddy, M. J. Swamy, *J. Phys. Chem. B*, 2010, 114, 13710–13717

CP-07**Purification, Biophysical Characterization, Lipid Binding Properties and Chaperone-like Activity of The Major Donkey Seminal Plasma Protein, DSP-1**

Sk Alim, Sudheer K. Cheppali, Musti J. Swamy
School of Chemistry, University of Hyderabad, Hyderabad-500046
e-address: alim26@uohyd.ac.in
correspondence e-address: mjswamy@uohyd.ac.in

Seminal fibronectin type-II (FnII) proteins are the major constituents of mammalian seminal plasma which specifically bind to choline phospholipids present on the sperm plasma membrane and induce efflux of cholesterol and choline phospholipids, which leads to sperm capacitation¹. Recent studies have shown that these proteins from bovine and horse seminal plasma can act as ATP-independent chaperones and this activity can be modulated by various factors such as pH, membrane binding, surfactants etc^{2,3,4,5}.

In the present study, we have purified DSP-1, a FnII protein from donkey seminal plasma, using affinity chromatography and reverse phase HPLC. The amino acid sequence determined by mass spectrometry and computational modeling studies revealed that DSP-1 is homologous to other mammalian seminal plasma proteins, including bovine PDC-109 and equine HSP-1/2. High-resolution LC-MS analysis indicated that the protein is heterogeneously glycosylated and also contains multiple acetylations, occurring in the attached glycans. Structural and thermal stability studies on DSP-1 employing CD spectroscopy and differential scanning calorimetry showed that the protein unfolds at ~ 43°C and binding to phosphorylcholine (PrC) - the head group moiety of choline phospholipids - increases its thermal stability. Further studies indicated that DSP-1 exhibits chaperone-like activity (CLA) and protects various client proteins against thermal and oxidative stress. Lipid binding and membrane binding aspects of DSP-1 were also investigated and it was found that DSP-1 shows greater affinity towards choline phospholipids and exhibits membrane destabilizing activity against supported and model cell membranes.

References:

1. Plante, G. et al. *Cell Tissue Res.* 363 (2016) 105-127.
2. Sankhala, R. S., Swamy M. J. *Biochemistry* 49 (2010) 3908-3918.
3. Sankhala, R. S., Damai, R. S., Swamy, M. J. *PLoS ONE* 6 (2011) e17330
4. Kumar, C. S., Swamy M. J. *Biochemistry* 55 (2016) 3650-3657.
5. Kumar, C. S., Swamy M. J. *Int. J. Biol. Macromol* 96 (2017) 524-531.

CP-08

Modeling Covid-19 transmission dynamics using diffusion based hybrid model

H. Rahaman, D. Barik

School of Chemistry, University of Hyderabad, Central University P.O., Hyderabad, 500046, Telangana, India
e-address: hrahaman809@gmail.com

Coronaviruses are a family of viruses that causes common cold, Middle East respiratory syndrome (MERS) and severe acute respiratory syndrome (SARS). The rapid spread of Covid-19, since December 2019, has become a global challenge with millions of deaths. Therefore understanding the spreading dynamics of Covid-19 is crucial in containing the spread of this deadly virus. Here we considered the role of airborne transmission, through diffusion, in the spreading of the virus. In this study, we developed a computational framework which is based on the hybrid discrete continuum (HDC) method in which the human population and viral factors are considered as discrete agents and continuous variable, respectively. Considering the diffusive spreading of virus, we investigated the spreading of infection and viral mortality in major European countries. We determined the effects of viral diffusion, movement of population, mask usage, lockdown period, age specific infection and death probability, viral incubation period and disease recovery period on the spreading of infection.

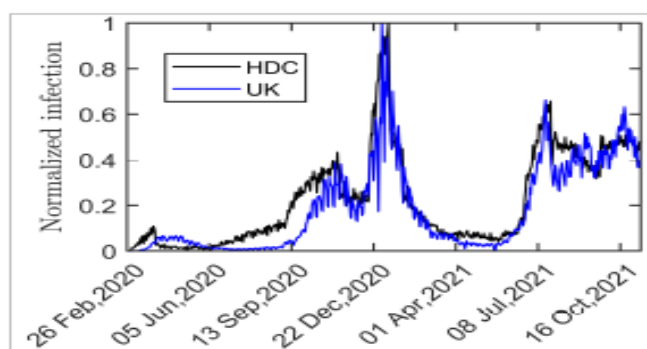


Figure 38: Comparison of normalized daily infection counts between the model and data from United Kingdom.

CP-09

Phase Behaviour and Supramolecular Organization of O-acyl- β -alaninols and Characterization of Equimolar Catanionic Complex

Suman Kumar Choudhury, D. Shivaramakrishna, M. J. Swamy

School of Chemistry, University of Hyderabad, Hyderabad-500046, India

e-address: sumankumar3394@gmail.comcorrespondence e-address: mjswamy1@gmail.com

Fatty acid amide hydrolase (FAAH) and NAE-hydrolyzing acid amidase (NAAA) play a central role in the degradation of endogenous lipid mediators like N-acylethanolamines (NAEs)¹. Studies show that O-acyl- β -alaninols (OABAs) are potent inhibitors of NAAA². Therefore, it is important to characterize the properties of OABAs. In this work, a homologous series of O-acyl- β -alaninols bearing 14-19 C atoms in the acyl chain have been synthesized and characterized with respect to phase transition, molecular structure and supramolecular organization. Differential scanning calorimetric (DSC) studies showed that the transition temperatures (T_t) in dry state exhibit odd-even alternation, with the even-chain-length compounds having higher T_t values. On the other hand, enthalpies (ΔH_t) and entropies (ΔS_t) of OABAs exhibit linear dependence on the acyl chain. DSC measurements on hydrated samples show all three parameters exhibit linear dependence on the acyl chain length. The molecular structure, packing properties, and intermolecular interactions of OABAs with 14 and 16 C atoms in the acyl chain were determined by single crystal X-ray diffraction, which showed that the hydrocarbon chains are packed in a tilted head-to-head (and tail-to-tail) bilayer format. d-Spacings obtained from powder X-ray diffraction studies exhibited an odd-even alternation. Turbidimetric, fluorescence spectroscopic, and isothermal titration calorimetric (ITC) studies established that in aqueous dispersions, O-myristoyl- β -alaninol hydrochloride (OMBA·HCl) and sodium dodecyl benzene sulphonate (SDBS) form an equimolar complex.

References:

1. N. Ueda, K. Tsuboi, & T. Uyama, Prog. Lipid Res. 2010, 49, 299–315.
2. Y. Yamano, et al. Bioorganic Med. Chem. 2012, 20, 3658–3665.

CP-10**De novo design of peptides as hydrolase model**Kalpana Kumari ,^a Vibin Ramakrishnan^a^a Department of Biosciences and Bioengineering, Indian Institute of Technology Guwahati, Guwahati-781039, Assam
e-address: k.kalpana@iitg.ac.in

Peptides have been a preferred choice for the design of bioinspired functional materials. Structural diversity, high loading capacity, and biocompatibility make them suitable candidates for synthesizing and characterizing their designed functional property at medium to large scales¹. The catalytic efficiency and stereo-selectivity shown by enzymes are the sources of inspiration to mimic them. Recent success in the design of novel peptide-based molecular systems that can catalyze reactions with comparable efficiency yet with remarkable stereo-selectivity provides hope for such an attempt. Such bioinspired catalytic scaffolds or their nano-assemblies mimic the active sites of a natural enzyme, with the minimum number of amino acids in their sequences^{2,3}.

Short peptides offer a direct analogy to enzymes because peptide catalysts have the same primary constituent amino acid molecule⁴. Hence, we can say that peptide catalysts can offer similar mechanistic origins for enantioselectivity. To achieve this, we have proposed to mimic the catalytic site of the catalytic system, i.e., Human carbonic anhydrase II. This project mainly aims to address: (i) Mimicking carbonic anhydrase active site by using peptide catalyst (ii) catalytic rate of peptide catalyst (iii) catalytic rate of peptide catalyst at adverse conditions such as higher temperatures (iv) and its Carbon dioxide capture ability. Hence, the construction of 'molecular mimics' for the molecular model system is the core Objective of this study.

References:

1. C. Zhang, X. Xue, Q. Luo, Y. Li, K. Yang, X. Zhuang, Y. Jiang, J. Zhang, J. Liu, G. Zou and X.-J. Liang, *ACS Nano*, 2014, 8, 11715–11723.
2. J. K. Kim, C. Lee, S. W. Lim, J. T. Andring, A. Adhikari, R. McKenna and C. U. Kim, *IUCrJ*, 2020, 7, 985–994.
3. D. J. Mikolajczak and B. Kocsch, *Catalysts*, 2019, 9, 1–4.
4. C. M. Rufo, Y. S. Moroz, O. V. Moroz, J. Stöhr, T. A. Smith, X. Hu, W. F. Degrado and I. V. Korendovych, *Nat. Chem.*, 2014, 6, 303–309.
5. D. J. Mikolajczak and B. Kocsch, *Catalysts*, 2019, 9, 903.

CP-11

Effect Of Macromolecular Crowding On Lectin-Carbohydrate Interaction

Sneha Banerjee , Musti J. Swamy

School of Chemistry, University of Hyderabad, Hyderabad - 500046, India

e-address: sneha112banerjee@gmail.com

Protein-carbohydrate interactions play a crucial role in various biological phenomena including cell-cell adhesion, cellular differentiation, mitogenicity, microbial infection etc. Our understanding in this area is largely due to a class of proteins called lectins, which are carbohydrate-binding proteins of non-immune origin that are devoid of enzymatic activity. In view of their ability to differentiate between normal and tumor cells, lectins are also being investigated as potential agents in developing target-specific drug delivery systems. In this context, it is important to understand how the crowded environment inside the cells modulates the carbohydrate binding properties of lectins.

Jacalin (*Artocarpus integrifolia* lectin), α -galactose-specific lectin, present in the seeds of jackfruit, recognizes the tumor-specific T-antigen.¹ In this study, we have investigated the effect of macromolecular crowding on the binding of methyl- α -D-galactopyranoside (Me- α -Gal) to Jacalin. Binding experiments were carried out employing isothermal titration calorimetry (ITC) and fluorescence spectroscopy in presence of polymeric dextrans of different sizes as crowding agents and at different concentrations in order to mimic the in vivo system.^{2,3} The results obtained showed that increasing the size of the crowders from 20 kDa to 70 kDa led to an increase in the binding affinity (see table in following Fig.). CD spectroscopic studies revealed that the secondary structure of the protein was unaltered in presence of these crowding agents.

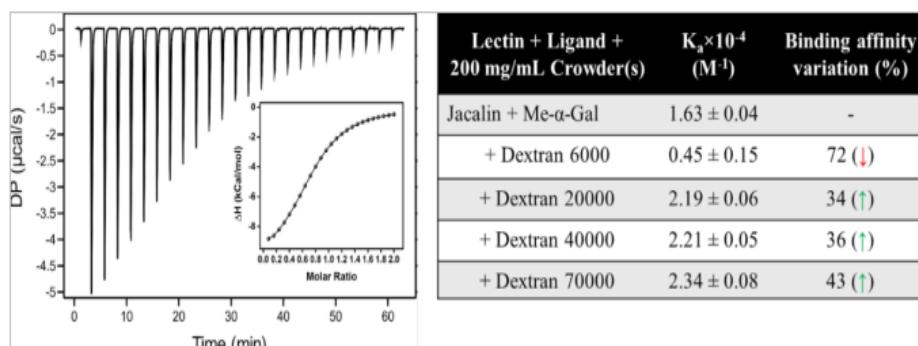


Figure 39: Left panel - ITC profile for binding of Me- α -Gal to Jacalin. Right panel - Binding affinities of crowders affecting binding of Me- α -Gal to Jacalin at different concentrations.

References:

1. M. V. K. Sastry et al., J. Biol. Chem. 1986, 261, 11726-11733.
2. S. Biswas et al., ACS Omega, 2018, 3, 4316-4330.
3. S. Biswas et al., J. Phys. Chem. B. 2016, 120, 12501-12510.

CP-12

Study of Transport Properties of a Driven Brownian Ratchet in a Rough Periodic Potential

Archana G.R.^a, Debashis Barik^a

^a School of Chemistry, University of Hyderabad, Telangana-500046, India
e-address: grarchana93@gmail.com

Brownian ratchets rectify unbiased thermal fluctuations leading to noise induced directed motion of particles and have vast applications in many transport processes of physical, chemical and biological systems. Although smooth periodic potential has been considered widely in the Brownian ratchets, however spatial heterogeneity in the potential landscape is well established in physical and biological systems such as in protein folding, structural glasses and super-cooled liquids. Previous studies showed that the roughness in the periodic potential act as a hindrance to the barrier crossing dynamics and can have conflicting roles in the transport of over-damped Brownian particle. We investigated the effect of roughness in the asymmetric periodic potential on the transport and diffusion of an inertial Brownian particle driven by a time-periodic force in a Gaussian environment. We find that moderate roughness leads to the loss of transient anomalous diffusion, and it helps to establish normal diffusion in the weak noise limit. In this limit, small amplitude roughness leads to the enhancement of directed transport. The deterministic dynamics of the system reveals that the chaotic dynamics in the rough potential may be the origin of enhancement of transport¹. We further studied the various aspects of roughness induced current reversal of a driven diffusive system in a symmetric rough periodic potential under the presence of an external load.

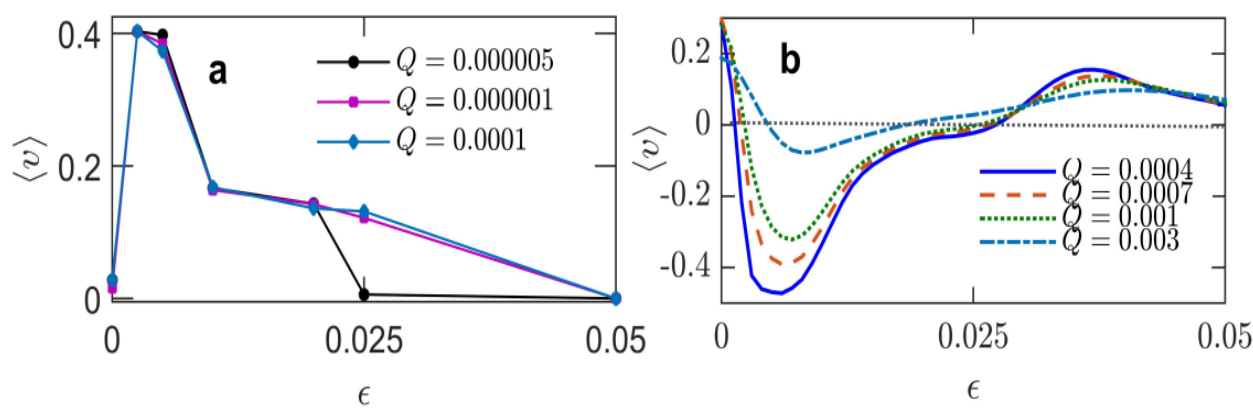


Figure 40: Effect of roughness in the magnitude (a) and direction (b) of velocity of a driven Brownian particle moving in a rough periodic potential

Reference:

1. Archana G. R. and D. Barik, Phys. Rev. E 104, 024103 (2021).

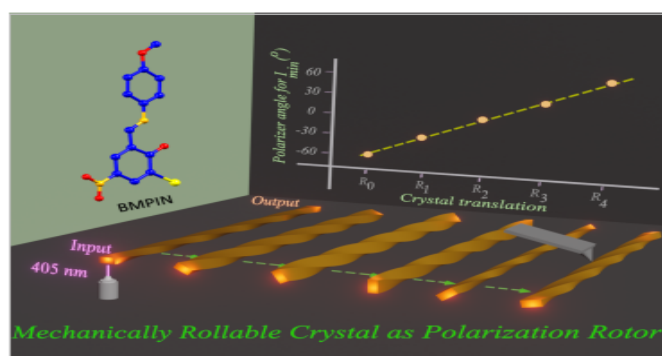
CP-13

Micromechanically-Powered Rolling Locomotion of Twisted-Crystal Optical-Waveguide-Cavity as a Mobile Light Polarization Rotor

Mehdi Rohullah,^a Vuppu Vinay Pradeep,^a Jada Ravi,^a Avulu Vinod Kumar,^a Rajadurai Chandrasekar^a

^aSchool of Chemistry, University of Hyderabad
e-address: roohullahmehdi@gmail.com

We demonstrate mechanically-powered rolling locomotion of twisted microcrystal optical waveguide cavity on the substrate, rotating the output signal's linear-polarisation. Self-assembly of (E)-2-bromo-6-(((4-methoxyphenyl)imino)methyl)-4-nitrophenol produces naturally twisted microcrystals. The strain between several intergrowing, orientationally mismatched nanocrystalline fibres dictates the pitch lengths of twisted crystals. The crystals are flexible perpendicular to twisted (001) and (010) planes due to $\pi\cdots\pi$ stacking, C-H...Br, N-H...O and C-H...O interactions. The twisted crystals in their straight and bent geometries guide fluorescence along their body axes and display optical modes. Depending upon the degree of mechanical rolling locomotion, the crystal waveguide cavity correspondingly rotates the output signal polarization. The presented twisted-crystal cavity with a combination of mechanical locomotion and photonic attributes unfolds a new dimension in mechanophotonics.



Reference:

M. Rohullah⁺, V. Vinay Pradeep⁺, A. Vinod Kumar, J. Ravi, R. Chandrasekar, *Angew. Chem., Int. Ed.* 2022, 2, 114. <https://doi.org/10.1002/anie.202202114>

CP-14

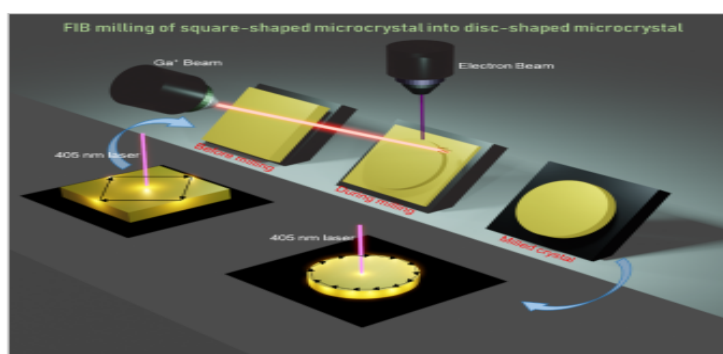
Micromanufacturing of Geometrically- and Dimensionally-Precise Molecular Single-Crystal Photonic Micro-Resonators via Focused Ion Beam Milling

Vuppu Vinay Pradeep , ^aRajadurai Chandrasekar ^a

^aSchool of Chemistry, University of Hyderabad

e-address: vinaypradeep777@gmail.com

Highly reproducible manufacturing of organic optical crystals with well-defined geometry and dimension is important to realize industrially relevant all-organic microelectronic and nanophotonic components, and photonic integrated circuits. Here, we demonstrate programmed shape and size alteration of perylene crystal resonators into disk and rectangular geometries using focused-ion beam (FIB) milling technique. Due to highly reproducible nature of the employed technique, the fabricated smaller sized disk and rectangular crystal resonators displaying shape and size dependent optical modes are suitable for commercial nanophotonic applications.



Reference:

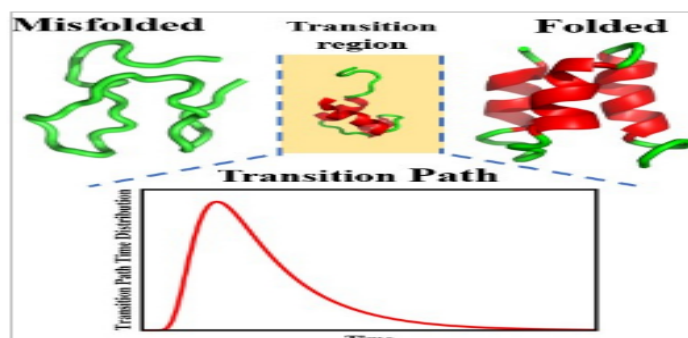
V. V. Pradeep, and R. Chandrasekar* "Micromanufacturing of geometrically- and dimensionally-precise molecular single-crystal photonic micro-resonators via focused ion beam milling" arXiv:2203.14218v1 [physics.optics].

CP-15

A Generalized Langevin Equation Approach for Barrier Crossing Dynamics in Conformational Transitions of Proteins

Vishal Singh^{a,b}, Parbati Biswas^a^aDepartment of Chemistry, University of Delhi, Delhi-110007^b Delhi School of Public Health, Institution of Eminence, University of Delhi, Delhi-110007e-address: pbiswas@chemistry.du.ac.in, dsph.vsingh@ioe.du.ac.in

Barrier crossing dynamics in conformational transitions of proteins are investigated in the framework of the inertial generalized Langevin equation with an exponential memory kernel in a parabolic potential¹. This approach yields an exact analytical expression for the time dependent Grote-Hynes rate and the transmission coefficient, which typically determines the kinetics of such transitions. The complete transition path time distribution (TPTD) and the mean transition path time (MTPT) are evaluated as a function of the frictional coefficient and barrier curvature. The results of TPTD show an excellent agreement with the experimental results of TPTD for the PrP prion protein and theoretical results in the high friction limit^{2,3}, while they exhibit a considerable deviation from the results of theory at the intermediate and low friction limits. The inertial terms significantly affect the short time dynamics of such transitions⁴. The results of the TPTD and MTPT are discussed at low and high frictional limits with varying curvatures of the potential barrier^{1,5}. The TPTD decreases with an increase in the barrier curvature at the high friction limit and exhibits an exponential decay at long times¹. The MTPT decreases with an increase in the curvature of the barrier.



References:

1. V. Singh, P. Biswas, *J. Stat. Mech.: Theory Exp.*, 2021 (2021) 063502
2. K. Neupane, D. A. Foster, D. R. Dee, H. Yu, F. Wang, M. Woodside, *Science*, 352 (2016) 239
3. E. Carlon, H. Orland, T. Sakaue, C. Vanderzande, *J. Phys. Chem. B*, 122 (2018) 11186
4. M. Laleman, E. Carlon, H. Orland, *J. Chem. Phys.*, 147 (2017) 214103
5. B. Peters, *Reaction Rate Theory and Rare Events*, Elsevier: Amsterdam (2017)

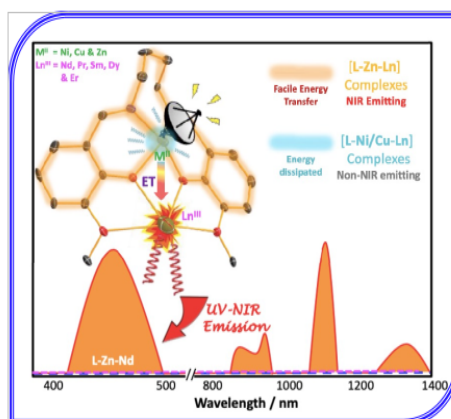
CP-16

The importance of d-metal Ion in determining the Fate of NIR emission from Ln^{III} ions: Ligand Influence Versus Electronic Configuration

Satyen Saha,^a Abhineet Verma^a

^a Department of Chemistry, Institute of Science, Banaras Hindu University, Varanasi, India.
e-address: satyen.saha@gmail.com

Lanthanides (Ln^{III}) are well known for their characteristic emission in the near-infrared region (NIR). Emission from Ln^{III} ions is a fundamentally important process as evident from a continuously expanding range of applications starting from biology to materials, for various purposes like lasers, OLED, optical fibres, WLED etc. However, direct excitation of lanthanides is not feasible, as restricted by Laporte's parity selection rule. Here we have presents several new NIR emitting [L–M–Ln] complexes (where L = an organic ligand, M = a d-block metal ion, and Ln = a lanthanide ion). [L–M] moiety acts as an antenna to absorb the excitation light and transfer to Ln^{III} energy levels. Based on fifteen lanthanide complexes having Cu^{II}, Ni^{II} and Zn^{II} d-block, it is demonstrated for the first time that the electronic configuration of the d-block metal ion is very crucial for obtaining NIR emission. With same Ln^{III} ion and the ligand, while [L–Zn–Ln] complexes shows very prominent NIR emission along with in visible range fluorescence, Cu^{II} and Ni^{II} complexes do not show any NIR emission.



References:

1. A. Verma, S. K. Saddam Hossain, S. S. Sunkari, J. Reibenspies, S. Saha*. Ligand influence versus electronic configuration of d-metal ion in determining the fate of NIR emission from Ln^{III} ions: a case study with Cu^{II}, Ni^{II} and Zn^{II} complexes. *New J. Chem.*, 2021, 45, 2696-2709.
2. N. Dwivedi, S. K. Panja, A. Verma, T. Takaya, K. Iwata, S. S. Sunkari, S. Saha*. NIR luminescent heterodinuclear [Zn^{II} Ln^{III}] complexes: Synthesis, crystal structures and photophysical properties. *J. Lumin.*, 2017, 192, 156-165.

CP-17**Ferrous ion - Carboxylate coordination-based crosslinking in XNBR**

Suraj W. Wajge, ^a Chayan Das ^a

^a Department of Chemistry, Visvesvaraya National Institute of Technology (VNIT), Nagpur-440011, India.

e-address: suraj.wajge1@gmail.com

Non-covalent crosslinking in rubber materials has drawn immense attention, due to its reversibility, self-healing, and shape memory effect. Addition of suitable metal ion crosslinker to the functional elastomer could result in crosslinking with unique property. In this work, Ferrous sulphate is employed to XNBR matrix to introduce crosslinks via interaction with carboxyl functional groups present in XNBR backbone. This is supposed to enhance the mechanical properties and improve viscoelastic property. Moreover, this could impart self-healing, and recyclability. The formation of metal-ligand bond between carboxylate groups and ferrous ions, is confirmed from attenuated total reflectance FTIR study. This is an approach to prepare a self-healable polymer based on non-covalent interaction between metal and ligand as an alternate to traditional crosslinking. The present study is expected to promote comprehensive research and industrial application of reversible non-covalent metal-ligand coordination bond in elastomer composite.

References:

1. Chino K, Ashiura M (2001) Thermoreversible cross-linking rubber using supramolecular hydrogen-bonding networks. *Macromolecules* 34(26):9201–9204.
2. McMullin E, Rebar HT, Mather PT (2016) Biodegradable thermoplastic elastomers incorporating poly(2,2,5-trimethyl-1,3-dioxane) (POTM): Synthesis, microstructure, and mechanical properties. *Macromolecules* 49(10):3769–3779.
3. Polgar LM, van Duin M, Broekhuis AA, Picchioni F (2015) Use of diels–alder chemistry for thermoreversible cross-linking of rubbers: The next step toward recycling of rubber products? *Macromolecules* 48(19):7096–7105.
4. Chen Y, Tang Z, Liu Y, Wu S, Guo B (2019) Mechanically robust, self-healable, and reprocessable elastomers enabled by dynamic dual cross-links. *Macromolecules* 52(10):3805–3812.

CP-18

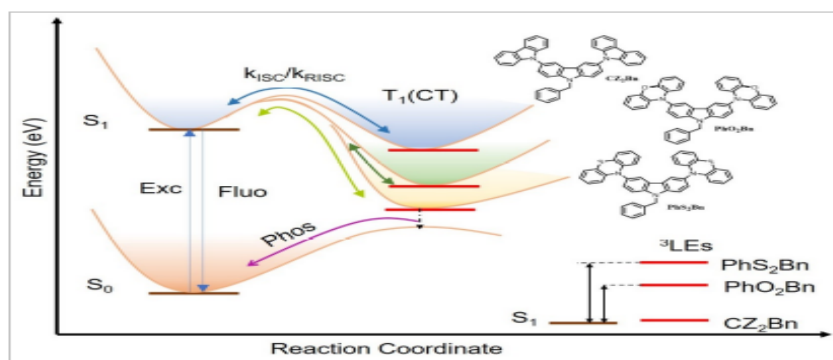
Regulating the 'Locally excited states' to facilitate spin-flip processes in efficient 'acceptor free' TADF emitters

Madalasa Mondal, Ratheesh K Vijayaraghavan

Department of Chemical Sciences IISER Kolkata, Mohanpur, West Bengal – 741246, India

e-address: mm18rs042@iiserkol.ac.in

Thermally activated delayed fluorescent materials are emerging as promising emissive layer materials for the next-generation organic light-emitting diodes (OLEDs) due to their high internal quantum efficiency. This would assist the development of low power operational devices with high luminescence efficiency and device durability. The overall efficiency of the process is known to be limited on the triplet to singlet up-conversion mechanism and the rate constant (k_{RISC}) of this process. The conventional TADF emitters consists of Donor -Acceptor (D-A) units in the chemical structure to facilitate the k_{RISC} , by reducing the singlet triplet energy offset. At the same time the geometrical distortion reduces the oscillator strength considerably thereby reducing the rate of singlet radiative processes. Our strategy to improve the k_{RISC} without compromising on the singlet radiative processes was achieved by introducing tailor designed locally excited state (LE) which is isoenergetic with the charge transfer states (CT) energy levels. This approach provides an effective strategy for designing effective TADF emitters without the conventional Donor-acceptor (D-A) structural backbone by managing LE and CT energy level alignments to facilitate the up-conversion process enhancing reverse intersystem crossing rate. In the present poster, three TADF emitters are considered for comparison that consisting carbazole as the core unit with different peripheral donor groups covalently connected to it, in particular CZ₂Bn having almost similar LE and CT energy levels exhibited efficient TADF feature and exciton utilization.



References:

1. Noda, H.; Nakanotani, H.; Adachi, C. *Sci Adv.* 2018, 4, eaao6910.
2. Noda, H.; Chen, X. K.; Nakanotani, H.; Hosokai, T.; Miyajima, M.; Notsuka, N.; Kashima, Y.; Brédas, J. L.; Adachi, C. *Nat. Mater.* 2019, 18, 1084-1090

CP-19

Organic Spiral waveguides for Photonic Circuit Applications

Avulu Vinod Kumar, Rajaduari Chandrasekar

School of Chemistry, University of Hyderabad.

e-address: vinod.avulu@gmail.comCorrespondence e-address: r.chandrasekar@uohyd.ac.in

The superior qualities of organic flexible crystals like high exciton-binding energy, photoluminescence quantum yield and good refractive index offer tremendous potential to apply these materials for photonic device applications¹. Here, we envisioned the design, and synthesis of extremely flexible blue-emitting organic molecule, namely, Cz-2CF₃. The unprecedented mechanical compliance displayed by the crystals can be attributed to the slip planes formed along [001] direction supported by supramolecular interactions like F...F, π ... π and C-F...H interactions. The microscopic photonic and mechanical properties of Cz-2CF₃ was explored using mechanophotonics approach. The micromechanical compliance was further exploited to fabricate, first of its kind, organic micro-architectures like circular, elliptical, rectangular, and triangular spiral waveguides (SW) using micromechanical operations like bending, moving, and pressing. The optical waveguiding properties of these microstructures were thoroughly investigated. The integration of spiral waveguides with different flexible crystals produces photonic circuits for diverse applications. Importantly, the post-fabrication modification and stability of the constructed SW under ambient and cryogenic temperatures were established, which might open-up new dimensions to use these materials for space applications.² The state-of-the-art results suggest the material's untapped potential as an alternative to Si-photonics.

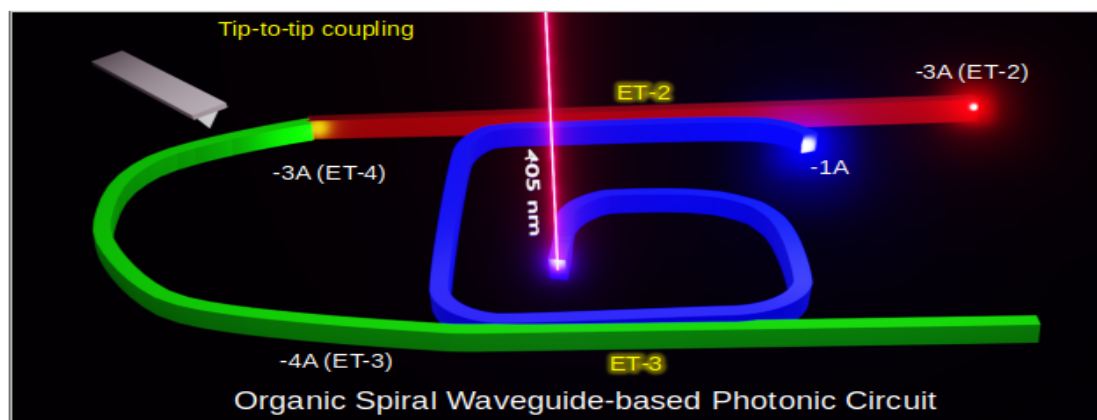


Figure 41: Effect of roughness in the magnitude (a) and direction (b) of velocity of a driven Brownian particle moving in a rough periodic potential

Reference:

1. R. Chandrasekar, Chem. Commun. (2022), 58, 3415-3428.

CP-20

ANTI-INFLAMMATORY, ANTI-CANDIDAL ACTIVITY AND IN SILICO PREDICTION OF PHARMACOKINETIC PROPERTIES OF NARDOSTACHYS JATAMANSI

Beena Rachotimath, Basavaraj Padmashali

Rani Channamma University, Department of Chemistry, Belagavi-591156,India

Corresponding author's e-address: basavarajpadmashali@yahoo.com

The earlier reports on Nardostachys jatamansi show contain avarious class of chemical constituents that have influenced the anti-inflammatory and anti-candidal activities. The present study reports the evaluation of anti-inflammatory and anti- candidal activities of N. jatamansi and also studies

pharmacokinetic properties using in-silico model. In ongoing research work, weused individual extracts of dichloromethane,

ethyl acetate, methanol, and water were prepared. The anti- inflammatory activity of different solvent extracts was carried

out using gelatin zymography through detection of MMP-2 and MMP-9 and on other side anti-candidal activity was carried out using Nitro blue tetrazolium assay (NBT).Bioactivity and pharmacokinetic parameters of all extracts were calculated using the property calculation online toolkit. From the results, it is observed that, among all the tested extracts, ethyl acetate extract wasfound to be more potent towards phagocytosis (more than 5 MPN) and Candida albicans (41%) at 100 $\mu\text{g}/\text{mL}$

while dichloromethane extract possesses profound anti- inflammatory activity towards MMP-2 (90%) and MMP-9

(85%) as compared to standardtetracycline HCl (positive control) followed by other extracts. Desoxo-Narchinol A, Narchinol B, Selinidin/ Jatamansin, Nardosinone and Valerenal were chosen as representative compounds of N. Jatamansi for the prediction of pharmacokinetic parameters, in-silico and bioactivity scores. All the compounds were showed results in line with Lipinski Rule of 5 and best acted as enzyme inhibitors with a score greater than 0.00. In light of the above result findings, N. jatamansi was found to possess anti-inflammatory and anti-candidal activities.This suggests extensive investigation of chemical components present in the active extracts to establish a structure-based activity relationship.

Keywords:

Nardostachys jatamansi, Narchinol B, Valerenal.

LA-01**Knockdown of Sperm associated antigen 11 A (Spag11a) enhances the susceptibility of epididymis and prostate to chemically induced carcinogenesis**

Aisha Jamil, Suresh Yenugu

Department of Animal Biology, School of Life Sciences, University of Hyderabad, Hyderabad-500046

e-address: aishajamil2023@gmail.com

Sperm-associated antigen 11a (Spag11a), an epididymis specific gene, is expressed in the principal cells of the caput. Our recent studies report that the ablation of SPAG11A protein by active immunization promotes oncogenesis in rats. This study aims to determine the changes in the epididymal transcriptome that is related to oncogenesis in Spag11a knockout mice. Further, we investigated the susceptibility of Spag11a knockout mice to chemically induced carcinogenesis. Spag11a knockout mice were administered a very low dose (0.05 ppm) of N, N-diethylnitrosamine (DEN) via drinking water for 12 weeks. A comparison of the caput transcriptomes of wild type and Spag11a knockout mice revealed that 601 genes were differentially expressed, of which 280 and 321 were up-regulated and down-regulated respectively. Interestingly, 2090 genes were uniquely present in the caput of Spag11a knockout mice (not detected in wild type) and 1700 genes that were not detected in the Spag11a knockout mice. Processes related to cell cycle and cell division-related genes were dysregulated. The KEGG pathway analyses suggested that the absence of Spag11a may activate microRNAs associated with cancer, chemical carcinogenesis-receptor activation and chemical carcinogenesis-DNA adducts pathways, which may contribute to the promotion of oncogenesis in the epididymis. Further, the epididymis and prostate of Spag11a knockout mice appeared to be more susceptible to DEN induced carcinogenesis compared to wild type mice, which is evident by histopathological examination. Hyperplasia, anaplasia, dysplasia, neoplasia, and inflammation in the epididymis and prostate of Spag11a knockout mice, while that of wild type mice displayed normal anatomical structure. Our results provide concrete evidence that the loss of Spag11a makes the epididymis and other tissues more susceptible to chemical carcinogenesis. The involvement of an epididymal gene in carcinogenesis is being demonstrated for the first time and also provides possible answer to the complex question of as to why epididymal cancers are rare.

LA-02**Bioaccumulation of heavy metals in different fishes of Gangetic river system in Varanasi and its health risk assessment**Gautam Geeta J.^a, Bhargawi Mishra^b, Vijay Nath Mishra^c^{a,c}Department of Neurology, Institute of Medical Sciences, Banaras Hindu University, Varanasi, India^bDepartment of Zoology, Mahila Mahavidyalaya, Banaras Hindu University, Varanasi, Indiae-address: geeta2713@gmail.com

Heavy metal load is one of the factor causing deterioration of river and aquatic species health. Present article is an attempt to evaluate the potential human health risks posed by four heavy metals (Pb, Mn, Cr and Cd), found in seven consumable fish species (Channa punctatus, Baikari, Mastacem-belus armatus, Mystus tengara, Cyprinus carpio, Johnus coitor and Oreochromis niloticus) randomly collected from the wild from river Ganga in Varanasi, Uttar Pradesh, India. The highest concentration of all the metals were recorded at Ganga-Varuna confluence point with Pb 1.29 mg/L, Mn 1.325 mg/L, Cr 0.169 mg/L and Cd 0.161mg/L, which was above than the permissible limits stated by Environment protection agency EPA in drinking water.

Highest accumulation of Pb was observed in Cyprinus carpio liver (8.86 $\mu\text{g/g}$) and lowest in Baikari muscles (0.07 $\mu\text{g/g}$). Cd was higher in C.punctatus, Telapia i.e O. nilotus and C. carpio. Except Cd in C. carpio, every metal was below the hazard quotient. Total THQ value i.e. hazard index (HI) of metals was recorded in following sequence: C.carpio > O. nilotus > C.punctatus > J.coitor > M.armatus > M.tengara > Baikari. Average HI value for C. carpio and O. nilotus was found above 1 which indicates that intake of heavy metals through these species may cause health hazard for human. Maximum HI was recorded in Carpio, which is highly consumed fish by human, hence may be harmful to them.

From our findings, it becomes necessary that regular monitoring of metals in fishes be performed in order to be aware of occurrence of heavy metals in the frequently consumed fishes. This would also act as a biomarker for monitoring the pollution status of river water and health risk assessment's on the human beings.

LA-03

Chromatin Association Dynamics Of Wip1

Vaishnavi Varadarajan^a, B J Rao^b^aIndian Institute of Science Education and Research, Karakambadi Road, Mangalam (B.O.), Tirupati, AP, India^bSchool of Life Sciences, University of Hyderabad, Prof. C R Rao Road, Gachibowli, Hyderabad 500046, Telangana, Indiae-address: vaishnaviv_iisert@uohyd.ac.in

Wip1 (wildtype p53-induced phosphatase-1, also called as PPM1D) is a serine-threonine phosphatase which predominantly dephosphorylates a large number of proteins involved in DNA repair, apoptosis and cell-cycle regulation. During stress recovery, Wip1 protein levels cross the threshold and by dephosphorylating, it switches off the stress signalling pathway. Thus, Wip1 has been termed as the 'homeostatic regulator' or the 'signal terminator' of the DNA damage response. In our study, we used a Wip1 overexpressed system in HEK293 cells (C-terminal FLAG tag). Upon replication stress induction by HU (hydroxyurea), protein levels and localization of Wip1 are highly regulated. We further report that the interaction dynamics of Wip1, as monitored by immunoprecipitation assays changes during the replication stress and recovery paradigm emphasising on the fluidity and the regulation of the system.

It has been suggested that chromatin association of Wip1 might regulate its functions. To understand the chromatin association dynamics of Wip1, we found in both endogenous and overexpression systems Wip1 was eluted in high salt fractions upon chromatin fractionation, i.e., it is a strong chromatin-binding protein. Furthermore, we showed for the first time that Wip1 phosphatase coimmunoprecipitates with DNA damage sensor protein PARP1. PARP1 PARylates and activates various proteins in the DNA damage pathway. PARP1 can influence and regulate proteins to bind to the chromatin. Preliminary studies showed that upon PARP1 inhibition, the affinity of Wip1 binding to chromatin decreased. This might hint towards the importance of PARP1 in governing Wip1 to bind to the chromatin. We further aim to understand the biological significance of PARP1 interaction with Wip1 and the regulatory mechanism of PARP1 governing Wip1 chromatin-binding dynamics.

LA-04

Mechanistic Insights on Mitochondrial Transport Defects in P301L Neurons

Anusruti Sabui^a, Mitali Biswas^a, Pramod Rajaram Somvanshi^b, Prasad Tammineni^a

^a Department of Animal Biology, School of Life Sciences, University of Hyderabad, India.

^b Department of Systems and Computational Biology, University of Hyderabad, India.

e-address: 20laph13@uohyd.ac.in

Correspondence e-address: prasadtammineni@uohyd.ac.in

Mitochondria are essential organelle required for neuronal homeostasis. Mitochondria supply ATP and buffer calcium at synaptic terminals. However, the complex structural geometry of neurons poses a unique challenge in transporting mitochondria to synaptic terminals. Kinesin motors supply mitochondria to the axonal compartments, while cytoplasmic dynein is required for retrograde transport. Despite the importance of presynaptic mitochondria, how and whether axonal mitochondrial transport and distribution are altered in tauopathy neurons and remain not well studied. In the current study, we have shown that anterograde transport of mitochondria is reduced in P301L neurons, while there is no change in the retrograde transport. Consistently, axonal mitochondrial abundance is reduced in P301L neurons. We further studied the possible role of two opposing motor proteins on mitochondrial transport and found that mitochondrial association of kinesin is decreased significantly in P301L cells. Interestingly, fitting our experimental data into mathematical equations suggested a possible rise in dynein activity to maintain retrograde flux in P301L cells. Our data indicate that decreased kinesin-mediated transport coupled with sustained retrograde transport might reduce axonal mitochondria in tauopathy neurons, thus contributing to the synaptic deficits in AD and other tauopathies.

Keywords:

Axon transport, Kinesin, Dynein, Tau, Alzheimer's Disease

Reference:

Sabui A, Biswas M, Somvanshi P and Tammineni P. Decreased Anterograde Transport Coupled with Sustained Retrograde Transport Contributes to Reduced Axonal Mitochondrial Density in Tauopathy neurons. *Front. Mol. Neurosci.* 2022; Sec. Brain Disease Mechanisms. doi: 10.3389/fn-mol.2022.927195 (Accepted, In Press)

LA-05**Role of hydrophobic hydration on the cold-induced denaturation of protein**

Sanjay Kumar , N. Prakash Prabhu

Department of Biotechnology & Bioinformatics, School of Life Sciences, University of Hyderabad, Hyderabad – 500 046, India.
e-address: sanjay.mynet@gmail.com

Protein denaturation by temperature variation can be categorized into two different transition regions, heat- and cold-induced denaturation. Except for a few proteins, the cold melting temperature of the proteins is well below the freezing point of water. It is proposed that hydrophobic hydration is the driving factor for the cold-denaturation of proteins¹; however, there is no direct evidence to verify these interactions. Surfactants are the molecules that denature the proteins through polar interactions at low concentrations and predominantly through hydrophobic interactions at their micellar concentrations². In the present work, the effect of hexatrimethyl ammonium bromide (HTAB), a cationic surfactant, on the thermal denaturation of apo-myoglobin (apo-Mb) is studied. HTAB does not affect the cold denaturation of apo-Mb at lower concentrations where the surfactant is mostly in its monomeric form. At the concentrations above its CMC, it clearly shows the inhibition of cold-induced denaturation of the protein. Further, the urea, a chemical denaturant that interacts with protein via hydrogen bonding, is found to destabilize the protein and induce early-unfolding. The addition of HTAB could counteract the effect of urea and stabilize the proteins against cold denaturation. These results clearly indicate that the hydrophobic interaction of HTAB with apo-Mb could prevent the hydration of the hydrophobic residues under sub-zero temperatures, thus stabilizing the protein.

References:

- 1.Naidu, K. T., Prabhu, N. P. (2020) J. Phys. Chem. B. 124, 10077-10088.
- 2.Otzen, D. (2011) Biochem. Biophys. Acta. 1814, 562-591.

LBC-01**Restoration of Mitochondrial Fusion Reduces Ovarian Cancer Progression by modulating AMPK/mTOR/ERK axis**

Rahail Ashraf, Sanjay Kumar

e-address: rahail.ashraf@students.iisertirupati.ac.in

correspondence e-address: sanjay@iisertirupati.ac.in

Mitochondrial dynamics, a balanced event of the fusion and fission process, determine the mitochondrial shape and size and are crucial for many physiological functions of the cells. Ovarian cancer (OC) cells display fragmented mitochondria, which indicates an imbalance in mitochondrial dynamics. We hypothesized that restoring mitochondrial fusion would balance mitochondrial dynamics in OC cells, normalize their function, and reduce tumorigenicity. Hence, we elucidated the potential role of Mfn2-induced mitochondrial fusion in OC cell survival and progression and their underlying mechanism. We determined that increased Mfn2 promotes autophagy, reduces ROS levels, and thus suppresses OC cell growth by activating the AMPK/mTOR-S2481/ERK signaling pathway. We also determined that increased Mfn2 expression reduces OC cell migration and invasion by reducing epithelial-to-mesenchymal transition EMT. Our data suggest that Mfn2-mediated mitochondrial fusion suppresses OC progression, and targeting Mfn2-mediated fusion could be a potential candidate for clinical applications.

LBC-02**Refolding and Biophysical characterization of leptospiral complement Regulator-acquiring protein A (LcpA)**

Umate Nachiket Shankar, Pankaj Kumar, Mohd. Akif

Laboratory of Structural Biology, Department of Biochemistry, School of Life Sciences, University of Hyderabad, Prof. CR Rao Road, Gachibowli, Hyderabad, Telangana (500046)
e-address: akif@uohyd.ac.in

Many pathogens establish a successful infection by evading the host complement system, an important arm of innate immunity. Pathogenic *Leptospira* is reported to evade complement-mediated killing through recruiting the host complement regulators by its lipoproteins or outer surface proteins. One of the lipoproteins/outer surface proteins, leptospiral complement regulator-acquiring protein A (LcpA), is known to recruit complement regulator, C4BP on the bacterial surface. LcpA doesn't have any homology with any other proteins. 3-dimensional structural organization LcpA and the structural basis of its interaction with the C4BP are not known. Here, we report the expression and refolding of recombinant LcpA from an inclusion body of *E. coli* as well as its purification at a large scale. Secondary structure analysis reveals that protein consists of 12%, 51%, and 46%, α -helix, β -strand, and random coil, respectively. T_m of the protein was found to be 50°C. Fluorescence quenching experiments demonstrate the binding of Zn^{2+} ions with the protein. Moreover, crystallization trials have yielded few crystallization hits, and same is being optimized. In our understanding, this is the first report of large-scale purification of LcpA through refolding experiments and preliminary structural characterization of LcpA. This study may provide additional information on the structural basis of complement evasion in leptospira.

Keywords:

Leptospira, Complement evasion, LcpA, Refolding, C4BP, Biophysical Characterization, Crystallization.

LBC-03**Regulation of protein homeostasis via SUMOylation in *Candida glabrata***

Dipika Gupta , Renu Shukla, Krishnaveni Mishra

Department of Biochemistry, School of Life Sciences University of Hyderabad, Hyderabad, Telangana 500046

e-address: dipikagupta592@gmail.com

Protein SUMOylation is a post-translational modification that plays critical regulatory roles in diverse cellular processes including gene transcription, cell cycle regulation, DNA replication and repair. The SUMO (Small Ubiquitin like Modifier) protein belongs to a group of ubiquitin-like modifiers, present in organisms ranging from yeast to humans, and is covalently attached to other proteins to modify their function. SUMOylation is a reversible process with deSUMOylating enzymes removing the SUMO from target proteins. In addition, polySUMOylation, wherein SUMO chains are added to the target proteins plays a significant role in protein homeostasis. These polySUMOylated proteins are further ubiquitinated by a group of ubiquitin-ligases and are targeted for proteosomal degradation, termed as SUMO-targeted ubiquitin ligases (STUbLs). SUMO has been identified in pathogenic fungi, and studies suggest that it is important either for survival and/or pathogenicity. In *Candida glabrata*, we had earlier identified the SUMO conjugation pathway and demonstrated that perturbation of SUMOylation reduces the virulence of *C. glabrata*. Of note, SUMO protease Cgulp2 deletion results in decreased cell survival and reduced adhesion. Based on sequence homology, we have now identified the components of the SUMO conjugation pathway and STUbLs in multiple pathogenic fungi. Mutant strains lacking STUbLs results in reduced cell survivability under various stress conditions. We have shown that loss of Ulp2 leads to accumulation of increased polySUMOylated protein that were degraded by proteasome via the STUbL pathway. These observations show the connection between SUMOylation and ubiquitination and also highlight the importance of SUMOylation in protein homeostasis.

LBC-04

Hydroxynitrile Lyase Employed Asymmetrization of Environmentally Challenging Aliphatic Aldehydes Into Value Added Chiral β -Nitroalcohols

Ghufrana Abdus Sami, Santosh Kumar Padhi

Biocatalysis and Enzyme Engineering Laboratory, Department of Biochemistry, School of Life Sciences, University of Hyderabad, Hyderabad- 500046, India

e-address: 17lbph14@uohyd.ac.in

Hydroxynitrile lyases (HNLs) are versatile biocatalysts which perform nucleophilic addition of hydrogen cyanide/ nitroalkanes to various carbonyls leading to enantiopure α -hydroxynitrile/ β -nitroalcohols (BNA), both of which are potential building blocks for several fine chemicals, pharmaceuticals and bioactive molecules¹. So far HNLs have been explored (a) majorly towards the chiral cyanohydrin synthesis² than the β -nitroalcohol by promiscuous reactivity, (b) broadly using aromatic aldehydes while very limited studies has been done with aliphatic aldehydes as substrates^{1,3}, and (c) exclusively using MeNO₂ as the nucleophile among nitroalkanes.^{1,2} Surprisingly aliphatic BNAs especially the short chain ones are precursors in the synthesis of various WHO listed essential drugs, e.g., methylergonovine, saffingol etc. and play an indirect role in corneoscleral crosslinking⁴. To address the above limitations of HNLs as well as to access the synthesis of significantly important aliphatic BNAs, we focused on HNL catalyzed chiral nitroaldol synthesis using exclusively aliphatic aldehydes with diverse nitroalkanes and further deepened our investigation with toxic halogenated aldehydes that are listed as environmental pollutants⁵.

Herein, we successfully achieved asymmetrization of various short chain toxic aliphatic aldehydes into enantiopure BNAs using wild type or engineered HNLs, i.e., R-selective *Arabidopsis thaliana* HNL and S-selective *Baliospermum montanum* HNL, as biocatalyst. Rational mutagenesis at selected amino acid positions have produced variants that enhanced the catalytic efficiency and stereoselectivity. Multilayered screening using bulky nitroalkanes as nucleophiles and aliphatic substrates furnished a series of stereocomplementary BNA enantiomers and diastereomers with significant improvement in conversion and stereoselectivity (up to 98% ee and 80% de). The synthesized enantiomers and diastereomers of both antipods owing to employment of R and S selective HNLs could act as active ingredient towards valuable fine chemicals, pharmaceuticals and medicinal formulation.^{1,2,6}

Keywords:

Biocatalysis, Hydroxynitrile lyase, stereocomplementary, asymmetrization, aliphatic aldehydes, β -nitroalcohols.

References:

1. M. Liu, D. Wei, Z. Wen and Jian-bo Wang, *Front. Bioeng. Biotechnol.*, 9 (2021), 653-682.
2. D. H. S. Rao, A. Chatterjee and S. K. Padhi, *Org. Biomol. Chem.*, 19 (2021), 322-337.
3. K.I. Fuhshuku, Y. Asano, *J. Biotechnol.* 153 (2011) 153-159.
4. Bo Li, J. Zhang, Bei-Bei Yang, Li Li and Xiao-Xiao Yang, *RSC Adv.*, 7 (2017), 45714-45720. (b) D.C. Paik, Q. Wen, R.E. Braunstein, S. Airiani, S.L. Trokel, *Investig. Ophthalmol. Vis. Sci.* 50 (2009) 1098-1105.
5. R. M. LoPachin and T. Gavin, *Chem. Res. Toxicol.* 27, 7 (2014), 1081-1091. (b) P. J. O'Brien, A. G. Siraki and N. Shangari, *Crit. Rev. Toxic.* (2008), 609-662.
6. T. Purkarthofer, W. Skranc, C. Schuster, H. Griengl, *Appl. Microbiol. Biotechnol.* 76 (2007) 309-320.

LBC-05

Podocyte Derived TNF- α Mediates Monocyte Differentiation and Contributes to Glomerular Injury

Sumathi Ravi Raj, Rajkishore Nishad, Atreya S.V Paturi, Anil Kumar Pasupulati

Department of Biochemistry, University of Hyderabad

e-address: 20lbph04@uohyd.ac.in

Diabetic kidney disease is the leading cause of end-stage kidney disease. Macrophage accumulation predicts the severity of kidney injury in human biopsies and experimental models of diabetic nephropathy (DN). However, the mechanism underlying macrophage recruitment in diabetic glomeruli is unclear. Elevated plasma growth hormone (GH) levels in type I diabetes and acromegalic individuals impaired glomerular biology. In this study, we examined whether GH-stimulated podocytes contribute to macrophage accumulation. RNA-seq analysis revealed elevated TNF- α signaling in GH-treated human podocytes. Conditioned media from GH-treated podocytes (GH-CM) induced differentiation of monocytes to macrophages. On the other hand, neutralization of GH-CM with the TNF- α antibody diminished GH-CM's action on monocytes. The treatment of mice with GH resulted in increased macrophage recruitment, podocyte injury, and proteinuria. Furthermore, we noticed activation of TNF- α signaling, macrophage accumulation, and fibrosis in DN patients' kidney biopsies. Our findings suggest podocytes could secrete TNF- α and contribute to macrophage migration, resulting in DN-related renal inflammation. Inhibition of either GH action or TNF- α expression in podocytes could be a novel therapeutic approach for DN treatment.

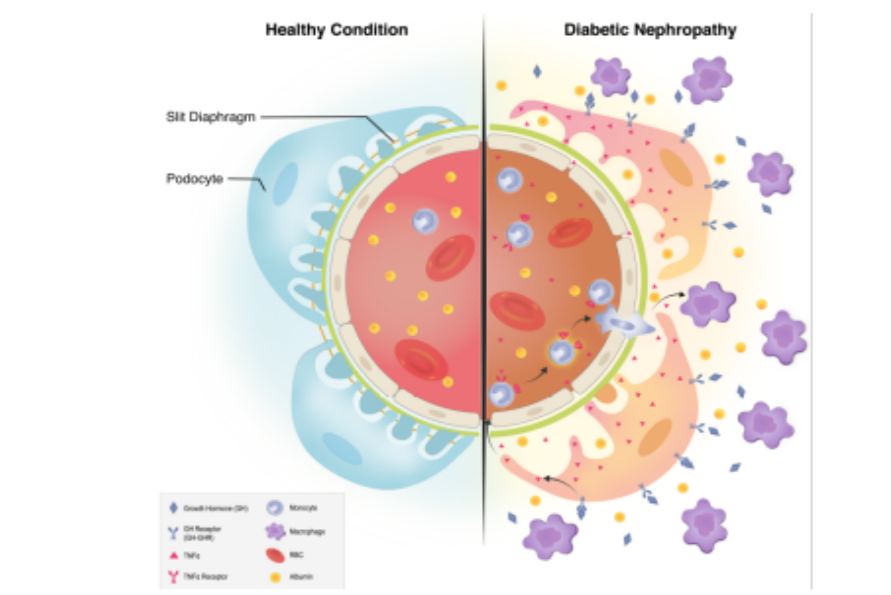


Figure 42: Schematic representation of paracrine action of GH on podocytes to induced monocyte-to-macrophage differentiation.

LBC-06**Beta N-acetyl-hexosaminidase from Snake Gourd: Purification and Biochemical Characterization**

Kavyashree Sakharayapatna Ranganatha , Nadimpalli Siva Kumar

Department of Biochemistry, School of Life Sciences, University of Hyderabad, Hyderabad-500046

e-address: kavyashree282@gmail.com

Beta N-acetyl hexosaminidases (EC 3.2.1.52) are exoglycosidases which cleave N-acetylglucosamine (GlcNAc) or N-acetylgalactosamine (GalNAc) from the non-reducing terminal of oligosaccharides, glycolipids, glycoproteins and other glycoconjugates. They possess wobbling specificity which cleave different substrates in both gluco- and galacto- configurations depending on enzyme source in a variable ratio. β -hexosaminidases are postulated to involve in glycoprotein metabolism during seed germination and seedling development. In the present study, β -hexosaminidase from crude extracts of Snake gourd seeds has been purified by ammonium sulfate precipitation, phenyl Sepharose, anion exchange, and lectin affinity chromatography. The purified Snake gourd β -hexosaminidase (SGH) migrated as a single band corresponding to \sim 220 kDa on native PAGE under non-reducing conditions. Under reducing conditions, SGH resolves into four subunits with an approximate molecular mass ranging from 88-55 kDa and into two subunits ($M_r \sim$ 220-190 kDa) under non-reducing conditions upon SDS-PAGE analysis. Zymographic analysis authenticates the purity and homogeneity of SGH. The pH optimum, temperature optimum and K_M were found to be 5.0, 50°C and 1.208 mM respectively with para-nitro-phenyl-N-acetyl- β -galactosaminide. Whereas with para-nitro-phenyl-N-acetyl- β -glucosaminide, the pH optimum, temperature optimum and K_M were found to be 5.0, 60°C and 3.228 mM respectively. Galactosamine, glucosamine, GalNAc and GlcNAc inhibited SGH in noncompetitive, uncompetitive and competitive mode respectively. SGH catalyzed the hydrolysis of acetylated chitooligomers. SPR analysis revealed the binding affinity of SGH with simple and amino sugars, sugar derivatives and disaccharides. Lectin binding studies demonstrated the binding of SGH only with Con A. The detailed biochemical characterization of SGH confirmed the chitinolytic activity in addition to hexosaminidase activity. This comprehensive biochemical study provides the basic framework to understand the structure-function relationship and the potential application of SGH as an efficient glycomic tool.

LBC-07**Proteomic study of purified alpha-mannosidase from bitter gourd seeds: understanding possible potential application in plant glycosylation**

Shivaranjani Vutharadhi , Siva Kumar Nadimpalli

Protein Biochemistry and Glycobiology Laboratory, Department of Biochemistry, School of Life Sciences, University of Hyderabad, Hyderabad-500046, Telangana, India
e-address: vshivaranjanik@gmail.com

Plant glycosylation is an essential post translational modification to better understand the crucial role of protein stability in endomembrane system. In particular, a fruit ripening specific N-glycan α -mannosidase is an exoglycosidase which plays an important role in removing terminal α 1-2, α 1-3 and α 1-6 linkages. These are essential for the 'Asparagine' linked glycosylation (N-glycosylation) that are involved in both glycan biosynthesis as well as catabolism. In the present study, we partially purified α -mannosidase from the defatted seed extract of bitter gourd (*Momordica charantia*) by a combination of hydrophobic interaction, lectin affinity, gel filtration chromatography and subsequently purified by anion exchange chromatography techniques. The purified α -mannosidase migrated as a single band in native PAGE corresponding to molecular weight \sim 238 kDa under non-reducing conditions and its purity was also authenticated by zymogram analysis using 4-methylumbelliferyl α -D-mannopyranoside as a substrate. In SDS PAGE, under reducing conditions it is dissociated into four sub units in the range \sim 70, 30, 23 and 18 kDa which showed immunoreactivity with antiserum raised against jack bean α -mannosidase through western blot analysis. In gel digestion followed by partial protein sequencing using tandem mass spectroscopy revealed sequence identity to the genomic sequence of *Momordica charantia* with a score of 59 (30% sequence coverage). The pH and thermal optima of purified α -mannosidase were found to be 5.0 and 60° C respectively. Further detailed biochemical characterization of the purified enzyme should reveal its physiological function and as a potential tool in glycomics.

LBC-08

Characterization of Lysosomal Enzymes From Hydra: An Attempt to Understand the Role of Lysosomal Enzymes During Hydra Regeneration

Lakshmi Surekha Krishnapati , Poorna Manasa Bhamidimarri, Siva Kumar Nadimpalli
Protein Biochemistry and Glycobiology Laboratory, Department of Biochemistry, School of Life Sciences, University of
Hyderabad, Hyderabad-500046, Telangana, India
e-address: skrishnapatimsc@gmail.com

Tissue regeneration is a dynamic process and involves complex interactions between cellular components. One of the fundamental mechanisms by which the plasma membranes are repaired involves calcium induced exocytosis of lysosomes. Although these processes are understood to a certain extent in vertebrates, mechanism(s) involved in invertebrate wound healing and regeneration are not clear. Here, we used Hydra, the fresh water Cnidarian to study regeneration due to its spectacular ability to regenerate the lost body parts. Hydra shows two modes of regeneration, morphallaxis and epimorphosis types, which involves different mechanisms. To identify the roles of lysosomal enzymes during both types of regeneration, it was initially necessary to identify, clone and characterize them. Genes encoding β -hexosaminidase, acid phosphatase, β -glucuronidase and α -fucosidase were cloned and confirmed by in silico analysis and sequencing. Localization studies of β -hexosaminidase, acid-phosphatase and β -glucuronidase showed endodermal expression suggesting possible role in digestion. α -fucosidase expression was seen in cnidocytes of the ectoderm, and in the endodermal epithelial cells, while it is absent in the cells undergoing oogenesis. Mid-gastric and apical bisections carried out for different time intervals and measurement of specific activities of lysosomal enzymes revealed alterations in their activities suggesting key role during epimorphic and morphallaxis types of regeneration.

Acknowledgements:

Research work in the laboratory is supported by the DST-SERB. LSK thank DST-SERB for funding and NPDF Fellowship. LSK, PMB and NSK thank UGC-SAP-DRS-1 and DST-FIST for funding to the Department of Biochemistry.

LBC-09**Characterization of cyanobacterial isocitrate dehydrogenase enzyme under the influence of citrate**

Balakynthiewshisha Lyngdoh Kynshi, Mayashree B. Syiem

Department of Biochemistry, North-Eastern Hill University, Shillong – 793022, Meghalaya, India

e-address: balalynz17@gmail.com

The enzyme isocitrate dehydrogenase (IDH) catalyzes the decarboxylation of isocitrate to α -KG, and it strongly depends on NADP^+ and $\text{Mn}^{2+}/\text{Mg}^{2+}$ as cofactors. The substrate isocitrate in TCA cycle is made from citrate by the enzyme aconitase. In this study, the IDH enzyme of the cyanobacterium *Nostoc muscorum* Meg 1 was characterized under the influence of citrate. The binding characteristics of isocitrate, NADP^+ and citrate on the IDH enzyme was analyzed by molecular docking and kinetic studies. Kinetic analysis revealed the values of K_m and V_{max} of the IDH with respect to isocitrate to be $25.47 \mu\text{M}$ and 0.295 units/mg protein and $30.25 \mu\text{M}$ and 1.48 units/mg protein with respect to NADP^+ . In the presence of citrate, the K_m and V_{max} were $30.32 \mu\text{M}$ and 0.3 units/mg protein (isocitrate) and $29.42 \mu\text{M}$ and 1.43 units/mg protein (NADP^+). Line-weaver Burk plot exposed that the binding of citrate to IDH is competitive with respect to isocitrate and non-competitive with respect to NADP^+ . Molecular docking studies also displayed that citrate binds to IDH with a high negative binding energies (BE) (-6.88 in specific docking and -7.03 in blind docking), which is very similar to the BE of isocitrate to IDH (-7.29 in specific docking and -7.07 in blind docking). Supplementation of $100 \mu\text{M}$ citrate in the growth medium showed increased in IDH enzyme activity, IDH protein expression (western blot analysis), and its mRNA content (RT-PCR), indicating that with the increased availability of the source of isocitrate, more enzyme was synthesized and thereby augmented the enzyme activity. Presence of $250 \mu\text{M}$ citrate showed very similar results compared to control, whereas $500 \mu\text{M}$ citrate significantly lowered all IDH parameters studied, indicating that at this concentration citrate is toxic to the organism.

Keywords:

IDH; Kinetics; Molecular Docking; Western blot; RT-PCR

AbbreviationsIDH- Isocitrate dehydrogenase; NADP^+ - Nicotinamide adenine dinucleotide phosphate; TCA- Tricarboxylic acid; BE- Binding energies; RT-PCR- Real-time Polymerase chain reaction

LBC-10

Zn Tolerance Exhibited By Carbon And Nitrogen Fixation Machinery Of A Cyanobacterium Isolated From Coal Mine Wastewater: A Potential Zn Bioremediator

Sukjailin Rynthathiang , Meguovilie Sachu, Mayashree B. Syiem
Department of Biochemistry, North Eastern Hill University, Shillong-793022, Meghalaya
e-address: suk.rynth@gmail.com

The cyanobacterium *Anabaena variabilis* MEGCH1 was isolated from coal-mining wastewater where several heavy metal ions were found to be present in varying concentrations. Amongst the metal ions, Zn was present at high concentrations (13.9 μ M). This elicited our interest to see how tolerant was this cyanobacterium towards Zn exposure. As a result, the effects of Zn exposure (10 - 60 μ M) on some major parameters of carbon and nitrogen fixation were analyzed in the organism. These include photosynthetic pigments, rates of photosynthetic and respiratory electron transport chain activities, protein contents of RuBisCO, nitrogenase, and GS enzymes, heterocysts frequency, nitrogenase, and glutamine synthetase enzyme activities, and production of total proteins and carbohydrates. The majority of these biochemical parameters studied demonstrated clear tolerance to Zn exposure up to a concentration of \sim 30 μ M. However, at higher Zn concentrations, the organism displayed significant changes in all parameters studied. The elevation in the total proline content seen in the Zn-treated culture clearly indicated that the organism was under obvious stress. However, that the organism could tolerate a Zn concentration as high as 30 μ M and was functional under the presence of Zn in the culture medium pointed toward the fact that this isolate could be further researched for its biotechnological applications as a Zn bioremediator from wastewater.

Keywords:

Zn toxicity, *Anabaena variabilis* MEGCH1, Carbon and Nitrogen fixation and assimilation, Western blot, SEM and TEM

Abbreviations:

Zn - Zinc, μ M - micromolar, RuBisCO - Ribulose-1,5-bisphosphate carboxylase/oxygenase, GS - Glutamine synthetase, SEM - Scanning electron microscopy, TEM-Transmission electron microscopy.

LBC-11**Toxicity of the herbicide 2,4-D on cyanobacterial CO₂ and N₂ fixations is mediated via molecular interaction with some vital proteins**

Meguovilie Sachu , Mayashree B. Syiem

Department of Biochemistry, North-Eastern Hill University, Shillong – 793022, Meghalaya, India

e-address: meguosac@gmail.com

Among the non-target microorganisms residing in crop fields that are potentially vulnerable to herbicides are cyanobacteria. Their capability to fix atmospheric nitrogen and Carbon dioxide immensely contributes to the maintenance of soil quality and fertility. The present study used molecular docking analysis to check the herbicide 2,4-D's interaction with some core proteins and enzymes involved in CO₂ and N₂ fixations in a cyanobacterium *Nostoc muscorum* Meg 1 isolated from a rice field in Meghalaya. Further, how 2,4-D influences various parameters of CO₂ and N₂ fixations in the cyanobacterium were also investigated. These include various photosynthetic pigments, the oxygen-evolving complex activity of the PSII, the protein contents of RuBisCO, D1 protein, IDH, nitrogenase, and GS enzymes, the heterocyst frequency, nitrogenase, and GS enzyme activities, and the production of total proteins and carbohydrates in the cyanobacterium under varying doses of 2,4-D (50-125 ppm). The mRNA levels of several proteins were also analyzed using RT-PCR analysis. Under exposure to different doses of 2,4-D, all biochemical parameters studied were found to be highly compromised. Herbicide-induced morphological and ultrastructural changes in the organism were highly evident under scanning and transmission electron microscopes. Thus, this study's significance emanates from the detailed examination of the effects of 2,4-D at the biochemical, physiological, and molecular levels.

Keywords:2,4-D; *Nostoc muscorum* Meg 1; Molecular docking; RT-PCR; Western Blot; TEM, SEM**Abbreviations:**

2,4-D- 2,4-Dichlorophenoxyacetic acid; CO₂- Carbon dioxide; N₂- Atmospheric nitrogen; PSII- Photosystem II; RuBisCO- Ribulose-1,5-bisphosphate carboxylase/oxygenase; IDH- Isocitrate dehydrogenase; GS- Glutamine synthetase; mRNA- Messenger ribonucleic acid; RT-PCR- Real Time-Polymerase chain reaction; SEM- Scanning electron microscopy; TEM- Transmission electron microscopy

LBC-12**Enzymatic And Non-Enzymatic Antioxidant Response To Cd²⁺ Stress In A Cyanobacterium**

Lanakadaphi Rangat Chullai , Meguovilie Sachu, Mayashree B. Syiem

Department of Biochemistry, North Eastern Hill University, Shillong-793022, Meghalaya

e-address: chullai_la@yahoo.com

The oxidant-antioxidant homeostasis in the cyanobacterium *Nostoc muscorum* Meg 1 was analyzed under Cd²⁺ exposure. The presence of different Cd²⁺ doses (10 and 20 μM) showed an increase in the ROS content by 63 % and 105 % as compared to the control. Exposure to increasing Cd²⁺ concentration results in an increase in protein oxidation and lipid peroxidation which indicated cellular damage. Subsequently, there was a substantial incline in the activities of various oxidant mitigating enzymes such as CAT, SOD, GR, and GPx upon exposure to 10 μM Cd²⁺ by 44 %, 30 %, 46%, and 34% respectively. The non-enzymatic antioxidants (proline, ascorbic acid, GSH, phytochelatin, cysteine, total thiol content, phenol, and flavonoid) also recorded a significant rise when exposed to 10 μM Cd²⁺ concentration, indicating that the cells were equipped to mount a multi-pronged attack on the increased ROS. The whole antioxidant defense mechanism was highly compromised in presence of 20 μM Cd²⁺. The total amount of CAT, SOD, GR, and GPx under western blot analysis indicated disruption of new protein synthesis and breakdown of their existing enzyme molecules when exposed to higher Cd²⁺ concentrations. Furthermore, SEM and TEM images revealed several undesirable changes in the morphology and ultrastructure of the organism due to Cd²⁺ exposure. Nevertheless, this study elucidates how the microbe gathered a range of various cellular metabolites to combat oxidative stress caused by heavy metal exposure such as Cd²⁺.

Keywords:

Cd²⁺, ROS, Antioxidants, Western blot, SEM, and TEM

Abbreviations:

Cd²⁺- cadmium ions, ROS- Reactive oxygen species, CAT- catalase, SOD- superoxide dismutase, GR- glutathione reductase, GPx- glutathione peroxidase, GSH- reduced glutathione, SEM- scanning electron microscope, TEM- transmission electron microscope

LB-01**Comparative Analysis of Relative Efficacy of Synthetic and Natural Drugs in Endometriosis Through Computational Approach**Indra Singha ^a, Ranjit Shawb ^b, Pritha Sahab ^b, Krishna Kumar Ojhac ^c, Radha Chaube ^b^aSchool of Biotechnology, Banaras Hindu University, Varanasi-221005, Uttar Pradesh, India^bDepartment of Zoology, Institute of Science, Banaras Hindu University, Varanasi-221005, Uttar Pradesh, India^c Department of Bioinformatics, Central University of South Bihar, Gaya-824236, Indiae-address: chauberadha@rediffmail.com

Endometriosis is a chronic, inflammatory condition of high incidence and with serious consequences. Several drugs are used for the treatment of this disease, but the treatment is mainly to ameliorate the symptoms and cannot be used to completely check the disease. Recently, several synthetic compounds have proved to be useful in treating its symptoms by inhibiting aromatase, which is responsible for the pathogenesis of this painful illness. Nevertheless, synthetic drugs pose several side effects, including headaches, osteoporosis, and so on. This dire scenario advocates the search for therapeutic formulations based on natural compounds. Thus, the present study was hypothesized to evaluate the comparative efficacy of the synthetic and natural drugs used in endometriosis, using the bioinformatics approach. A thorough investigation of the relative efficacy of these drugs for endometriosis is essential for the development of novel treatment approaches for this debilitating condition. CB-Dock was employed to perform molecular docking of the aromatase enzyme with two synthetic and three natural drugs to predict their molecular interactions, and binding affinities. The curcumin-aromatase complex was further subjected to MD simulations to determine its stability, with the goal of applying it to natural compound-based computer-aided drug discovery. Among the natural drugs, curcumin was observed to dock (showing a docking score of -8), with greater binding interaction with aromatase. The RMSD profile, hydrogen bonds, RMSF, and Rg values of the complex were stabilized after 50 ns, which was an indicator of the stable binding pose of the curcumin-aromatase complex. These in-silico findings are the basis for proposing that curcumin can be considered as a potential binding agent to inhibit the aromatase enzyme in the treatment of endometriosis. Molecular modelling and dynamics results suggest that curcumin and aromatase are forming a stable complex and that curcumin can be targeted as a drug in the treatment of endometriosis.

Keywords:

Endometriosis; Synthetic; Natural drug; Aromatase; Estrogen; Molecular docking; Molecular dynamics simulation; Curcumin; In-silico; Treatment.

Acknowledgements:

Partial funding of IOE, BHU is acknowledged.

References:

1. C. Mehedintu, et al., Endometriosis still a challenge, *Journal of medicine and life* 7 (3) (2014) 349-357, <https://pubmed.ncbi.nlm.nih.gov/25408753/>
2. L.C. Giudice, Clinical practice: Endometriosis, *The New England Journal of Medicine* 362 (25) (2010) 2389-2398, <https://doi.org/10.1056/NEJMc1000274>
3. D. L. Olive, *Endometriosis in Clinical Practice*, London and New York: Taylor and Francis (11) (2005)
4. M. Fukunaga, Uterus-like mass in the uterine cervix: superficial cervical endometriosis with florid smooth muscle metaplasia? *Virchows Archiv* 438 (3) (2001) 302-305, <https://doi.org/10.1007/s004280000299>.

LB-02**Metastable Intermediates During Fibril Formation of Mutant Forms α -Synuclein and Their Relation with Fibril Stability and Disease Progression**

G. Priyanka , Archi Saurabh, N. Prakash Prabhu

Department of Biotechnology and Bioinformatics, School of Life Sciences, University of Hyderabad, Hyderabad – 500046, India.
e-address: gpriyanka27496@gmail.com

α -Synuclein (α -syn) is a 140 amino acid intrinsically disordered protein (IDP) found predominantly in the presynaptic neuron terminals in the brain. The abnormal accumulation of α -synuclein called Lewy bodies is the main characteristic of synucleopathies such as Parkinson's disease (PD)¹. Experimental studies suggest that α -syn transforms into fibril through exposure to hydrophobic surfaces at the central region of the protein referred to as the fibril core covering the residues V37 to D98². Five PD familial mutations located in the fibrillar core region include E46K, H50Q, and A53T which cause early onset of PD while G51D, and A53E cause late onset³. The conformational changes driving the fibril assembly of these mutants are not fully understood. The present study analyses the conformational plasticity in the fibrillar core region using replica exchange molecular dynamics (REMD) simulations of wild type (WT) and its mutant forms. The conformations obtained were analysed using c-PCA and clustering methods to identify the important metastable intermediate structures in WT and mutant forms. The differences in the number of inter-chain hydrogen bonds, center of mass distance between the chains, solvent accessible surface area (SASA), inter and intra-chain salt bridges, radius of gyration (Rg), solvation energy, and inter-chain interaction energy for all the intermediate structures obtained were analysed and compared. The results show that the plasticity of the fibril core residues shows significant differences in their inter- and intra-chain interactions and backbone torsion angles. The fibril pathway is also affected by the variation in the mutants, thus affecting the final fibril stability.

References:

1. Oliveira, L. M. A. et al. Alpha-synuclein research: defining strategic moves in the battle against Parkinson's disease. *npj Park. Dis.* 7, 65 (2021).
2. Meade, R. M., Fairlie, D. P. and Mason, J. M. Alpha-synuclein structure and Parkinson's disease – lessons and emerging principles. *Mol. Neurodegener.* 14, 29 (2019).
3. Guerrero-Ferreira, R., Kovacic, L., Ni, D. and Stahlberg, H. New insights on the structure of alpha-synuclein fibrils using cryo-electron microscopy. *Curr. Opin. Neurobiol.* 61, 89-95 (2020)

LB-03

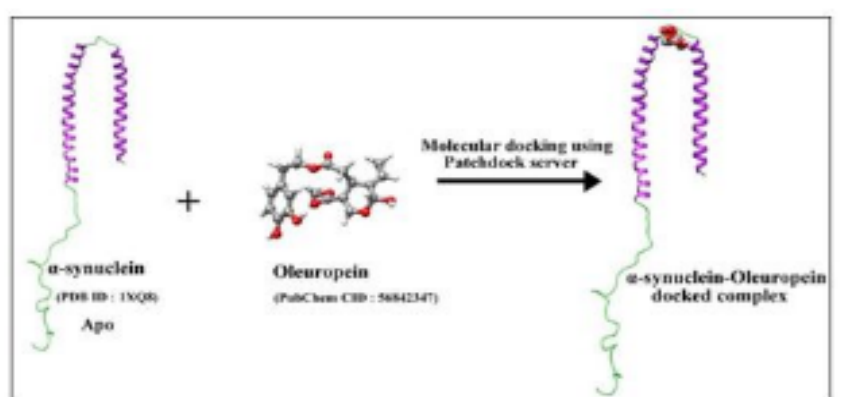
An in-silico investigation on the role of Oleuropein aglycone on the aggregation propensity of α -Synuclein

Priyanka Borah, Venkata Satish Kumar Mattaparthi

Molecular Modelling and Simulation Laboratory, Department of Molecular Biology and Biotechnology, Tezpur University, Assam, India.

e-address: psumuborah@gmail.com

After Alzheimer's disease, Parkinson's disease (PD) is the second most common progressive neurodegenerative brain disorder. The misfolding and aggregation of Alpha-synuclein (α -synuclein) is the primary pathogenesis of this disease. It is distinguished by the Lewy bodies and Lewy neurites, which are aggregated fibrillary forms of α -synuclein. Preventing α -synuclein misfolding and subsequent aggregation is one of the most promising strategy for treating Parkinson's disease. Oleuropein aglycone (OleA) has recently been shown to stabilise the monomeric structure of α -synuclein, allowing non-toxic aggregates to develop. Understanding the conformational dynamics of the α -synuclein monomer in the presence of OleA is therefore crucial. Using Molecular Dynamics (MD) Simulation, we studied the influence of OleA on the conformational dynamics and aggregation propensity of α -synuclein. The intramolecular distance between the non-amyloid-component (NAC) domain and the C-terminal domain of α -synuclein was enhanced when OleA was bound to α -synuclein, according to MD trajectory analysis. OleA was discovered to engage with the N-terminal domain of α -synuclein, thereby blocking this area from interacting with membranes and lipids and thus prevents formation of cellular hazardous aggregates. We found that the binding affinity between α -synuclein and OleA is certainly high based on the binding free energy (BFE) analysis. The influence of OleA on the structure and stabilisation of α -synuclein monomer, which favours the creation of stable and non-toxic aggregates, is thus substantiated by our findings in this work.



Acknowledgement:

The authors acknowledge Tezpur University for providing the research facilities. P.Borah acknowledges DST for the grant of DST-INSPIRE Fellowship (IF190310) for research purpose.

References:

1. Borah, P. et al. Computational investigation on the effect of Oleuropein aglycone on the α -synuclein aggregation. *Journal of Biomolecular Structure and Dynamics*, 39(4), 1259-1270, 2021.
2. Palazzi, L. et al. Oleuropein aglycone stabilizes the monomeric α -synuclein and favours the growth of non-toxic aggregates. *Scientific reports*, 8(1), 8337, 2018.

LB-04

Effect of pY39 Post-translational modification on the interactions between α -Synuclein and Lipid Membrane

Dorothy Das , Venkata Satish Kumar Mattaparthi

Molecular Modelling and Simulation Laboratory, Department of Molecular Biology and Biotechnology, Tezpur University, Tezpur-784 028, Assam, India.
e-address: dorthyds.1010@gmail.com

The nature of abnormal accumulation and aggregation of amyloid fibrils of α -synuclein causing formation of lewy bodies and neurites at the synaptic terminals acts as a major pathological hallmark of Parkinson's disease and other synucleopathies. It is well studied that Post-translational modifications (PTMs) in proteins may act as crucial factor in inhibiting its functionality on interaction with biological membranes and membrane proteins that are important for the release of neurotransmitters and the plasticity of synapses. Recently one of such PTMs in α -synuclein is demonstrated to be phosphorylation at Tyrosine 39 residue that controls the biological function of α -synuclein in regulating synaptic vesicles as it is dependent on its association to the lipid bilayer which can be crucial for both pathological dysfunction and normal function. From the Molecular Dynamics study, we found that phosphorylation at Y39 position in α -synuclein to have marked effect on its interaction with the lipid membrane. The conformational snapshots of α -synuclein obtained from 100ns molecular dynamics simulation showed high degree of fluctuation in N-terminal region resulting in the disruption of helix-2 binding region and thereby affecting the binding to the lipid bilayer. As a result, aggregation of α -synuclein may take over through its interaction with other proteins and vesicles.

Acknowledgement

We acknowledge for the support and guidance of our funding agency DST-SERB

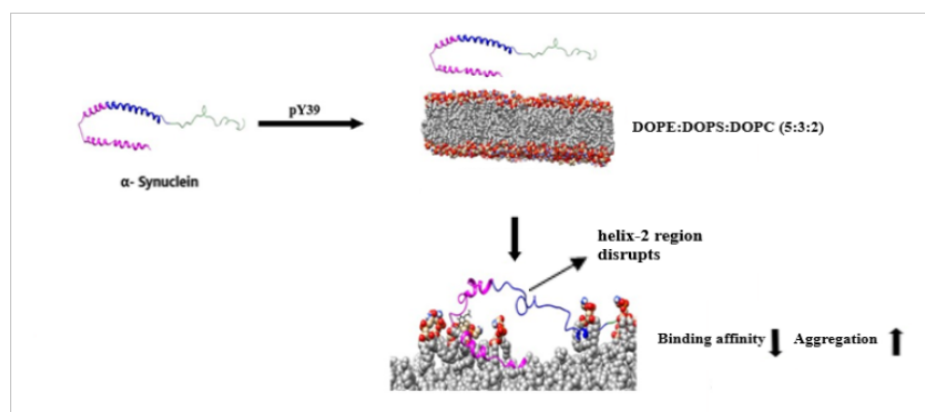


Figure 43: Graphical representation of association of pY39 α -synuclein with Lipid Membrane during 100 ns Molecular Dynamics simulation

References:

1. Zhao, K. et.al. Parkinson's disease-related phosphorylation at Tyr39 rearranges α -synuclein amyloid fibril structure revealed by cryo-EM. 2019, PNAS, 1-11.
2. Dikiy, I. et.al. Semisynthetic and in vitro phosphorylation of alpha-synuclein at Y39 promotes functional partly-helical membrane-bound states resembling those induced by PD mutations. 2016, ACS Chem, Biol., 11(9), 2428-2437.

LB-05**Immunoinformatics Analysis of Antigenic Epitopes and Designing of a Multi-epitope Peptide Vaccine from Putative Nitro-reductases of *Mycobacterium tuberculosis* DosR**

Mohd Shiraz , Surabhi Lata, Pankaj Kumar, Umate Nachiket Shankar, Mohd. Akif,
Department of Biochemistry, School of Life Sciences, University of Hyderabad, Hyderabad 500046, India
e-address: mohd.shiraz1992@gmail.com

Mycobacterium tuberculosis (Mtb) resides in alveolar macrophages as a non-dividing and dormant state causing latent tuberculosis. Currently, no vaccine is available against the latent tuberculosis. Latent Mtb expresses ~48 genes under the control of DosR regulon. Among these, putative nitroreductases have significantly high expression levels, help Mtb to cope up with nitrogen stresses and possess antigenic properties. In the current study, immunoinformatics methodologies are applied to predict promiscuous antigenic T-cell epitopes from putative nitro-reductases of the DosR regulon. The promiscuous antigenic T-cell epitopes prediction was performed on the basis of their potential to induce an immune response and forming a stable interaction with the HLA alleles. The highest antigenic promiscuous epitopes were assembled for designing an in-silico vaccine construct. A TLR-2 agonist Phenol-soluble modulin alpha 4 was exploited as an adjuvant. Molecular docking and Molecular Dynamics Simulations were used to predict the stability of vaccine construct with the immune receptor. The predicted promiscuous epitopes may be helpful in the construction of a subunit vaccine against latent tuberculosis, which can also be administered along with the BCG to increase its efficacy. Experimental validation is a prerequisite for the in-silico designed vaccine construct against TB infection.

LB-06

CHOLAR: Characterization of lncRNA from raw reads

Haneesh Jindal , Anubha Dey , Manjari Kiran

Department of Systems and Computational Biology, School of Life Sciences, University of Hyderabad.

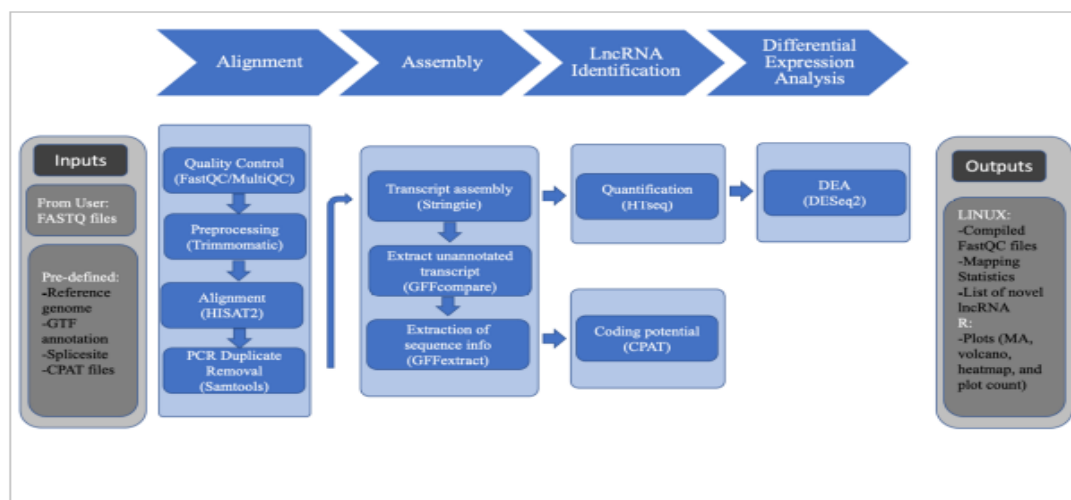
e-address: schosio@protonmail.com

Objectives:

Development of RNA-seq analysis pipeline with GUI.

Background:

RNA-sequencing has been used for numerous discoveries in research, from distinguishing immune cell subtypes to differential gene expression between cancer versus normal tissue types. Another application of RNA-seq is identifying novel transcripts involved in various biological processes. The most relevant are context and cell-type-specific non-coding RNAs, such as long non-coding (lncRNAs), which have become a case point for most transcriptomic studies proving their role in regulating gene expression, post-transcriptional regulation, and epigenetic regulation. It is crucial to check the relation expression of lncRNAs in transcriptomic-wide studies.



Results:

Our group has developed an automated lncRNA expression and differential expression analysis pipeline. The only requirement from the user side is raw data in FASTQ format. The user gets a list of known and novel lncRNAs and differential gene expression between condition(s). The pipeline comes with a user-friendly GUI, eliminating the need for the user to be versed in complex transcriptome analysis and the UNIX environment.

Code availability:

The source code for the tool is available under an open-source license at <https://github.com/schosio/CHOLAR>.

LB-07**Screening Of Disease Candidates in Hepatocellular Carcinoma by Gene Ontology inferred through a Protein-Protein Interaction Graph**Satya Kiran Veera ^a, V. Siva Ranjani ^b, S. B. Rao ^c, P Manimaran ^d^aAccolite Digital, Nanakaram Guda, Hyderabad-500 032, Telangana, India.^bDepartment of Plant Molecular Biology and Bioinformatics, Tamil Nadu Agricultural University, Coimbatore-641 003, India.^cCR Rao Advanced Institute of Mathematics Statistics and Computer Science, University of Hyderabad Campus, Gachibowli, Hyderabad-500 046, India.^dSchool of Physics, University of Hyderabad, Gachibowli, Hyderabad -500 046, Telangana India.e-address: vskirann@gmail.com

Prediction of disease genes elucidate lead candidates for drug design in medical research. Hepatocellular (liver) Carcinoma, prevalent more in men than women, contributes to high incidence of mortality worldwide. There is extensive research on identifying genes critical to liver carcinoma that involves both experimental and in-silico methods. Most of the studies have a broad perspective that might lack a targeted approach to elucidate specific attributes. In this paper we employed an alternate method to determine highly probable gene targets by adopting a protein protein interaction network and using gene ontology terms. In our study, we came across candidate genes which are potential targets for disease progression in hepatocellular carcinoma.

Keywords:

Hepatocellular carcinoma, Human Cancer Gene Network, centrality measures.

LB-08

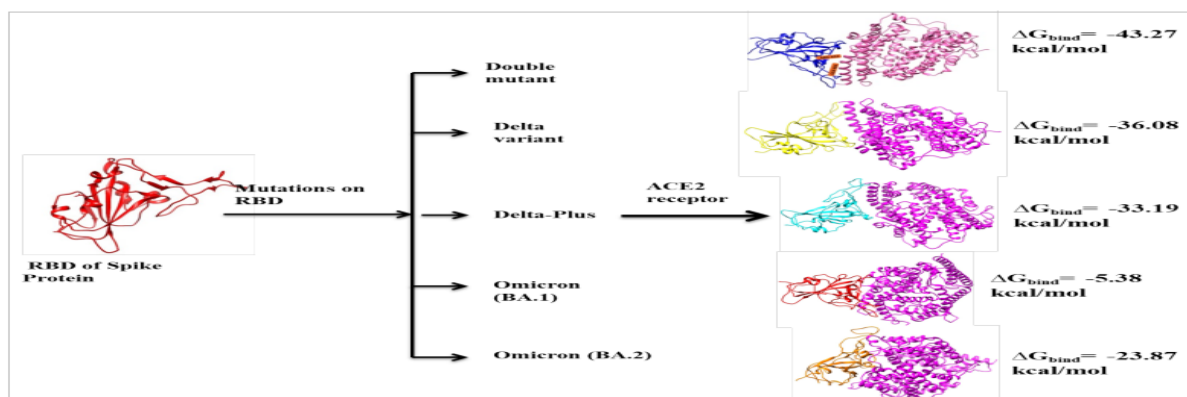
Effect of mutations on the RBD of spike protein on its interaction with the ACE2 receptor of human host

Chaine Das, Venkata Satish Kumar Mattaparthi

Molecular Modeling and Simulation Laboratory, Department of Molecular Biology and Biotechnology, Tezpur University, Tezpur, Assam, 784 028, India.

e-address: chainedas97@gmail.com

The ongoing spread of an infectious COVID-19 is caused by SARS-CoV-2. Due to its high prevalence and protracted incubation period, SARS-CoV-2, an encapsulated positive-stranded RNA virus, poses exceptional challenges for the healthcare system. The SARS-CoV-2 spike protein has gained significant attention since the outbreak of the COVID-19 pandemic due to its role in the entry of the virus into the host cell. Recent studies have shown that SARS-CoV-2 has undergone mutations and generated several variants, with new variants of the virus showing up in different places across the globe. Some of the widespread SARS-CoV-2 variants are Double mutant (DM) (B.1.617), Delta (B.1.617.2), Delta-Plus (B.1.617.1) and Omicron variants that include (BA.1, BA.2). Here, we have focused on the effect of various mutations in the RBD (Receptor Binding Domain) region of spike protein on its binding to the host cell receptor protein, angiotensin-converting enzyme 2 (ACE2). From the molecular dynamics simulation, we observed that the mutated spike protein utilizes unique strategies to achieve stable binding to ACE2. Using MM-GBSA algorithm, the binding affinity between the RBD of spike protein (Wild type, DM, Delta, Delta-Plus, BA.1 and BA.2) and ACE2 were determined. We found ΔG_{bind} value to be -28.23 kcal/mol for Wild type, -43.27 kcal/mol for Double Mutant, -36.08 kcal/mol for Delta, -33.19 kcal/mol for Delta-Plus, -5.38 kcal/mol for BA.1 and -23.87 kcal/mol for BA.2. For a virus to enter the host cells, the spike protein must maintain a stable binding with ACE2 receptor. And it has been observed that those mutations enable stable binding of spike protein to its receptor ACE2.



Acknowledgement

The authors extend their deepest gratitude to Tezpur University and University Grants Commission, India, for the start-up grant.

References:

1. Das, C., Hazarika, P.J., Deb, A., Joshi, P., Das, D., Mattaparthi, M.V.S., 2022. Effect of Double Mutation (L452R and E484Q) in RBD of Spike Protein on its Interaction with ACE2 Receptor Protein.

Biointerface research in applied chemistry, 13, pp. 97.

2. Das, C., Mattaparthi, M.V.S., 2022. Effect of mutations in the SARS-CoV-2 spike RBD region of Delta and Delta-plus variants on its interaction with ACE2 Receptor Protein. Biointerface research in applied chemistry (Accepted).

LB-09**Microsatellite Based Molecular Diversity Among Selected Segregants Derived from Mahateora X Biol-212 and Berhampore Local X Mahateora In Grasspea**

Pratik Saha , Sayani Bandyopadhyay, Raghunath Sadhukhan, Md. Nasim Ali

Department of Agricultural Biotechnology, Faculty of Agriculture, Bidhan Chandra Krishi Viswavidyalaya, Mohanpur, Nadia, West Bengal 741252,

^bDepartment of Genetics and Plant Breeding, Faculty of Agriculture, Bidhan Chandra Krishi Viswavidyalaya, Mohanpur, Nadia, West Bengal 741252,

e-address: pratiksaha0906@gmail.com

Grasspea (*Lathyrus sativus* L.) belongs to the family Fabaceae and the tribe *Vicieae* having chromosome number ($2n = 2x = 14$). India is the largest producer of lathyrus which is the third most important pulse crop after chickpea and pigeon pea. It is one of the most important crops with respect to climate resilience since it can thrive overcoming both biotic and abiotic stresses. The desirability of the crop is constrained by the presence of an anti-nutritional compound β -N-oxalylamino-L-alanine (BOAA) or β -N-oxalyl-L- α , β -diaminopropionic acid (ODAP) which causes neurolathyrism, a paralytic disorder. In the present study, the genetic diversity of the segregating populations (F_2 and F_3) developed from two sets of crosses (Mahateora x BIO L-212 and Berhampore Local x Mahateora) was assayed using microsatellite markers. A total of 30 SSRs were used for molecular diversity of which 19 were found to be polymorphic. After PCR amplification, a binary matrix was constructed and the segregants were clustered using DARwin v6 software. A total of 7 distinct groups were formed and Cluster V being the largest with 15 cluster members. This study identified 8 SSR markers showed higher Polymorphism Information Content and Marker Index value indicating that they can be used in molecular diversity analysis in lathyrus for future breeding programmes.

Keywords:

Cluster, Grasspea, Genetic diversity, Microsatellite and Segregating population.

LB-10**Assessing Biochemical Descriptors Affecting Fibre Quality of Tossa Jute**Sayani Bandyopadhyay, ^a Pratik Saha ^a, Subhojit Datta ^b, Md. Nasim Ali ^a^aDepartment of Agricultural Biotechnology, Faculty of Agriculture, Bidhan Chandra Krishi Viswavidyalaya, Mohanpur, Nadia -741252, West Bengal, India,^b Biotechnology Unit, Crop Improvement Division, ICAR-Central Research Institute for Jute and Allied Fibres, Barrackpore, Kolkata- 700121, West Bengal, Indiae-address: sayanichitrangada@gmail.com

Jute fibre is a bio-degradable and environmental friendly bast fibre in nature which are utilized for commercial purposes. Jute fibre has more lignin content and less cellulose content compared with the other bast fibre crops. These reduce the fibre quality which needs to be improved to replace synthetic fibre. The Objective of the present work was to understand the biochemical factors affecting the fibre quality in jute. Here, we selected two *tossa* jute varieties named JRO 524 with coarse fibre and JBO 1 with finer fibre. We estimated the acid insoluble lignin, cellulose content and performed the Phenylalanine Ammonia Lyase (PAL) and Cinnamyl Alcohol Dehydrogenase (CAD) enzyme assay which are involved in lignin biosynthesis from the fibre of those two varieties at 30 and 60 Days after germination (DAG). The fibre of JBO 1 contained less acid insoluble lignin content and more cellulose as compared with JRO 524. The activities of PAL and CAD enzymes were higher in the fibre of JRO 524 than JBO 1 at both developmental stages. This finding signifies that the lignin content negatively correlated with fibre fineness where as cellulose content positively correlated with fibre bundle strength. Thus, JBO 1, having less lignin and more cellulose content, could be used as a genetic resource in order to improve the fibre quality.

Keywords:

Tossa jute, PAL, CAD, lignin and cellulose

LB-11**Differential Effect Of Dihydric Alcohols On Thermo- And Cryo-Stability Of Apo-myoglobin**

Subhasree Ghosh, N. Prakash Prabhu

Department of Biotechnology & Bioinformatics, University of Hyderabad, Hyderabad - 500046.

e-address: subhasreeghosh4@gmail.com

Protein stability is a major issue of consideration in diverse areas of biotherapeutic and biotechnological applications^{1,2}. Naturally occurring osmolytes are well known to stabilize proteins against environmental stress. A wide range of synthetic osmolytes are also being used to enhance protein stability in industries. Earlier studies established that alcohols are effective protein denaturant and its efficiency amplifies with the increased chain length. However, it is also observed that ethylene glycol destabilizes proteins like alcohols at room temperature and above, while at sub-zero temperatures it stabilizes.³ The present work analyzes whether this differential effect is a generic property of all dihydric alcohols using apo-myoglobin (ApoMb) as a model protein. Thermal and cold denaturation of the protein in the presence of varying concentrations of five different dihydric alcohols: ethylene glycol, 1,2-butanediol, 1,4-butanediol, 1,2-hexanediol and 1,6-hexanediol was carried out and compared with a well-known stabilizing osmolyte, glycerol. The free energy change over the entire temperature range was analysed. Further, structural changes at different temperatures ranging from -10 to 70 oC were also examined using CD and fluorescence techniques. The investigation suggests that all five dihydric alcohols stabilize ApoMb against cold denaturation and shifts the temperature of maximum stability to lower temperature, whereas they destabilize the protein during thermal unfolding in a concentration-dependent manner. The results also show that all the dihydric alcohols have similar characteristic with the highest stabilizing effect observed in 1,6-hexanediol. These cosolvents increased the stability of secondary structures and the compaction of the protein at sub-zero temperature conditions.

References:

1. Authelin, J.-R. et al. Freezing of Biologicals Revisited: Scale, Stability, Excipients, and Degradation Stresses. *J. Pharm. Sci.* 109, 44–61 (2020).
2. Rathore, N. & Rajan, R. S. Current perspectives on stability of protein drug products during formulation, fill and finish operations. *Biotechnol. Prog.* 24, 504–514 (2008).
3. Naidu, K. T., Rao, D. K. & Prabhu, N. P. Cryo vs Thermo: Duality of Ethylene Glycol on the Stability of Proteins. *J. Phys. Chem. B* 124, 10077–10088 (2020).

LB-12**Characterization of leishmanial arginyl synthetase for the development of novel therapeutics**Fouzia Nasim, Insaf Ahmed QureshiDepartment of Biotechnology and Bioinformatics, School of Life Sciences University of Hyderabad, Hyderabad 500046, India
e-address: insaf@uohyd.ac.in

Visceral leishmaniasis, caused by the protozoan parasite *Leishmania donovani* affects the human population worldwide and has no proper treatment till date. Since aminoacyl tRNA synthetases have been considered as promising drug targets in case of bacteria, fungi etc., it would be interesting to validate these macromolecules for the development of antileishmanials. In the current study, arginyl tRNA synthetase of *Leishmania donovani* (LdArgRS) was cloned, purified and characterized by various biophysical and biochemical approaches. It exhibited critical differences in the ligand binding sites when compared to its human counterpart and the presence of novel insertion of 110 amino acids within its catalytic domain. Circular dichroism study revealed that the protein comprised of more α -helices when compared to β -sheets. The T_m of the protein was observed to be 41°C while its structural integrity destabilised with lower concentrations of guanidine hydrochloride than that of urea. However, binding of ligands to the protein did not affect T_m values on a larger scale. On subjecting the protein to different pH conditions, the α -helical content decreased gradually towards both extremities on a pH scale. Furthermore, intrinsic fluorescence analysis depicted that the protein shows a blue shift towards acidic pH and minimal red shift in basic conditions. Although, varying acrylamide concentration could quench the fluorescence of the protein, no effect was seen for potassium iodide. LdArgRS depicted more affinity towards ATP than L-arginine even in the absence of tRNA^{arg} and its highest activity was observed at pH 6.5 and 40°C. Simultaneously, the enzymatic activity was found to be higher with manganese and potassium ions among various divalent as well as monovalent ions tested. We are now screening the compound library on a pursuit of finding a suitable compound that can inhibit this leishmanial enzyme at minimal concentrations.

LB-13**Advanced Glycated End-Products Activate Notch1 Signaling In Podocytes: Implications In Diabetic Nephropathy**

Ashish Kumar Singh ^a, Rajkishor Nishad ^a, Prajakta Meshram ^a, G Bhanuprakash Reddy ^b, Anil Kumar Pasupulati ^a

^aDepartment of Biochemistry, University of Hyderabad, Hyderabad, India,

^bDepartment of Biochemistry, National Institute of Nutrition, Hyderabad, India

e-address: 19lbph05@uohyd.ac.in

Advanced glycation end-products (AGEs) are implicated in the pathogenesis of diabetic nephropathy (DN). Previous studies have shown that AGEs contribute to glomerulosclerosis and proteinuria. Podocytes, terminally differentiated epithelial cells of the glomerulus and the critical component of the glomerular filtration barrier, express the receptor for AGEs (RAGE). Podocytes are susceptible to severe injury during DN. In this study, we investigated the mechanism by which AGEs contribute to podocyte injury. Glucose-derived AGEs were prepared in vitro. Reactivation of Notch signaling was examined in AGE-treated human podocytes (in vitro) and glomeruli from AGE-injected mice (in vivo) by quantitative reverse transcription-PCR, western blot analysis, ELISA, and immunohistochemical staining. Further, the effects of AGEs on epithelial to mesenchymal transition (EMT) of podocytes and the expression of fibrotic markers were evaluated. Using human podocytes and a mouse model, we demonstrated that AGEs activate Notch1 signaling in podocytes and provoke EMT. Inhibition of RAGE and Notch1 by FPS-ZM1 (N-Benzyl-4-chloro-N-cyclohexylbenzamide) and DAPT (N-[N-(3,5-Difluorophenacetyl)-L-alanyl]-S-phenyl glycine t-butylester), respectively, abrogates AGE-induced Notch activation and EMT. Inhibition of RAGE and Notch1 prevents AGE-induced glomerular injury and proteinuria. Furthermore, kidney biopsy sections from people with DN revealed the accumulation of AGEs in the glomerulus with elevated RAGE expression and activated Notch signaling. The data suggest that AGEs activate Notch signaling in the glomerular podocytes. Pharmacological inhibition of Notch signaling by DAPT ameliorates AGE-induced podocytopathy and fibrosis. Our observations suggest that AGE-induced Notch reactivation in mature podocytes could be a novel mechanism in glomerular disease and thus could represent a novel therapeutic target.

LB-14**Utilization Of Tannery Solid Waste For Enzyme Induced Carbonate Precipitation Process**

Parthasarathy Baskaran Sujiritha , Vijan Lal Vikash, Ganesan Ponesakki, Niraikulam Ayyadurai,
Numbi Ramudu Kamini

Department of Biochemistry and Biotechnology, CSIR - Central Leather Research Institute, Chennai, 600020, Tamil Nadu, India
e-address: sujirithabaskaran@gmail.com

Rapid industrialization and urbanization increases the demand of cement, a major construction material used for infrastructure development and ground improvement applications. The process of manufacture of cement is extremely energy intensive process and a major source of carbon dioxide emissions. Therefore, researchers are making efforts to reduce the consumption of cement in soil stabilization through the use of biocementation techniques. Biocementation via enzyme induced carbonate precipitation (EICP) is an emerging ground improvement technique that utilizes free urease enzyme for calcium carbonate precipitation. In EICP, the urease enzyme catalyses the hydrolysis of urea and in the presence of calcium ions, the calcium carbonate (CaCO_3) is precipitated. The precipitated calcium carbonate coats the soil particles, fills the void space and increase the strength and stiffness of the soil matrix. In the present study, the feasibility of utilizing tannery lime liquor as calcium source for EICP process with an extracellular urease enzyme produced by *Arthrobacter creatinolyticus* MTCC 5604 was investigated. The EICP was optimum with 1000 U of urease, 1.0 M urea and 1.0 M $\text{CaCl}_2 \cdot 2\text{H}_2\text{O}$ for test tube experiments. Sand columns treated by EICP with laboratory grade $\text{CaCl}_2 \cdot 2\text{H}_2\text{O}$ exhibited unconfined compressive strength (UCS) of 810 kPa, while the sand column treated with calcium solution obtained from lime liquor yielded 780 kPa. The crystalline phases and morphology of the CaCO_3 precipitate were analyzed by XRD, FTIR and SEM-EDX. The results showed the formation of calcite and vaterite polymorphs of calcium carbonate. Utilization of lime liquor in EICP could reduce the pollution load and sludge formation that are generated during the pre-tanning operations of leather manufacturing. This study could be a viable approach to achieve sustainable biocementation for large scale applications.

LB-15

Preferential Anti-Apoptotic and Imaging Potentials of Dual Acting Oleyl Chitosan Coated Quercetin Nanocomposite: In Vitro Perspectives

Thiagarajan Hemalatha , Numbi Ramudu Kamini, Niraikulam Ayyadurai

Department of Biochemistry and Biotechnology, CSIR – Central Leather Research Institute, Chennai – 600020, Tamil Nadu, India
e-address: hemabiotek.t@gmail.com

Quercetin is a multifunctional hydrophobic bioflavonoid abundantly found in plant foods. Quercetin exerts anti-tumor effect on a wide range of cancer cell lines. The major limitations hampering the pharmacological property of quercetin include its poor water solubility, low oral bioavailability and rapid gastrointestinal digestion. Nanoformulations of quercetin are the emerging effective strategies to overcome the above limitations. Therefore, the study aims to prepare a quercetin-based nanocomposite (QNC) with theranostic potential i.e., for use in diagnostics and cancer therapeutics. Nanocomposite comprising of iron/gold nanohybrid particles, coated with oleyl chitosan, conjugated with folic acid and loaded with quercetin was synthesized and physico-chemically characterized. Presence of iron/gold hybrid nanoparticles served as dual modality contrast agents for both magnetic resonance imaging (MRI) and computed tomography (CT) imaging. Presence of folic acid in the nanocomposite acted as a ligand for targeting cell membrane and enhancing nanoparticle endocytosis via folate receptor. The preferential cytotoxicity exhibited by QNC towards cancer cell line (MDA-MB-231) and non-toxic effect towards normal cell line (NIH 3T3), is yet another promising aspect of QNC. Together, the results prove that, QNC could be used as dual modality contrast agent for both MRI and CT, and it also demonstrated significant anti-cancer effect on tumor cell line.

LB-16**Fleshings Extract As An Alternate Nitrogen Source For Production Of Industrial Enzymes**

Mannankatti Ramkumar, Puhazhendi Puhazhselvan, Numbi Ramudu Kamini

Department of Biochemistry and Biotechnology, CSIR - Central Leather Research Institute, Chennai, 600020, Tamil Nadu, India
e-address: ramkumarbio97@gmail.com

Leather industry gains prominence in economy of under-developed and developing countries through generation of enormous employment and foreign exchange. However, the discharge of huge quantities of solid and liquid wastes have raised serious concerns on account of their environmental impacts. Among the solid wastes, fleshing waste is the major hazardous solid waste, which is susceptible to putrefaction and also emits obnoxious smell due to the presence of ample quantity of protein and moisture. In India, around 700,000 tons of skins and hides are converted to leather annually, which results in the generation of 100,000 tons of fleshing wastes. The valuable biomolecules such as lipids (4-18%) and proteins (50-60%) present in the fleshing waste have potential for various application. In the present study, the fleshings extract was prepared by enzymatic hydrolysis of the tannery fleshing wastes followed by the spray drying. The process parameters such as atomization pressure, flow rate and inlet air temperature were standardized by RSM to obtain maximum recovery of product with less moisture content. The RSM results showed that the recovery of product was 96.70% under optimum conditions of inlet air temperature, 175 °C, atomization pressure, 1 kg/cm² and feed flow, 2.0 ml/min. Total nitrogen and amino nitrogen of fleshings extract was 13.19 and 3.62%, respectively and was similar to the nitrogen content of commercial nitrogen sources. The results on enzyme production revealed that fleshings extract could be used as nitrogen source by replacing the soybean meal, meat extract and corn steep liquor towards production of enzymes such as *Bacillus subtilis* protease, *Arthrobacter creatinolyticus* urease and *Aspergillus niger* lipase, respectively. Thus, the development of microbiological media supplement could provide sustainable solution to the issue of fleshing waste disposal and the process serve as baseline for circular economy approach.

LB-17**Preparation and Characterization of Bioactive Composite Material for Tissue Regeneration Application**

Vinayagamurthy Kalaiselvi , Vijan Lal Vikash, Niraikulam Ayyadurai, Numbi Ramudu Kamini,
Ponesakki Ganesan

Department of Biochemistry and Biotechnology CSIR-Central Leather Research Institute (CLRI) Adyar, Chennai – 600 020,
Tamil Nadu, India

e-address: kalaiselvi564@gmail.com

One of the primary goals of tissue engineering and regenerative medicine is to develop a matrix or scaffold system that mimics the structure and function of native tissue. With an increasing demand for skin regeneration products, there is a noticeable development in biomaterial research on the fabrication of various composite materials for wound healing and skin tissue engineering application. Though several keratin-based biomaterials are developed and are being utilized for various applications, the interaction of keratin-derived molecules with cells and their role in supporting the cells needs to be explored in detail. The present study aimed to fabricate a composite gel material composed of keratin hydrolysate derived from animal hair waste, polyvinyl alcohol (PVA) and gellan gum loaded with α -tocopherol, and polycaprolactone-encapsulated cephalixin for skin tissue engineering application. Keratin hydrolysate with a protein content of 620 $\mu\text{g}/\text{ml}$ was cross-linked with 0.5 % gellan gum (w/v) and 5 % PVA (w/v) to form a hydrogel containing 400 IU of α -tocopherol and cephalixin. The composite material was analysed for its physiochemical and morphological properties using FTIR and SEM, respectively. The swelling property and the degradation rate of the developed material were measured. The antioxidant potential of the composite material was examined by DPPH assay. The biocompatibility of the prepared composite material was tested in NIH-3T3 fibroblast cells. The FTIR results indicated the presence of functional groups associated with keratin and α -tocopherol. A uniform porous structure was observed through SEM analysis, and the pore size was comparatively smaller than that of the control material. The material had compatible swelling capacity with total porosity of $85.68 \pm 0.29\%$ and a degradation rate of $57.9 \pm 0.56\%$ (after three weeks). It exhibited higher DPPH radical scavenging potential compared to the control material. The biocompatibility analysis showed that the prepared composite material supports the adhesion and proliferation of NIH-3T3 fibroblast cells. The data emphasize that keratin-derived biomolecules could be effectively utilized to fabricate porous composite gel along with antioxidants and antibiotic nanoparticles to enhance cellular activities, which will be translated for skin tissue regeneration.

LB-18**Genetically Encoded Fluorescent Protein as a Sensor for Cancer
Theranostics**

Suresh Prem, Pachaiyappan Mohandass, Asuma Janeena, Sundarapandian Ashokraj, Jayaraman Narayanan, Shanmugam Easwaramoorthi, Numbi Ramudu Kamini, Niraikulam Ayyadurai
Department of Biochemistry and Biotechnology CSIR – Central Leather Research Institute, Chennai, 600020, Tamil Nadu, India
e-address: premsuresh5@gmail.com

There are more than eighteen thousand bladder cancer cases in India in 2020 with males being more susceptible than females. The main presenting symptom of all bladder cancers is painless haematuria. Bladder cancer occurs due to the abnormal expression of genes like TP63, EGPF, and Ras protein. It could be treated when diagnosed early but due to the wall layer stratification it cannot be entirely defined even using sophisticated techniques like MRI. It is important to find a suitable sensor that gives good sensitivity and selectivity for the diagnosis of bladder cancer in the early stage. There are reports that show intake of zinc supplement reduces prostate cancer. There are research papers that states excess level of zinc (Zn) concentration in urine indicates bladder cancer. We have developed a genetically encoded redox amino acid (DOPA) in green fluorescent protein and fabricated the same on an electrode surface for the selective and sensitive detection of zinc ions. The genetically encoded protein showed better redox activity and metal coordination with zinc. The zinc sensor showed linear responses to the protein fabricated electrode with a detection limit of 0.129 nM. The stability of the protein fabricated electrode showed consistent performance. The developed sensor is highly selective and sensitive for detecting zinc ions in real-time spiked urine samples and could be applied for bladder cancer diagnostics.

LB-19

Enzyme mediated Biofuel production using nanomaterials

Shubhashree Barik, Dr. Moumita Saharay
e-address: 20lsph02@uohyd.ac.in

Biofuel or bio-ethanol from biomass is one of the environment friendly alternatives to fossil fuel. In nature, some organisms feed on wood and other plant materials, for example, termites. The gut microbiome of termite consists of battery of enzymes, known as cellulases, that can breakdown tightly packed cellulose chains present in the plant cell wall into smaller sugar molecules containing one or two glucose units. Industrial production of bioethanol requires these cellulase enzymes as catalytic agents for the decomposition of cellulosic biomass and the yield of simple sugar is readily fermented into ethanol. For a cost-effective biofuel production, these enzymes need to be recycled by immobilizing them on nanomaterials, e.g. Graphene, Carbon Nanotubes (CNTs), and Magnetic Nanoparticles (MNPs), while retaining their catalytic activity. We studied the binding of Graphene and CNTs on CelS, a microbial cellulase enzyme, using molecular dynamics simulation techniques to provide insights into molecular interactions between these species.

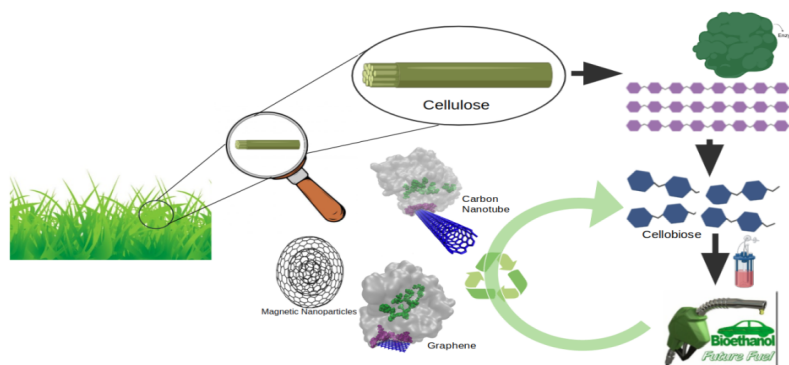


Figure 44: The figure explains how plant biomass is treated by cellulase enzyme in industries and for cost-efficient production of biofuel by immobilizing cellulase on nanomaterials.

LB-20**Role of dengue virus capsid protein on mitochondrial homeostasis**

Preeti Chauhan, Dr.M.Vekataramana

Department of Biotechnology and bioinformatics,school of Life Science,University of Hyderabad
e-address: 18ltp09@uohyd.ac.in

The dengue virus (DENV) is the leading cause of mild febrile illness to severe hemorrhagic fever worldwide. The genome of this virus is a positive sense single stranded RNA that expresses as a single open reading frame (ORF). This ORF yields three structural (Capsid, pre-Membrane and Envelope) and seven non-structural (Ns1, 2A, 2B, 3, 4A, 4B and 5) proteins. Some of these proteins are shown to mitigate mitochondrial function. In this study, we intend to analyze the role of capsid protein on mitochondrial homeostasis. The DENV capsid protein plays an essential structural role in protecting the viral genome and its assembly plays an important role in the viral life cycle. It has been reported that the multifunctional C protein is essential in the viral replication, assembly, RNA encapsidation, as well as pathogenesis. The role of Capsid protein in inducing apoptosis by activating caspase-3 and caspase-9 leading to mitochondrial dysfunction was reported. This virus replication occurs in the infected cell cytoplasm. The data suggested the mitochondrial localization of capsid protein transfected in HEK293T cells. The western blotting analysis confirmed the above observation. The Denv1 Capsid also has a nuclear localization signal (NLS) that mediates entry into the nucleus. Furthermore, we also determined that in the presence of mitochondrial lysate this protein assembles in oligomer form. In Conclusion:, the Mitochondria localization of the dengue Capsid may play critical roles in viral replication and Capsid induced apoptosis. Hence the role of the localized capsid protein in mitochondrial homeostasis will be discussed.

LB-21**Designing Inhibitors Against Cathepsin Targeting HIV-1 Viral Infection**

Sarita Swain, Satyajit Mukhopadhyay, Anand K. Kondapi

Department of Biotechnology and Bioinformatics, School of Life sciences, University of Hyderabad

e-address: Swain.sarita27@gmail.com

Human Immunodeficiency Virus has been considered as chronic disease that attacks the immune system and interfere with the ability to fight infection. There are highly active anti-retroviral treatments (HAART), a combination of nucleoside transcriptase inhibitors (NRIs), non-NRIs, protease inhibitors (PIs) and integrase inhibitors available to suppress the HIV replication. Among the HIV drugs, 26 drugs are approved by FDA from which ten are HIV protease inhibitors. These inhibitors block the viral protease to stop the polyprotein processing resulting inhibition of replication process. In HIV life cycle, proteases play vital role for replication. HIV proteases are homo-dimeric aspartyl proteases that cleaves the polyprotein precursor. It cleaves Gag and Gag-Pol polyprotein encoded by HIV virus genome at nine processing site to produce mature active proteins. In recent studies, it has been found that protease cleavage site on HIV glycoprotein recognized by three major proteases (cathepsin S, L and D) which is important for antigen processing and presentation. These proteases cleave HIV gp120 and form different polypeptides based on the extent of proteolysis. One of the polypeptide with mol wt reported to exhibit 70kDa was chosen for the study. Based on the above background, a series of dicoumarin molecules that have been developed for inhibition of HIV gp120 (Reverse Transcription) also been used for analysis of protease inhibitors. The molecules has been designed and minimized using Chems sketch and Sybyl software. Then docking has been performed for the analysis of interaction between cathepsin and dicoumarin molecules. From this procedure 6 dicoumarin molecules have been chosen based on the higher binding score (Affinity) i.e. -9.2, -10.2, -9.2, -9.7, -10.3, -10.0 and further evaluated for their biological activity.

References:

1. Georgio Kourjian, Marijana Rucevic, Matthew J. Berberich, Jens Dinter, Daniel Wambua, Julie Boucau, and Sylvie Le Gall. HIV Protease Inhibitor-Induced Cathepsin Modulation alters Antigen Processing and Cross-Presentation. *J Immunol* 2016; 196:3595-3607
2. Zhengtong Lv* Yuan Chu* Yong Wang Department of Immunology, School of Basic Medical Science, Xiangya School of Medicine, Central South University, Changsha, Hunan, People's Republic of China. HIV protease inhibitors: a review of molecular selectivity and toxicity. *HIV AIDS (Auckl)*. 2015; 7: 95-104
3. Bin Yu, Dora P. A. J. Fonseca, Sara M. O'Rourke, Phillip W. Berman. Protease Cleavage Sites in HIV-1 gp120 Recognized by Antigen Processing Enzymes Are Conserved and Located at Receptor Binding Sites. *J Virol*. 2010 Feb; 84(3):1513-26
4. Kammari K, Devaraya K, Bommakanti A, Kondapi AK. Development of pyridine dicoumarols as potent anti HIV-1 leads, targeting HIV-1 associated topoisomeraseII β kinase. *Future Medicinal Chemistry* 2017; 9:1597-1609.

LB-22**Importance of Mitochondrial Electron Transport Chain in Sustaining Brassinosteroid Enhanced Photosynthesis in *Arabidopsis thaliana* Mesophyll Protoplasts**

Kandarpa Mahati , Kollipara Padmasree

Department of Biotechnology and Bioinformatics, School of Life Sciences, University of Hyderabad, Hyderabad-500046

e-address: kmahati91@uohyd.ac.in, kpssl@uohyd.ac.in

The Cyanide-sensitive cytochrome oxidase (COX) pathway and the Cyanide-resistant alternative oxidase (AOX) pathway of the mitochondrial electron transport chain (mETC) are known to play a significant role in optimizing photosynthesis. Apart, the external application of Brassinolide (BL), an important form of brassinosteroid hormone (BR) to plants is known to increase the capacity of photosynthesis through enhancement in the activity of the Calvin-Benson cycle (CBC) enzymes. In the present study, the mesophyll cell protoplasts of *Arabidopsis thaliana* are treated with BL in the presence of mETC inhibitors antimycin-A (AA) and salicylhydroxamic acid (SHAM) to unveil the importance of COX and AOX pathways in BR stimulated photosynthesis. A broad range of BL concentrations from 0.05 pM to 5 pM was applied to mesophyll protoplasts and pre-incubated in light ($1000 \mu\text{E m}^{-2}\text{s}^{-1}$). Soon after pre-incubation, the samples were transferred to a Clark-type oxygen electrode cuvette to monitor the effect of BL on respiratory O_2 uptake, bicarbonate-dependent photosynthetic O_2 evolution (CBC activity) and p-benzoquinone-dependent O_2 evolution (PS-II activity). The addition of optimal concentration of BL stimulated the total respiratory activity, CBC and PSII activities. Besides, the addition of BL increased the capacity of both COX and AOX pathways. However, the contribution of AOX pathway capacity was more pronounced than COX pathway capacity. Further, the transcript levels of CBC enzymes and glucose-6-phosphate, a major product of carbon assimilation as well as the precursor for sucrose synthesis increased significantly when treated with BL. Furthermore, the total cellular ATP/ADP ratio, reactive oxygen species (ROS) and the ROS scavenging enzymes increased upon treatment with BL. However, the application of BL to mesophyll protoplasts in presence of AA or SHAM could not stimulate the CBC activity, transcript level of its enzymes and glucose-6-phosphate, indicating the importance of COX and AOX pathways in sustaining the BR promoted photosynthesis. An enhancement in the decrease of total cellular ATP/ADP ratio upon treatment with BL in presence of AA suggests its role in keeping high the CBC activity by meeting the cellular demands for ATP during BR promoted photosynthesis. Also, aggravation in the rise in ROS levels and the transcripts of antioxidant enzymes parallel to a decrease in CBC activity upon treatment with BL in presence of AA or SHAM suggest the significant contribution of COX and AOX pathways in maintaining cellular ROS at optimal levels during BR promoted photosynthesis.

LB-23**Structural and functional attributes of Microrchidia family of chromatin remodelers**

Chutani, Namita , Singh, A.K., Kadumuri, R.V., Chavali, S., Pakala, S.B.

e-address: namitachutani@students.iisertirupati.ac.in

Cellular DNA is dynamically organized in the form of chromatin in the nucleus. Several chromatin remodeling proteins modulate chromatin states and associated cell-type specific function(s). Chromatin remodelers affect the spatio-temporal dynamics of global gene-expression through its ATPase domain and a histone-code/protein binding domain(s). Microrchidia (MORC) family is a relatively new addition to the four well-studied families of chromatin remodeling proteins viz. (i) SWItching defective/Sucrose Non-Fermenting (SWI/SNF) family, (ii) the Imitation SWItch (ISW1), (iii) the Chromodomain, Helicase, DNA binding (CHD) and (iv) the INOitol requiring 80 (INO80) family. Dysregulation/dysfunction of MORCs are associated with various disease types, such as inflammation, neurodegeneration and cancer progression. Through extensive literature search and computational analysis, we explored the participation of MORCs in phase-separated structures, possible influence on various biological processes through protein–protein interactions, and potential extra-nuclear roles. We will present a holistic understanding and comparative views of the various biological roles of MORCs from molecular, structural and systems-level perspectives.

LB-24**iMCLAPE: A multi-class classifier for epistatic interaction**

Anubha Dey , Manjari Kiran

Department of Systems and Computational Biology, School of Life Sciences, University of Hyderabad 500 046,
e-address: 19lsph01@uohyd.ac.in**Background**

Cancer is a deadly disease due to uncontrolled cell proliferation. Tumor cells are the result of mutated or overexpressed genes in otherwise normal cells. Over the last decade, clinicians have started implementing targeted therapy approaches that selectively target cancerous cells while sparing the normal cells. Synthetic lethality (SL) and synthetic viability (SV) are the two most important genetic interactions (GI) known in the targeted therapy approach. Synthetic Lethality is a GI, where inhibiting either of the genes does not have any effect on the cancer cell survival, but inhibiting both the genes leads to a lethal phenotype. Whereas in synthetic viability inhibiting one of the genes makes the cancer cell sick, but inhibition of the other gene rescues the effect of the mutation and promotes cell viability.

The Gap in the field:

Many experimental approaches have been employed to successfully identify genetic interactions. Most of these approaches are time-consuming, laborious, and expensive. The computational tools for SL prediction involve statistical models and machine learning approaches. Almost all the machine learning tools are binary classifiers and involve the identification of only SL pairs. There are limited methods and no machine learning tool to identify synthetic viable gene pairs. Most importantly, there are limited numbers of properties known that best describe and differentiate a GI from the other. To the best of our knowledge, there is no multi-class classifier to predict whether a pair is SL, SV, or NOT a genetic interaction.

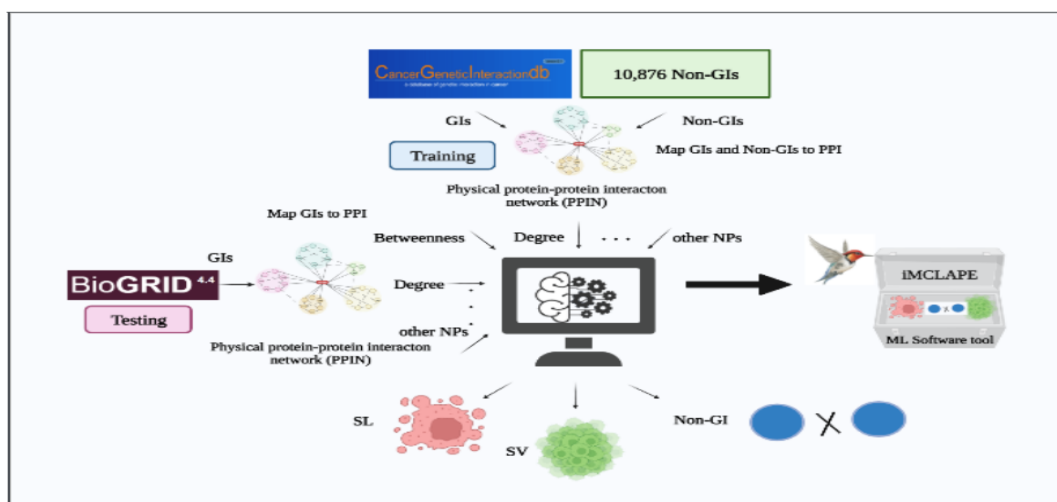
Results:

We have developed iMCLAPE (Multi-Class cLassifier APproach for Epistatic Interactions). This is a multi-class model for GI pairs' prediction using machine-learning methods. Literature supports utilizing networks to classify whether a pair is SL or NOT. We have calculated different network properties in the present work and fed them into the model as features. Removal of redundant pairs, selection of discriminatory features, and proper data balancing have been incorporated for better model building and prediction. Various supervised learning approaches have also been employed to build a multi-classifier that is able to predict the different classes of GIs. Amongst all the models, random forest outperforms and identifies discriminatory variables leading to better accuracy. The model has been trained on the CGIdb (Cancer Genetic Interaction database) dataset and tested on the BioGRID dataset (The Biological General Repository for Interaction Datasets) of genetic interaction. A 100-fold cross-validation test has been implemented that results in an accuracy of 92.17 on the training dataset, and an accuracy of $\sim 70\%$ for the test set.

Discussion:

This study aims to build a multi-class classifier that can predict different classes of GIs and also identify features that best differentiate the three classes of GIs. As there is no multi-class model to predict genetic interactions this makes the study novel and intriguing. We have limited our analysis to three classes of prediction but future versions may incorporate more classes such as synthetic dosage

lethality, and collateral lethality. To further improve the model accuracy one might add more features to the model. With the inclusion of more classes and features, the model will learn variety and novelty and may perform better. The findings of this study will create a new research domain to explore, enhance drug efficacy and improve patients' survival.



LB-25**AN ORIGINAL RESEARCH WORK GREEN ENGINEERED SILVER NANOPARTICLES OF SPONDIAS PINNATA LEAVES & ITS APPICATIONS - AN ECO-FRIENDLY APPROACH**

V Arun Reddy ^a, Dr T Sowmya ^b, V Narmada ^a, Dr E Sujatha ^c

^aDepartment of Pharmacy, Pharmaceutical Analysis & QA, University College of Technology(A), Osmania University, Tarnaka, Hyd-500 007, TS, India

^b UGC Assistant Professor, Forensic Science Unit, Department of Chemistry, University College of Science, Osmania University, Tarnaka, Hyd-500 007, TS, India

^c Associate Professor & PRO, Department of Botany, University College of Science, Osmania University, Tarnaka, Hyd-500 007, TS,India

e-address: Vakitiarunreddy939@gmail.com

Aim:

The main aim of present research work is Green fabrication(Synthesis) of silver nanoparticles (AgNPs) of spondias pinnata leaves and biological activity.

Introduction:

Nanotechnology has changed the outlook of researchers towards science and technology. The enhanced surface area of the particles due to their nano size is contributing to the wide range of applications are used.

Objective:

Find new applications of AgNPs.

Background:

No reports of green synthesis of silver nanoparticles.

Methodology:

Hot Plate/ Microwave Assisted methods are used for synthesis of AgNPs and characterization was done by SEM, TEM, FTIR, UV, XRD, EDAX & Nanoparticle analyzer(Size & Zeta potential). Activities such as Antimicrobial, Anticancer, Antiucler, Drug identification and DNA Binding studies.

Conclusion::

An eco friendly, rapid & a convenient green method for synthesis of AgNPs was reported. Antimicrobial & Anticancer.

Keywords:

Green Synthesis, Spondias pinnata, AgNPs, SEM, Antimicrobial, Anticancer.

MS-01

A Tendon Substitute For Orthopaedic Reconstructive Surgery - Acellular Tissue Matrix With Phyto-extract of *Cuminum cyminum*

Niveditha K^{a,c}, Resmi Rajalekshmi^b, Roy Joseph^b, Annie Abraham^a, Annie John^{a,d}

^aDepartment of Biochemistry;

^d Advanced Centre for Tissue Engineering (ACTE); ^c Department of Biotechnology, University of Kerala, Thiruvananthapuram-695581, Kerala, India.

^b Division of Polymeric Medical Devices, BMT Wing, Sree Chitra Tirunal Institute for Medical Sciences and Technology, Trivandrum, Kerala, India.

e-address: karippacheril@gmail.com

Background:

Mechanical force transmission during sports or trauma is a major cause of tendon injury and a challenge in Orthopedic Medicine. Currently, re-tear of synthetic substitutes is most likely to occur after suturing as regeneration of tendon is slow due to its avascularity and easily prone to re-injury. Hence alternate approaches are becoming imperative for this unmet clinical need. In this work, ayurvedic formulation of *Cuminum cyminum* seed extract (CCE) incorporated alginate dialdehyde (ADA) - gelatin (G) - (ADAGCCE) hydrogel dip coated decellularized rabbit tendon scaffold has been proposed as a substitute to assist the repair of injured/damaged tendon.

Methodology:

Decellularization (DT) of Rabbit tendon was performed by the chemical method (TBP and Triton X 100) and characterized using microscopic techniques. ADA was prepared by the oxidation of sodium alginate with sodium meta periodate. *Cuminum cyminum* seeds (10g) soaked in 100ml water formed the CCE which was qualitatively analysed for the presence of various bioactive molecules. CCE in the range 12.5 μ l to 200 μ l were added to ADAG. An optimum formulation of ADAGCCE hydrogel was prepared by mixing 10% ADA, 10% Gelatin and 50 μ l of 10% cumin aqueous extract, dip coated on DT and evaluated for functional groups (FTIR), water uptake %, degree of crosslinking and porosity. *In vitro* cytotoxicity, cytocompatibility and proliferation of Adipose Derived Mesenchymal Stem Cells (ADMSCs) seeded ADAGCCE dip coated DT scaffolds were also analyzed by MTT and LDH assays.

Results and Discussion:

DT samples were assessed by Microscopy for its acellularity. Alkaloids, phenols, flavonoids, steroid, terpenes and tannins were present in CCE. FTIR spectra of ADAG hydrogel showed a peak at 1609 cm^{-1} due to the Schiff's base formation with the aldehyde groups in ADA and amide groups in gelatin. In the FTIR spectra of ADAGCu, there was a peak at 1608 cm^{-1} indicating the Schiff's base formation. When the concentration of cumin was increased the degree of crosslinking decreased from 36.35 ± 1.25 to 26.75 ± 1.98 . As the concentration of cumin increased from 12.5 μ l to 200 μ l the water uptake % increased from 969.76 ± 6.25 to 1087.36 ± 12.85 . Hence 50 μ l of cumin extract can be added to ADAG hydrogel without much change in its properties. The dip coating time was optimized for 30 min with the result obtained from water uptake % (78.55 ± 2.9). Similar to ADAG hydrogel, an open porous structure with interconnected pores was observed in ADAGCCE hydrogel by scanning electron microscopy (SEM). *In vitro* evaluation of ADMSCs seeded DT dip coated ADAGCCE scaffolds by confocal microscopy visualized the presence of abundant viable cells on the scaffolds. Furthermore, SEM also displayed adhesion and uniform distribution of cells expanded on DT scaffolds manifesting its role as a cell friendly noncytotoxic and cyto-compatible scaffold for tendon substitute to replace damaged/injured tendon.

The relevance of the study:

A combination of biomimetic properties of surrogate ECM from DT with the regenerative potential of *Cuminum cyminum* may be a promising surgeon-friendly substitute for tendon defect healing - a boon to athletes, geriatric population, labour intensive groups etc.

Keywords:

Tendon Tissue Engineering, Decellularization, Cuminum cyminum, Hydrogel

Acknowledgements:

Authors gratefully acknowledge University of Kerala and Dept. of Biochemistry for the facilities; Funds received from ICMR (NK, AJ, AA -File No: 5/3/8/322/2017-ITR) and ICMR Emeritus Scheme (AJ - 74/2019) are gratefully acknowledged.

MS-02**Treatment of Ischemic Brain Injury with optimized mesenchymal stem cells and their secretome through the intermittent hypoxic physiological environments**

Subathra Radhakrishnan^{a,b}, Catherine Ann Martin^b, Subbaraya Narayana Kalkura^c,
Shanmugaapriya Sellathamby^a, Mohamed Rela^b

^aDepartment of Biomedical Science, Bharathidasan University, Tiruchirappalli, TN, India.

^bNational Foundation for Liver Research, Cell laboratory, Chromepet, Chennai, TN, India.

^cCrystal Growth Center, Anna University, Chennai, TN, India.

Hypoxia is considered a key factor in cellular differentiation and proliferation, particularly during embryonic development; the process of early neurogenesis also occurs under hypoxic conditions. Apart from these developmental processes, hypoxia preconditioning, or mild hypoxic sensitization develops resistance against ischemic stroke in deteriorating tissues. We, therefore, hypothesized that neurons resulting from hypoxia-regulated neuronal differentiation could be the best choice for treating brain ischemia, which contributes to neurodegeneration. In this study, infrapatellar fat pad (IFP), an adipose tissue present beneath the knee joint, was used as the stem cell source. IFP-derived stem cells (IFPSCs) are totally adherent and are mesenchymal stem cells. The transdifferentiation protocol involved hypoxia preconditioning, the use of the hypoxic-conditioned medium, and maintenance in a maturation medium with α -lipoic acid. The differentiated cells were characterized using microscopy, reverse transcription PCR, real-time PCR, and immunocytochemistry. To evaluate the epigenetic reprogramming of IFPSCs to become neuron-like cells, methylation microarrays were performed. Hypoxia preconditioning stabilized and allowed for the translocation of hypoxia-inducible factor 1 α into the nucleus and induced achaete-scute homologue 1 and doublecortin expression. Following induction, the resultant cells expressed neuronal markers neuron-specific enolase, neurofilament-light chain, growth-associated protein 43, synaptosome-associated protein 25, and β -III tubulin. The differentiated neural-lineage cells had functional gene expression pertaining to neurotransmitters, their release, and their receptors. The molecular signaling mechanisms regulated developmental neurogenesis. Furthermore, the *in vitro* physiological condition regulated neurotransmitter respecification or switching during IFPSC differentiation to neurons. Thus, differentiated neurons were fabricated against the ischemic region to treat neurodegenerative diseases.

Keywords:

Mesenchymal stem cells, hypoxic sensitization, DNA methylation, neuronal differentiation, neurotransmitter respecification.

MS-03**Mobile Health (mHealth) Technology for Non-Communicable Disease Services: Enhancing the Performance of Community Health Workers.**

K.Jyothi , Dr. C.T. Anitha

University of Hyderabad

e-address: 19muph03@uohyd.ac.in

Background:

There are 1.2 billion mobile customers in India, and the smartphone users in rural India were 67.6% in 2021. Mobile health (or mHealth) refers to delivering healthcare services and managing patient data using portable electronic devices and software applications. Noncommunicable diseases (NCDs) account for 41 million annual deaths globally, and 85% of premature deaths occur between 30 and 69 years due to NCDs in Low and Middle Income Countries (LMICs). Community health workers (CHWs) serve as a bridge between the communities and the health centers. In India, 10.4lakh Accredited Social Health Activists (ASHAs) and 2lakh Auxiliary Nurse Midwives (ANMs) serve as CHWs. Their services have contributed to a decrease in maternal and infant morbidity and mortality rates as well as the burden of communicable diseases. To facilitate tasks and enhance outcomes, mobile technologies are developed, tested, and deployed by community health professionals. Our study aimed to examine and qualitatively determine the potential of mobile phone technology in improving CHWs' performance and effectiveness in the delivery of NCD services.

Methods:

A qualitative study with 30 in-depth interviews with ASHAs, ANMs, and supervisor were conducted from selected Primary Health Centers (PHCs) and Subcenters in the Suryapet district of Telangana in 2021. The CHWs were asked about their experience using mobile technology to deliver NCD health services. The in-depth interviews were audio recorded, transcribed verbatim, and coded using the software Atlas.ti.

Results:

Inductive thematic analysis was adopted to analyze the data. The themes identified were enlisted as beneficial: 1)Reduction in CHWs workload, 2)Improvement in the data collection, 3)Increasing service access and quality, 4)Training and supervision of personnel management, 5)Reporting and monitoring, and 6)Better organization of CHWs tasks and improvement in community health outcomes. The CHWs reported a few challenges to using mobile phones, such as a lack of training on new mHealth solutions, weak technical support, and systemic challenges.

Conclusion::

mHealth interventions are essential to aid in CHWs' performance and can improve patient outcomes and reduce the burden of NCDs. The study found an increasing technical uptake, acceptance, and steady decline in costs provide scope to expand mHealth technology in LMICs in the future.

Keywords:

NCD screening, Mobile phones, ANM, ASHA, Chronic diseases

MS-04**Streptozotocin-induced Animal Model as a model to study Diabetic Complications**

J.Ram Mukka Raju , Athar H Siddiqui

School of Medical Sciences, University of Hyderabad, Hyderabad-500046

e-address: 17bmph02@uohyd.ac.in**Introduction:**

Diabetes is a multi-factorial metabolic disease, characterized by sustained hyperglycemia, associated with either lack of Insulin or Insulin resistance. The function of the renin-angiotensin system (RAS), an important component of the body's physiological functions, is altered under diabetic conditions. There are numerous evidences that indicate the differential function of RAS in diabetes and its dysregulation that could lead to acute and chronic complications including renal and cardiovascular disorders. In our present study, we have used the Streptozotocin-induced diabetic animal model to assess diabetic complications and validate it as an effective tool to study diabetic complications associated with the kidneys, to identify the induced renal conditions.

Methodology:

Male Sprague Dawley (SD) rats were used in the present study. The animals were divided into two groups, n=4: Vehicle and Streptozotocin (STZ) -induced rats. A single intraperitoneal injection of STZ (55mg/kg BW), dissolved in the Na-Citrate buffer was administered to induce diabetes. Vehicle groups of animals were injected only with Na-Citrate buffer. Forty-eight hours after the injection, blood glucose was measured and the animals having plasma glucose of 300 ± 50 mg/dl were included in our study. During the course of treatment, their daily consumption of food and water was monitored and recorded. The rats were placed in metabolic cages 3 days before the scheduled sacrifice. Furthermore, urine was also collected for analysis. All data are expressed as Mean \pm SEM and statistical significance was set at $p < 0.05$

Results:

After two weeks of STZ treatment, the STZ-induced diabetic rats showed significantly increased blood glucose levels (381.8 ± 15.51 Vs 108.3 ± 2.136) they had increased water intake (98.59 ± 9.497 vs 29.09 ± 0.1986) and food consumption (23.20 ± 1.739 vs 17.18 ± 0.1109), accompanied by weight loss (10.56 ± 4.918 vs 22.82 ± 2.852), as compared to vehicle rats. The urine flow (28.33 ± 2.150 vs 7.100 ± 0.2198) and Urine protein were also significantly higher in the Diabetic rats (62.33 ± 5.918 vs 16.04 ± 0.4915), compared to the vehicle group.

Conclusion::

The STZ-induced diabetic rats displayed all the clinical manifestations of Diabetes thus making it an important animal model to study the clinical ramifications of Diabetes. The induction of proteinuria in diabetic rats reveals an acute injury to the kidneys in the diabetic rats and this could serve as an important initiating step to study the progressive renal damage associated with diabetes and evolve newer therapeutic strategies and targets to delay or prevent the onset of renal damage in diabetes.

Financial Acknowledgment and sponsorship:

This work was financially supported by the DST-PURSE, Institute of Eminence, University of Hyderabad, and ICM

Conflicts of interest:

There are no conflicts of interest

MS-05**A gelatin based 3D matrix with adipose derived stem cells and exclusive ascorbic acid signalling emerged as a novel neural tissue engineering construct**

Catherine Ann Martin ^{a,b}, Subathra Radhakrishnan ^b, Mettu Srinivas Reddy ^b, Mohamed Rela ^b,
Narayana Kalkura Subbaraya ^a

^aCrystal Growth Centre, Anna University, Chennai-25

^b Stem Cell Laboratory, National Foundation for Liver Research, Chrompet, Chennai-44

The current study investigated a triad, which comprises of adipose tissue derived stem cells isolated from infrapatellar fat pad and gelatin/PVA based matrix with exclusive ascorbic acid signalling. Though, the bio-mechanical properties of the gelatin-PVA blended scaffolds in wet condition are equivalent to the ECM of soft tissues in general, in this study, the triad was tested as a model for neural tissue engineering. Apart from being cytocompatible and biocompatible, the porosity of the scaffold has been designed in such a manner that it facilitates the cell signalling and enables the exchange of nutrients and gases. The highly proliferative stem cells from passage 2 were characterized using both, mesenchymal and embryonic stem cell markers. As an initial exploration the mesenchymal stem cells at passage 4 were exposed to ascorbic acid and bFGF signalling for neuronal differentiation in 2D environment independently. The MSCs successfully differentiated and acquired neuron specific markers related to cytoskeleton and synapses. Subsequently, three phases of experiments have been conducted on the 3D gelatin/PVA matrix to prove their efficacy, the growth of stem cells, growth of differentiated neurons and the *in-situ* growth and differentiation of MSCs. The scaffold was conducive and directed MSCs to neuronal lineage under specific signalling. Overall, this organotypic model triad could open a new avenue in the field of soft tissue engineering as a simple and effective tissue construct.

Keywords:

adipose derived stem cells (ASCs), ascorbic acid, soft tissue engineering, triad, neuronal differentiation.

MS-06

Synthesis Of Cysteine Graphene Oxide And Assessing Its Antimicrobial Activity.

Mukkaragari krupa, Dr. Nagaraju Konda

School of Medical Sciences, University of Hyderabad, Prof C R Rao Road, Gachibowli, Hyderabad, 500046.

e-address: 17moph02@uohyd.ac.in

In past few years, nanoparticles antimicrobial activity has been improved and destroying pathogenic organisms without being toxic to the surrounding tissues, Graphene and graphene based materials (GBMs) like graphene oxide, graphite oxide, reduced graphene oxide shown good antimicrobial activity with increasing concentration, l- cysteine is a semi essential amino acid biosynthesized by organisms and has three active functional groups like NH_2 , $-\text{COOH}$ and $-\text{SH}$, it is biocompatible, inexpensive and easily obtained. The l-cysteine acts as a reducing and bridging agent to functionalize graphene oxide which resulted in increasing in conductivity of the product and improved by four to five orders of magnitude when compared to graphene oxide. The functionalized l-cysteine reduces the layer- stacking of graphene oxide this is due to that it acts as a dispersant when inserted into graphene oxide layers. there is no sufficient data regarding the biocompatibility of l-cysteine-graphene oxide and no studies on antimicrobial activity of l-cysteine- graphene oxide composite but antimicrobial activity of graphene oxide studies alone, hence there is a need of such materials which are biocompatible and have excellent antimicrobial activity together. Here we synthesized cysteine graphene oxide by using the coupling agent like 1-ethyl-3- (3-dimethylaminopropyl)-carbodiimide (EDAC) with different concentrations and characterized the synthesized product by Raman spectroscopy, Fourier-transform infrared spectroscopy (FTIR), Uv -visible spectroscopy, field emission scanning electron microscopy (FESEM).

References:

1. Chandraker, K., Nagwanshi, R., Jadhav, S. K., Ghosh, K. K., and Satnami, M. L. (2017). Antibacterial properties of amino acid functionalized silver nanoparticles decorated on graphene oxide sheets. *Spectrochimica Acta Part A: Molecular and Biomolecular Spectroscopy*, 181, 47-54.
2. Mu, L., Gao, Y., and Hu, X. (2015). L-Cysteine: A biocompatible, breathable and beneficial coating for graphene oxide. *Biomaterials*, 52, 301-311.

MS-07

Revisiting the Effects of *Ocimum sanctum* Shade-Dried Leaves Powder on Body Length and Wing Length of *Drosophila melanogaster*

Sanjay Saraswati , Sudipta Saraswati

Behavioural Neuroscience Laboratory, Centre for Neural and Cognitive Sciences, University of Hyderabad, Hyderabad, India
e-address: sanjaydbt322@gmail.com

Drosophila melanogaster has been widely used as a model organism to study the developmental mechanisms that regulate body and organ size (Mirth and Shingleton, *Frontiers in Endocrinology*, 2012). Such studies have elucidated the involvement of the insulin signalling, the target of rapamycin (TOR) signalling, and the Hippo signalling pathways—all of which are evolutionarily conserved—in regulating body size in *Drosophila* adults (Mirth and Shingleton, *Frontiers in Endocrinology*, 2012). Agrawal and Yadav (*Indian Journal of Life Sciences*, 2015) reported that *Drosophila melanogaster* grown in food medium supplemented with *Ocimum sanctum* (Tulsi) leaves extract exhibit an increase in both body length and wing length in comparison with control *Drosophila* grown in the absence of the above-mentioned extract. This finding raises an interesting question: What is the mechanism(s) underlying this observed effect? As an important first step to answer this question, we carried out investigations to confirm the observed results reported by Agrawal and Yadav (*Indian Journal of Life Sciences*, 2015). Our approach was to grow one set of *Drosophila melanogaster* in standard food and another set in food supplemented with 3% shade-dried leaves powder of *Ocimum sanctum*, and investigate whether the progeny of *Drosophila* grown in these two different food media have any statistically significant difference with each other in their body length and wing length. We observed that there is no statistically significant difference in body length and wing length between the two groups of *Drosophila* raised in two different food media. Our results demonstrate that contrary to published results reported by Agrawal and Yadav (*Indian Journal of Life Sciences*, 2015), under our experimental conditions, the chemical contents of *Ocimum sanctum* leaves have no observable effect on body length and wing length in *Drosophila melanogaster*. Thus, our result calls into question the reproducibility of an interesting finding published earlier.

References:

1. Agrawal, S. and Yadav, R. (2015). Effect of *Ocimum sanctum* leaf extract on *Drosophila*. *Indian Journal of Life Sciences* 5, 133-134.
2. Mirth, C. K. and Shingleton, A. W. (2012). Integrating body and organ size in *Drosophila*: recent advances and outstanding problems. *Frontiers in Endocrinology*, 3, 1-13.

MS-08**New approach for Dry Eye Diagnosis: using Tear Film Lipid Layer Thickness and Meibomian Gland Loss**

Sandhya Esam ^a, Geeta K.Vemuganti ^a, Dr.Nagaraju.Konda ^a, Dr. Swati Singh ^b

^aSchool of Medical Sciences, University of Hyderabad, Prof C R Rao Road,Gachibowli Hyderabad 500046.

^b Assistant ophthalmologist Ophthalmic Plastic Surgery Service Centre for Ocular Regeneration,L.V. Prasad Eye Institute, Kallam Anji Reddy Campus, L V PrasadMarg, Hyderabad – 500034
e-address: 18moph02@uohyd.ac.in

Purpose:

Dry eye disease (DED) is a multifactorial disease due to disrupted three layered tear film homeostasis ,with the prevalence of 20 – 50% DED, has become the significant global health problem ,there is no “gold standard” diagnostic test for DED, due to limitations,poor correlation of signs & symptoms, DED diagnosis is still remaining as challenge in ophthalmology field.While studies have addressed the aqueous and mucin deficiency,but lipid layer deficiency DED are not well understood. As the meibomian gland is the primary source of tear film lipid layer,we attempted to compare the structural and functional correlation of meibomian glands and lipid layer thickness among different ages in normal and dry eye cases

Methods:

With the approval of IEC dry eye (n=25) patients and (n=25)healthy/controls were recruited ,based on DEWS II(Dry eye workshop II) classification, like Symptoms, Tear-secretion evaluation etc,then measured the lipid layer thickness(LLT) and meibomian gland loss from lipi view II and those photographs were quantified with Image analysis.

Results:

Our study found thin lipid in dry eye compared to normal eye

Conclusion:

Measurement of LLT and Meibomian gland loss are a better guide for clinical diagnosis of dry eye.

Keywords:

Lipid layer thickness, Meibography, Lipi view II , Dry eye, Tear film.

References:

1. Craig JP, Nichols KK, Akpek EK, et al. TFOS DEWS II definition and classification report. *Ocul Surf*2017;15:276–283. [PubMed] [Google Scholar]
2. Blackie, Caroline A., et al. "The relationship between dry eye symptoms and lipid layer thickness." *Cornea* 28.7 (2009): 789-794.

MS-09**Dimensions of access to mobile based tobacco cessation services among Municipal waste workers in Hyderabad, Telangana.**

Laxmi Ramitha Koneti^a, C.T. Anitha^b

^aResearch scholar in Public Health, School of Medical Sciences, University of Hyderabad,

^b Associate Professor, School of Medical Sciences, University of Hyderabad.

e-address: 19muph06@uohyd.ac.in

Introduction:

Globally, tobacco use accounts for over 8 million annual deaths with 1.35 million annual deaths in India. The World Health Organization (WHO) observed that only 3% of smokers were successful in quitting without any assistance. Hence, WHO identified Mobile based Tobacco Cessation Services (MTCS) as an effective tool to boost tobacco cessation promotion. Existence of quitlines is more in High Income Countries (60%) than Middle (32%) and Low-income (8%) countries. The use of these quitlines was less in Low- and Middle Income Countries (LMICs) as per the findings of Global Adult Tobacco Survey. MTCS including quitlines, smart phone applications have been recently gaining recognition in promoting reduction of tobacco use in India including the mCessation programme. It is a short text message-based free of cost mobile health service developed by the Government of India to aid quitting tobacco. While these digital technologies are advancing, end user adoption is necessary for them to have an influence on health. The ownership of a mobile phone becomes a primary necessity for implementation of MTCS. Mobile divides with gender gaps were found in Venezuela, India and Philippines, a way different from advanced economies such as South Korea, Netherlands and Israel where about nine-in-ten adults own a mobile. Therefore this study aims to assess the facilitators and barriers to access mobile phones for MTCS among Municipal Waste (MW) workers in Hyderabad, Telangana.

Methodology:

A cross-sectional study was conducted among 236 MW workers during February-April, 2022 in their occupational setting the Greater Hyderabad Municipal Corporation. The modified WHO STEPS questionnaire was used. Data analysis was done in MS-Excel.

Results:

The mean age of the study population was 40.32 ± 8.89 years among whom 38.13% were males and 61.86% were females. Almost 61% of them had no formal education and their average salary was Rs.18,414 \pm 11,180. Tobacco users were 40% (94/236) with 21.27% and 67% using smoke and smokeless form of tobacco respectively. Some (11.7%) used both forms of tobacco. An attempt to quit was noticed among 19.14% (18/94) of tobacco users. Among the tobacco users who visited a healthcare provider in the past 30 days more than half of them i.e. 56.25% (18/32) received quit advice. Regarding ownership of mobile phones, 68.08% (64/94) of tobacco users owned a mobile with majority being male (65.62%) than female (34.37%). Among mobile owners, women did not own smart phone while a very few men had a smart phone. Women who did not own mobile phone reported to depend on mobile phones of fellow workers or family members. Almost 74.57% of MW workers reported television as the major source for information on harms of tobacco.

Conclusion:

The study highlights the digital divide including low literacy, less access to mobiles especially among women accompanied by meagre wages and less quit attempts. These form access barriers to uptake of

MTCS which leads to health disparities among population groups like MW workers. The digital-based health efforts could be underutilized as engaging end users is compromised. The greater reach of mass media such as television could aid in creating awareness about utilizing the MTCS especially among tobacco users willing to quit. In years to come, digital technology can aid the healthcare provider to initiate MTCS and facilitate quit attempts.

MS-10**Internalization of exosomes in Retinoblastoma tumor progression**

Attem Jyothi , Dr. Geeta K Vemuganti

School of Medical Sciences, University of Hyderabad, Hyderabad-500046

e-address: 18bmph01@uohyd.ac.inCorrespondence e-address: gvmd@uoh.ac.in**Introduction**

Exosomes have been shown to contain 'cargo' that is specific to their cell of origin, with this cargo being able to manipulate several cellular functions, including modification of their immediate environment in inflammation, degenerative disease, and cancer. There is numerous evidence that has proven that exosomes released by tumor cells play a key role in the tumor microenvironment and participate in different pathological stages of angiogenesis, proliferation, invasion, and metastasis, as well as therapeutic resistance. However, the mechanism underlying exosome-mediated tumor progression is not clear. Hence, in this present study, we attempted to evaluate the exosome characterization and internalization by source cell and target cell in Retinoblastoma. This understanding is a promising avenue for the development of effective clinical applications.

Methodology

RbY79 and bone marrow mesenchymal cell cultures (BM-MSc) grown in RPMI 1640, and DMEM without fetal bovine serum (FBS) and 1% anti-antimycotic (100X) solution at 37°C in 5% humidity and 5% (v/v) CO₂. Conditioned media was collected after passage 3, followed by exosome isolation using ultracentrifugation. Morphological and Size analysis of exosomes was done by Transmission electron microscopy. Size distribution and dispersion index were determined by dynamic light scattering (DLS). Moreover, confirmation of exosomes was done by the surface marker of exosomes. Finally, the internalization of exosomes by source cells (RbY79) and target cells (BM-MSc) was confirmed by confocal microscopy at different time points (4hr, 6hr, 12hr, and 24hr).

Results

In the study, we observed that the isolated exosomes from Rb Y79 cells as well as BM-MSc cells were confirmed to be in size ($<200\text{nm}$), shape (cup shape), poly dispersion index (0.328), the range of zeta potential - 12.8 mV, (showing that the isolated exosomes were stable), and phenotype (CD63, CD9, TSG101, HSP-70, and β -actin) were identified. This study demonstrates that the ultracentrifugation method of exosomal isolation from conditioned media yielded higher was a suitable method for getting higher exosomes. Internalization of exosomes was observed at 12hr in RbY79 cells and BM-MSc cells as compared to control without exosomes. Further *in-vitro* and *in-vivo* functional studies are warranted to understand the role of exosomes in tumor progression and metastasis.

Conclusion:

The isolated exosomes showed all the characteristics of exosomes isolated by other researchers. The internalization of exosomes, in target cells BM-MSc (metastatic site) thus makes it important in the Retinoblastoma clinical ramifications. This could serve as an important initiating step to study the progressive tumor growth associated with retinoblastoma and evolve newer therapeutic strategies and targets to delay or prevent the onset of tumor progression.

Financial Acknowledgment and sponsorship:

This work was financially supported by the DST-PURSE, Institute of Eminence, University of Hyderabad, CSIR, and SERB.

Conflicts of interest:

There are no conflicts of interest

MS-11

Ocular Surface Analyser as an emerging diagnostic modality for Dry Eye Disease and Meibomian Gland Dysfunction

Dr. Yash Agarwal , Dr. Gautam Singh Parmar

Sadguru Netra Chikitsalaya, Janaki kund, Chitrakoot, Satna 210204, Madhya Pradesh, India.

e-address: dryashagarwal2011@gmail.com

Dry eye disease is one of the most commonly encountered ophthalmic conditions in an eye specialist's clinic. An overt digital media usage in the recent times and identification of phenomena like computer vision syndrome have further increased the footfalls. Meibomian gland is touted as the leading cause behind dry eye disease (with excessive tear evaporation) attributable to 46.2% to 69.3% of dry eye in Asian population, particularly in patients of rural settings, because of associated factors like dry hot climate, use of *chulhas* by rural women, poor eye hygiene, etc. Apart from being supplemented with a subjective dry eye questionnaire, it primarily deals with objective evaluation of "non-invasive tear film break-up time, lipid layer interferometric analysis, lower lacrimal meniscus height with non-contact meibography" as its highlight feature quantifying the meibomian gland losses/drop-outs. Ocular Surface Analyser serves as a *non-invasive* and objective diagnostic tool for a quick but reliable analysis and quantification of tear film parameters in clinic-based settings, augmenting the diagnosis and treatment of dry eye disease and meibomian gland dysfunction.

MS-12

Application of Technology for Diagnostics Devices and Tools for Life Sciences

Anshu Sarje , Anjali Singh, Vamsidhar Nayak
International Institute of Information Technology, Hyderabad,
e-address: anshu.sarje@iiit.ac.in

Breakthrough in understanding life sciences has been made due to advancement in engineering and technology. In this poster, we present some of our work in the area of technology implementation for enhancing sensing, diagnostics and patient monitoring. The goal of this abstract is to introduce the audience to application of engineering in life sciences. While microscopy and electrophysiology were breakthroughs made in early years, today advancement of technology is evident from cutting edge technology like MEMs (Micro Electro Mechanical Systems) and Nano-technology which has given tools like genome sequencing, non-invasive surgeries, wearable devices etc. to medical sciences. We present our project on lab-on-chip type device and patient monitoring system highlighting some key advantages of the technology. Microfluidics, micro machining and micro fabrication provide a platform for complete processing of diagnostic samples (body fluid) on a small chip instead of conventional processing in a huge laboratory. This lab-on-a-chip reduces the requirement of sample size, volume of reagents, energy consumption as well as processing time and hence is ideal for sensors and diagnostic devices which can reach out to masses in remote areas and provide timely diagnosis or sensing. We are also integrating electronics with micro-fluidics and MEMs to further enhance the processing capabilities of such chips. The second project shows usage of integrated electronic circuits for patient monitoring and prosthetics development. We are developing wearable ECG and EMG monitoring device for continuous monitoring of a patient with minimal interference due to the device. This wearable device provides medical quality output with minimal distortions. To use it around the patient's body, the system design has to be ergonomic, flexible -wearable. We show some test signal and actual ECG signals recorded using the device. The flexible electrodes technology will ensure that the signal is collected with minimal distortion and can be on the patient for long periods of time.

References:

1. A. Sarje, MSE Thesis, "Characterisation of particles using dielectrophoresis ", 2005, John Hopkins University.
2. Vamsidhar Naik Guggulothu, A. Sarje, "Wearable System Design for EMG Study", submitted to IEEE Silicon, 2022
3. Venkata P. P. , A. Sarje, "Fabrication and characterisation of low cost humidity sensor", IEEE FLEPS, July 2022, Vienna.

MS-13**Nanoparticles enhance infection susceptibility: a multi-parametric cellular analysis using ECIS**

Amalu Navas, Moon Moon Bagalri, A. Maya Nandkumar

Division of Microbial Technology, BMT wing, Sree Chitra Tirunal Institute for Medical Sciences and Technology,
Thiruvananthapuram, Kerala, India.e-address: moonb@sctimst.ac.incorrespondence e-address: anmaya@sctimst.a.cin

A robust multiparametric platform for assessing cell behaviour would provide a new paradigm compared to invasive end-point analysis which requires time and labour. New in-vitro methods are the need of the hour as today data analysis and data mining are important for understanding both simple and complex phenomenon. The need is for maximum inferences to be obtained from a single assay. In our study, the effect of nanoparticles on infection susceptibility was understood using an impedance-based method. Electrical cell-substrate impedance sensing (ECIS) is a morphological biosensor which records the electrical properties of cell-covered microelectrodes in an AC circuit including impedance (ohm), resistance (ohm), and capacitance (μ Farad). The measurement when taken over multiple frequencies (62.5Hz-64k Hz), we were able to differentiate between junctional impedance and impedance caused by cell-substrate interactions as well as the cell membrane capacitance. In the current study, fluctuations in the electrical properties of cell-covered microelectrodes reflect dynamic changes in cell morphology resulting from disrupted cell monolayers following exposure to bacteria. Using the ECIS system, real-time changes in cell morphology and disruption of monolayer integrity of cell cultures in vitro were revealed for A549 cells pre-exposed to carbon black nanoparticle (CBNP) and infected with *Pseudomonas aeruginosa* over a multi-frequency scan (62.5Hz -64kHz). The exposure to CBNP for 24hrs resulted in a dose-dependent change in impedance readings of the cell. Resistance measurements after infection with *P. aeruginosa* showed a drastic reduction which was time-dependent as well as dependant on the dose of pre-exposed CBNP. The highest concentration of CBNP caused the measured resistance (ohm @4 kHz) to drop faster than its' immediate lower concentrations. The 3-Dimensional graph analysis of frequency v/s time v/s impedance showed well-to-well differences in barrier integrity as well as membrane capacitance. To evaluate correlation with $-Z-$ spectra modelling data, parallel, biochemical assays were performed. Functionally, cytokine responses were different between nanoparticle exposed cells and further bacterial infected cells. In Conclusion:, we observed that nanoparticle exposure induces infection susceptibility in epithelial cells facilitated by loss of barrier integrity and loss in membrane capacitance. Our findings indicate that ECIS provides a means to quantify, automate, and measure the influence of various insults or injury or chemical challenges on cell barrier functions, which could be used as first line of high throughput analysis in drug discovery, cancer therapeutics and virological assays.

Keywords:

ECIS, Barrier integrity, infection susceptibility, impedance

MS-14**In-vitro model to study *Clostridium sporogenes* interaction with the gut epithelial cells.**

Moon Moon Baglari , Dr. A Maya Nandkumar, Amalu Navas, Umate Nachiket Shankar, Mohd.

Akif,

Division of Microbial Technology, Sree Chitra Tirunal Institute for Medical Sciences and Technology, India

e-address: 1993moonb@gmail.com

correspondence e-address: anmaya@sctimst.ac.in

The *Clostridium sporogenes* is a spore-forming, facultative or strict anaerobic, rod shaped, Gram-positive bacteria. *Clostridium sporogenes* is rarely considered to be a pathogen. The cellular components and metabolites, like butyrate, secondary bile acids and indole propionic acid, play a probiotic role by energizing intestinal epithelial cells, strengthening the intestinal barrier. The metabolites produced by gut microbes are crucial mediators of diet-induced host-microbial interaction. *C. sporogenes* are able to convert tryptophan to IPA, which strengthens the epithelial cells. It also can form biofilm which helps them in the colonization. Our studies show that, *C. sporogenes* produces slime, referring to the ability to form biofilm. In our study, we have used Caco2 and HT29 cell line, gut epithelial cells as a model to study the interaction with the *C. sporogenes*. We have demonstrated the adherence property of *C. sporogenes* onto the gut epithelial cell, Caco2 and HT29. The main idea is to look at the role of *C. sporogenes* as probiotics. To find out if *C. sporogenes* are able to prevent the adhesion of *C. difficile*. For this interaction study, will be looking at, 2D culture system and Trans well co-culture system.

References:

1. Henrik M. Roager and Tine R. Licht, (2018) Microbial tryptophan catabolites in health and disease, Nature Communications, doi: 10.1038/s41467-018-05470-4.
2. Pingting Guo, Ke Zhang, Xi Ma, and Pingli He, (2020) *Clostridium* species as probiotics: potentials and challenges, doi: 10.1186/s40104-019-0402-1.

MS-15

Screening the Perception of Quality of Life among Parents of Retinoblastoma(Rb) Survivors of 2-5 years of age group in Tertiary Care Eye Hospital in Hyderabad: A Crosssectional Study

Krishnasri Padamandala,^a Rolika Bansal,^b Santosh G Honavar,^b Surya Durga Prasad,^a Geeta K Vemuganti^c,

^aSchool of Medical Sciences, University of Hyderabad.

^bCentre for Sight, Banjara Hills, Hyderabad.

^cCentre for Health Psychology, University of Hyderabad.

e-address: krishnasri.p6931@gmail.com

Purpose:

To study the perception of the pediatric quality of life among the parents and or caretakers of Rb survivors as compared to an age matched control group.

Methods:

A total of 51 parents (bilateral/unilateral/enucleated and chemo and radio therapy) of Rb survivors and 45 parents of age-matched controls from a tertiary eye care center, were given a validated questionnaire Paediatric quality of life 4.0 generic core scale which contains four deductive themes Physical health (8 variables), Emotional health (5 variables), School health (5 variables), Social health. Difficulties related to understanding of questionnaire were also evaluated and estimated on the Likert scale.

Results:

Of the total 96 subjects(51 parent of affected children and 45 controls) the childrens age group was 2-5 years with a M:F::1.1: Type of respondents among cases were Mother 29.4%, Father 64.7%, Caretakers 5.9%, and in controls Mother, 33.3%, father 64.4%, 2.2% were caretakers. As compared to the controls, children affected with Rb had reduced Physical health activities (42%) (walking, running, bathing; School health (22%) Emotional health (27%) and Social health 24% as compared to control group which were normal on all dimensions. There was no reporting of problem in understanding the questionnaire on a Likert scale of 0-4.

Conclusion::

The data of Rb survivors of parents' perception suggests that the QoL is affected is affected RB treatment more so with physical activities moderately affecting Emotional health, Social and school health linearly than the age-matched control group. This study is warranted, counselling of parents and children regarding QoL should be considered as part of treatment protocols for Two to Five years of Rb survivors.

Keywords:

Quality of life, Rb survivors, Parent perception, Retinoblastoma.

Conflicts of interest:

There are no conflicts of interest.

References:

1. DeVita et al., *Cancer: Principles and Practice of Oncology*, 5th ed, p2104.
2. Dhingra H, Arya D, Taluja A, Das S, Mahajan A. A study analyzing the health-related quality of life of retinoblastoma survivors in India. *Indian J Ophthalmol* 2021;69:1482-6.
3. Abramson DH. Retinoblastoma in the 20th century: past success and future challenges the Weisenfeld lecture. *Invest Ophthalmol & Vis Sci.* 2005;46:2684–91.
4. Zhang L, Gao T, Shen Y. Quality of life in children with retinoblastoma after enucleation in China. *Pediatr Blood Cancer.* 2018 Jul;65(7):e27024. DOI: 10.1002/pbc.27024. Epub 2018 Mar 12. PMID: 29528176.
5. Current therapeutic trends for tinnitus cure and control – a scoping review Vatsal A Chhaya, DivyaG Patel, ShamikP Mehta, JigneshP Rajvir, Vinodkumar Jhinjhuwadia, Pranshuta Sehgal, KapilM KhambholjamedRxiv 2021.06.29.21259450; DOI: <https://doi.org/10.1101/2021.06.29.21259450>.

MS-16**Mobile Based Health Interventions for Health Promotion among adults with Non-alcoholic Fatty Liver Disease.**Bhargava Bharam ^a, Kalyankar Mahadev ^b, Anitha C.T. ^b^a Research scholar in Public Health, School of Medical Sciences, University of Hyderabad,^b Associate Professor, School of Medical Sciences, University of Hyderabad.e-address: 20muph04@uohyd.ac.in**Introduction**

Non-alcoholic fatty liver disease (NAFLD) is the build-up of extra fat in liver cells that is not caused by alcohol. Due to the substantial relationship with various metabolic abnormalities, NAFLD is now regarded as a part of the spectrum of metabolic syndromes (MS). Due to sedentary lifestyles and excessive intake of processed energy-rich foods, NAFLD has recently become a significant concern in both developed and developing countries. A study in Japan, one of the developed countries reported an overall prevalence of NAFLD as 24.6% (68.5% in obese subjects and 15.2% in non-obese subjects).(1) The prevalence of NAFLD among the general population in India ranges from 9% to 53%, with a higher incidence amongst overweight/obese and diabetic/prediabetic patients.(2) The risk of NAFLD is more among adults with sedentary life style, obesity and diabetes. Globally there are 3.8 billion estimated smartphone users implying that roughly 50% of people worldwide have access to mobile phones.(3) A billion smartphones are anticipated to be used in India by 2026. (4)This easy access of mobile technology enables one to use mobile health services for lifestyle interventions which helps in preventing NAFLD. Many mobile phone applications are available to monitor the dietary intake and daily physical activity. Therefore, the aim is to review the mobile based health interventions among adults with NAFLD across various countries.

Methodology

Drawing from literature on the lifestyle interventions, this review summarizes the mobile based health interventions among adults with NAFLD across various countries. Electronic databases PubMed, Google scholar, Scopus and Web of science Libraries were searched for potential studies published from 2012 to 2022 using Keywords: NAFLD AND mHealth, NAFLD AND eHealth, lifestyle change AND eHealth. All the literature published in English will be considered.

Results:

A randomized control trial (RCT) in Singapore assessed lifestyle intervention using Nutritionist Buddy (nBuddy) mobile app for weight loss among NAFLD patients. Comparing the intervention group to the control group at 6 months, the intervention group had a 5-fold increased likelihood of achieving a $\geq 5\%$ weight loss. Similarly, Fitbit app was used in an RCT in the USA where 50% of NAFLD adults had reduction of weight after 6 months. Web based program was designed in a study in Italy reaching the 10% weight target among 5%, 13% and 20% of NAFLD adults in intervention group at 6, 12 and 24-month follow. Mobile based lifestyle interventions are implemented either alone or along with general physician advice. There are no many studies for mobile based lifestyle intervention among adults with NAFLD in India though a few studies focused on lifestyle interventions in general or among diabetics or obese groups.

Conclusion::

Recent years have seen a rise in the use of mobile applications that help people lose weight through self-monitoring of dietary intake and physical activity. This can be carried out with the convenience of

mobile devices. The studies across other countries have shown significant effectiveness of mobile phone applications for intervening those with NAFLD. Such studies are recommended among NAFLD adults in India as the prevalence of NAFLD has been increasing silently over years. Mobile applications have a greater chance of extending the reach and effectiveness of lifestyle interventions for the prevention of NAFLD.

MS-17

Analysis of Wing Expansion Behaviour in Rice Grasshopper *Hieroglyphus banian*

Kamala Soren, Sudipta Saraswati

Behavioural Neuroscience Laboratory, Centre for Neural and Cognitive Sciences, School of Medical Sciences, University of Hyderabad, Hyderabad, India
e-address: kamalasoren@gmail.com

Soon after eclosion, winged insects undergo an evolutionarily conserved stereotyped motor behaviour called wing expansion behaviour. This behaviour has been thoroughly studied in *Drosophila melanogaster* (White and Ewer, 2014). However, to the best of our knowledge, wing expansion behaviour in rice grasshopper, *Hieroglyphus banian* has not been reported yet. We carried out an investigation into the wing expansion behaviour of *Hieroglyphus banian*. Here, we report the results of our study on wing expansion behaviour in *Hieroglyphus banian*. We observed that in *Hieroglyphus banian*, wing expansion behaviour consists of a stereotyped sequence of different motor programmes, which starts with spontaneous locomotion followed by perching on a vertical wall. We also observed that under the perched condition, *Hieroglyphus banian* repeatedly exhibits a sequence of motor activities such as abdominal contraction, wing spreading etc., which is culminated in the expansion of two pairs of wings. The results of our study will help not only in investigating the neurobiological processes underlying wing expansion behaviour in *Hieroglyphus banian*, but also in identifying which aspects of wing expansion behaviour are conserved and which aspects are not conserved across different winged insect species.

Reference:

Benjamin H. White, and John Ewer (2014). Neural and Hormonal Control of Postecdysial Behaviors in Insects. Annual Review of Entomology. 59:363–81

MS-18

Prevention and Control of Workplace Violence Among Health Care Professionals: Use of Technology

Gadapati Suresh , Prof.Shamanna BR

University of Hyderabad

e-address: 19muph02@uohyd.ac.in

Aim:

To explore recent literature on the use of technologies to prevent and reduce workplace violence against healthcare professionals.

Background:

Workplace violence (WPV) is a thriving public health problem among healthcare professionals (nurses, doctors, physicians, etc.) globally. It's a major occupational hazard in India. The intentional use of power, threatened, against HCPs in work-related circumstances, that results in injury, death. Prevalence of WPV among health care professionals (HCPs) up to 38% and 62% globally and In India about 75%. The healthcare industry has been working to improve effectiveness and efficiency with the adoption of technology. It underwent a considerable transformation and enhanced working conditions and quality of healthcare service delivery. New technologies are significantly cost-effective, provide effective services and bring innovative solutions for the violence against the healthcare providers during their work.

Method:

We reviewed the literature, including information from Google Scholar, Scopus, PubMed, ProQuest Central, CINAHL, and ERIC. A narrative analysis was done on peer-reviewed articles released in English between 2011 and 2021.

Findings:

The finding of the review shows the new technologies such as cameras, badge controlling systems, monitoring systems, visitor management systems (weapon detection), barrier protection, audio analytics (sensing raised voices), mobile duress system(real-time location systems (RTLS)), security robots and systems to identify and flag clients with a history of violence. Implementing these new technologies protects and supports healthcare professionals at work while significantly lowering their stress levels and high risks. Improving worker safety is necessary. It's an integral part of a thorough plan to avoid workplace violence is an investment in security technologies.

Conclusion::

This study adds to the existing literature and practice point of view by offering a clear picture of the present state of the art in preventing violence against HCPs in the hospitals with the help of technology. Unfortunately, this phenomena is still being studied, and it is unclear which frameworks may be used to define the possible successful solutions, as well as how cultural, contextual, and organizational variables might be included.

Keywords:

Attack, Assaults, Threat, Caregivers, health providers, Nurses, Doctors

LP-01**Melatonin modulates the nitrogen metabolism and autophagy differentially under drought stress in upland cotton (*Gossypium hirsutum* L.)**

Laha Supriya , Gudipalli Padmaja

Department of Plant Sciences, School of Life Sciences, University of Hyderabad, Hyderabad 500 046, Telangana, India

Melatonin (N-acetyl-5-methoxytryptamine) is a multifunctional hormone having a wide range of phyto-protectant activities including tolerance to abiotic stresses. The role of melatonin in regulation of nitrogen metabolism and autophagy under drought stress is still elusive. Here, melatonin-mediated effects on nitrogen metabolism and autophagy during drought stress were studied in drought-sensitive (L-799) and drought-tolerant (Suraj) varieties of upland cotton (*Gossypium hirsutum* L.). Melatonin-priming enhanced the activities of nitrate reductase (NR), nitrite reductase (NiR), glutamine synthase (GS) and glutamate synthase (GOGAT) enzymes besides increasing the nitrate and lowering the ammonium contents in drought stressed plants thus showing the improved N₂-metabolism under drought in L-799 variety. Interestingly, melatonin-primed drought-stressed plants of Suraj did not show any significant changes in the enzyme activities of NR, NiR, GS and GOGAT as well as nitrate and ammonium contents compared to un-primed stressed controls. The lowered transcript levels of autophagy-related genes (ATG) including autophagosome formation in L-799 variety under drought stress could be due to unregulated production of ROS levels that could have restrained the autophagy induction. The expression levels of two genes viz., TOR (target of rapamycin) and COST1 (constitutively stressed-1) that are negative regulators of autophagy decreased by 9- and 21- folds, respectively in melatonin-primed stressed plants of L-799 which is pointing towards the involvement of melatonin in accelerating the autophagy initiation under drought stress. Besides, upregulated expression of ATG-genes (ATG2, ATG9, ATG18a, ATG5, ATG12 and ATG7), along with higher ratio of lipidated-ATG8 and free ATG8 protein levels with elevated autophagosomes in primed-stressed plants proves the beneficial effect of melatonin-priming in phagophore membrane and autophagosome maturation in sensitive variety (L-799) under drought stress. On the other hand, drought stress alone stimulated autophagy initiation in Suraj possibly due to its inherent tolerant nature whereas melatonin priming caused a decrease in ATG8-PE protein level and autophagosome formation when subjected to drought stress. ROS being the main effector molecule to induce autophagy pathway, melatonin-priming might have lowered the intracellular ROS below the levels necessary for the activation of autophagy process under drought-stressed conditions in drought-tolerant variety (Suraj). Thus, the study showed that exogenous melatonin differentially modulates nitrogen metabolism and autophagy in two drought-distinguished varieties of upland cotton under drought stress.

Keywords:Cotton, Melatonin priming, Drought stress, N₂-Metabolism, Autophagy.

LP-02**Functional elucidation of a Phosphorus starvation inducible Respiratory burst oxidase SlRbohH gene in the reprogramming of root system architecture.**

Akash, Rahul Kumar

Department of Plant Sciences, School of Life Sciences, University of Hyderabad, Gachibowli, Hyderabad, India.

e-address: 17lpph10@uohyd.ac.in

Phosphorus (P) is an essential nutrient, but its low concentrations in inorganic form (Pi) in soil limits plant growth and reproduction. To adapt to low Pi availability, plants have developed intricate regulatory mechanisms that integrate the environmental stimuli with internal cues in order to exploit the use of P. As an initially acquired molecule, Pi is a primary signal that directly regulates Pi starvation responses and generation of subsequent signals, such as hormones, sugars, P-containing metabolites, mobile RNAs and Reactive oxygen species (ROS). ROS are detrimental to plant health when generated in excess, however, can act as signals, when produced at low levels, to regulate diverse cellular processes during plant development. In the present study, we have screened tomato genotype for RSA under P-deficient condition and observed that primary root length, root hairs density, total carbohydrate, anthocyanin and ROS content significantly increased. Cell growth is a fundamental process in all organisms, and NOXs genes have been implicated in polarized cell growth in plants. In the light of these facts, we have identified eight NOX members in tomato. To identify PSI Rboh (Respiratory Burst Oxidase Homologues), we studied their expression profiles under P deficient condition and performed VIGS of RbohH gene which led to decline Pi content, root hairs density and ROS generation whereas enhanced the anthocyanin and carbohydrate content. Further, RbohH promoter was shown positive interaction with transcription factor Phosphate starvation response (PHR), which may be helping to regulate many PSI genes.

Keywords:

Phosphate Starvation Response (PSR), NADPH oxidases (NOXs), VIGS and PHR

LP-03**Genetic polymorphism revealed by RAPD and ISSR markers in different accessions of *Pterocarpus santalinus* L.**Priyanka S. ^a, Pattanaik S. ^b, Padmaja G. ^a^aDepartment of Plant Sciences, School of Life Sciences, University of Hyderabad, Hyderabad 500 046, Telangana^bInstitute of Forest Biodiversity, Dulapally, Hyderabad 500 100, Telanganae-address: psaxena.biotech@gmail.com

Pterocarpus santalinus L., commonly known as red sanders is a popular tree species of Fabaceae family having multiple industrial and pharmaceutical applications. The knowledge on genetic diversity of red sanders in natural populations using molecular markers is limited. Such information is necessary to develop appropriate plans for management, conservation and repopulation of this species. In this study, RAPD (Random Amplified Polymorphic DNA) and ISSR (Inter Simple Sequence Repeat) markers have been used to estimate the genetic variation in 40 different accessions of red sanders representing 8 forest regions of 3 states (Andhra Pradesh, Tamil Nadu, and Telangana). Out of 42 RAPD primers screened, 20 primers resulted in amplification which were used to analyze the genetic variation. The total number of bands amplified were 122 out of which 83 bands were polymorphic accounting to 68.03% polymorphism, with an average of 6.1 bands per primer. Maximum polymorphism of 100% was detected by 3 RAPD primers, viz., OPF-11, OPO-08 and OPS-05 whereas 13 RAPD primers detected polymorphism higher than 60%. In ISSR analysis, 33 primers were screened initially, out of which 20 primers produced amplified bands. Out of 140 amplified bands, 109 bands were polymorphic, with an average of 77.85% polymorphism and 7.2 bands per primer. Further, 17 ISSR primers detected more the 60% polymorphism. Overall, 6 RAPD and 7 ISSR primers generated PIC values greater than 0.4 in the 40 accessions analyzed. Hierarchical clustering and Neighbor joining tree based on dissimilarity index generated from combined RAPD and ISSR markers revealed 2 major clusters, with the first major cluster amassed accessions from 4 forest locations viz., Ahobilam and Redwood Park of Andhra Pradesh, and Nayapakkam and Amrithi of Tamil Nadu indicating greater similarities among the accessions of these locations. All accessions from one forest location (Medireddypalli) of Andhra Pradesh always found to be out-grouped in a separate major cluster or sub-cluster suggesting that they are genetically distinct from the accessions of other forest locations. The results presented here are of significance as it helped in the identification of polymorphic RAPD and ISSR markers that detected genetic variation and also revealed the genetic relationships among accessions of 8 forest locations in red sanders.

LP-04**Silencing of a ripening-associated UDP-glycosyltransferase SIUGT1 gene leads to inhibited ripening in tomato fruits**

Stuti Kujur , Rahul Kumar

Department of Plant Sciences, School of Life Sciences, University of Hyderabad, India

e-address: stutikujur@gmail.com

Tomato is an important food crop across the globe because of its edible fleshy fruits, rich in carbohydrates, Vitamin C, Vitamin K and antioxidants like lycopene and β -carotene. However, post-harvest spoilage and over-ripening of fruits during storage and transport causes significant loss to the total harvest. Improving fruit quality and increasing fruit shelf-life is thus crucial for reducing financial drain upon farmers. Auxin is a key phytohormone in tomato fruit ripening besides being involved in cell elongation, organogenesis, development, tropic and stress responses. In tomato, fruit ripening initiation is accompanied by ethylene peak and a concomitant sharp decline in auxin - a prerequisite for ripening in fleshy fruits. External application of auxin, silencing and knockout of auxin homeostasis genes have shown to delay fruit ripening in many plants including tomato, banana, strawberry, papaya, grapevine, and avocado. UDP-glycosyltransferases (UGTs) are class of enzymes which catalyse glycosylation of molecules like hormones, xenobiotics and secondary metabolites, affecting their transport, solubility and activity. Numerous studies have identified UGTs involved in glycosylation of hormones including Indole-3-Acetic Acid (IAA, predominant form of auxin in plants) which have been found to alter growth and morphology of the plant. Their precise role in fruit ripening in tomato is yet unclear. Our work focuses on identification and characterisation of auxin-inducible fruit ripening-related UGTs in tomato.

Keywords:

Auxin, UDP Glycosyltransferase, Fruit ripening, Tomato

LP-05**Cryo-milled nano-DAP for enhanced growth of plants**

Naorem Ronald Reagan Singh^a, Sreedhara Sudhakara Sarma^b, Tata Narsinga Rao^b, Harita Pant^c, Venkata Satya Siva Srikanth^c, Rahul Kumar^a

^aDepartment of Plant Sciences, University of Hyderabad, India.

^bARCI, Hyderabad, India.

^c School of Engineering Sciences and Technology, University of Hyderabad, India.

e-address: henjunahanaorem@gmail.com

Phosphorus (P) is a limiting macronutrient that regulates plant growth and development based on the bioavailability of its inorganic form, i.e., orthophosphate (Pi). P plays a critical role in cell development, and it is a key component of ATP, DNA, lipids, and cell signaling machinery. Without the exogenous application of P fertilizers, the yield of crops will not meet the ever-growing demand in today's world. However, due to the non-renewable nature of natural P reserves and simultaneous rapid human population growth, food crops must be ultimately produced more than ever by using a lower P fertilizer input. Hence, the strategy of preparing nano-fertilizers was conceptualized and demonstrated with great success. However, nano-fertilizers cannot be produced on a large scale using the currently available processing methods. Herein, a novel processing strategy, namely cryo-milling, is demonstrated to prepare nano-diammonium phosphate (n-DAP) on a kg-scale without altering DAP's bonding structure from commercial granular DAP (c-DAP). Cryo-milling procuded n-DAP with particle size ~ 5000 times smaller but specific surface area ~ 14000 times greater than that of c-DAP and at at 75% lower input than c-DAP, enhanced the growth of monocot (wheat) and dicot (tomato) plants due to improved bioavailability of Pi even for a far lower input than c-DAP.

Keywords:

Phosphorus, orthophosphate (Pi), nano-fertilizers, cryo-milling, diammonium phosphate.

References:

1. J.M. Mogollón, A.H.W. Beusen, H.J.M van Grinsven, H. Westhoek and A.F. Bouwman. Future agricultural phosphorus demand according to the shared socioeconomic pathways. *Global Environmental Change*. 2018, 50, 149-163.
2. M. Gargouri, C. Chtara, P. Charrock, A. Nzihou and H. El Feki. Synthesis and Physicochemical Characterization of Pure Diammonium Phosphate from Industrial Fertilizer. *Industrial and Engineering Chemistry Research*. 2011, 50, 6580-6584.

LP-06**Insights into the chitin-active repertoire of *Paenibacillus* sp. LS1 and its implication in chitooligosaccharides production**

Saumashish Mukherjee , Jogi Madhuprakash

Department of Plant Sciences, School of Life Sciences, University of Hyderabad, Gachibowli, Hyderabad – 500046, India.

e-address: saumashish.13sm@outlook.com

Chitin, an insoluble homopolymer of β -1,4 linked N-acetyl-D-glucosamine (GlcNAc), is the second-most abundant and a highly crystalline polysaccharide on Earth. This makes it recalcitrant and limits efficient valorization towards the production of bio-active chitooligosaccharides (CHOS). In nature, microorganisms (particularly bacteria) are known for their inherent ability to degrade chitin for nutrition. Hence, tapping into the chitinolytic reservoir of potential bacterial systems is a promising step towards the refining of chitin valorization process and thus efficient production of bioactive molecules. Genome analysis of the novel isolate *Paenibacillus* sp. LS1 revealed the chitin- active enzyme repertoire comprising of six GH18 chitinases, three GH3 β -N- acetylglucosaminidases and four polysaccharide deacetylases of CE4 family. The genome also encodes a potential transporter system involved in CHOS transport and metabolism. Gene expression analysis using qRT-PCR confirmed the up-regulation and possible involvement of the predicted chitin-active genes during degradation of crystalline chitin substrates, α - and β -chitin. Further, heterologous expression and in-depth characterization of two chitinases - the uni-modular chitinase, Chi3 and a multi-modular chitinase, Chi5 were also performed. Both Chi3 and Chi5 were optimally active at pH 5.0, and at 40°C and 45°C, respectively. HPLC analysis revealed Chi5 to be active on natural crystalline chitin substrates while, Chi3 showed activity on the less-crystalline colloidal chitin and CHOS. Furthermore, difference in product profiles for both the chitinases revealed Chi5 as a major chitobiose producer, while Chi3 generated only GlcNAc. The results taken together proposes promising implications towards utilizing the chitin-active enzymes of *Paenibacillus* sp. LS1 for efficient production of CHOS from natural chitin.

Keywords:

Chitin, chitin-active CAZymes, GH18, chitobiose, GlcNAc

LP-07**Understanding the genetic regulatory mechanism controlling PUE and PAE upon mycorrhizal colonization in tomato**

Rajat srivastava, Gayathri A G, Rahul kumar

Department of Plant Science, School of Life Science, University of Hyderabad, Gachibowli, Hyderabad, 500046, Telangana, India
e-address: 17LPPH13@uohyd.ac.in

The arbuscular mycorrhizal (AM) fungi symbiotic associations in cereal crops are known to regulate growth in cultivar-specific manner. Plant have developed several adaptive strategies to overcome phosphate (Pi) limitation. The association of roots with soil borne AMF is one of them. In the present study, we studied the growth response of an Indian tomato cultivar Pusa Ruby in the presence of *Glomus* species and noticed that AM-inoculated seedlines performed better, and accumulated more biomass than their non-AM counterparts. AM-inoculated seedlings displayed higher Pi levels and Pi acquisition efficiency (PAE), indicating it to be one of the reasons behind the observed growth promotion. The enhanced Pi levels were highly correlated with the elevated transcripts level of multiple Pht1 transporters in AM-than their control. The expression profiling also identified a receptor kinase gene (*MYRK*) as a promising candidate involved in the promotion of AM colonization in tomato roots. Interestingly, this gene promotes root mycorrhization better under Pi deprivation condition. Altogether, we discuss the role of this gene in determining the P acquisition efficiency in tomato, a non legume crop for the first time.

Keywords:

Arbuscular mycorrhizae, orthophosphate (Pi), phosphate acquisition efficiency

Reference:

Indrasumunar, Arief, Julia Wilde, Satomi Hayashi, Dongxue Li, and Peter M. Gresshoff. "Functional analysis of duplicated Symbiosis Receptor Kinase (SymRK) genes during nodulation and mycorrhizal infection in soybean (*Glycine max*)." *Journal of plant physiology* 176 (2015): 157-168.

LP-08**Heterologous expression of Melon Necrotic Spot Virus recombinant Coat Protein for invitro assembly studies**

Swati Verma, Dr. Gopinath Kodetham

Department of Plant Sciences, School of Life Sciences, University of Hyderabad, Hyderabad-500046

e-address: swativerma900@gmail.com

Melon Necrotic Spot Virus (MNSV-HYD) is (+) a single-stranded spherical shaped RNA virus with a genome of 4.3 kb, belongs to the genus *Carmovirus*; family *Tombusviridae*, and infects *Cucurbitaceae* family members. Coat Protein (CP) is involved in various aspects like encapsidation, cell-to-cell / systemic movement, and also regulates the viral RNA accumulation for the formation of virion particles. Viral infections result in substantial loss of crops that cause a socio-economic burden on farmers and thus immediate measures for disease control is required. *In vitro* viral assembly studies may provide insights into remediation or disease control where two purified components (CP and RNA) are mixed directly in an optimized buffer. In order to understand this, we have initiated our studies with MNSV-HYD strain, as a model system. Using molecular biology techniques, MNSV CP gene was amplified with different combination of histidine tagged-primers and cloned into TA-vector followed by sub-cloning in pET28a expression vector. The CP constructs were overexpressed at different temperatures (18°, 24°, 30° and 37°C) in *E. coli* microbial host with 1mM IPTG. However, optimal expression was observed at 37°C except in the case of C-His terminal CP construct. The expressed recombinant CP was present in inclusion bodies therefore, tried to solubilize it using pH, arginine and anionic detergents. The CP solubility was achieved using 0.3% Sodium lauryl sarcosinate. The soluble coat proteins with a poly-histidine tag at N-terminal was purified using Ionized Metal Affinity Chromatography (IMAC). The soluble CP fractions were layered onto 10% to 40% sucrose gradient. However, CP was unable to self-assemble into capsids and further studies is in process.

Keywords:

Coat protein, Overexpression, Solubilization, Arginine, Sodium lauryl sarcosinate, Sucrose gradient, IMAC, capsid assembly.

LP-09**Insights into the chitinolytic machinery of *Streptomyces* sp. UH6**

Lal Duhsaki , Jogi Madhuprakash

Department of Plant Sciences, School of Life Sciences, University of Hyderabad, Gachibowli, Hyderabad – 500046, India.
e-address: lalduhsaki29@gmail.com

Chitin is a natural, second most prevailing homopolymeric polysaccharide which can be found in diverse life forms. Chitinolytic bacteria secrete enzymes that can hydrolyze chitin and convert them into valuable products. In this study, the chitinolytic machinery of *Streptomyces* sp. UH6, isolated from the campus of University of Hyderabad is characterized using genomic and biochemical analyses. Genome analysis revealed the size of the genome to be 6.51 Mb and there are 6990 coding sequences present in the genome, out of which 63% were functionally annotated. Furthermore, two possible chitin-utilization pathways which employ chitin active lytic polysaccharide monooxygenases and family-18 glycoside hydrolases (GHs) were identified in the genome. Intriguingly, the genome also codes for six family-4 polysaccharide deacetylases which have a role in converting chitin to chitosan, as well as two chitosanases belonging to GH46 and GH75 families. The Conclusion: of phylogenetic and genomic analyses suggests that the isolate, *Streptomyces* sp. UH6 secretes chitin-active enzymes responsible for chitin to chitosan conversion. In addition, biochemical characterization of the secretome and comparison of the secretome with two well-studied *Streptomyces* sp. suggests that *Streptomyces* sp. UH6 is indeed an efficient chitin degrader which can degrade even the most crystalline form of chitin. The study further proposes the potential of utilizing UH6 isolate for the process of biomass conversion in biorefineries.

Keywords:

Chitin, chitosan, chitinolytic machinery, genomic analyses, *Streptomyces*, secretome.

LP-10**Molecular cloning and characterization of a new chitinase from *Flavobacterium johnsoniae***Vandhana T M, Jogi Madhuprakash

Department of Plant Sciences, School of Life Sciences, University of Hyderabad, Gachibowli, Hyderabad – 500046, India.

e-address: 19lpph03@uohyd.ac.in

Chitinases (E.C. 3.2.1.14) are glycoside hydrolases of families GH18 and GH19, that degrade chitin in either exo- or endo- manner to generate chitooligosaccharides (CHOS) which finds immense application in the fields of agriculture, industry, food and medicine.

Chitinases are often associated with binding domains known as Carbohydrate binding modules (CBMs). These non-catalytic entities bring the catalytic domain into intimate and prolonged association with the crystalline substrate and therefore helps to increase the rate of catalysis.

Here we report the heterologous expression and characterization of a chitinase, ChiC from the Bacterioidetes, *Flavobacterium johnsoniae*. FjChiC is a multimodular chitinase which has a GH18 catalytic domain and a CBM6 module appended to it. Family 6 CBMs are previously reported to be associated with xylanases, mannanases, β -glucanases, agarases and arabinases; but its function in chitinases is yet to be explored. FjChiC was optimally active at an acidic pH of 4 and at 45°C. MALDI-TOF MS and HPLC analysis revealed that FjChiC can efficiently hydrolyse α - and β -chitin generating chitobiose as the major product. Further, binding studies confirmed the affinity of FjCBM6 to both α - and β -chitin. In addition to this, we also observed that truncation of FjCBM6 reduced activity of the full-length chitinase on glycol chitin thus confirming the essential role of CBM6 in chitin hydrolysis. The work may contribute to the understanding of a versatile chitinase and its appended binding module towards efficient degradation of natural chitin for CHOS generation.

Keywords:Chitin, *Flavobacterium johnsoniae*, GH18, CBM6, CHOS.

LP-11**Understanding PGPR Mediated Salt Stress Tolerance In Tomato Plants**

Koyel Bardhan , Jogi Madhuprakash

Department of Plant Sciences, School of Life Sciences, University of Hyderabad, Gachibowli, Hyderabad – 500046, India.

e-address: koyelbardhan@gmail.com

Soil salinity alter soil properties causing detrimental effects not only on plant growth and crop production but also on cultivable areas worldwide. Plant Growth Promoting Rhizobacteria (PGPR) residing in rhizospheric region help plants grown under harsh ecosystems cope with abiotic stress factors by positively influencing plant physiology, development, and environmental adaptation. The present work is aimed to understand the role of PGPR in promoting growth and salt stress tolerance in tomato plants by investigating their physiological and biochemical responses under green house conditions.

Six bacterial cultures isolated from the soil samples collected at University of Hyderabad (UH) were found to have potential PGPR activity. All the isolates were able to tolerate excess salt conditions, but UH6 remains unaffected. Subsequently, tomato plants inoculated with six isolated PGPR were subjected to 150 and 200 mM salt stress. Increment in the number of leaves, root-shoot length, and biomass in PGPR inoculated plants compared to uninoculated plants under salt stress are the evidence of the same. Apart from the morpho-physiological evidences, decreased MDA content (marker of lipid peroxidation), increased proline content, enhanced antioxidant enzyme activity (associated with reduction in ROS level) such as peroxidase, catalase, ascorbate peroxidase, and superoxide dismutase in UH isolate(s) treated plants were observed compared to the untreated plants. Of all the six cultures, UH isolates inoculated tomato plants were healthy, exhibited less senescence, thereby, showed the most prominent salt-tolerant ability at both 150 and 200 mM salt concentrations. Along with these, combinations of isolates i.e., UH1+UH2, UH1+UH3, UH2+UH3, UH3+UH4, and UH3+UH6 showed significant salt stress-tolerant ability compared to the individual cultures. Taken together, the current results confirm that the UH culture(s) inoculation effectively induces an antioxidant system in tomato plants under salt stress, which leads to overall plant protection. Our findings represent a promising sustainable solution to improve agricultural production under the forthcoming climate change conditions.

Keywords:

PGPR; ROS; Salt stress; Antioxidants; Tomato

LP-12**Azolla plants attenuate Aluminium toxicity in Rice plants, and escalate their development under acidic soil conditions**

Karishma Agarwal , Markkandan Ganesan

Department of Life Sciences, Presidency University, Kolkata 700073, West Bengal, India.

e-address: karishma64@gmail.com

Soils with a pH lower than 5 become unsuitable for cultivation of food crops, especially due to the formation of complex metal ions in the wet soil, which obstruct the uptake of mineral ions. Rice is one of the most important crops cultivated in soils with excess of water. This leaches the soil of their nutrients, as well as causes formation of phytotoxic Aluminium ion complex with protons, thereby further reducing the pH of the soil. Hence, we grow Azolla plants, an aquatic pteridophyte with nitrogen fixing and phytoremediation properties, along with rice plants under both Aluminium (Al) and acid soil stress. We observed that at a higher concentration of ≥ 30 μ M Al and pH ≤ 5 , roots of Azolla plants get affected and start falling, while germination of rice seedlings increase with the presence of Azolla. Also, Rice seedlings were found to have reduced oxidative stress when grown together with Azolla plants. Furthermore, the hydroponics media was found to have increased nitrate content in presence of Azolla plants.

LP-13**Tolerance of cotton to Aluminum is regulated by GhMATE1 and overexpression of GhMATE1 intensifies acid soil tolerance of Arabidopsis**

Atreyee Sur Roy Chowdhury , Markkandan Ganesan

Department of Life Sciences, Presidency University, Kolkata 700073, West Bengal, India

e-address: atreyee.em@gmail.com

In acid soil conditions, the ionic form of Aluminum (Al^{3+}) is one of the elements that plants should avoid. Al-induced activation of membrane transporters, which has the effect of accelerating the release of organic acids from the root region, is one of the main functional tools for plant Al tolerance. In the rhizosphere, the released organic acids—typically citrate, oxalate, and malate—form stable, harmless complexes with Al. To comprehend how plants tolerate acid soil, several genes were characterized. In instance, Al-activated malate and citrate release from the roots are key components of processes that efficiently reduce acid soil stress. The cotton citrate [Gossypium hirsutum Multidrug and Toxic compound Extrusion 1 (GhMATE1)] transporters have been cloned and characterized in Cotton based on the aforementioned mechanisms. The GhMATE1 (GhMATE1-RNAi) system's downregulation enhanced the sensitivity to Al and proton. Furthermore, compared to control plants, plants missing GhMATE1 generated a very little amount of citrate. Under Al stress conditions, GhMATE1-RNAi-lines' main and secondary root growth was severely suppressed. Additionally, GhMATE1-RNAi lines did not exhibit any changes in the expression of Al stress-responsive genes, including Gossypium hirsutum Aluminum-activated Malate Transporter 1 (GhALMT1), Gossypium hirsutum Sensitive to Proton toxicity 1 (GhSTOP1), and Gossypium hirsutum Aluminum Sensitive 3 (GhALS3). Furthermore, compared to control plants, transgenic Arabidopsis plants overexpressing GhMATE1 showed rapid root growth and improved citrate excretion, as well as Al-tolerant traits. The findings demonstrated that GhMATE1 regulates citrate-mediated Al^{3+} sequestration and is Al inducible in expression. These findings suggested that GhMATE1 is a crucial gene involved in the arrest of lateral root growth and citrate release triggered by Al.

